1-1-1982

Discharge and resistance of streams with multiple roughness.

Andrew Hok-Bun Lau
University of Windsor

DISCHARGE AND RESISTANCE OF STREAMS WITH MULTIPLE ROUGHNESS

by

Andrew Hok-Bun Lau
B.A.Sc., B.A.

A Thesis
submitted to the Faculty of Graduate Studies through the
Department of Civil Engineering in Partial Fulfillment
of the requirements for the Degree of
Master of Applied Science at
The University of Windsor

Windsor, Ontario, Canada
1982

LAU, Andrew Hok-Bun Discharge and resistance of streams... MASc.1982
PRINTING ON LEAVES 190 TO 256 IS FAINT AND BROKEN. WOULD NOT PRODUCE A GOOD MICROFICHE.

To my parents

ABSTRACT

This thesis describes the influence of multiple roughness on the conveyance capacity of streams. Experimental studies were made of covered or open-channel flow in cross-sections lined entirely or partially with various roughness materials. Friction factors which were expressed in terms of Manning's and Chezy's roughness coefficient were determined and detailed velocity distributions were also measured. Theoretical analysis was made on the boundary shear stress distribution and velocity profiles, and relating these parameters to different configurations of the channel cross-section. A finite strip method was developed here in describing the velocity flow pattern within a channel, and the results would be very useful for the determination of stream flow characteristics in natural rivers.

ACKNOWLEDGEMENTS

The writer wishes to express his sincere gratitude to Dr. S. P. Chee, Head of Civil Engineering Department for his constant guidance and encouragement and for critically reviewing this thesis.

In addition, many thanks must be given to Dr. J. A. McCorquodale, Professor of Civil Engineering Department and Dr. M. R. Haggag for their concern and assistance throughout this study.

The financial support provided by the National Research Council and the Civil Engineering Department of the University of Windsor is gratefully acknowledged.

TABLE OF CONTENTS

APPENDIX (continued)

LIST OF FIGURES

Figure (continued) Page

Figure (continued) Page

LIST OF TABLES

CHAPTER I

INTRODUCTION

1.1 Introductory Remarks

The regimesof rivers are continually being altered both by nature and man. The effects of such alter-ations often extend far distance up and down the stream from the actual site. Hence a complete assessment of the impacts of such changes is important to future planning of water resources development and control. Although laboratory studies which involve turbulent flow of water in flumes, lined channels, and other conduits of homogeneous boundary roughness are well understood in their overall aspects, yet these studies have depended either on very generalized descriptions of the natural rivers or on very idealized laboratory models of the rivers. Such simplicities are seldom found in natural streams. It is quite common to find marked lateral variations of bed configuration and roughness in such streams which associated with variations in depth as well. Therefore, the extent to which the laboratory results apply to the behaviour of natural streams is limited by many idealized test conditions.

In order to estimate the resistance to flow which is encountered, the question arises as to the extent to which existing mathematical models derived from flume data are applicable. As far as the composite roughness is concerned, a variety of formulas can be found based on different assumptions. It has been pointed out by some previous investigators that these assumptions are generally too optimistic.

The aim of this study is to develop a more rational model for the prediction and presentation of data on the velocity profiles, the shear stress distributions and friction factor of a composite channel.

1.2 Definition of the Problem

Channel sections with different roughnesses along the wetted perimeter are often encountered in design problems, such as man-made and natural watercourses. Typical design problems include partly lined canals and tunnels with different construction materials used for the bottom and the sides.

In order to solve the problem, a more general solution has to be developed. There are two major aspects which have to be considered.

Firstly, the model has to be applicable to a multiple-roughness channel, with or without a buoyant cover.

Secondly, it can also be applied to channels of different configurations, without neglecting the sidewall effects.

The need for such a solution is obvious, both for design purposes and for laboratory investigation.

CHAPTER II

LITERATURE REVIEW

2.1 Introduction

As stated in the previous chapter, most laboratory experiments on the resistance to flow in open channels have been conducted under carefully controlled, idealized conditions. But these experimental conditions fail in important ways to reflect the characteristics of natural streams, in which lateral variation in depth and roughness may be very pronounced.

Past experience indicates that the roughness coefficient should be a function of the following independent variables: the Reynolds number; the roughnesses of the wetted perimeter; the cross-sectional shape; the non-uniformity of the channel in both profile and plan; the Froude number; and the degree of unsteadiness [38].

It is worth noting that many investigators have been studying the effects of these variables. Their invaluable experiences, which form the ground for future investigations, are going to be discussed in the following sections.

For the sake of simplicity, some of the notations used in different literature reports have been modified to agree

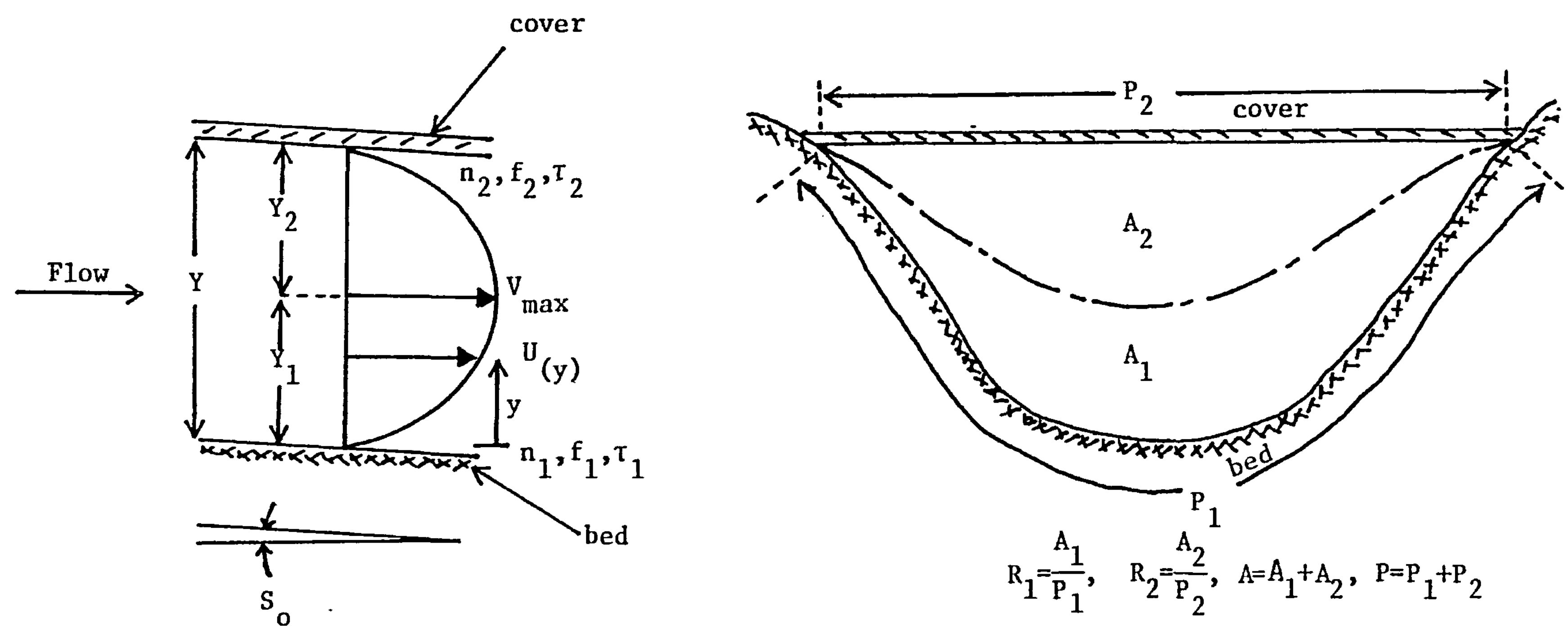

Fig. 2.2.1 Schematic Depiction of Flow Under an Ice Covered Channel

with those adopted in this thesis.

2.2 Development of Equivalent Roughness Equations

Basically the development was first studied for the determination of the equivalent roughness of an ice covered channel and the related problem of predicting the shear stress on the wetted perimeter. Later on different methods had been developed to obtain a more general solution to the problem of equivalent roughness.

By considering a segment of an ice covered stream as shown in Fig. 2.2.1, a common feature of practically all the analysis is the division of the whole flow section into two parts: area A_1, which is dominated by the bed; and the balance of the section A_2, for which the streamwise gravity force is balanced by the shear on the ice cover. The method for dividing the section into A_1 and A_2 differs from one analysis to another. The corresponding wetted perimeters are P_1 and P_2, and the Manning coefficients, the Darcy-Weisbach friction factors and shear stresses are n_1, n_2, f_1, f_2 and τ_1, τ_2 respectively.

In 1931 Pavlovskiy [33] was the first to calculate the composite roughness n_t, by equating the gravity force along the channel to the sum of the shear forces exerted on the channel bed and the ice cover

$$\gamma R_t S_o = \frac{\tau_1 P_1 + \tau_2 P_2}{P_1 + P_2} \tag{2.2.1}$$

where

γ is the unit weight of the fluid

S_o is the energy slope of the channel

R_t is the hydraulic radius of the channel

The shear stress τ_i is obtained from Manning's equation in metric form

$$\tau_i = \frac{V^2\gamma}{(\frac{1}{n_i} R_i^{1/6})^2}, \quad i = 1, 2 \qquad (2.2.2)$$

where V is the mean velocity.

He assumed $R_t = R_1 + R_2$ and introduced Eq. (2.2.2) into Eq. (2.2.1) to obtain

$$n_t^2 = \frac{n_1^2 + a\, n_2^2}{1 + a} \qquad (2.2.3)$$

where $a = P_2/P_1$. Equation (2.2.3) states that n_1^2 and n_2^2 are weighted in the composite n_t by P_1 and P_2. It is apparent from Eq. (2.2.2) that τ_i/n_i^2 is constant, under the assumptions that R_i, i = 1,2, are equal and V_i, i = 1,2, are common to all sections.

In 1933 Lotter [33] based his analysis on both the Chezy formula and continuity, developed the relation for composite Chezy's coefficient,

$$Q = AC_t \sqrt{R_t S_o} = A_1 C_1 \sqrt{R_1 S_o} + A_2 C_2 \sqrt{R_2 S_o} \qquad (2.2.4)$$

Where V_i and C_i are the mean velocities and Chezy's coefficients for the flow sections. By the introduction of R_i = constant, and $a = P_2/P_1$ Eq. (2.2.4) yields

$$C_t = \frac{C_1 + aC_2}{1 + a} \tag{2.2.5}$$

When the equation is expressed in terms of n_i, Eq. (2.2.5) becomes

$$n_t = \frac{1 + a}{\frac{1}{n_1} + a\frac{1}{n_2}} \tag{2.2.6}$$

In 1938 Belokon [33] used a power-law velocity distribution, with an exponent of 1.5, for each of the subsections A_1 and A_2, and assumed that $V = V_1 = V_2$. The expression he derived was,

$$n_t = n_1 \left[1 + a \left(\frac{n_2}{n_1} \right)^{3/2} \right]^{2/3} \tag{2.2.7}$$

In the limiting case $n_1 = n_2$ and $P_1 = P_2$, Eq. (2.2.7) yields $n_t = 1.59\ n_1$, which is obviously incorrect.

In 1948 Sabaneev [33] utilizing a generalized form of the Chezy relation with

$$C_i = 1.486\ \bar{R}_i^{r}/n_i \tag{2.2.8}$$

where r is a nondimensional coefficient, which is equal to 1/6 in the Manning equation. Introducing Eq. (2.2.8) into the Chezy equation Eq. (2.2.4), and solving for A_i yields

$$A_i = \left[\frac{n_i V_i}{1.486 \sqrt{S_o}} \right]^{2/(2r + 1)} P_i \qquad (2.2.9)$$

Substituting Eq. (2.2.9) into $A_t = A_1 + A_2$ and assuming the equality of V_i leads to

$$n_t = n_1 \left[\frac{1 + a \left(\frac{n_2}{n_1}\right)^{2/(2r+1)}}{1 + a} \right]^{(2r+1)/2} \qquad (2.2.10)$$

In 1948 Levi [28], for a wide channel, applied the logarithmic velocity distribution to sections 1 and 2 to obtain

$$U_i(y) = \frac{1}{\kappa} \sqrt{\frac{gYS_o}{2}}\, \ell n \frac{y_i}{k_i}, \; i = 1, 2 \qquad (2.2.11)$$

where κ is Von Karman's constant; y_i are vertical displacements away from the corresponding boundaries and k_i is the hydraulic roughness height. Equating the maximum velocity by substituting $Y_i = y_i$ into Eq. (2.2.11) and with $Y = Y_1 + Y_2$ leads to

$$Y_i = Y \frac{k_i}{\Sigma k_i}, \; i = 1, 2 \qquad (2.2.12)$$

By applying the continuity equation together with the Chezy's relation, results in C_t,

$$C_t = \frac{\sqrt{g}}{\kappa} \left[\ln \frac{Y}{2k_m} - 1 \right] \tag{2.2.13}$$

where $k_m = \dfrac{k_1 + k_2}{2}$

In terms of Manning's n_t, Eq. (2.2.13) becomes

$$n_t = \frac{\kappa \left(\frac{Y}{2}\right)^{1/4}}{\sqrt{g} \left[\ln \frac{Y}{2k_m} - 1 \right]} \tag{2.2.14}$$

where k_m is given by the relation,

$$k_m = \frac{Y}{2} \exp \left[-1 - \frac{\kappa}{n_t \sqrt{g}} \left(\frac{Y}{2}\right)^{1/4} \right] \tag{2.2.15}$$

Levi recommended the use of Eq. (2.2.15) for each n_1 and n_2 to solve for k_1, k_2, and k_m and introducing k_m into Eq. (2.2.14) for the required n_t.

In 1958 [16] a "Task Force on Flow in Large Conduits" of the Committee on Hydraulic Structures (A.S.C.E.) was authorized to assemble and evaluate information on hydraulic characteristics in large pipes, tunnels, and conduits.

According to Colebrook, when a conduit is lined circumferentially with two different materials, a relationship can be used to weight the composite friction factor slightly in the direction of greater roughness, that is,

$$n_t = n_r \left[\frac{P_r + P_s \left(\frac{n_s}{n_r}\right)^{3/2}}{P_r + P_s} \right]^{2/3} \tag{2.2.16}$$

in which r and s represent the rough and smooth sections respectively.

In 1959 Chow [11] by following Pavlovskiy, utilized the static balance expression Eq. (2.2.1) together with the Chezy equation, obtained the expression

$$\frac{1 + a}{C_t^2} = \frac{1}{C_1^2} + \frac{a}{C_2^2} \tag{2.2.17}$$

where $a = P_2/P_1$, which in terms of the Manning equation, becomes

$$\frac{(1 + a)\, n_t^2}{R_t^{1/3}} = \frac{n_1^2}{R_1^{1/3}} + \frac{a n_2^2}{R_2^{1/3}} \tag{2.2.18}$$

by assuming $R_t = R_1 + R_2$ and the maximum discharge condition expressed by

$$\frac{d}{d(R_1/R_2)} (n_t) = 0 \tag{2.2.19}$$

Equation (2.2.18) becomes

$$n_t = \frac{n_2}{\sqrt{1+a}} \left[a^{3/4} + \left(\frac{n_1}{n_2}\right)^{3/2} \right]^{2/3} \tag{2.2.20}$$

In the limiting case $n_1 = n_2$ and $a = 1$ Eq. (2.2.20) yields $n_t = n_1 (2)^{1/6}$.

For channel with multiple roughness coefficients, he assumed that each part of the channel section has the same mean velocity which is equal to the mean velocity of the whole cross-section, the equivalent roughness coefficient can be obtained from,

$$n_t = \left(\frac{\sum_{i=1}^{N} P_i \, n_i^{3/2}}{P_t} \right)^{2/3} \qquad (2.2.21)$$

where i = 1, 2...N. By assuming that the total force resisting the flow is equal to the sum of the forces resisting the flow developed in the divided areas, another expression for n_t can be derived,

$$n_t = \left(\frac{\sum_{i=1}^{N} P_i \, n_i^{2}}{P_t} \right)^{1/2} \qquad (2.2.22)$$

Further assume that the total discharge is equal to the sum of the discharges of the subdivided parts, the equivalent roughness coefficient can be expressed by

$$n_t = \frac{P_t R_t^{5/3}}{\sum_{i=1}^{N} \frac{P_i R_i^{5/3}}{n_i}} \qquad (2.2.23)$$

In 1961 Shiperko [39] used the assumptions that for a given channel section with roughness coefficients n_1 and n_2, the average velocity and discharge must be a maximum. Thus the equivalent roughness coefficient can be obtained as,

$$C_t^{\,2} = \frac{P_1}{P_t} C_1^{\,2} + \frac{P_2}{P_t} C_2^{\,2} \qquad (2.2.24)$$

By further assuming that $R_t = R_1 = R_2$, and in term of Manning's n_t, Eq. (2.2.24) becomes

$$n_t = \sqrt{\frac{1}{\dfrac{P_1}{P_t n_1^{\,2}} + \dfrac{P_2}{P_t n_2^{\,2}}}} \qquad (2.2.25)$$

In 1962 Dul'nev [13], by following Lotter and by further assuming that the hydraulic radii R_t, R_1 and R_2 were equal, he came up with an expression for the equivalent roughness coefficient as

$$n_t = \frac{1}{\dfrac{P_1}{n_1 P_t} + \dfrac{P_2}{n_2 P_t}} \qquad (2.2.26)$$

In 1965, Sinotin [40], by applying Nikitin's law of velocity distribution for uniform flow in a wide channel ($R \simeq Y$),

$$\frac{U}{V_{*i}} = 6.45 \log y/Y_i + 5.6 + 2.8 \frac{y/Y_i - 1}{y/Y_i} \qquad (2.2.27)$$

where V_{*i} are the shear velocities of section 1 and 2, to $i=1,2$
both the cover and bed sections of the channel, he obtained a hydraulic division relationship $\frac{Y_1}{Y} = F(\frac{n_1}{n_2})$ as,

$$\frac{Y_1}{Y} = 0.6 \log \frac{n_1}{n_2} + 0.5 \qquad (2.2.28)$$

He concluded that the formula for determining the reduced coefficient of roughness with variation of $\frac{Y_1}{Y}$ by Eq. (2.2.28) as,

$$n_t = \frac{n_1}{1.67 \left[(0.6 \log (\frac{n_1}{n_2}) + 0.5)^{1.75} + \frac{n_1}{n_2} (0.5 - 0.6 \log (\frac{n_1}{n_2})^{1.75} \right]} \qquad (2.2.29)$$

In 1966 Carey [2, 3], by basing his analysis on the Karman-Prandtl resistance equation for turbulent flows in pipes, he developed a framework for analysis and presentation of data. The resistance equations for the channel subsections can be written in terms of the effective size of roughness projections, k_i, as

$$\frac{V_i}{\sqrt{8gR_iS_o}} = 2 \log \frac{2R_i}{k_i} + 1.74 \qquad (2.2.30)$$

$$i = 1,2$$

By obtaining data on the stream discharge, channel geometry, and k_i, Eq. (2.2.30) can be solved for R_i and A_i by a trial and error procedure. Then, by employing Darcy's friction relation,

$$f_i = \frac{8gR_iS_o}{V_i^2}, \quad i = 1,2 \qquad (2.2.31)$$

the quantities f_i can be calculated.

In the following year, 1967 [4], he presented two different approaches for computing total discharge.

The first computation method called the "Pipe-flow-equation method," he modified the Darcy-Weisbach equation in the form of

$$Q = \sqrt{\frac{8g}{f_{MOD}}}\, A_t\, R_t^{1/2}\, S_o^{1/2} \qquad (2.2.32)$$

where Q is the total discharge for the covered channel,

f_{MOD} is the modified Darcy-Weisbach friction factor for the channel,

to evaluate the total discharge of a covered channel.

The second method called the "Stage-fall-relation method" is based on an analogy between ice-covered streams and streams having variable slopes caused by backwater during periods of open water. Basically, it involves two graphical relationships: (1) a relation between stage and discharge for some fixed condition of fall of the water surface; (2) a relation between discharge ratios and corresponding fall ratios.

Since the relationships in both methods are developed with data either recorded or measured in the field, it cannot be used for general applications.

In 1967 Sumbal and Komora [41], based on the studies of the flow under an ice covered channel, derived a method for solving the equivalent composite roughness.

He assumed that the velocity profile can be divided into several parts, pertaining to the walls and bottom and to the ice cover, where equal average velocity and equal energy slope exist.

For a given channel, as shown in Fig. 2.2.2a ,from the assumed values of the n_1, n_2 and n_3 at a given discharge area, the relative distance of maximum velocities from the bottom $\frac{Y_1}{Y}$ is determined by means of a monograph [41]. The coefficient of $n_{1,2}$ can be defined by Eq. (2.2.33),

$$n_{1,2} = \frac{n_1 n_2}{\left[n_2 \left(\frac{Y_1}{Y}\right)^{5/3} + n_1 \left(1 - \frac{Y_1}{Y}\right)^{5/3} \right]} \qquad (2.2.33)$$

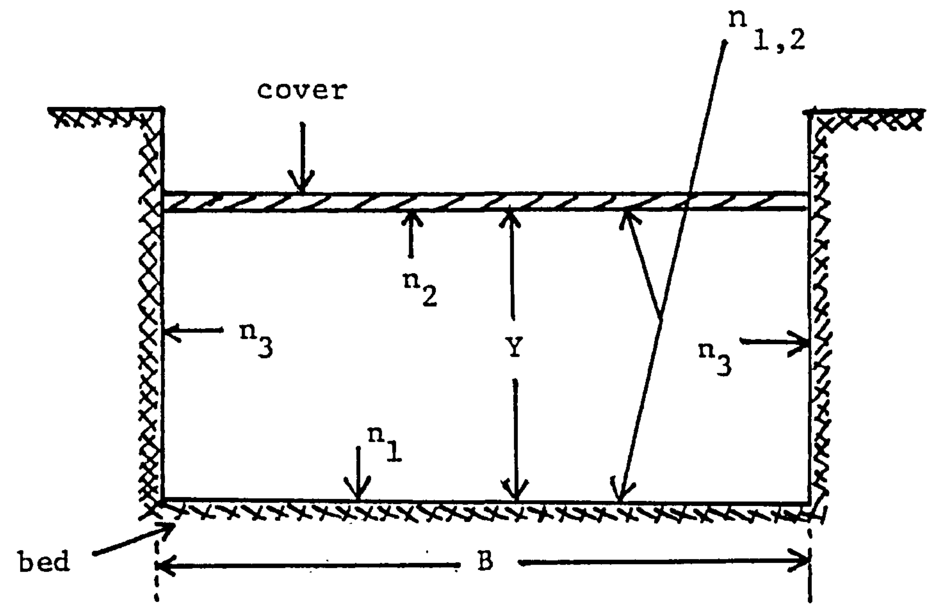

Fig. 2.2.2a Covered Channel with Three Different Boundary Roughnesses (After Sumbal and Komora [41]).

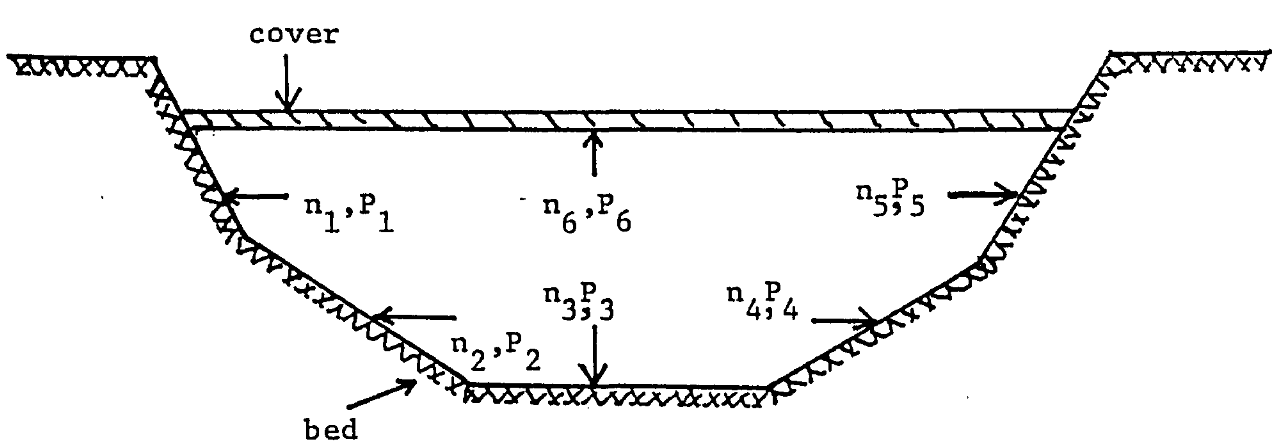

Fig. 2.2.2b Scheme of the Uniform Channel with Common Shape and Multiple Boundary Roughnesses (After Sumbal and Komora [41]).

Finally, the equivalent roughness coefficient n_t by Eq. (2.2.34), as,

$$n_t \left[\frac{n_{1,2}^{3/2} + \frac{Y}{B} n_3^{3/2}}{1 + \frac{Y}{B}} \right]^{2/3} \tag{2.2.34}$$

where

Y is the maximum depth of the channel,

B is the width of the channel.

In the same year they examined several composite roughness equations which had been derived by previous investigators. By following Pavlovskiy's approach and the introduction of the Manning-Strickler equation, they obtained an expression for the hydraulic division ratio as,

$$\frac{Y_1}{Y} = \frac{n_1^{3/2}}{n_1^{3/2} + n_2^{3/2}} \tag{2.2.34a}$$

and a composite roughness equation

$$n_t = n_1 \left[\frac{1 + \left(\frac{n_2}{n_1}\right)^{3/2}}{2} \right]^{2/3} \tag{2.2.34b}$$

By further assuming that Eq. (2.2.34b) can be applied to a uniform channel of common shape as shown in Fig. 2.2.2b to obtain a simple expression as,

$$n_t = \frac{\left[\sum_{i=1}^{N} n_i^{3/2} P_i\right]^{2/3}}{\sum_{i=1}^{N} P_i} \qquad (2.2.34c)$$

In 1967 Bruk and Volf [1] had established a mathematical scheme which utilized Manning's equation to determine the roughness coefficients for very irregular rivers with large flood plains. The reach of the river is divided into k sections (Fig. 2.2.3), and each section is subdivided into a main channel and several strips of the flood plain. By applying the Manning equation to each strip, together with the continuity equation, they derived a system of equations.

$$\sum_{i=1}^{m} n_i^{-1} A_{ij} R_{ij}^{2/3} S_j^{1/2} - Q = 0 \qquad (2.2.35)$$

where

Q = total measured flow rate

A_{ij} = cross-sectional area of each strip

R_{ij} = hydraulic radius of each strip

S_j = energy slope for each section

i = number of strips within one section

j = number of sections within the reach

Since the channel geometry, total discharge and slope are measured, the only unknown variables of the k equations are the m roughness coefficients. The number of k equations are then reduced to m normalized equations by the method of

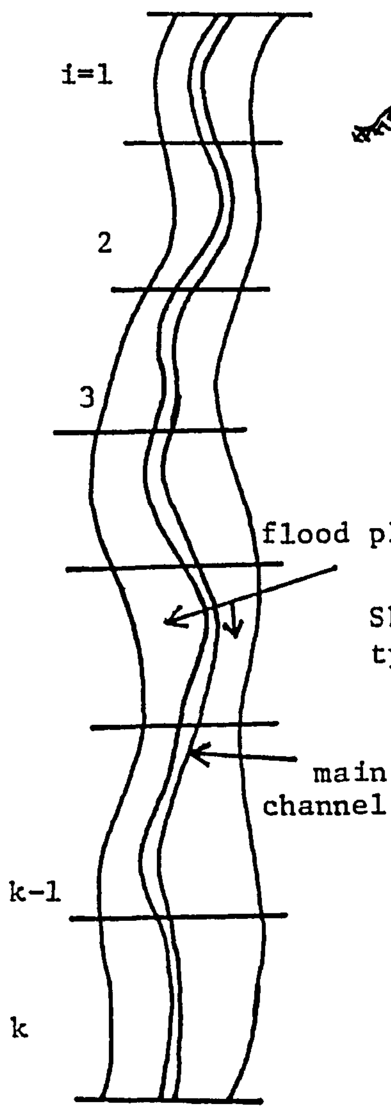

Plan View of the Main Channel and Flood plain

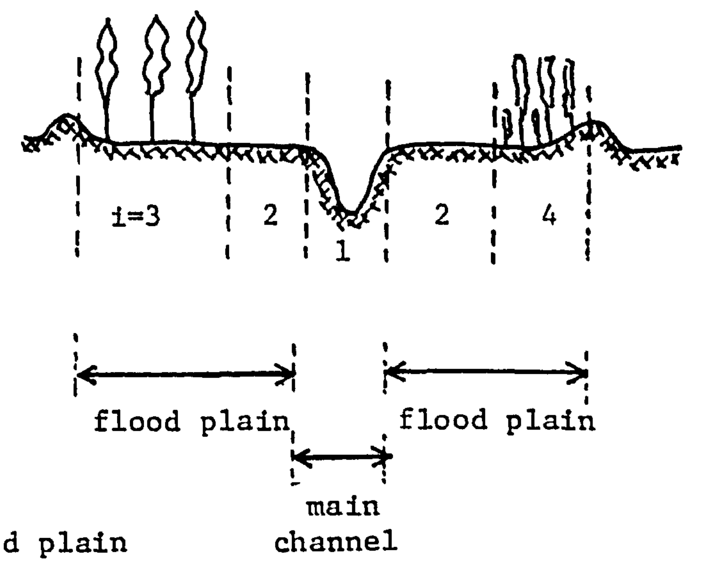

Sketch-diagram of a River with Various types of Vegetation.

1. Main Channel
2. Grass
3. Planted Timber
4. Natural Forest

Fig. 2.2.3 Irregular River with a Large Flood Plain (After Bruk and Volf [1]).

least squares, with the additional condition that the total head loss along the given reach be equal to its measured value H;

$$Q^2 \sum_{j=1}^{k} L_j \left[\sum_{i=1}^{m} n_i^{-1} A_{ij} R_{ij}^{2/3} \right]^{-2} = \sum_{j=1}^{k} \Delta h_j = H \tag{2.2.36}$$

where L is the length along each section.

The computation is initiated by assuming **m** roughness coefficients for the sections and the recalculations of these coefficients by the above method.

In 1967 Hancu [18] [45] took the velocity defect law as the starting point for his investigation of the composite roughness channel. The velocity defect relation is

$$V_{max} - U_i(y) = \sqrt{\frac{\tau_i}{\rho}} \frac{1}{\kappa} \ell n \frac{Y}{Y_i}, \quad i = 1,2 \tag{2.2.37}$$

where κ is Von Karman's constant.

$$\tau_i = \frac{\rho}{2} \lambda_i' V_i^2, \quad i = 1,2 \text{ shear stress on the boundaries} \tag{2.2.38}$$

$$\lambda_i'^{-1/2} = 4 \log \frac{Y_i}{k_i} + 4.25, \quad i = 1,2 \text{ friction coefficients} \tag{2.2.39}$$

k_i are the absolute roughnesses

ρ is the density of fluid.

By integrating Eq. (2.2.37) and eliminating V_{max}, the resulting expression is then combined with the force equilibrium of flow, pressure gradient and continuity equation which will yield,

$$\lambda' = 1/2 \left[\left(\frac{V_1}{V}\right)^2 \lambda_1' + \left(\frac{V_2}{V}\right)^2 \lambda_2' \right] \qquad (2.2.40)$$

where λ' is the composite friction coefficient.

The parameters V_1, V_2, Y_1, Y_2, λ_1' and λ_2' are the unknowns to be solved for using the given values of κ, k_i, V and Y. Hancu presented a series of figures [18] to evaluate all these parameters, and the final expression in terms of Manning's friction coefficients is

$$n_t = n_1 \left[1/2 \left(\frac{Y}{Y_1}\right)^{1/3} \left[\left(\frac{V_1}{V}\right)^2 + \left(\frac{V_2}{V}\right)^2 \left(\frac{n_2}{n_1}\right)^2 \left(\frac{Y_1}{Y_2}\right)^{1/3} \right]\right]^{1/2} \qquad (2.2.41)$$

In 1968 Yu, Graf and Levine [47] reviewed the available formulas and then developed a semi-empirical relationship for n_t both for ice covered and ice free channels. First they adopted a modified form of Manning's equation.

$$V_i = \frac{1.49}{n_1} \left(\frac{A_i}{P_i Z}\right)^{(r + 1/2)} S_o^{1/2} \qquad (2.2.42)$$

where $r = 1/6$, an empirical constant

$Z = \left(\frac{n_2}{n_1}\right)^{1/6}$ which is determined experimentally.

By using the geometrical relation $A_t = A_1 + A_2$ and the equality of V_i, they came up with an expression for n_t, as,

$$n_t = n_1 \left[\frac{1 + a^Z (n_2/n_1)^{3/2}}{(1 + a)^Z} \right] \qquad (2.2.43)$$

In 1969 Larsen [25], for wide and constant depth channels, he applied the logarithmic velocity distribution to the subsections which is given by

$$U_i(y) = 2.5\ V_{*i}\ \ell n \frac{30}{k_i} y_i,\ i = 1,2 \qquad (2.2.44)$$

where y_i is the distance from the boundary of A_i

k_i is the roughness of the boundary

v_{*i} is the shear velocity of A_i.

By evaluating the common maximum velocity and the mean velocities for both sections, together with the Manning equation applied to A_1 and A_2, he came up with a hydraulic division ratio expression of Y_1/Y_2.

$$\frac{Y_1}{Y_2} = \left[\frac{\ell n\frac{30}{k_2} Y_2 \ (\ell n\ \frac{30}{k_1} Y_1 - 1)\ n_1}{\ell n\ \frac{30}{k_1} Y_1 \ (\ell n\frac{30}{k_2} Y_2 - 1)\ n_2} \right]^{3/2} \qquad (2.2.45)$$

which, together with the continuity equation and the Manning equation applied to A_t, A_1 and A_2 yields

$$n_t = \left[\frac{0.63 \left(\frac{Y_2}{Y_1} + 1\right)^{5/3}}{\frac{Y_2}{Y_1}^{5/3} \quad \frac{1}{n_2} + \frac{1}{n_1}} \right] \quad (2.2.46)$$

The quantity $\frac{Y_1}{Y_2}$ can be expressed as a function of n_i and $(\frac{30}{k_i})Y_i$ by Eq. (2.2.45). For the practical ranges of k_i and Y_i, the expression $\ell n\ (\frac{30}{k_i})Y_i$ is usually greater than unity and Y_1/Y_2 is only a function of n_1/n_2. Thus n_t/n_2 can be related to n_1/n_2 by Eq. (2.2.45) and (2.2.46).

In 1972 Krishnamurthy and Christensen [24] presented a paper on the equivalent roughness coefficient of a wide channel. They assumed that the channel is so wide and shallow that the side wall effect can be neglected. The channel is subdivided into segments as in Fig. 2.2.4 . Through the continuity equation, the discharge, ΔQ, in any subdivided section is expressed as,

$$(\Delta Q)_i = (V_{mean})_i\ (Y_i)\ (P_i),\ i = 1,2,3,\ldots N \quad (2.2.47)$$

The logarithmic velocity distribution $U(y)_i$, at any distance y from the bed and the roughness expressed in terms of hydraulic roughness k is

$$\left(\frac{U(y)}{V_*}\right)_i = 8.48 + 2.5\ \ell n\ \left(\frac{Y}{k}\right)_i,\ i = 1,2,3,\ldots N \quad (2.2.48)$$

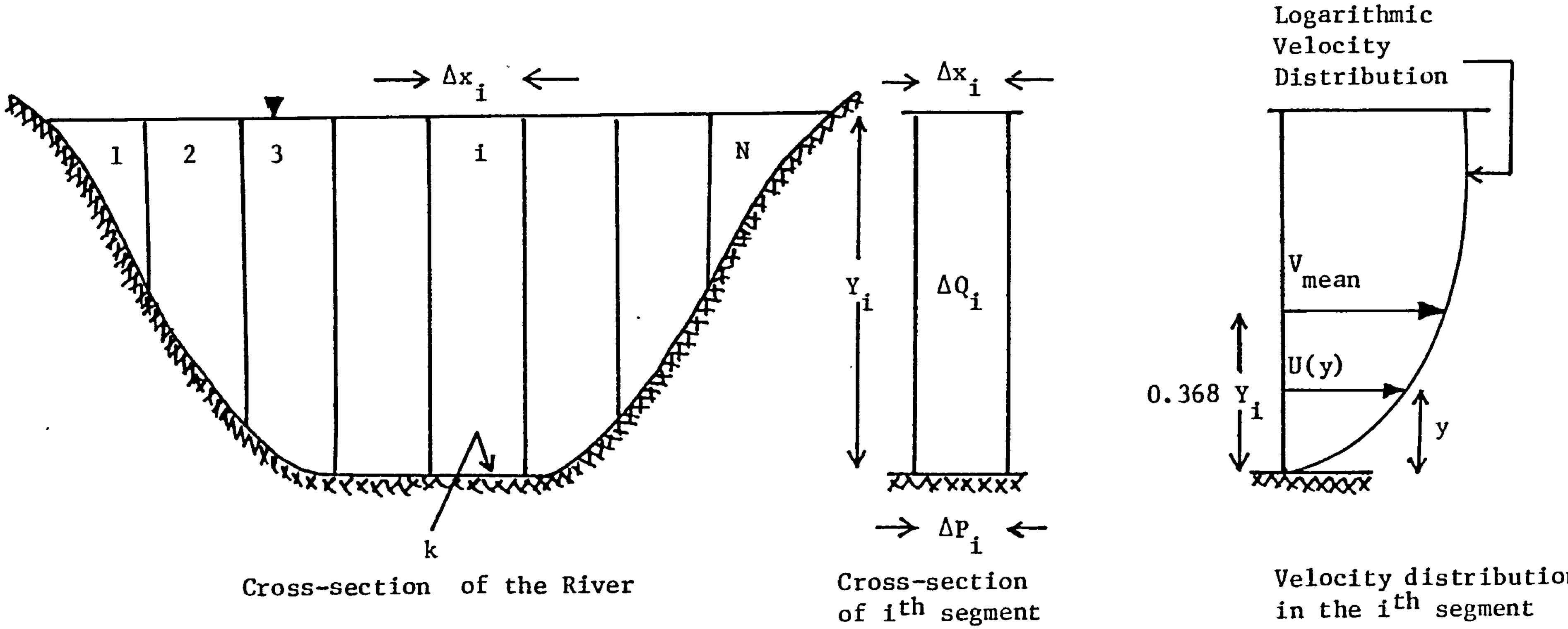

Fig. 2.2.4 Cross-Section and Velocity Distribution at River Section (After Krishnamurthy and Christersen [24]).

where V_* is the shear velocity

k is the hydraulic roughness, $k = \left(\frac{n}{0.0342}\right)^6$

By using the assumption that the mean velocity occurs at a distance of 0.368 Y_i from the bed, and the sum of partial discharges equals to the total discharge, the equivalent roughness expression is,

$$n_t = \exp \left[\frac{\sum_{i=1}^{N} P_i Y_i^{3/2} \ell n \, n_i}{\sum_{i=1}^{N} P_i Y_i^{3/2}} \right] \qquad (2.2.49)$$

It is noted that Eq. (2.2.49) cannot be applied to rectangular channel sections and also covered channels.

In 1981 Lau and Krishnappan [26] presented a paper of an ice cover and its effect on stream discharge and flow mixing. They adopted the "k-e" turbulence model described by Launder and Spalding [27] to calculate the depth, velocity distribution, and turbulent eddy viscosity ν_t distribution for the given discharge, bed slope and boundary roughnesses. These results are then used in the two-dimensional mass transport equation for simulation. The final solution gives some indications of the effects of an ice cover on the flow and on the vertical mixing.

For steady, two dimensional channel flow, the equations of continuity, momentum and the transport equation for k and e take the following forms:

$$\frac{\partial U}{\partial x} + \frac{\partial V}{\partial y} = 0 \qquad (2.2.50)$$

$$\frac{\partial U^2}{\partial x} + \frac{\partial UV}{\partial y} = \frac{\partial}{\partial y}\left(\nu_t \frac{\partial U}{\partial y}\right) + gS_o - g\frac{dY}{dx} \qquad (2.2.51)$$

$$\frac{\partial Uk}{\partial x} + \frac{\partial Vk}{\partial y} - \frac{\partial}{\partial y}\left(\frac{\nu_t}{\sigma_k}\frac{\partial k}{\partial y}\right) + G - e \qquad (2.2.52)$$

$$\frac{\partial Ue}{\partial x} + \frac{\partial V}{\partial y} = \frac{\partial}{\partial y}\left(\frac{\nu_t}{\sigma_e}\frac{\partial e}{\partial y}\right) + C_1\frac{e}{k}G - C_2\frac{e^2}{k} \qquad (2.2.53)$$

$$\frac{\partial U\phi}{\partial x} + \frac{\partial V\phi}{\partial y} = \frac{\partial}{\partial y}\left(\frac{\nu_t}{\sigma_\phi}\frac{\partial \phi}{\partial y}\right) + S_\phi \qquad (2.2.54)$$

The coordinate system is shown in Fig. 2.2.5 where U, V are the velocity components in the x and y directions respectively.

Y is the flow depth

S_o is the channel bed slope.

σ_k, σ_e, σ_ϕ, C_1 and C_2 are empirical constants

e is rate of dissipation of turbulent energy

k is kinetic energy of turbulent motion

G is turbulent energy production by the mean motion ,

$$G = \nu_t \left[\left(\frac{\partial U}{\partial y}\right)^2 + 2\left(\frac{\partial V}{\partial y}\right)^2 \right]$$

ϕ is a scalar quantity such as concentration in mass transfer.

S_ϕ is the volumetric source rate of ϕ.

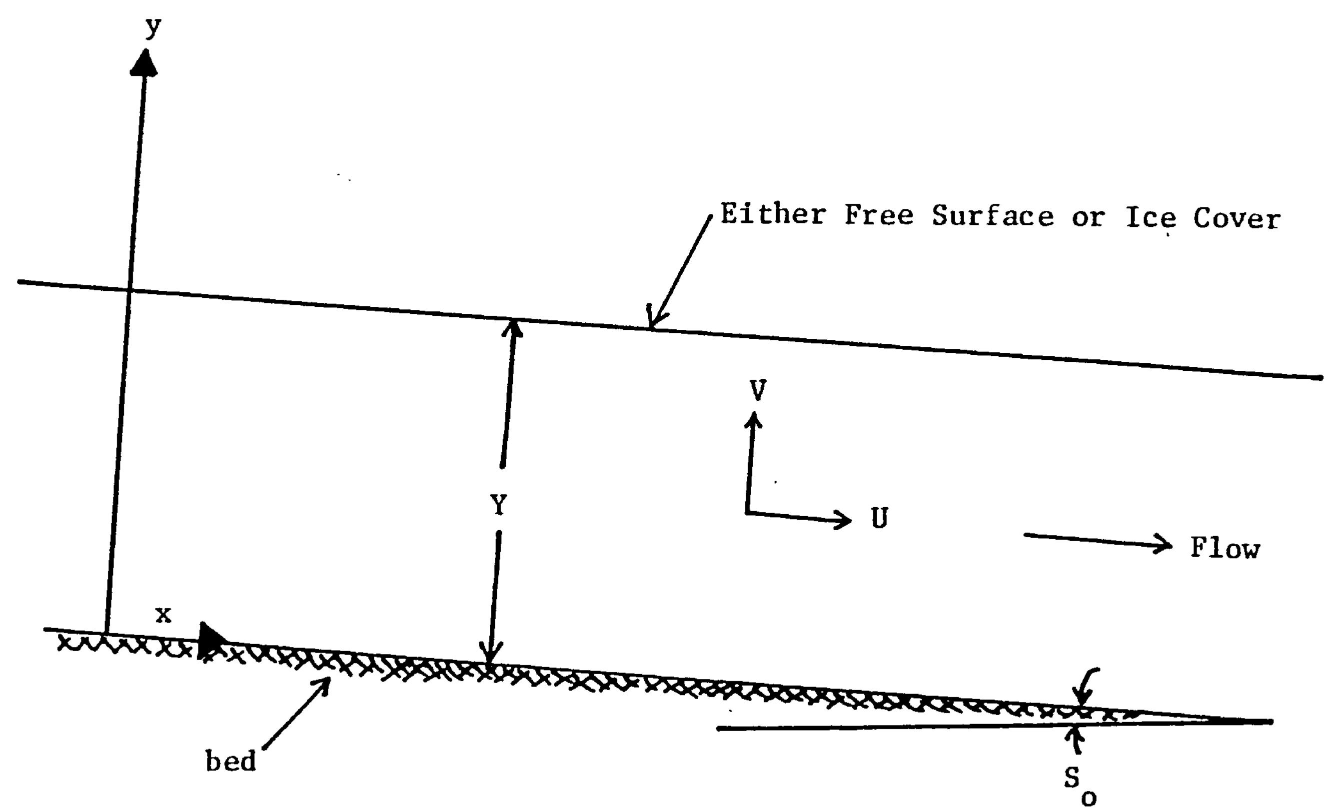

Fig. 2.2.5 Co-ordinate System (After Lau and Krishnappan [26].)

The governing equations listed in the foregoing are derived with the assumption that the flow is predominantly along the x-direction, and that the turbulent transports U, k, e and ϕ are negligible in that direction.

For the numerical scheme, the one which was proposed by Patankar and Spalding [37] is adopted. The forms of the above governing equations are such that one single numerical scheme can be used to solve all of them. An implicit form of the finite difference equations of Eq. (2.2.54) are arrived at by integrating the differential equation term by term over small control volumes.

The result shows that, the computed velocity and eddy viscosity distributions do not follow the logarithmic and parabolic distributions for the whole depth of flow. The vertical mixing rates is larger in the case of free surface flow than in ice-covered flows, due to the difference in the eddy viscosity between the two. The final computed energy slope S_o and the flow depth Y can be used to define the equivalent roughness coefficient through the application of Manning's equation.

2.3 Shape Effects on Channel Resistance

Prediction of discharge through a channel depends directly upon an accurate prediction of the resistance coefficient. One of the major governing factors is the channel geometry. Although the shape effects of the channel cross-section have received considerable attention from hydraulic engineers for many years, yet their results cannot be generalized. Some of the techniques previously used to deal with this problem are reviewed and their shortcomings are discussed.

In 1967 Marchi [30] presented a paper to show the validity, for the calculation on friction factor in open channels, of formulae analogous to those of circular pipes and also taking into account the influence of cross-sectional shape and the free surface.

By combining the "velocity-defect law" and the "logarithmic velocity law," the velocity distribution along normals to the side wall can be represented by,

$$\frac{U(y)}{\bar{V}_*} = \frac{1}{\kappa} \ln \eta_* + F(\eta_*, \xi_*) + \frac{V_{max}}{\bar{V}_*} \qquad (2.3.1)$$

in which

$\bar{V}_* = \sqrt{\bar{\tau}_o/\rho}$ the mean shear velocity,

$V_* = \sqrt{\tau_o/\rho}$ the local shear velocity

$\xi_* = \dfrac{V_*}{\bar{V}_*}$ the ratio between local shear velocity and mean shear velocity

$\eta_* = \dfrac{y}{Y}$ is the depth ratio from the boundary

$F(\eta_*, \xi_*)$ is a function which is equal to zero for $\eta_* = 1$, and becomes independent of η_* for small values of η_* $(\eta_* \rightarrow \frac{\delta}{Y})$, where δ is the thickness of the laminar sublayer, κ is the Von Karman constant

According to Eq. (2.3.1), the wall has a sensible influence on the value of the velocity which represents the beginning of the turbulent distribution, that is on the value of U(y) for $y = \delta$ in the smooth flow, but it has a negligible action on the variation of $(U(y)/\overline{V}_*)$ as the y increases. By using the experimental data observed by Tracy [43] on closed conduits and by Nikuradse [34] and Marchi [29] on open channels, Eq. (2.3.1) becomes, for smooth flow,

$$\frac{U(y)}{\overline{V}_*} = a \log \frac{y\overline{V}_*}{\nu} + F_S\ (\eta_*,\ \xi_*) \qquad (2.3.2)$$

and for fully rough flow (in conduits with a sand roughness ε),

$$\frac{U(y)}{\overline{V}_*} = a \log \frac{y}{\varepsilon} + F_r\ (\eta_*,\ \xi_*) \text{ with } a = 2.30/\kappa \qquad (2.3.3)$$

The integration over the cross-section of the velocity given by Eq. (2.3.2), (2.3.3) together with the Chezy relation, yields the following resistance equations:

For smooth channels

$$C = a \log \frac{N_R}{L} + a'_S \qquad (2.3.4)$$

in which

C is Chezy's coefficient for the channel

N_R is the Reynolds number $\frac{4RV}{\nu}$ and L is a constant unit length and the a'_S is an experimental coefficient.

For rough channels,

$$C = a \log \left(\frac{4R}{\varepsilon}\right) + a'_r \qquad (2.3.5)$$

where

a'_r is an experimental coefficient

ε is the sand roughness.

By assuming that the shear velocity distribution is a function of only the section shape, different from open to closed sections, but independent for the regime of turbulent flow, and with ψ a sectional shape coefficient which is introduced into Eq. (2.3.4), (2.3.5), yields:

For smooth boundary flow,

$$C = 5.75 \log \left(\frac{\psi N_R}{L}\right) \qquad (2.3.6)$$

For fully rough boundary flow,

$$C = 5.75 \log \left(\frac{13.3\ \psi R}{\varepsilon}\right) \qquad (2.3.7)$$

and for the transition region

$$C = 5.75 \log \left(\frac{L}{\psi N_R} + \frac{\varepsilon}{13.3 \psi R}\right) \qquad (2.3.8)$$

in which ψ is the shape factor which has to be determined experimentally.

In 1973 Yen and Overton [46] presented their study on the shape effects on the resistance in flood plain channels.

By assuming that secondary flow is non-existent both in laminar and turbulent flow, the equation of motion for a cross-section shown in Fig. 2.3.1 can be written as,

$$\frac{\nu V}{gb^2(-h_x)} \left(\frac{\partial^2 U_1}{\partial y_1^2} + \frac{\partial^2 U_1}{\partial z_1^2}\right) = 1 \qquad (2.3.9)$$

in which

$U_1 = \frac{u}{V}$; u is the local velocity at point (y,z), V is the mean velocity over the cross-section.

$y_1 = \frac{y}{b}$, $z_1 = \frac{z}{b}$ and $h_x = \frac{\partial h}{\partial x}$, peizometric head gradient in the flow direction.

In solving Eq. (2.3.9) for velocity distribution, the numerical method of relaxation was used, then, the boundary shear stress is computed from velocity gradient at various points on the boundary. By integrating the velocity over the entire cross-section and the shear stress over the wetted perimeter, the average velocity and average boundary shear stress were obtained. The Darcy-Weisbach resistance coefficient was then evaluated for various flow stages.

For resistance evaluation, the method suggested by Overton [36] was used to produce a resistance coefficient and an associated effective channel boundary for the channel cross-section. The effective channel boundary is an imaginary surface located at a distance of e from the actual

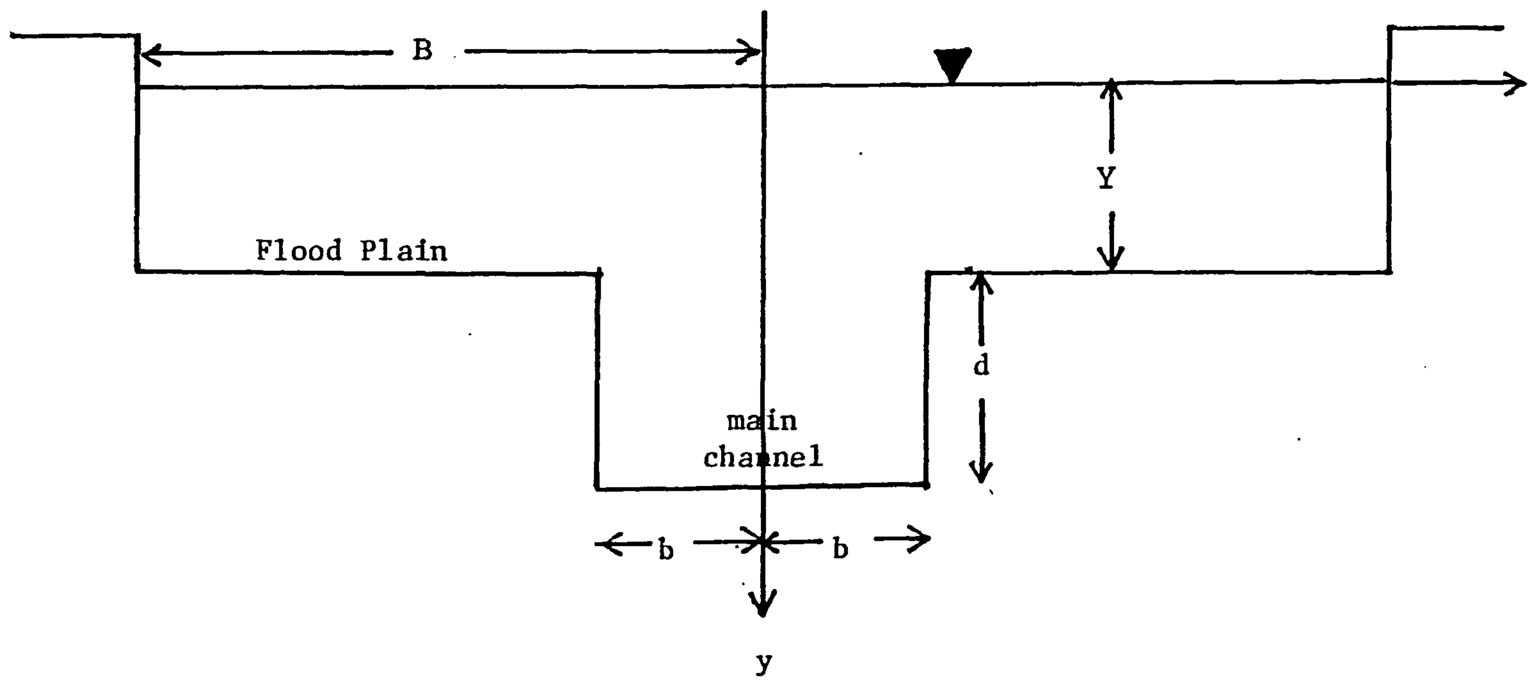

Fig. 2.3.1 Definition Sketch of Flood Plain Channel Cross-Section (After Yen and Overton [46]).

channel boundary.

By assuming that the Manning n-value for the channel is considered to be independent of the channel slope S_o, then, the following proportionality holds;

$$Q/\sqrt{S_o} \sim AR^{2/3} \tag{2.3.10}$$

where

Q is the total flow rate

A is the effective flow area

R is the effective hydraulic radius.

If $Q/\sqrt{S_o}$ is plotted versus the $AR^{2/3}$ term on a linear graph paper, the slope of the line of best fit would be equal to $1.49/n_t$, when using imperial units provided that the line intersects the origin. Since $AR^{2/3}$ is a function of e, the e value was chosen so that the line of best fit would pass through the origin. The objective fitting function such as the linear least squares can be used to solve the problem. The Manning n-value is calculated as,

$$n_t = 1.49 \frac{\Sigma\alpha_1^2 - \bar{\alpha}_1\Sigma\alpha_1}{\Sigma K_1\alpha_1 - \bar{K}_1\Sigma\alpha_1} \tag{2.3.11}$$

and the equation for the zero intercept is

$$\bar{K}_1 - \frac{1.49\ \bar{\alpha}_1}{n_t} = 0 \tag{2.3.12}$$

in which

K_1 is $Q/\sqrt{S_o}$ (2.3.13a)

α_1 is $AR^{2/3}$ (2.3.13b)

and the bar signifies the mean of observed values.

By eliminating n_t from Eq. (2.3.11) (2.3.12) yields

$$\overline{K}_1 \ \Sigma\alpha_1^2 \ - \ \overline{\alpha}_1 \ \Sigma K_1 \ \alpha_1 = 0 \qquad (2.3.14)$$

Since α_1 is a function of e, Eq. (2.3.14) can be written as,

$$\text{Funct (e)} = 0 \qquad (2.3.15)$$

Finally, the Newton-Raphson method is used to solve for e and n_t.

In 1979 Hey [19] presented a paper on the influence of shape factor on the resistance to uniform flow in straight gravel-bed rivers and derived a standardized approach for the estimation of flow resistance.

By adopting the Colebrook-White equation in its general terms,

$$\frac{1}{\sqrt{f}} = C_1 \log \left(\frac{aR}{k}\right) \qquad (2.3.16)$$

in which

$a = 10^{(E\kappa/2.30)}$, $C_1 = 2.30/(\kappa.\sqrt{8})$

E is a coefficient

κ is the Von Karman constant

k is the roughness height of the surface

f is the Darcy-Weisbach friction factor.

Various cross-sectional shapeswere evaluated to determine the relation between shape effects and the coefficient 'a' as in Eq. (2.3.16). A unique relation was found between R/Y the radius-depth ratio and 'a', where Y is the perpendicular distance from the perimeter to the point of maximum velocity; usually, it is the maximum flow depth unless flow width/ depth ratio is very small. He transformed a variety of channel cross-sections to their equivalent plane surface Fig. 2.3.2.a,b . Assuming that the flow is two-dimensional and provided the roughness heights, hydraulic radii, and slopes are the same in each case, the smaller the ratio of R/Y, the higher the average velocity. Since proportionately more of their flow area is at a distance greater than R from the solid boundary. As the flow resistance declines with R/Y, it implies that the coefficient 'a' is inversely related to R/Y. In order to evaluate the flow resistance of the channel, it is necessary to standardize the roughness height of the banks to that of bed material. This is achieved by reducing the effective hydraulic length of the bank, if the bed is rougher than the bank and the reverse, to obtain a common velocity gradient in the bed and bank flow areas, Fig. 2.3.2b . The effective hydraulic radius of the section can then be defined for use in the Colebrook-White equation Eq. (2.3.16)

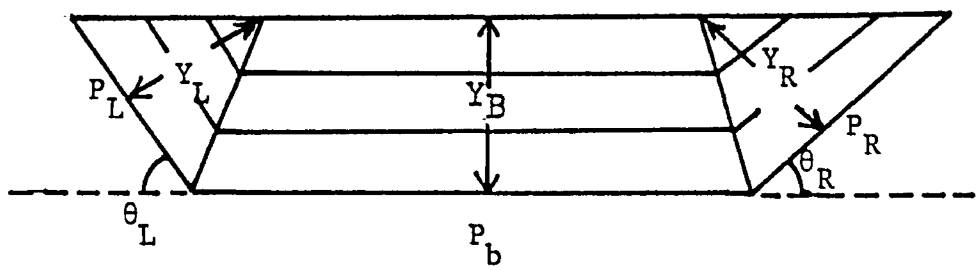

(a)

Idealized Distribution, Uniform
Shear Stress and 2D Flow

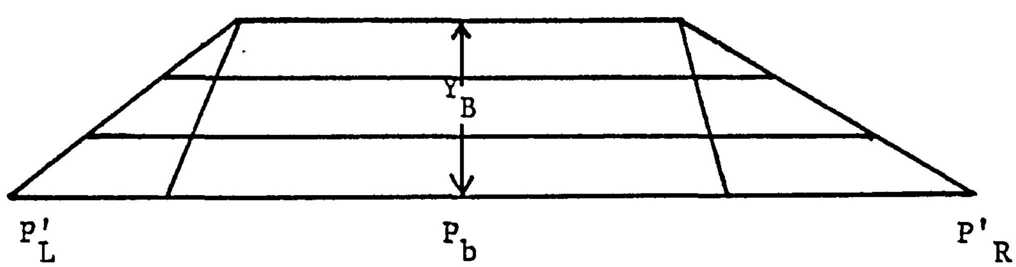

(b)

Transformed Distribution,
Standardized Velocity Gradients

Fig. 2.3.2.a,b Velocity Distribution in Trapezoidal Channel with Differing Bed and Bank Roughness (After Hey [19]).

By equating the wall flow areas in Fig. 2.3.2a and Fig. 2.3.2b , the effective wetted perimeter of the left and right banks are

$$P'_L = \frac{Y_L}{\text{Sin } \theta_L} \qquad (2.3.17)$$

$$P'_R = \frac{Y_R}{\text{Sin } \theta_R} \qquad (2.3.18)$$

the effective hydraulic radius will be

$$R' = A/P' \qquad (2.3.19)$$

where $P' = P_b + P'_L + P'_R$ is the effective wetted perimeter. Thus the flow resistance of the sections can be defined by using the effective hydraulic radius R' in Eq. (2.3.16).

In 1979 Kazemipour and Apelt [22] developed a method for dealing with shape effect from considerations of dimensional analysis and using the experimental data of previous investigators. The method employs parameters more representative of the effect of cross-sectional shape on flow resistance in open channels. The shape factor developed is

$$\psi = \psi_1/\psi_2 \qquad (2.3.20)$$

where ψ_1 is equal to $\sqrt{P/B}$, (P is the wetted perimeter, B is the width of the channel), reflects the effects of non-uniform distribution of shear stress on the boundary as the shape of cross-section departs from an infinitely wide channel and ψ_2 is a function of the width/average depth or aspect ratio of the cross-section. With this ratio, the value of ψ_2 can be obtained from the dimensionless plot of Tracy and Lester's and Shih and Grigg's experimental data [22].

The shape factor ψ can then be defined by Eq. (2.3.20). If the flow is in the smooth or transitional turbulent region, the adjusted channel friction factor f_* can be obtained from

$$\frac{1}{\sqrt{f_*}} = -2 \log \left(\frac{k_s}{14.84R} + \frac{2.51}{N_R\sqrt{f_*}}\right) \qquad (2.3.21)$$

where $N_R\sqrt{f_*} = (128R^3 g S_o/(\nu^2\psi))^{1/2}$ (2.3.22)

k_s is Nikuradse's sand roughness size

R is the hydraulic radius

N_R is the Reynolds number

ν is the kinematic viscosity

g is the acceleration due to gravity.

If the flow is in the fully rough turbulent region, the f_* will be obtained from

$$\frac{1}{\sqrt{f_*}} = 2 \log 14.84\ (R/k_s) \qquad (2.3.23)$$

The final friction factor f_c for the channel is obtained from

$$f_c = \psi f_* \qquad (2.3.24)$$

In any specific case, it may be necessary to complete a preliminary trial calculation in order to determine the smooth or fully turbulent regime.

In 1980 Chee, Haggag and Wong [6] presented a paper on the influence of channel shape on the conveyance capacity of streams.

By using the Reynolds form of the Navier-Stokes equation in two dimensional flow, the Prandtl-Von Karman mixing length theory, they came up with an equation which described the composite roughness of a covered channel

$$\frac{n_1}{n_t} = (\alpha+(1-\alpha)\lambda)^{-5/3} \; (\alpha+(1-\alpha)\frac{n_1}{n_2}\lambda^{5/3}) \qquad (2.3.25)$$

where

n_1 is the channel roughness

n_2 is the covered roughness

n_t is the composite roughness

λ is the hydraulic radius ratio R_2/R_1

α is the wetted perimeter ratio P_1/P

From observations in the laboratory for seven different channel shapes, they developed the shape factor ϕ such that,

$$\phi = n/n_t \qquad (2.3.26)$$

in which n is the measured composite roughness of the channel. From the plot of ϕ versus the Reynolds number N_R, an expression which related the shape factor to the Reynolds number can be obtained as

$$\phi = \left(\frac{3200}{N_R}\right)^{1.75} + C_1 \qquad (2.3.27)$$

in which C_1 is an experimental constant for different channel configurations [6], N_R is the Reynolds number.

2.4 Secondary Flow in Open Channel

Flow in noncircular channels of finite width has received considerably more attention to their motion pattern than channels with other shapes. The complexity of the channel configuration requires an additional dimension for its description. Irregularities in mean velocity distribution can be explained by reference to a system of secondary motions or superposed circulations in the plane of the conduit cross-section. Since these irregularities are not present in laminar motion, irrespective of boundary form, or in turbulent flow within circular pipes, it is usually concluded that the secondary motions are connected to the turbulent fluctuations in non-circular conduits.

Very few laboratory studies of this type of flow have been reported; J. Nikuradse [35], L. Howarth [20], H. A. Einstein and H. Li [14] are those among the earliest investigators. The result of their studies concluded that secondary currents may be expected to occur in open channel turbulent flows.

In 1961 Taylor [42] carried out exploratory studies on open channel flow over boundaries of laterally varying roughness. The laboratory work was done in a tilting rectangular flume with plywood for the smooth half of the bottom, and nominal one inch filter gravel for the rough half. Observations were made both for the determination of overall friction factors of different bed types as well as detailed velocity traverses which were necessary to determine the distribution of flow and existence of secondary currents.

The recorded velocity distributions show displacement of equal velocity curves toward corners of the cross-section, and the occurrence of the thread of maximum velocity, in open channel flow, at a point below the free surface. These features are thought to be the result of a pronounced system of secondary circulation. Although Taylor had not derived any mathematical model for solving the enigma of secondary circulation, yet the presentation of his results provided good evidence for the existence of secondary circulation in open channel flow.

In 1965 Tracy [43] presented a paper on "Turbulent Flow in a Three-Dimensional Channel." By examining the flow regions, he assumed that the condition of steady flow removes the dependency of any time averaged quantity on time; the condition of uniform motion causes the mean values of the fluctuating quantities to be independent of the x-direction;

the viscous terms of the equations of motion are insignificant in fully developed turbulence flow. For these conditions, the equations of motion become

$$V\frac{\partial U}{\partial y} + W\frac{\partial U}{\partial z} = -\frac{1}{\rho}\frac{\partial \bar{P}}{\partial x} - \left(\frac{\partial \overline{uv}}{\partial y} + \frac{\partial \overline{uw}}{\partial z}\right) \qquad (2.4.1)$$

$$V\frac{\partial V}{\partial y} + W\frac{\partial V}{\partial z} = -\frac{1}{\rho}\frac{\partial \bar{P}}{\partial y} - \left(\frac{\partial \bar{v}^2}{\partial y} + \frac{\partial \overline{vw}}{\partial z}\right) \qquad (2.4.2)$$

$$V\frac{\partial W}{\partial y} + W\frac{\partial W}{\partial z} = -\frac{1}{\rho}\frac{\partial \bar{P}}{\partial z} - \left(\frac{\partial \overline{vw}}{\partial y} + \frac{\partial \bar{w}^2}{\partial z}\right) \qquad (2.4.3)$$

and the equation of continuity is

$$\frac{\partial V}{\partial y} + \frac{\partial W}{\partial z} = 0 \qquad (2.4.4)$$

where x, y, z are the coordinate system referred to Fig. 2.4.1

U, V, W are mean velocities parallel to x, y, z directions respectively.

u, v, w are instantaneous values of velocities fluctuations parallel to the x, y, z

ρ is the fluid density.

By differentiating Eq. (2.4.2) with respect to z and Eq. (2.4.3) with respect to y, then, subtracting one from the other, and combining it with the continuity equation, Eq. (2.4.4), the equations yield:

$$W\frac{\partial \xi_R}{\partial z} + V\frac{\partial \xi_R}{\partial y} = \frac{\partial^2 \overline{vw}}{\partial z^2} - \frac{\partial^2 \overline{vw}}{\partial y^2} + \frac{\partial^2}{\partial y \partial z}(\bar{v}^2 - \bar{w}^2) \qquad (2.4.5)$$

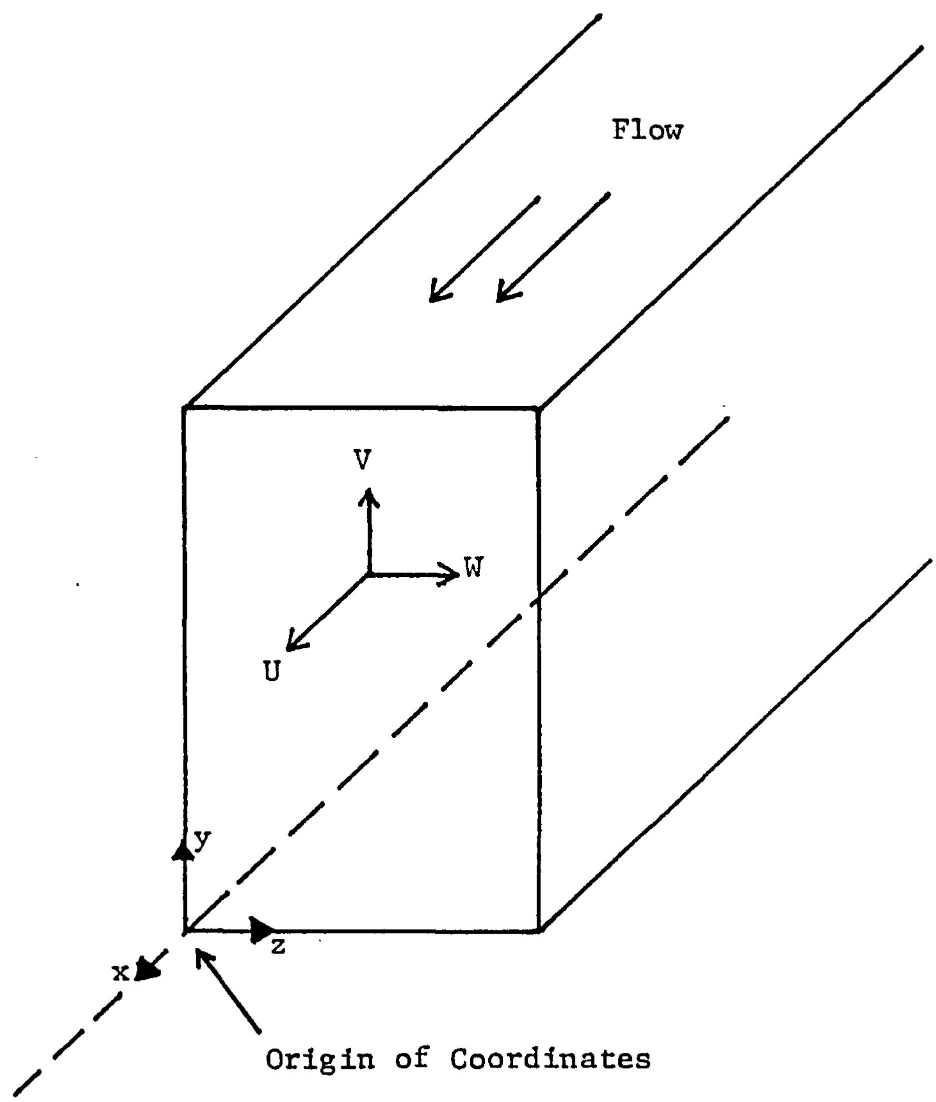

Fig. 2.4.1 Orientation of Test Channel (After Tracy [43]).

in which

$$\xi_R = \frac{\partial W}{\partial y} - \frac{\partial V}{\partial z} \qquad (2.4.6)$$

The quantity ξ_R is a measure of the rotation of a fluid particle about an axis normal to the y-z plane. The magnitudes of the normal stress terms $\overline{v}^2$ and $\overline{w}^2$ of the Eq. (2.4.5) are functions of the Reynolds number of the mean flow, the space coordinates of the point at which they were measured, and the shape boundary roughness of the channel. They are physically significant as additional normal or pressure forces superposed on an elementary particle as a result of the turbulence of the motion. It is therefore, reasonable to speculate that the secondary motions are sustained as a result of an imbalance in these forces.

A sufficient condition for the existence of the motions is the existence of nonzero values of $\overline{v}^2$ and $\overline{w}^2$ of Eq. (2.4.5). Since the symmetry condition of uniform flow in circular pipes will prevent the above condition to exist, thus secondary motions are not present in circular sections.

In 1981 Chiu and Hsuing [10] based on their earlier papers [7][8][9] dealing with various aspects of three-dimensional mathematical modeling of open channel flow, developed some relations and interactions among the secondary flow, shear stress distribution, and sediment concentration in alluvial channels. The analysis uses the framework of a curvilinear system consisting of isovels (equal velocity curves) of primary flow (measured or computed local velocities), marked as ξ curves and their orthogonal trajectories marked as η curves(Fig. 2.4.2). The equations for ξ and η can be written as

$$\xi = \left(\frac{x_2}{Y}\right) \left[\left(1 - \frac{|x_3|}{B_i}\right) e^{|x_3|/B_i} \right]^{\beta i} \qquad (2.4.7)$$

$$\eta = \left(\frac{x_2}{Y}\right)^2 + \frac{2B_i^2}{Y^2 \beta_i} \left(\ell n \frac{|x_3|}{B_i} - \frac{|x_3|}{B_i}\right) \qquad (2.4.8)$$

in which Y is the water depth at the x_2 axis

B_i; i = 1,2 are the transverse distances on the water surface between the x_2-axis and either the left or right bank of a cross-section;

ξ_o and β_i = empirical coefficients.

By applying the momentum equation in the x_1 direction in the ξ-η coordinate system directly gives the ξ component of the secondary flow.

$$V_\xi = \left(\frac{\rho}{h_\xi} \frac{\partial V_1}{\partial \xi}\right)^{-1} \left[-\rho \frac{\partial V_1}{\partial t} - \rho V_1 \frac{\partial V_1}{\partial x_1} - \frac{\partial}{\partial x_1} (\rho g H) + \frac{\partial \sigma_1}{\partial x_1} + \frac{1}{h_\xi} \frac{\partial \tau_{\xi 1}}{\partial \xi} + \frac{1}{h_\xi h_\eta} \frac{\partial h_\eta}{\partial \xi} \tau_{\xi 1} \right] \qquad (2.4.9)$$

while the continuity equation gives the η component of the flow

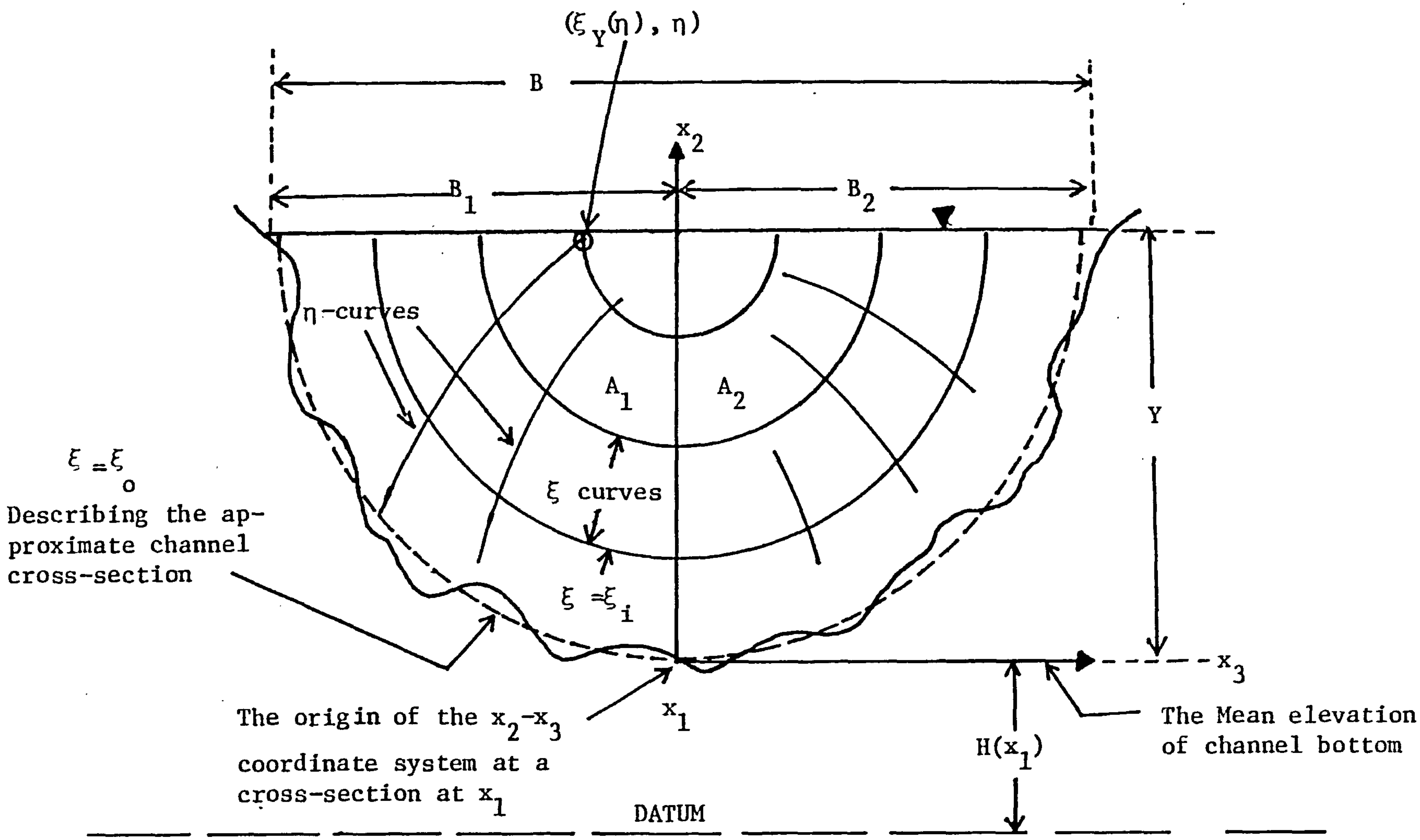

Fig. 2.4.2 Curvilinear Coordinate System (After Chin and Hsuing [10]).

$$V_\eta = -\frac{1}{h_\xi}\int_{\eta^*}^{\eta} \left(h_\xi h_\eta \frac{\partial V_1}{\partial x_1} + h_\eta \frac{\partial V_\xi}{\partial \xi} + V_\xi \frac{\partial h_\eta}{\partial \xi}\right) d\eta + V_\eta\Big|_{\eta=\eta^*}$$

(2.4.10)

in which h_ξ and h_η are the scale factors on the ξ and η curves

ρ is the fluid density

t is the time

V_1 is x_1 component of flow velocity

g is the gravitational acceleration

H is the mean elevation of the bottom of a transverse cross-section of open channel

$V_\eta{}^*$ is the value of V_η at a boundary point in which $\eta = \eta^*$

$\tau_{\xi 1}$ is the shear stress in the x_1 direction in the plane perpendicular to the ξ direction

σ_1 is the normal stress in the x_1 direction.

To compute secondary currents, Eq. (2.4.9) can be used first at every grid point of the ξ-η coordinate network to obtain V_ξ, the other component V_η can be obtained by integrating Eq. (2.4.10) along each ξ curve starting from a boundary point (point at water surface).

By re-arrangement of Eq. (2.4.9) and applying it to the bed boundary ($\xi_i = \xi_o$), for steady uniform flow in the x_1 direction, the equation for the shear stress in x_1 direction in plane perpendicular to ξ direction can be written as,

$$\tau_{\xi 1}(\xi_i,\eta) = \frac{1}{h_\eta(\xi_i,\eta)} \left[\rho g S_o \int_{\xi_i}^{\xi_Y(\eta)} h_\xi h_\eta d\xi - \rho \int_{\xi_i}^{\xi_Y(\eta)} h_\eta V_\xi \frac{\partial V_1}{\partial \xi} d\xi \right] \qquad (2.4.11)$$

in which S_o is the energy slope. Equation (2.4.11) can be used to compute the shear stress in the flow and along the channel bed, that includes among other things, the effect of secondary flow.

In a study of bank erosion problems, Eq. (2.4.11) should be used to determine the peak values of boundary shear (drag force) that tend to occur on the side walls and on the channel bottom near the side walls. Peak boundary shear along with convection by secondary flow near the side walls should be a major mechanism responsible for bank and bed erosion of alluvial channels.

2.5 Discussion on Literature Review

Determination of the composite roughness of a covered or open channel and the related problem of predicting the shear stress exerted by the flow are of central importance to several aspects of hydraulic engineering. Hence it is not surprising that this problem has received the continued attention of engineers since the early 1930's.

Based on the foregoing discussion, it can conclude that many existing models has involved one or more fundamental shortcomings which are vital in hydraulic analysis of covered or open channel flows. Some of these shortcomings are listed as follows:

1. The assumption of equal hydraulic radii ($R = R_1 = R_2$) regardless of the boundary roughness.

2. The assumption of an infinitely wide channel ($R \approx Y$) to a finite channel.

3. The assumption of equal velocities ($V = V_1 = V_2$), which is invalidated for most finite channels.

4. By assuming uniform distribution of shear stress along the wetted perimeter.

5. By assuming no sidewall and geometric shape effect on the flow region.

6. Most models cannot handle more than two boundary roughnesses.

7. By applying one- or two-dimensional models to three-dimensional flow.

8. By assuming no secondary circulations exist in the flow region.

To be more generally applicable, a mathematical model which can deal with the complex reality of three-dimensional flow, has to be developed in order to overcome the foremen-tioned problems.

CHAPTER III

THEORETICAL ANALYSIS

3.1 Introduction

The approach used to evaluate the effects of the multiple roughness of the wetted perimeter, and channel shape on the flow and stream resistance, is presented here based on the concepts developed in the earlier research by Chee and Haggag (1977)(1976) [17]. The procedure involves the Reynolds form of the Navier-Stokes equation in two-dimensional flow together with the Prandtl-Von Karman mixing length theory to develop the velocity profile equations. Through the use of Manning's equation, the momentum equation and the defined velocity profile equations, the composite roughness equation of the channel is thus derived. The relations are then applied into a numerical model to solve for the final solution.

The model is developed in a manner that it can handle any geometric shape effects and multiple roughness condition of a channel. The cross-section of a stream is divided into segments of corresponding depth and bed configuration, such that a composite result can be obtained by numerically integrating the velocity pattern over the entire stream cross-section. Also, the friction factors which are expressed in term of Manning's roughness and Chezy's coefficient can be calibrated through this method. The results obtained from this investigation can be extended for use in prototype covered or open-channels.

3.2 Theoretical Assumptions

The following assumptions are used in derivation of the relations:

1. The channel flow cross-section is divided into vertical finite strips, Fig. 3.2.1 . For each strip, it is again sub-divided into two small sections, an upper and a lower sub-section. Both subsections exert shear on and are affected by their boundary conditions respectively.

2. The dividing surface between the upper and lower sub-sections is the locus of no shear within the flow and is also the locus of maximum velocity. The boundary between two finite strips is considered as no shear within the flow.

3. The above assumptions also hold when the channel cross-section is sub-divided into horizontal finite strips, with each strip consisting of the left and right sub-sections, corresponding to the boundary conditions on both sides of the channel.

4. In case of open channel flow, the vertical finite strip will consist only of one sub-section, which is the lower sub-section corresponding to the channel bed.

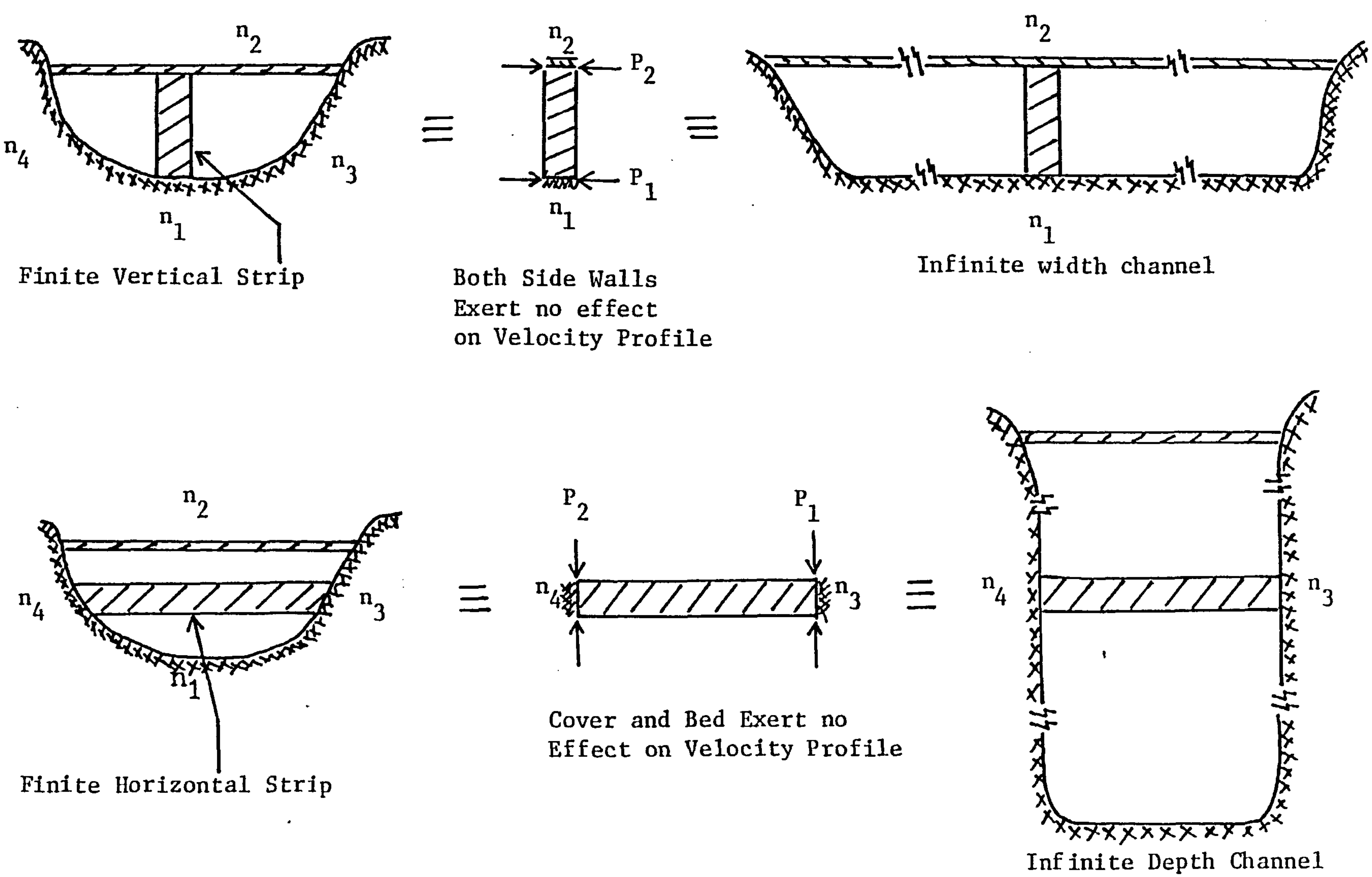

Fig. 3.2.1 Definition of Finite Vertical and Horizontal Strip Approach.

5. In the vertical strip approach, each strip is assumed to be a finite section within an infinitely wide channel, where the side walls exert no effect on that particular section. In the horizontal strip approach, each strip is assumed to be a finite section within an infinitely deep channel, where the surface and bed exert no effect on that particular section.

6. The hydraulic equations such as the continuity and Manning's equation can be applied to each finite strip separately.

7. The fluid is homogeneous, incompressible and the flow is steady and uniform.

3.3 Derivation of the Flow Equation

The derivation is based on a covered channel which is divided into two sub-sections. The division boundary line represents the locus of no shear and maximum velocity in relation to a vertical. The Reynolds form of the Navier-Stokes equation in two dimensional flow can be written as:

$$\rho\left(\frac{\partial \bar{U}}{\partial t} + \bar{V}\frac{\partial \bar{U}}{\partial y} + \bar{U}\frac{\partial \bar{U}}{\partial x}\right) = -\frac{\partial \bar{P}}{\partial x} + \frac{\partial}{\partial y}\left(\mu\frac{\partial \bar{U}}{\partial y}\right) + \frac{\partial}{\partial y}\left(-\overline{\rho U'V'}\right) + F_{ix} \qquad (3.3.1)$$

in which $\bar{U}$, $\bar{V}$ are average velocities in x and y directions;

U', V' are local velocity variations in the x and y directions;

ρ, μ are fluid density and viscosity;

$\overline{P}$ is the average pressure;

F_{ix} is the body force;

and the main flow characteristics and notations are shown in Fig. 3.3.1 and Table (3.3.1).

For the condition of steady flow, the change of the flow velocity with respect to time $\partial\overline{U}/\partial t$ will equal zero while $\overline{V}$ will vanish as it averages a random variation. And, as the flow is uniform with respect to the x-direction, both $\partial\overline{U}/\partial x$ and $\partial\overline{P}/\partial x$ will be zero.

Moreover, from Fig. 3.3.1 , the force due to gravity is the only body force which acts on the flow. This force is represented by the weight component in the x-direction. For unit volume of flow,

$$F_{ix} = \gamma \cdot \sin\theta \tag{3.3.2}$$

As θ is very small in most practical cases, the sin θ value can be substituted by the bed slope S_o and by replacing γ with ρg, Eq. (3.3.2) becomes

$$F_{ix} = \rho g S_o \tag{3.3.3}$$

Then, Eq. (3.3.1) can be simplfied as

$$\frac{\partial}{\partial y}\left(\mu \frac{\partial\overline{U}}{\partial y} - \rho\overline{U'V'}\right) = -\rho g S_o \tag{3.3.4}$$

The first term on the left side of Eq. (3.3.4), $\mu \frac{\partial\overline{U}}{\partial y}$

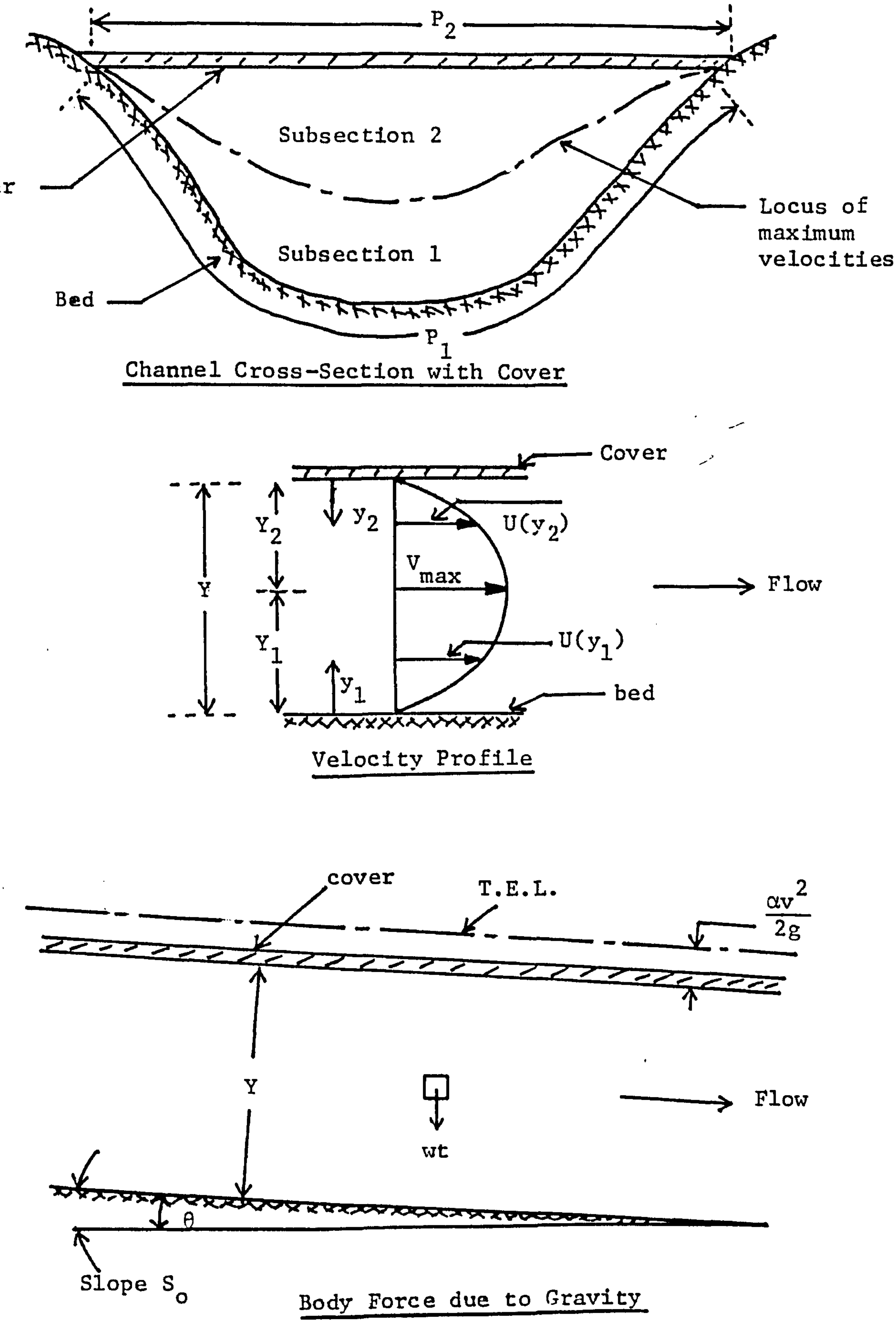

Fig. 3.3.1 Definition Sketch of Channel Cross-Section

TABLE 3.3.1

Assigned Notation

Parameter	Flow Cross-section	Channel Sub-section	Cover Sub-Section
Flow Area	A	A_1	A_2
Wetted Perimeter	P	P_1	P_2
Hydraulic Radius	R	R_1	R_2
Flow Depth	Y	Y_1	Y_2
Relative Depth Ratio	ε	ε_1	ε_2
Local Velocity	U	U_1	U_2
Mean Velocity	V	V_1	V_2
Manning's Roughness	n	n_1	n_2
Shear Stress	τ	τ_1	τ_2
Shear Velocity	V_*	V_{*1}	V_{*2}
Bed Slope	S_o	S_o	S_o

represents the laminar shear τ_L and the second term $\overline{\rho U'V'}$ represents the turbulent shear τ_t. Then Eq. (3.3.4) can also be written as

$$\frac{\partial}{\partial y} (\tau_L + \tau_t) = - \rho g S_o \qquad (3.3.5)$$

3.4 <u>The Shear Stress Distribution</u>

By integrating Eq. (3.3.5) with respect to each sub-section, the shear stress and velocity distributions can be obtained.

For the channel sub-section (1), the shear stress is given as

$$\tau_{L1} + \tau_{t1} = -\rho g S_o Y_1 + C_1 \qquad (3.4.1)$$

where C_1 is an integrating constant.

Since the upper boundary of sub-section (1) is the separation surface between the two sub-sections, which is presumed to be the locus of zero shear and lies at a distance Y_1 from the bed, therefore, when $y_1 = Y_1$, the laminar and turbulent shear will be

$$\tau_{L1} = \tau_{t1} = 0 \quad \text{When } y_1 = Y_1 \qquad (3.4.2)$$

From this boundary condition, C_1 can be obtained as

$$C_1 = \rho g S_o Y_1 \qquad (3.4.3)$$

and substituting it back to Eq. (3.4.1), yields

$$\tau_{L1} + \tau_{t1} = \rho g S_o (Y_1 - y_1) \tag{3.4.4}$$

The existence of a laminar sublayer close to the bed boundary at a very small distance of δ_1, only the laminar shear exists in this region. Therefore, when $y_1 = 0$, Eq. (3.4.4) yields

$$\tau_{01} = \tau_{L1} = \rho g S_o Y_1 \tag{3.4.5}$$

where τ_{01} is the total shear on the bed.

Since the laminar shear is very small outside the sublayer, it can be neglected from the total shear, and Eq. (3.4.4) becomes

$$\tau_{t1} = \rho g S_o (Y_1 - y_1) \tag{3.4.6}$$

where τ_{t1} describes the shear distribution between the range $Y_1 > y_1 > \delta_1$.

Similar shear stress distribution can be obtained for sub-section (2), with the changing of subscript 1 to 2 for the above expression, and they are shown as in Fig. 3.4.1

3.5 The Velocity Distribution

The velocity profiles of a channel can be obtained by employing the Prandtl-Von Karman mixing length theory. For the lower subsection (1) of a covered channel, the equation

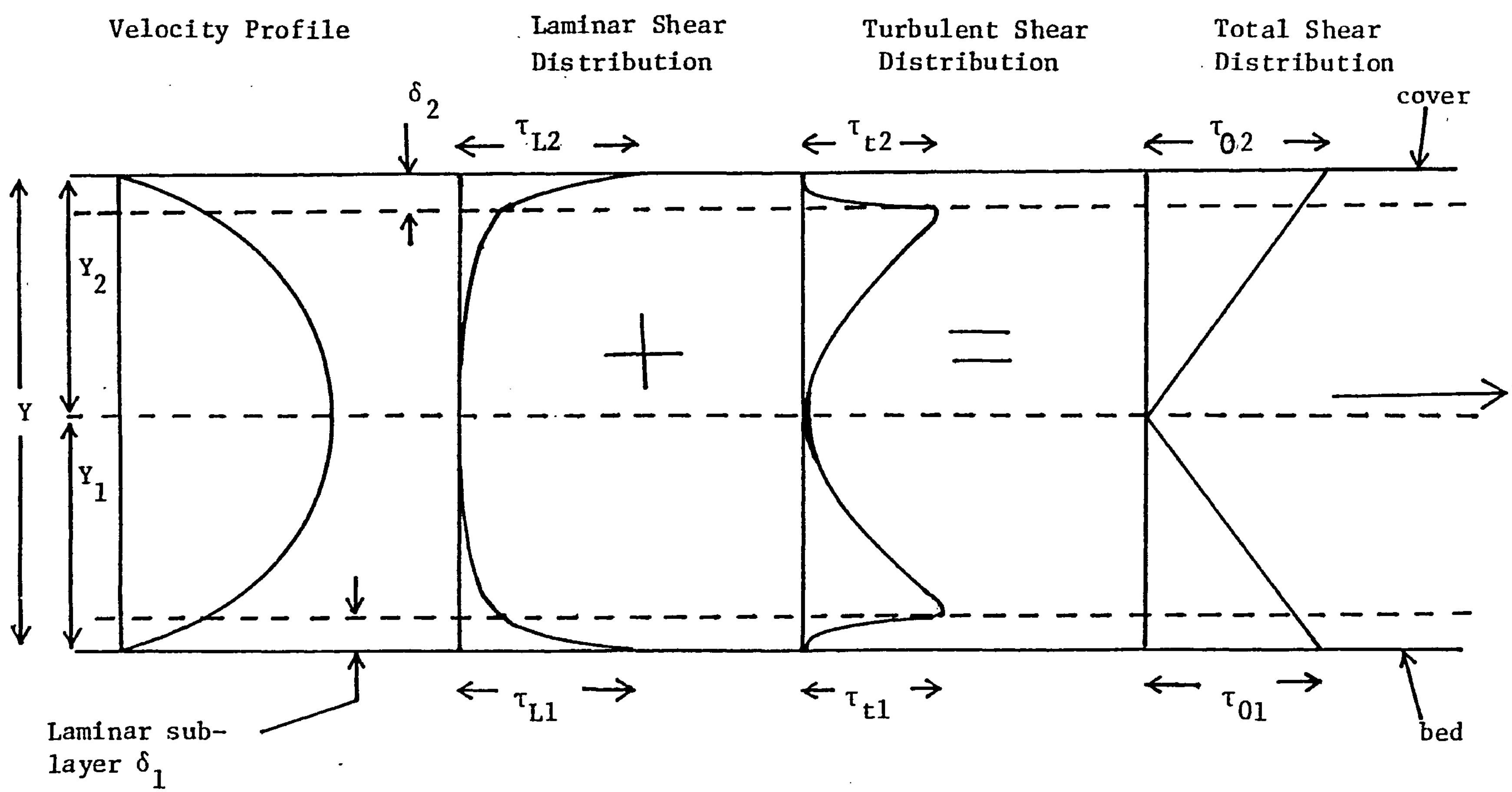

Fig. 3.4.1 Shear Stress Distributions.

is

$$\tau_{t1} = \rho\, L^2 \left(\frac{dU_1}{dy_1}\right)^2 \qquad (3.5.1)$$

where L, according to Von-Karman is defined as

$$L = \kappa y_1 \qquad (3.5.2)$$

where κ is the Von-Karman constant.

By substituting Eq. (3.5.2) into Eq. (3.5.1) gives

$$\tau_{t_1} = \rho\kappa^2 y_1{}^2 \left(\frac{dU_1}{dy_1}\right)^2 \qquad (3.5.3)$$

Combining Eq. (3.5.3) with Eq. (3.4.6) yields

$$\frac{dU_1}{dy_1} = \frac{1}{\kappa y_1} (gS_o)^{1/2} (Y_1 - y_1)^{1/2} \qquad (3.5.4)$$

which in terms of the relative depth ratio $\varepsilon_1 = \frac{y_1}{Y_1}$, becomes

$$\frac{dU_1}{d\varepsilon_1} = \frac{1}{\kappa} (gY_1 S_o)^{1/2} \frac{(1-\ \varepsilon_1)^{1/2}}{\varepsilon_1} \qquad (3.5.5)$$

Since the shear velocity of a wide channel can be expressed as,

$$V_{*1} = (gY_1 S_o)^{1/2} \qquad (3.5.6)$$

therefore, Eq. (3.5.5) becomes

$$\frac{dU_1}{d\varepsilon_1} = \frac{V_{*1}}{\kappa} \frac{(1-\varepsilon_1)^{1/2}}{\varepsilon_1} \qquad (3.5.7)$$

The velocity distribution in terms of ε_1 can be obtained by integrating Eq. (3.5.7) with respect to ε_1,

$$U_1(\varepsilon_1) = \frac{V_{*1}}{\kappa} F_1(\varepsilon_1) + C_1 \qquad (3.5.8)$$

where

$$F_1(\varepsilon_1) = 2(1-\varepsilon_1)^{1/2} - \ell n \frac{1+(1-\varepsilon_1)^{1/2}}{1-(1-\varepsilon_1)^{1/2}} \qquad (3.5.8a)$$

is a dimensionless velocity function and is shown in Fig. 3.5.1 .

By equating the mean velocity of the sub-section V_1 to the value computed from Eq. (3.5.8) and putting the relative depth $\varepsilon_1 = 1/3$, which is the location of the mean velocity in the sub-section, the constant C_1 can be obtained as,

$$C_1 = V_1 + 2/3 \frac{V_{*1}}{\kappa} \qquad (3.5.9)$$

Substituting Eq. (3.5.9) into Eq. (3.5.8) yields,

$$\frac{V_1 - U_1(\varepsilon_1)}{V_{*1}/\kappa} = -F_1(\varepsilon_1) - 2/3 \qquad (3.5.10)$$

which when simplified, gives

$$\frac{V_1 - U_1(\varepsilon_1)}{(2V_{*1}/\kappa)} = F_2(\varepsilon_1) \qquad (3.5.11)$$

in which F_2 (ε_1) is another dimensionless velocity function shown in Fig. 3.5.1 and can be expressed as

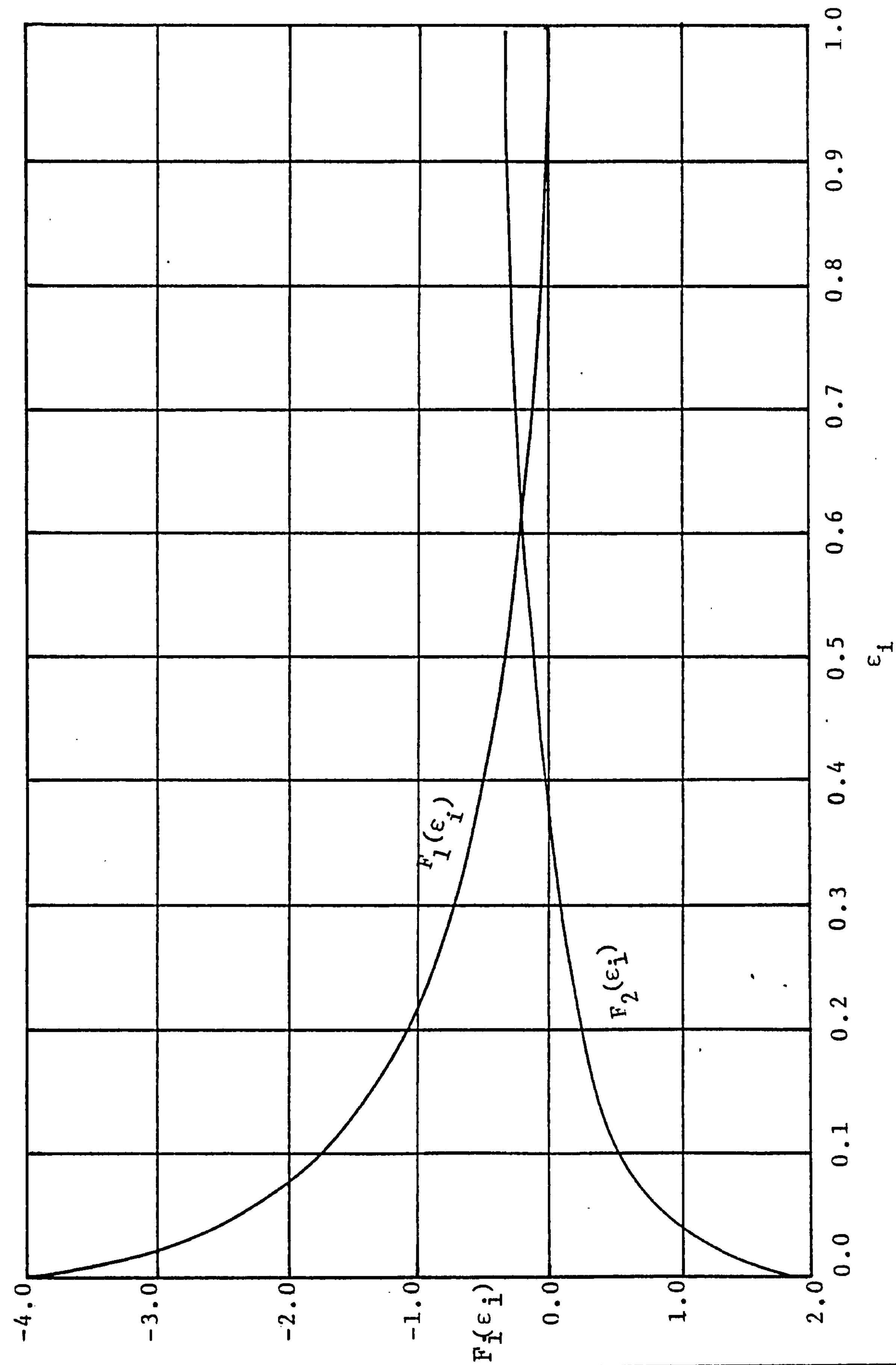

Fig. 3.5.1 Dimensionless Velocity Functions.

$$F_2(\varepsilon_1) = \ell n \frac{(\varepsilon_1)^{1/2}}{1-(1-\varepsilon_1)^{1/2}} - (1-\varepsilon_1)^{1/2} - 1/3 \qquad (3.5.12)$$

By applying another boundary condition, that is, when ε_1 equals unity, where the local velocity becomes equal to the maximum velocity and $F_1(\varepsilon_1)$ equal to zero, Eq. 3.5.8 becomes

$$U_1(\varepsilon_1) = V_{max} + \frac{V_{*1}}{\kappa} F_1(\varepsilon_1) \qquad (3.5.13)$$

Noticing that $F_1(\varepsilon_1)$ is always a negative function and when $\varepsilon_1 = 1/3$, $F_1(\varepsilon_1)$ is equal to -2/3. Putting it back into Eq. (3.5.13) gives

$$U_1(\varepsilon_1) = V_{max} - 2/3 \frac{V_{*1}}{\kappa} = V_1 \qquad (3.5.14)$$

which is the mean velocity of sub-section (1).

Similarly, the velocity equations for the upper sub-section of an covered channel can be derived as

$$U_2(\varepsilon_2) = V_{max} + \frac{V_{*2}}{\kappa} F_1(\varepsilon_2) \qquad (3.5.15)$$

or

$$\frac{V_2 - U_2(\varepsilon_2)}{(2V_{*2}/\kappa)} = F_2(\varepsilon_2) \qquad (3.5.16)$$

and the mean velocity of sub-section (2) as

$$U_2(\varepsilon_2) = V_{max} - 2/3 \frac{V_{*2}}{\kappa} = V_2, \text{ for } \varepsilon_2 = 1/3 \qquad (3.5.17)$$

Therefore, with the above equations, the velocity profile of a covered channel is completely defined.

3.6 Characteristic Equations for Velocity Distribution

The derived velocity equations show that as the boundary roughness coefficients of the two sub-sections are equal, their mean velocities will also be equal, and the maximum velocity will be located at the mid-depth of the cross-section. If the channel consists of different boundary roughness, then the difference between the two sub-section mean velocities can be expressed as

$$V_1 - V_2 = -\frac{2}{3\kappa}(V_{*1}-V_{*2}) \qquad (3.6.1)$$

in which V_1, and V_2 can be evaluated by applying Manning's equation to both sub-sections separately.

$$V_i = \frac{1.49}{n_i} R_i^{2/3} S_o^{1/2}, \; i = 1,2 \qquad (3.6.2)$$

and the maximum velocity which can be expressed as

$$V_{max} = 1/2(V_1+V_2) + \frac{1}{3\kappa}(V_{*1}+V_{*2}) \qquad (3.6.3)$$

will move away from the rougher boundary.

The velocity distribution also shows that, as the bed slope S_o increases, the curvature of the velocity profile will become more severe. The variations of the velocity profile are shown in Fig. 3.6.1

By using the continuity equation together with the above equations, the channel mean velocity can be written as

$$V = 1/2(V_1+V_2) - \frac{1}{3\kappa}(V_{*1}-V_{*2})\left(\frac{A_1-A_2}{A}\right) \qquad (3.6.4)$$

which when combined with Eq. (3.6.3), gives the ratio between V_{max} and V, as,

$$\frac{V_{max}}{V} = 1+\frac{2}{3\kappa}\left(\frac{V_{*1}}{V}\frac{A_2}{A} + \frac{V_{*2}}{V}\frac{A_1}{A}\right) \qquad (3.6.5)$$

Equation (3.6.5) also shows that, the rougher the boundaries, the higher the shear velocities V_{*i} and consequently the larger the V_{max}/V ratio.

3.7 The Hydraulic Radius Ratio Equation

The equation used to evaluate the hydraulic radius ratio can be obtained by substituting Eq. (3.5.6) for subsection (1) and (2) and Eq. (3.6.2) into Eq. (3.6.1) as

$$\frac{R_1^{1/6}}{n_1\sqrt{g}} = \frac{0.444(\lambda^{1/2}-1)}{\kappa(1-n_1/n_2\,\lambda^{2/3})} \qquad (3.7.1)$$

in which $\lambda = R_2/R_1$ is the hydraulic radius ratio.

By applying the momentum equation to the flow, for

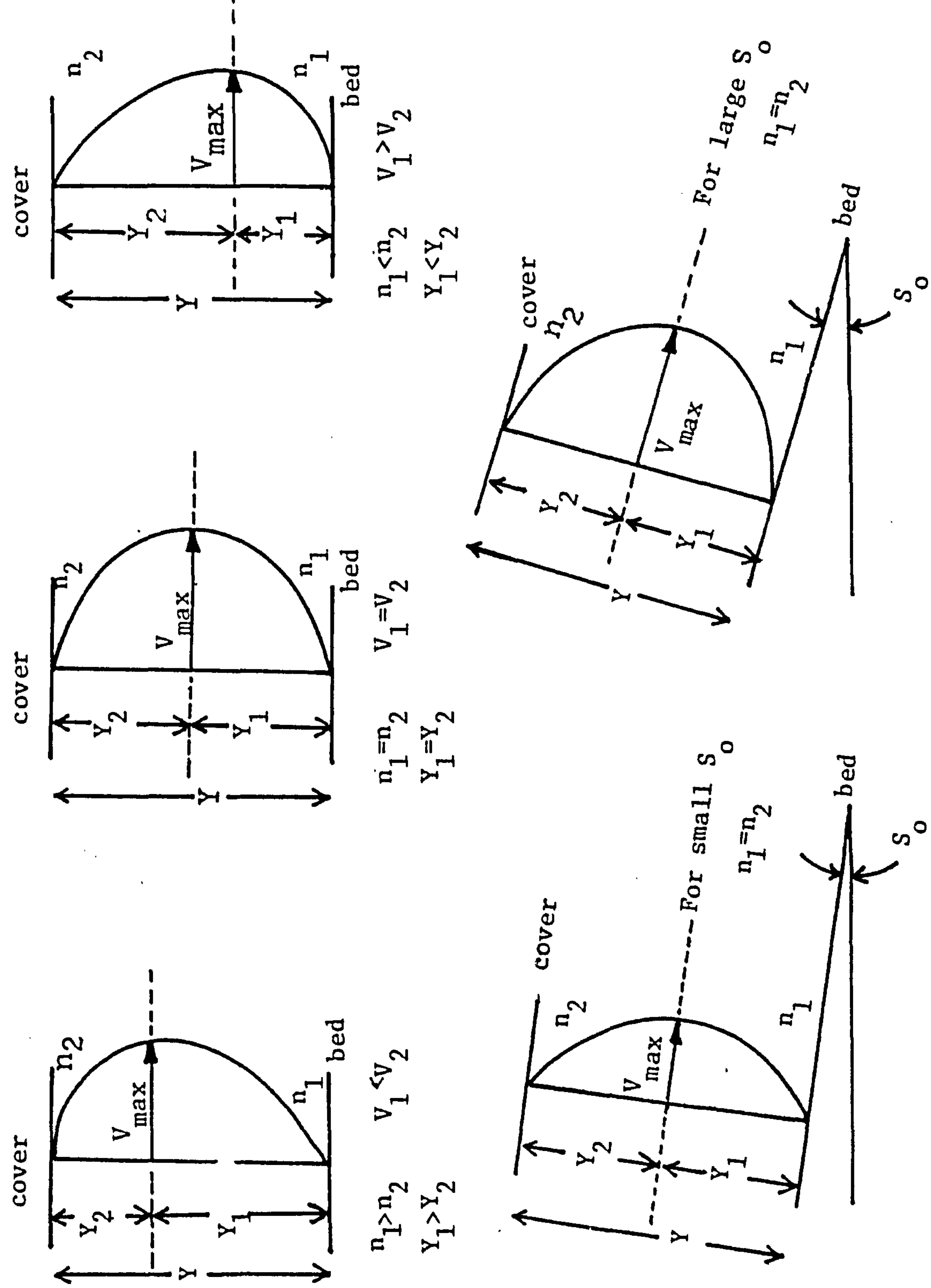

Fig. 3.6.1 Variations of Velocity Distribution.

unit length of channel in the flow direction

$$\gamma A S_o = \tau_1 P_1 + \tau_2 P_2 \qquad (3.7.2)$$

and substituting τ_i by $\gamma R_i S_o$, $i = 1,2$, for uniform flow, Eq. (3.7.2) becomes

$$R_1/R = 1/(\alpha + (1-\alpha)\lambda) \qquad (3.7.3)$$

where α is the wetted perimeter ratio P_1/P.

The final equation for the hydraulic radius ratio λ can be obtained by combining Eq. (3.7.1) and Eq. (3.7.3) and taking the value of $\kappa = 0.4$,

$$\frac{R^{1/6}}{n_1 \sqrt{g}} = 1.11 \frac{(\lambda)^{1/2} - 1}{1-(n_1/n_2)\ \lambda^{2/3}} (\alpha + (1-\alpha)\lambda)^{1/6} \qquad (3.7.4)$$

The location of the division surface between the two sub-sections can be obtained by solving Eq. (3.7.4) for the λ value.

3.8 The Composite Roughness Equation

By the definition of the hydraulic radius $R = A/P$, and the cross-section geometry, it gives

$$\frac{A_2}{A_1} = \lambda \frac{1 - \alpha}{\alpha} \qquad (3.8.1)$$

Introducing this equation into Eq. (3.6.4) together with Eq. (3.6.2) and Eq. (3.5.6) for both sub-sections, yields

$$\frac{n_1}{n_t} = 1/2 \left(\frac{1}{\alpha+(1-\alpha)\lambda}\right)^{2/3}\left(1+\frac{n_1}{n_2}\lambda^{2/3}\right) - \frac{n_1\sqrt{g}}{R^{1/6}}\frac{1}{4.47\kappa} \cdot$$

$$\frac{\alpha-(1-\alpha)\lambda}{(\alpha-(1-\alpha)\lambda)^{5/6}}(1-\sqrt{\lambda}) \qquad (3.8.2)$$

The above equation can be simplified by means of Eq. (3.7.4) to obtain,

$$\frac{n_1}{n_t} = (\alpha+(1-\alpha)\lambda)^{-5/3}(\alpha+(1-\alpha)\frac{n_1}{n_2}\lambda^{5/3}) \qquad (3.8.3)$$

This is the general composite roughness equation for a covered channel with only two boundary roughness.

In wide channels, the α value becomes 0.5 and Eq. (3.7.4) and Eq. (3.8.3) can be reduced to

$$\frac{R^{1/6}}{n_1\sqrt{g}} = \frac{\lambda^{1/2}-1}{1-(n_1/n_2)\lambda^{2/3}} \cdot (1+\lambda)^{1/6} \qquad (3.8.4)$$

and

$$\frac{n_1}{n_t} = \frac{1.587(1+(n_1/n_2)\lambda^{5/3})}{(1+\lambda)^{5/3}} \qquad (3.8.5)$$

3.9 Mathematical Model for General Solution

The difficulties of solving the channel flow problems arise from the fact that most natural channels usually consists of more than two roughnesses along their wetted perimeter. Also, the shear stress is not evenly distributed along the boundary.

The model used to solve these problems is illustrated in the channel shown in Fig. 3.9.1 . The cross-section is divided into vertical and horizontal finite strips corresponding to their local flow depths and boundary roughnesses. The relations derived in the previous sections are applied to the strips for their individual velocity profile. The dimensionless velocity profiles $(U_S/V_S)_{xy}$ and $(U_S/V_S)_{xz}$ are then used as coefficients of each other through a coefficient equation. The relative velocity at the intersecting point 'A' can be estimated. The successive evaluation of the local point velocities forms the solution field for the channel cross-section.

The coefficient Equation which describes the velocity distribution within the channel cross-section can be expressed as,

$$U/V = E1 \left[(U_S/V_S)_{xy} \cdot (U_S/V_S)_{xz} \right]^{E2} \qquad (3.9.1)$$

or

$$U/V = E3 \left[(U_S/V_S)_{xy} \cdot (U_S/V_S)_{xz} \right]^{E2}/(V_{max}/V) \qquad (3.9.2)$$

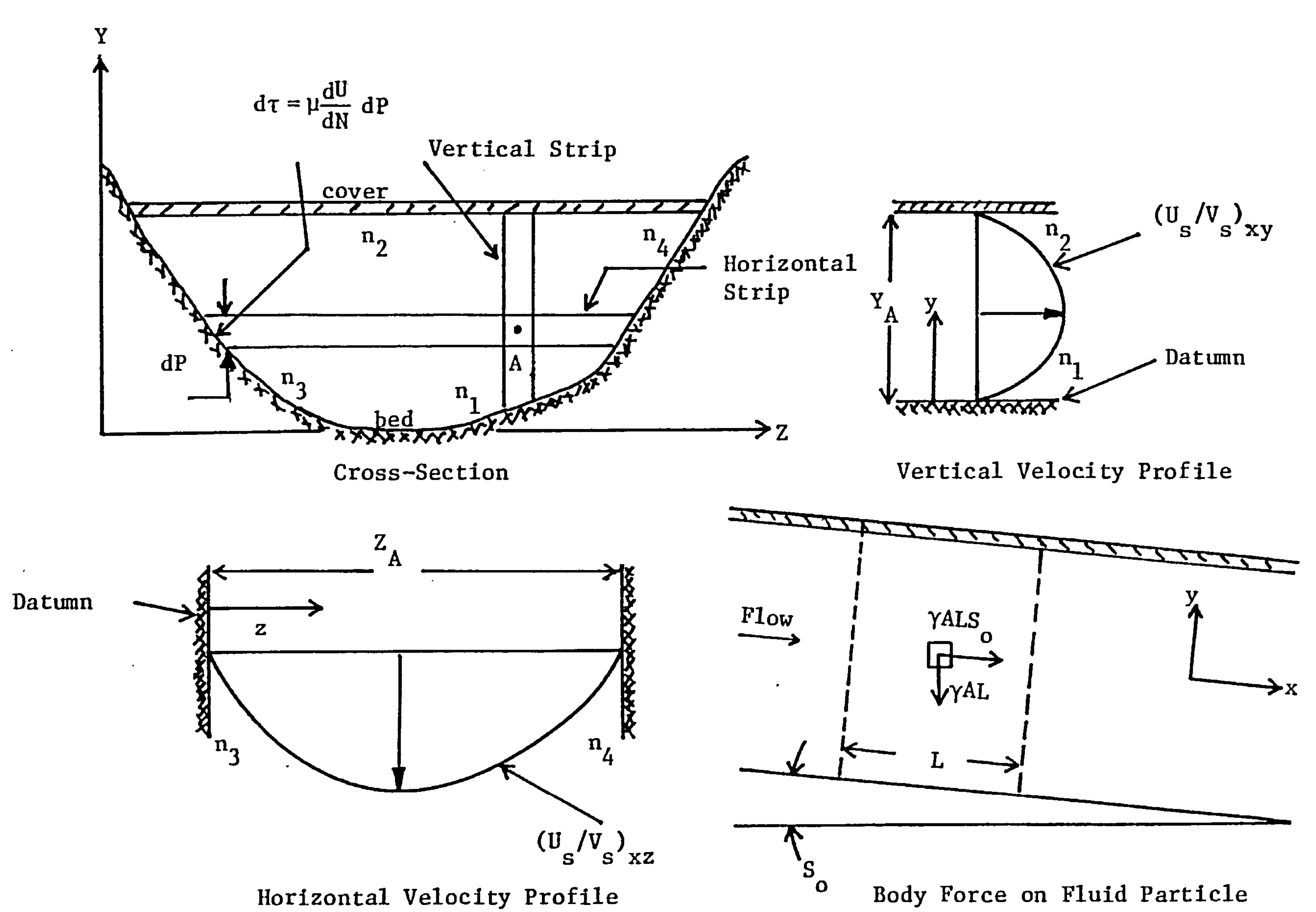

Fig. 3.9.1 Mathematical Model for Velocity Profile Determination.

in which

$(U_S/V_S)_{xy}$ is the dimensionless local velocity profile in the x-y plane

$(U_S/V_S)_{xz}$ is the dimensionless local velocity profile in the xz plane

U_s is the point velocity within the strip

V_S is the mean velocity for that particular strip

U is the final local velocity for the solution

V is the mean velocity for the cross-section

V_{max} is the maximum velocity of the cross-section

E1 is the velocity coefficient which indicates the magnitude of the flow

E2 is the velocity exponent which indicates the velocity gradient steepness

E3 is the velocity coefficient, where

$E3 = E1 \cdot (V_{max}/V)$

The coefficient equation (3.9.2) defines the solution set of any individual cross-section, whereas Eq. (3.9.1) defines the solution for the cross-section with a given flow rate designated by its (V_{max}/V) ratio.

The evaluation of the unknown coefficients E1, E2 in Eq. (3.9.1) or (V_{max}/V), E3, E2 in Eq. (3.9.2) can be done by satisfying the following boundary conditions:

1. Through the continuity equation, the total flow

rate of the cross-section should be equal to the integration of the velocity profile with respect to the elementary areas, that is,

$$\frac{1}{A}\int\frac{U}{V}\,dA = \frac{1}{AV}\int U\,dA = \frac{Q}{AV} = 1 \tag{3.9.3}$$

where A is the total flow area, Q is the total flow rate, V is the mean velocity.

2. By means of the momentum equation, the total driving force (gravitational body force) should be equal to the integration of the shear force along the wetted perimeter, under the steady state condition. For unit length along the flow direction (x axis)

$$\gamma A S_o = {}_P\int \tau_L\,dP \tag{3.9.4}$$

where $\tau_L = \mu\frac{dU}{dN}$ is the boundary shear stress

N is a displacement vector normal to the boundary surface, N=Funct. (y,z)

If θ_1 is the local product of $({}^{U}S/{}^{V}S)_{xy} \cdot ({}^{U}S/{}^{V}S)_{xz}$, Eq. (3.9.1) becomes

$$U/V = E1\,\theta_1^{E2} \tag{3.9.5}$$

By condition (1)

$$\frac{1}{A}\int\frac{U}{V}dA = \frac{E1}{A}\int\theta_1^{E2}\,dA = 1 \tag{3.9.6}$$

which can be written as,

$$E1 = \frac{A}{\int \theta_1^{E2} dA} \qquad (3.9.7)$$

By condition (2) and Eq. (3.9.5)

$$\frac{dU}{dN} = V.E1.E2.\theta_1^{(E2-1)} \frac{d\theta_1}{dN} \qquad (3.9.8)$$

Therefore, the total shear is

$$\int_P \mu \frac{dU}{dN} dP = \int_P \mu V.E1.E2.\theta_1^{(E2-1)} \frac{d\theta_1}{dN} dP = \gamma A S_o \qquad (3.9.9)$$

Using Eq. (3.9.1), (3.9.7) and (3.9.9), the coefficients E1, E2 can be defined.

Identical relations can be obtained for the coefficient equation (3.9.2), in order to solve for E2, E3 and (V_{max}/V) ratio. Finally, a complete model for solving the problem is well defined and this concludes the chapter on Theoretical Analysis.

CHAPTER IV

EXPERIMENTAL INVESTIGATION

4.1 Introduction

In trying to understand the flow situations and to estimate the composite roughness of a channel, the question arises as whether the derived mathematical method in Chapter III is applicable to all channels. Thus, experimental investigation is necessary, in order to answer this question.

Experiments were undertaken to examine those aspects such as:

1. The calibration of roughness materials,
2. the variations of geometric shape and multiple roughnesses in channel flow,
3. the verification of theoretically developed velocity profiles,

and to estimate their significance. The results of those experiments form the basis for this study.

4.2 The Test Equipment

4.2.1 Laboratory Facilities

Experimental observations were carried out in a 1.5' (0.457 m) width by 2.0' (0.61 m) depth flume with an uninterrupted length of 24' (7.315 m) (Ref. Fig. 4.2.1.1). The bottom and one side of the flume were made of plywood while the other side was made of clear plexiglass. The head tank, with a size of 4.25' (1.419 m) by 3.66' (1.18 m) in plan and 4' (1.219 m) in depth was provided at the upstream end of the flume, where an adjustable gate was also located. Gauge screens were installed between the outlet section of the tank and the flume, in order to reduce the air bubbles entrained within the water as well as the surface waves caused by turbulence.

At the downstream exit, a tail gate was installed to control the flow depth. The flume was served by a centrifugal pump capable of delivering up to 3500 USGPM (0.2267 m^3/s) in discharge with a 22.0' (6.71 m) head. It has an open loop system used together with a sump. The flow was adjusted by a gate valve installed between the pump and the inlet pipe of the head tank. An electromagnetic flow meter calibrated to 10 USGPM (6.31 x 10^{-4} m^3/s) was used for discharge measurements.

4.2.2 Measuring Equipments

Point gauges with electric bulb indicators were used to measure water surface elevations at three stations along the flume. They were calibrated to read up to 0.01" (0.025 cm) directly.

Pitot tubes were used for measuring point velocities

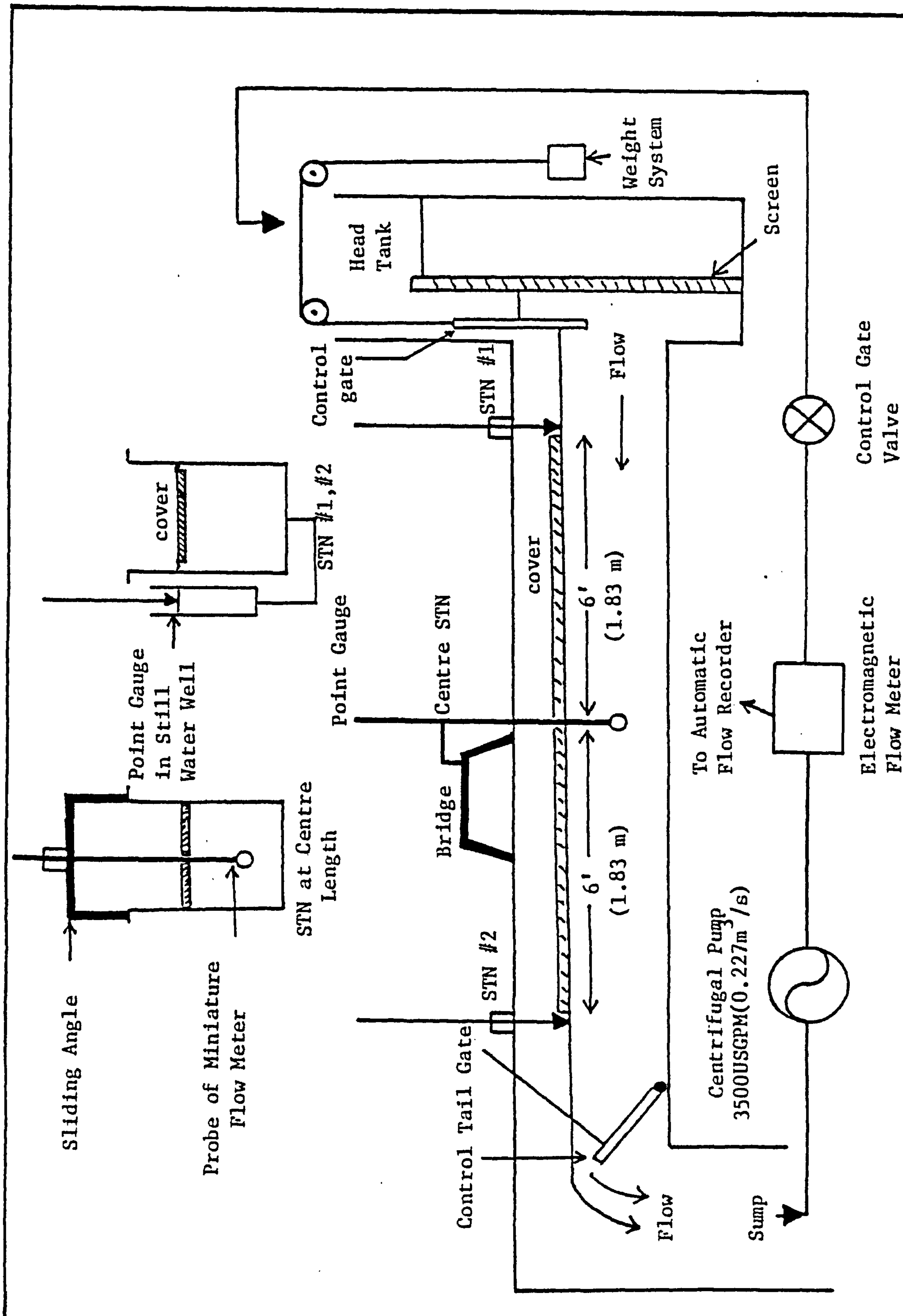

Fig. 4.2.1.1 Layout of Test Flume.

at the centre station. The manometer used read directly to 0.1" (0.254 cm).

A miniature current flow meter was also used to measure the point velocities at the cross-sections. The meter, together with two separate probes, could operate in four different ranges, with a maximum reading of 13.12'/s (4 m/sec). The sensitivity of the meter is 0.157"/s (0.4 cm/s).

All these equipments are shown in Fig. 4.2.2.1 to Fig. 4.2.2.2.

4.2.3 Experimental Channels

Seven different channel cross-sections had been used for observations. These channel shapes ranged from rectangular, semi-circular, trapezoidal, triangular, and compound variations of the last three shapes. The rectangular channel was actually the testing flume itself with bottom and one side made of plywood and the other side of plexiglass. The semi-circular channel was built with 20 gauge sheet metal, and inscribed in the flume. The trapezoidal and triangular channels were also built inside the flume, with 3/4" (1.905 cm) thick plywood. Several vent holes were drilled on the channel bottom near station (1) and (2), to balance out the static pressure built up under the channel.

There were seven partition blocks on each side beneath the channel bottom, to prevent any leakage flow in

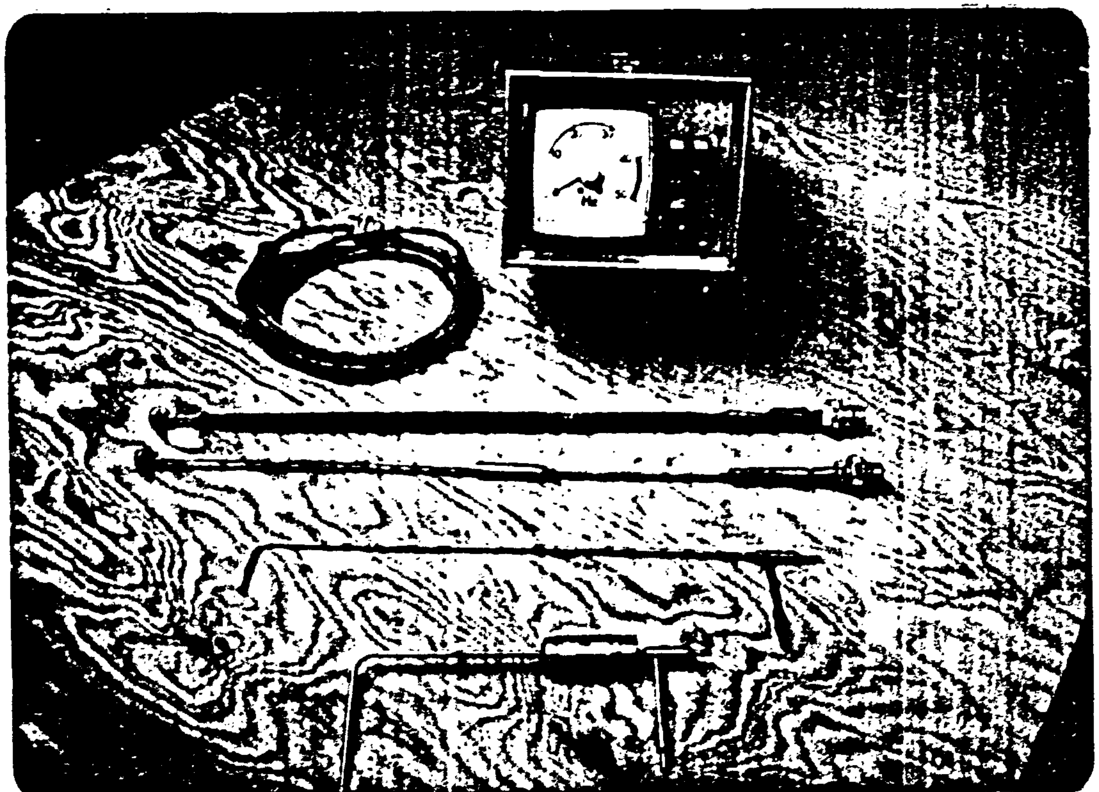

Miniature Current Flow Meter with High and Low Speed Probes, Pitot Tubes.

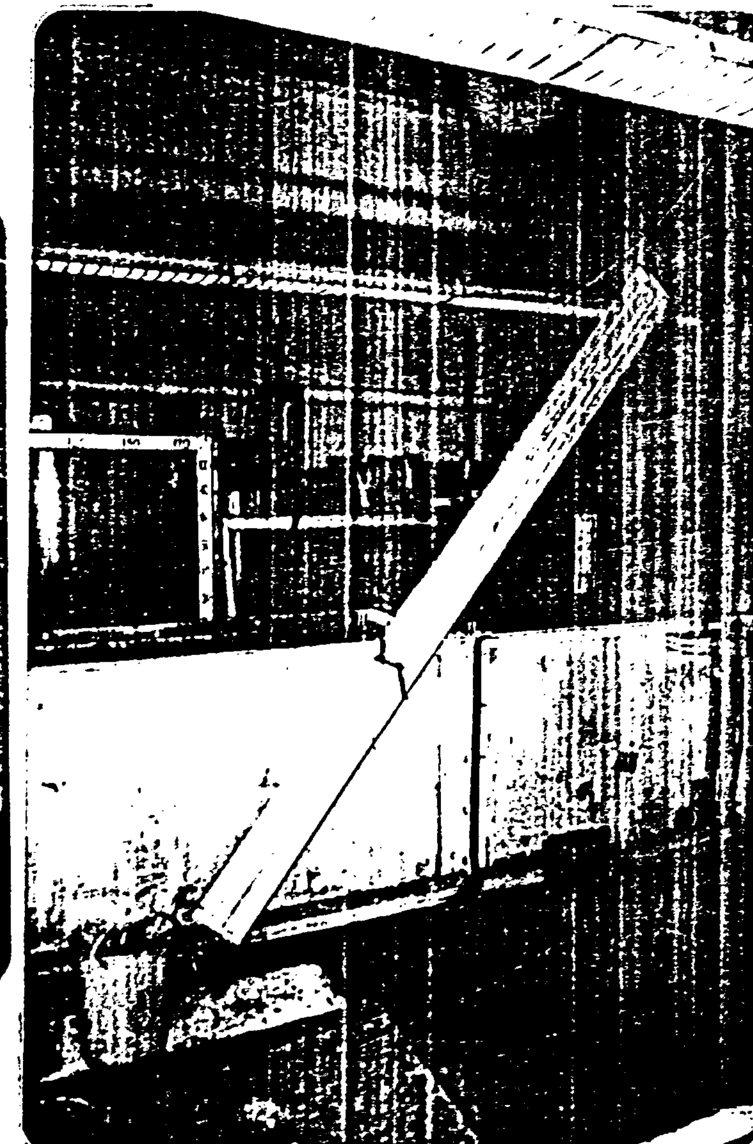

Sloping Manometer

Fig. 4.2.2.1 Measuring Equipment.

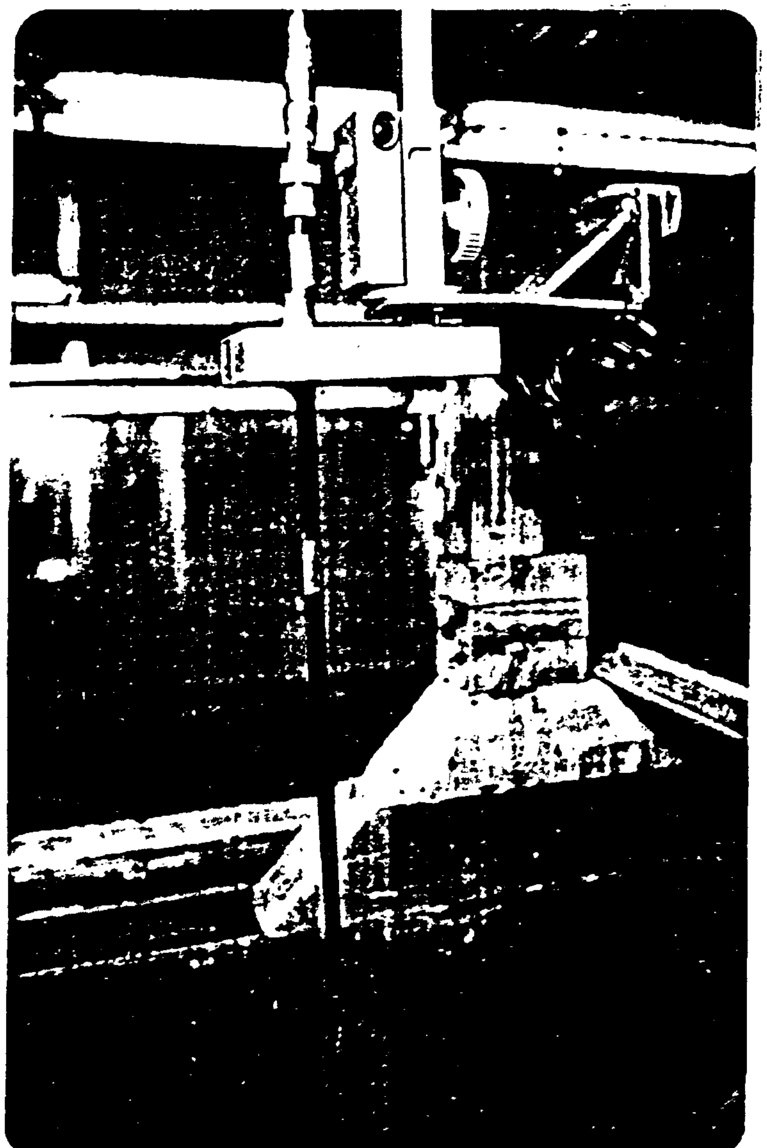

Point Gauge With Flow Meter's Probe

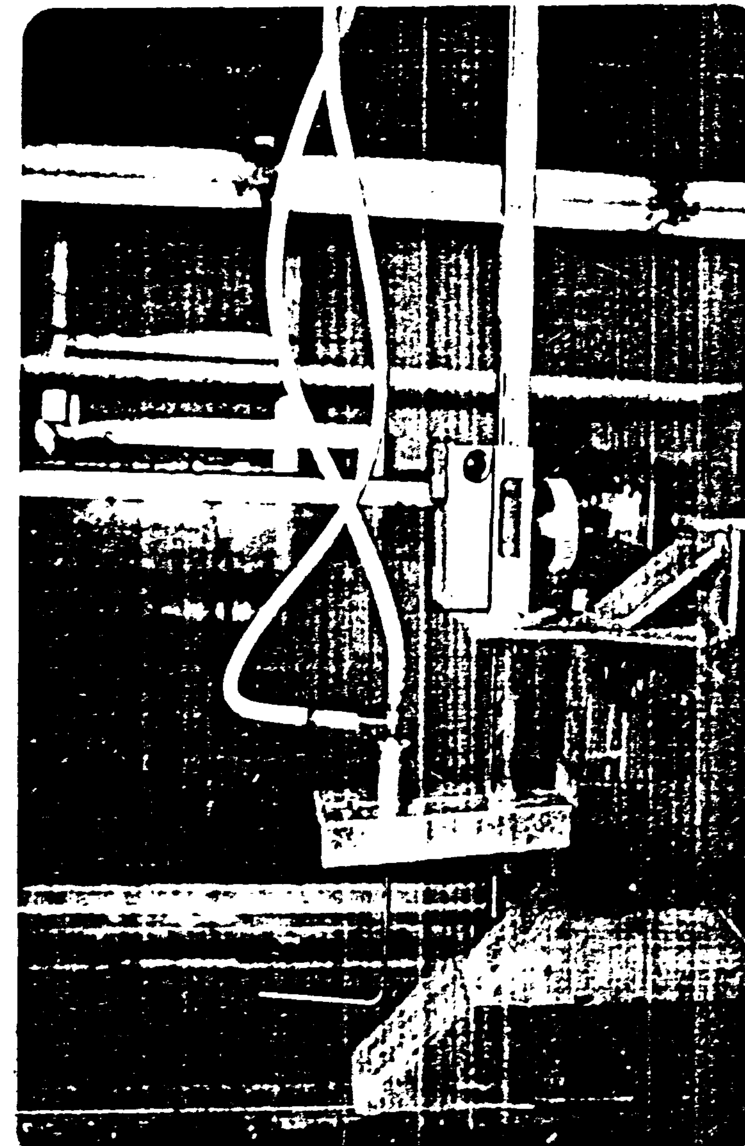

Point Gauge With Pitot Tube

Fig. 4.2.2.2 Measuring Equipment

that region. The details and dimensions of these channel cross-sections are shown in Fig. 4.2.3.1 , together with some of these sections in 4.2.3.2 and 4.2.3.3 .

4.2.4 Simulated Covers and Roughness Materials

In the cases of flow with covered channels, the floating covers were made of plywood boards with and without roughness elements attached to the underside. The size of the covers were 17" (43.2 cm) square by 1.5" (3.81 cm) thick. The specific gravity of the cover was 0.8.

Two different kinds of wire mesh, with diamond shape patterns, of sizes 2 1/2" x 1 1/4" (6.35 cm x 3.175 cm) and 1 1/2" x 3/4" (3.81 cm x 1.905 cm) had been used. These wire meshs together with the plywood would impose multiple roughnesses for different boundary conditions.

All these materials are shown in Fig. 4.2.4.1 . The symbols n_C, n_F and n_P are used to designate (2 1/2" x 1 1/4") wire mesh, (1 1/2" x 3/4") wire mesh and plywood respectively.

4.3 Experimental Program

This program consisted of groups of experiments which had been carried out along the investigation in order to meet the objectives of this study. The arrangements and procedures used in different groups are listed in the following sections.

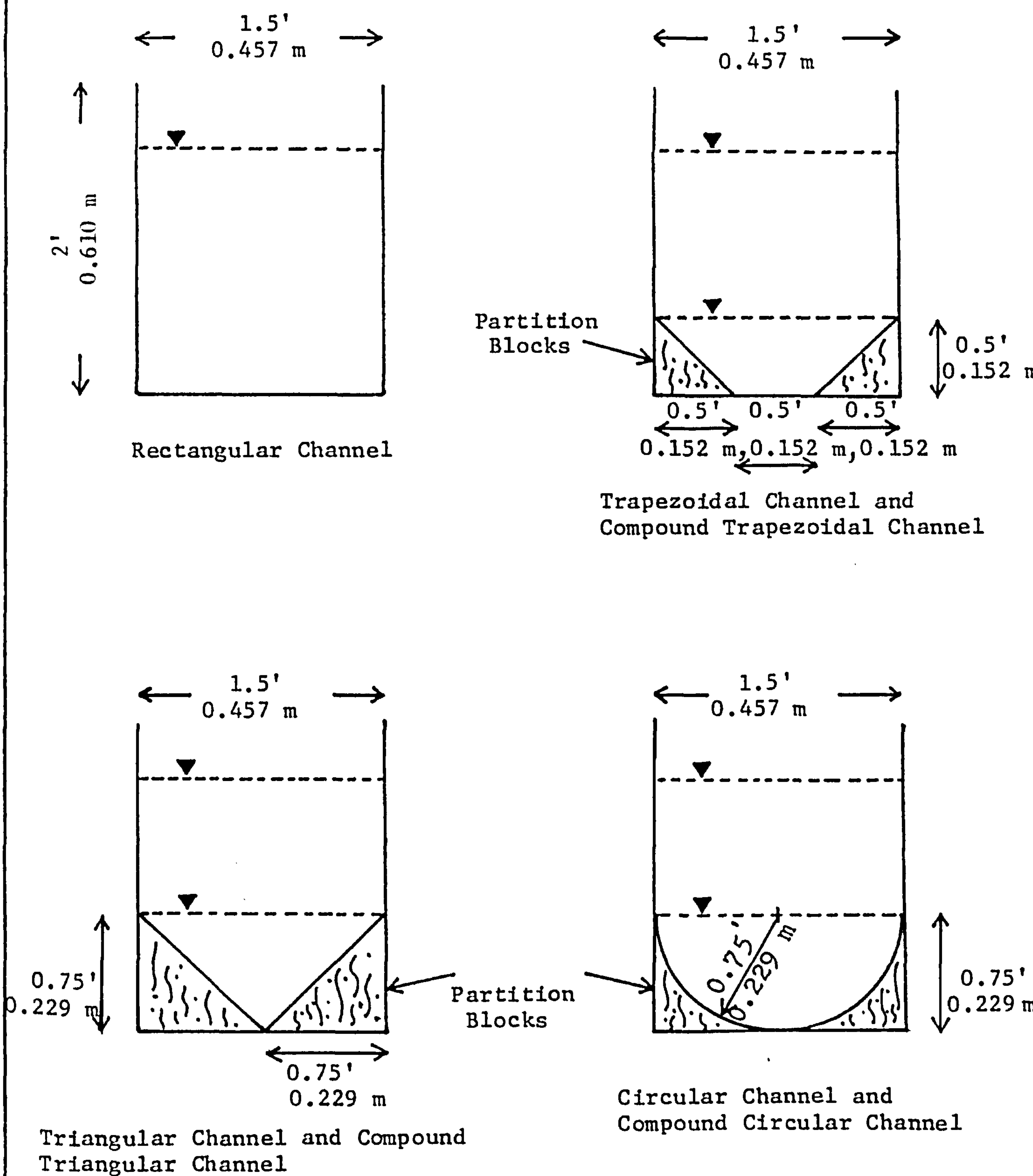

Fig. 4.2.3.1 Dimensions of Experimental Channel Cross-Sections.

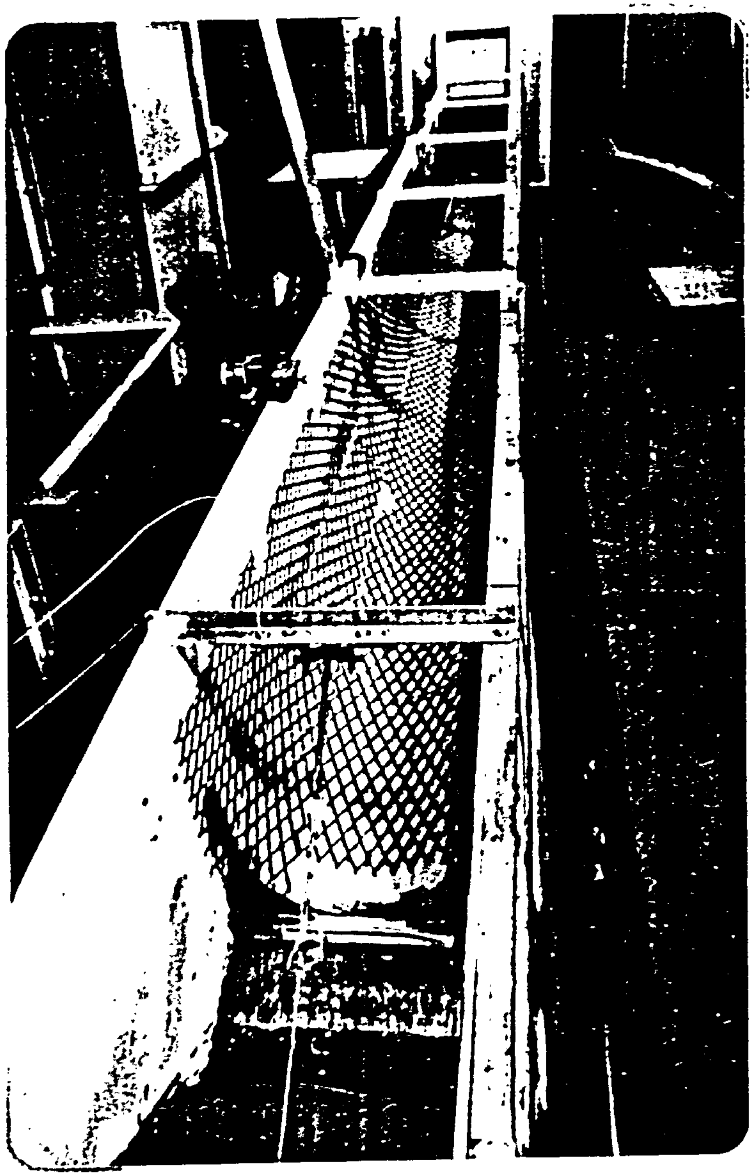

Semi-Circular Channel

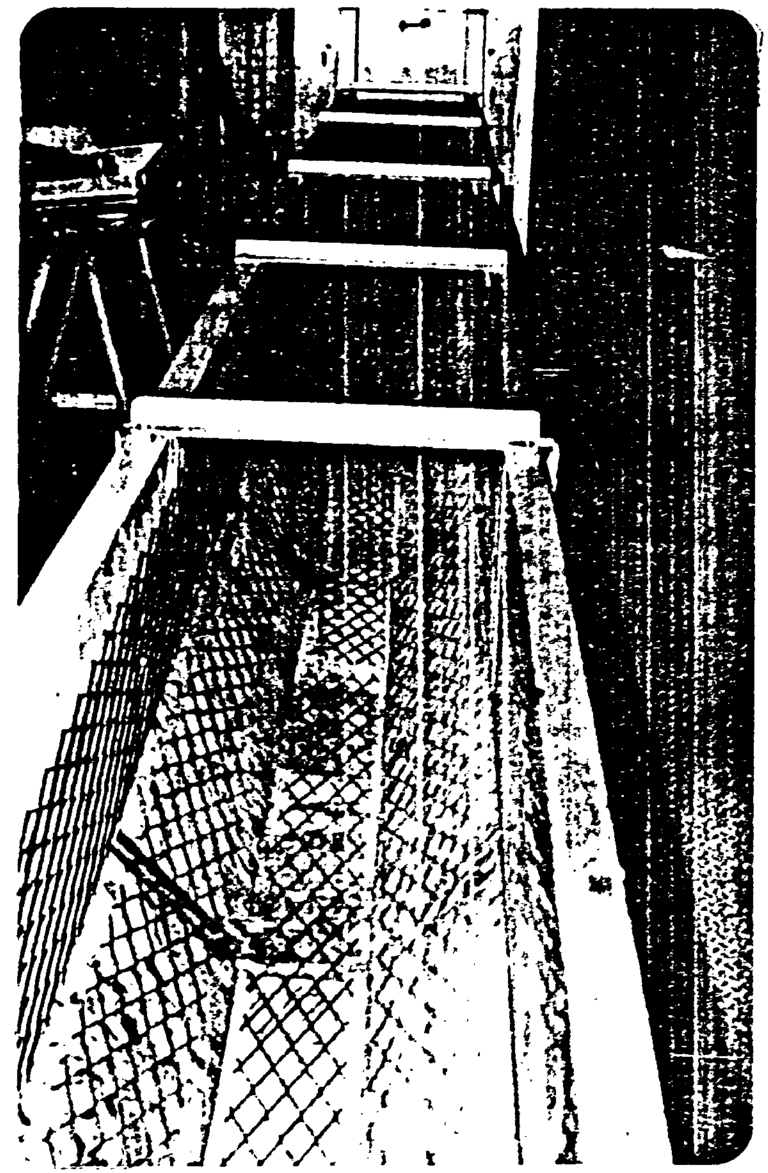

Trapezoidal Channel

Fig. 4.2.3.2 Experimental Channel Cross-Sections.

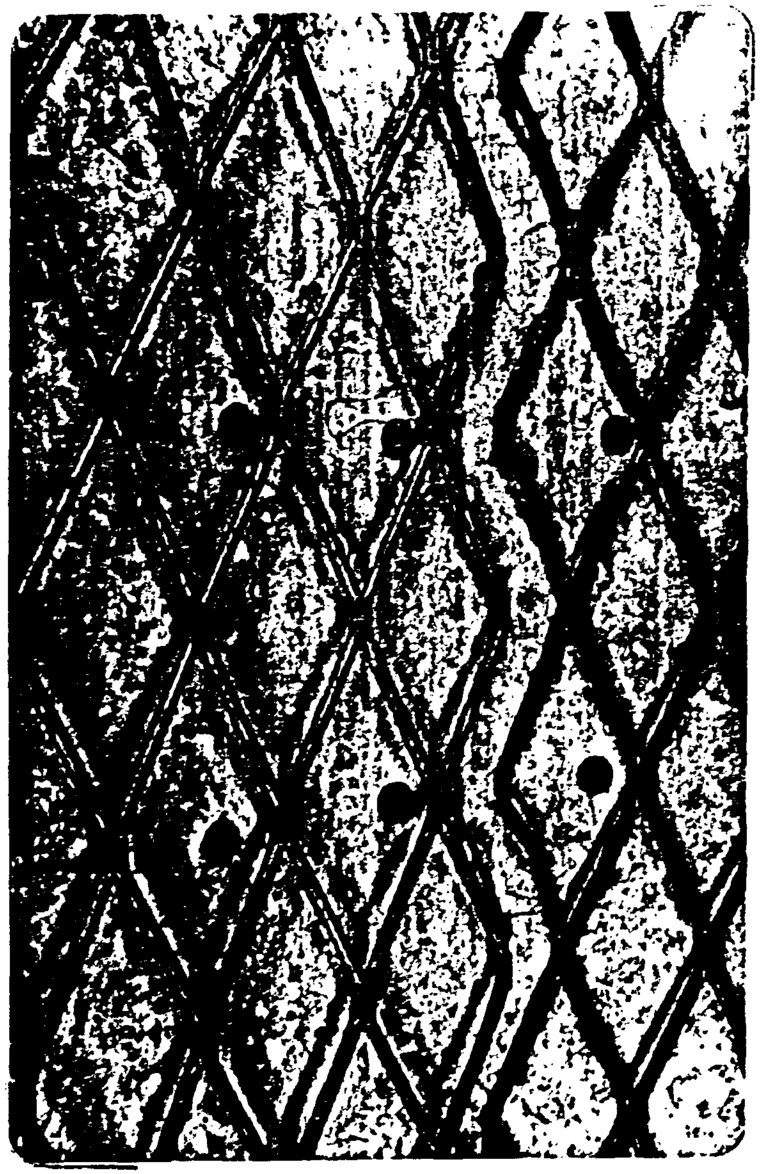

Vent Holes Used to Balance the Static Pressure Under the Channel Bottom

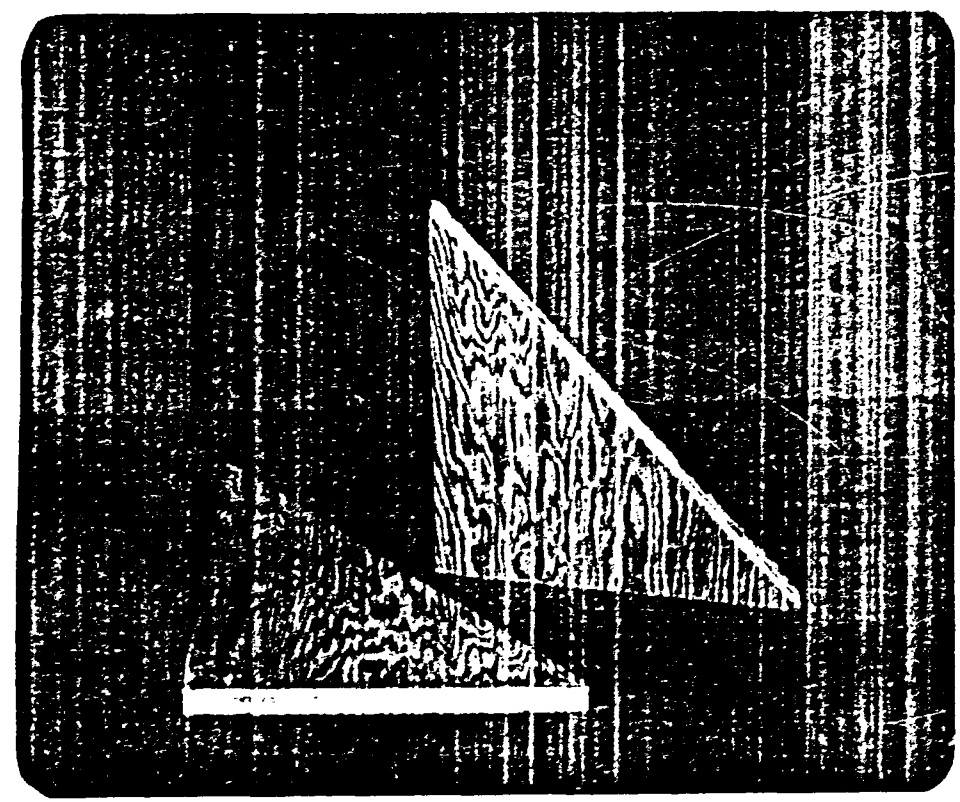

Partition Blocks Used to Prevent Leakage Flow Under the Channel Bottom.

Fig. 4.2.3.3 Model Channel Features.

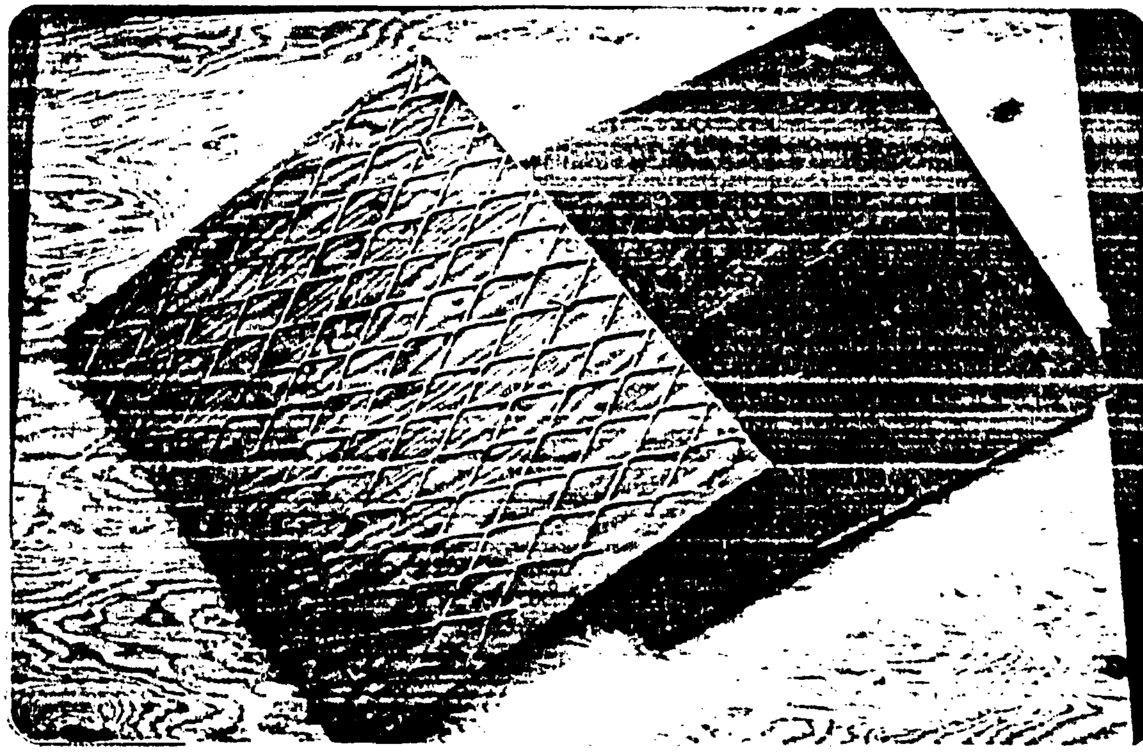

Simulated Cover Blocks With and Without Wire Mesh

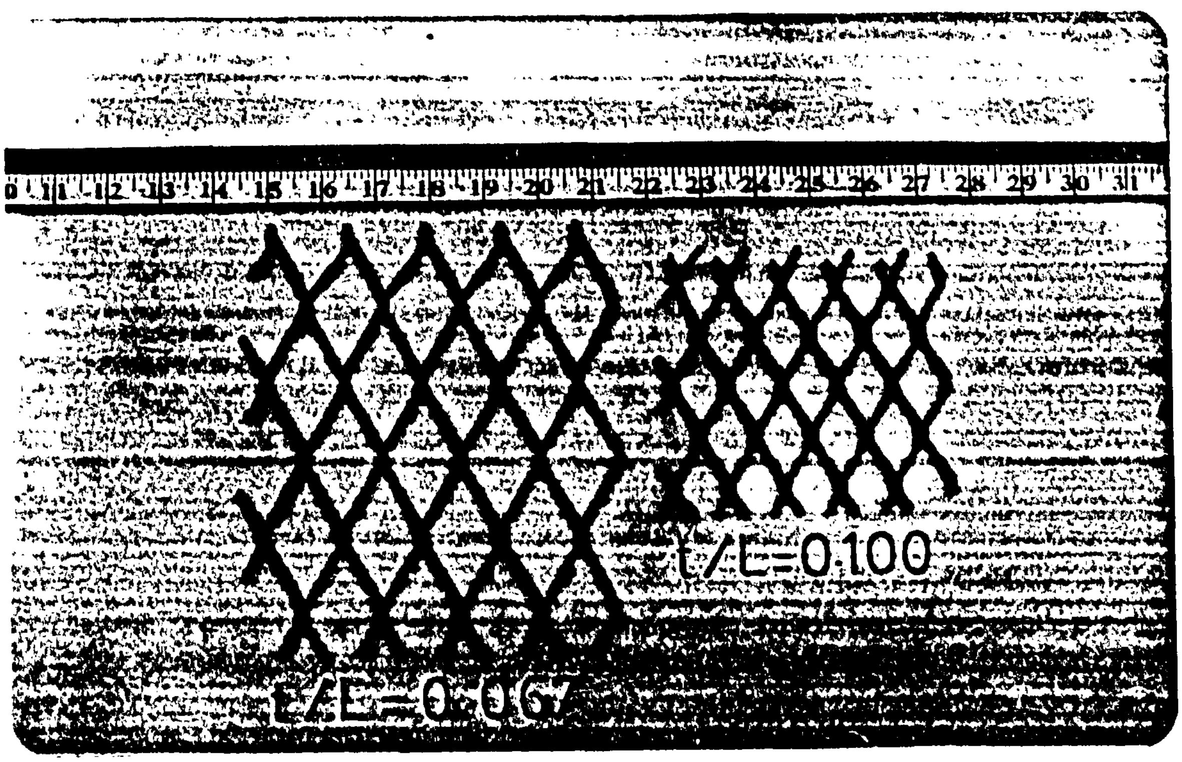

Diamond Wire Mesh of Sizes 2 1/2" x 1 1/4" (6.35 cm x 3.175 cm) and 1 1/2" x 3/4" (3.81 cm x 1.905 cm)

Fig. 4.2.4.1 Simulated Covers Blocks and Roughness Elements.

4.3.1 Calibration of Roughness Materials

Six different arrangements had been used for this calibration procedure. The rectangular channel was chosen as the standard shape for comparison. Only the bottom was lined with an unique wire mesh at a time. The energy slope, the total flow rate and the water surface elevations at station (1) and (2) were recorded in order to evaluate Manning's roughness coefficient. Two different approaches were used to measure the flow rate Q. The first one was using the flow rate recorded by the flow meter, which was the total flow rate through the flume. The second method is by means of a recorded velocity profile. The profile along the vertical centre line of the cross-section had been measured and was used to evaluate the discharge. These two sets of values were then compared.

4.3.2 Evaluation of Channel Composite Roughness

The experimental procedures were almost the same as described in the previous section. Instead of just using the rectangular flume, all seven channel cross-sections had been studied. The boundary roughness elements were also rotated for different settings. In this way, the significance of the geometric shape and multiple boundary roughness can be estimated.

4.3.3 Study of the Velocity Profile

Detailed velocity traverses through the flow depth and across the width of the channel were recorded by using pitot tube and miniature flow meter. The station which had chosen for taking measurements were located well beyond an initial length of 40 times the cover thickness to ensure the establishment of uniform flow away from the leading edge.

The coordinate system used in recording data was indicated in Fig. 4.3.3.1 . Elevations were measured as a ratio to the maximum flow depth. The spacing of the traverse stations were small near the sidewall of the channel.

All seven different configurations with rotating multiple roughness had been studied and sixty seven velocity traverses were recorded.

4.4 Experimental Results

A summary of the results obtained in the experimental investigation is given in Appendix C.

4.5 Experimental Errors

The sources of the experimental errors along with their expected values are discussed in Chapter V.

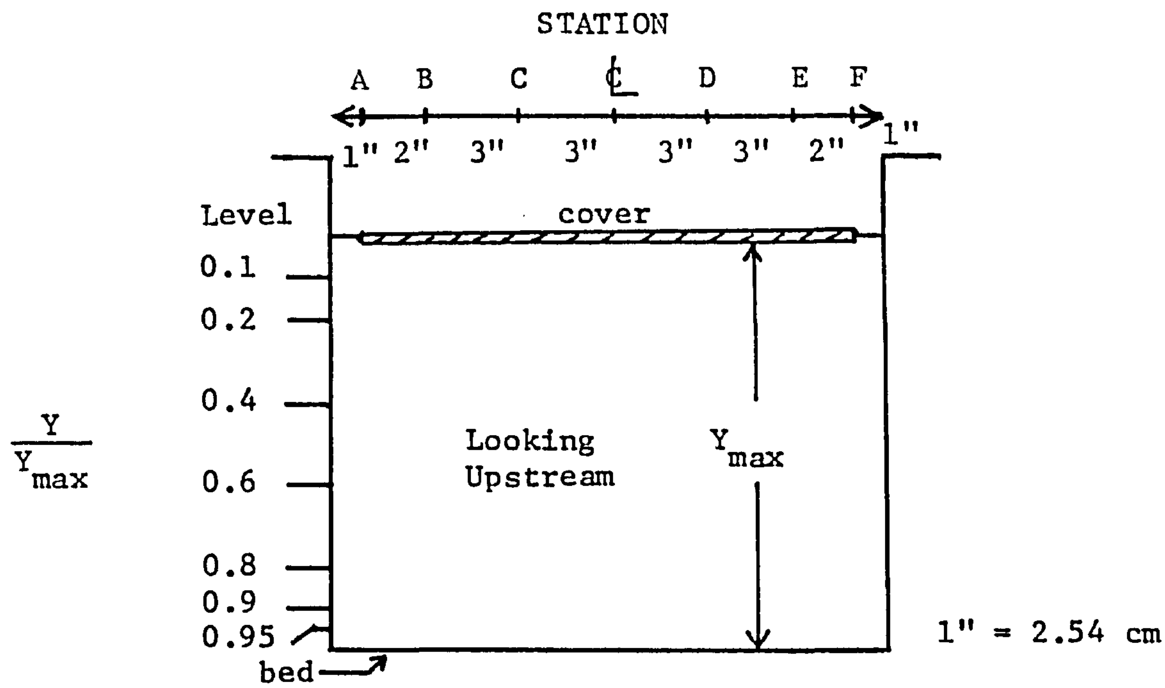

Coordinate System for Velocity Traverse at Center Station

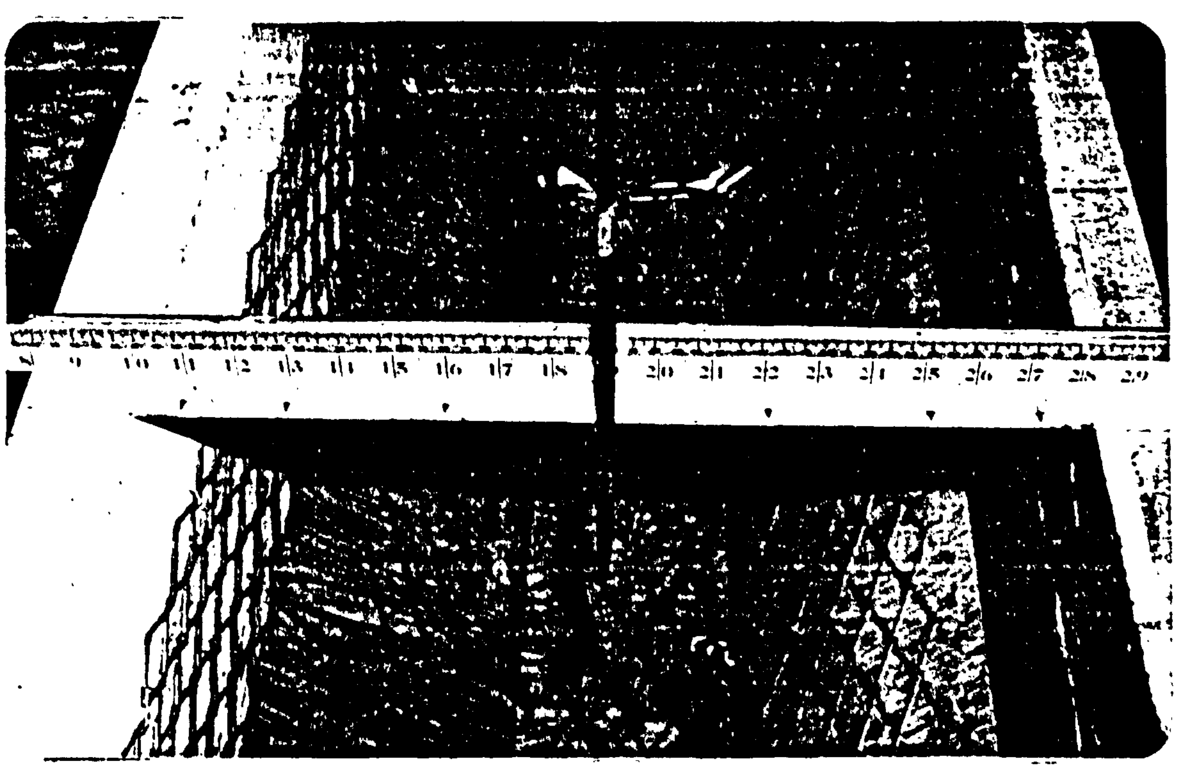

Locations of Traverse Stations (Looking Up-stream of the Flume)

Fig. 4.3.3.1 Velocity Traverse Arrangement.

CHAPTER V

DISCUSSION OF THEORETICAL AND EXPERIMENTAL RESULTS

5.1 Introduction

In this chapter the utilization of the analytical relations and the mathematical model developed in Chapter III are discussed. First, the behavior of various analytical relations to their independent variables, then the applicability of these relations to different model channels and comparisons with the experimental results. Finally, the application of the numerical model together with the above relations in solving composite channel problems, and verification of this procedure through the experimental results.

5.2 The Division Surface Equation

The analytical model mentioned in Chapter III involved the solving of the Division Surface Equation, Eq. (3.7.4), in order to locate the position of the division surface, which separates the two flow sub-sections in relation to the cross-section of the channel. Since the dependent variable λ can not be separated from the other parameters, no direct solution can be found.

In order to evaluate the values of λ, one method is to develop a kind of alignment chart which consists of a practical range of precalculated λ values.

By referring back to Eq. (3.7.4), successive numerical values of n_1, n_2, α and λ are used within a numerical subroutine in order to generate the corresponding values of Φ, where $\Phi = R^{1/6}/(n_1 g^{1/2})$ denotes a separate functional group of the equation.

During the computation process, the values of Φ was found to be very insensitive to the changes of α, thus the range of α values from 0.55 to 0.65 can be considered as a parameter with one unique value.

The Alignment Chart, Fig. 5.2.1 , is developed with a logarithmic base. It consists of a total of nine axes. The first axis from the left contains all pre-calibrated Φ values. The rest of the eight axes carry the values of λ corresponding to eight different n_1/n_2 ratios.

To distinguish the positions of the λ values on different axes, a reference point is placed on the far right side of the figure.

With a single set of λ and Φ data generated by an unique value of n_1/n_2 ratio, we can calibrate a single λ axis, by aligning the reference point with the corresponding values on the pre-calibrated Φ axis.

The use of this Alignment Chart to find λ values of certain given n_1/n_2, α and Φ value is demonstrated in Appendix A1.

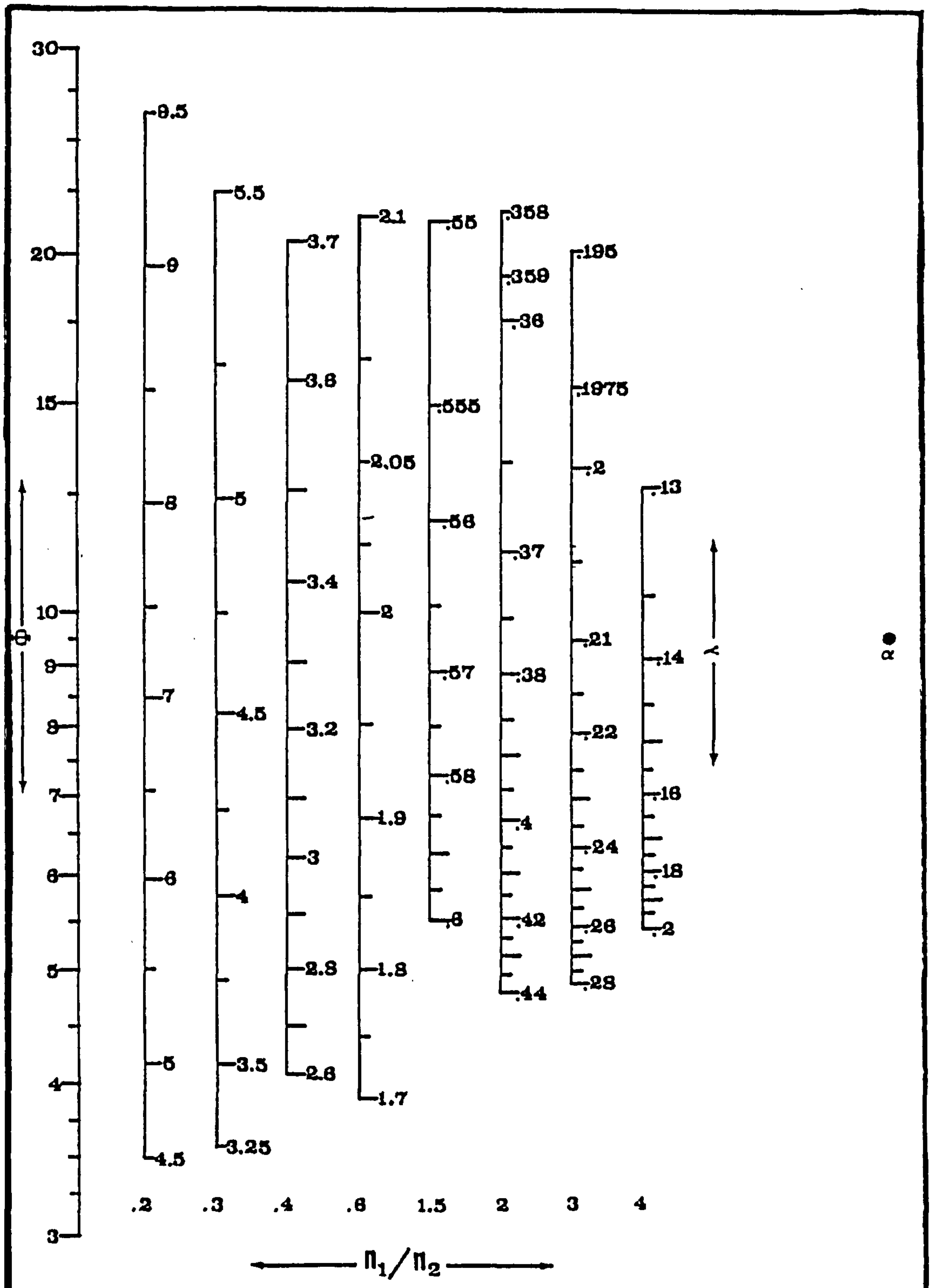

Fig. 5.2.1 Monograph for λ

5.3 The Composite Roughness Equation

The general equation for the estimation of the composite Manning's roughness factor n_t for a covered channel with any cross-sectional shape is referred to by Eq. (3.8.3).

Although the equation can be solved directly to get the value of n_t, yet it will involve a lot of mathematical operations. It is much more handy to develop another alignment chart to solve the equation graphically.

The development of the alignment chart is much similar to that described in the previous section. But this time, the composite roughness n_t is quite sensitive to the change in α values. Thus the chart has to be developed to take this effect into account.

In order to include the complete range of n_1/n_2 ratio, two separate charts, Fig. 5.3.1 and Fig. 5.3.2 , have been developed with one ranging from 0.2 to 0.6 and the other one from 1.5 to 4.0.

The first axis to the left contains all precalibrated λ values. The rest of the four axes carry the values of n_1/n_t corresponding to different n_1/n_2 ratios. For each axis, the left side of the axis is calibrated with α values equal to 0.55 and on the right equal to 0.65. For the rest of the n_1/n_t values within this α range, they can be obtained by interpolating between the 0.55 to 0.65 values.

The use of these Alignment Charts to find n_1/n_t values

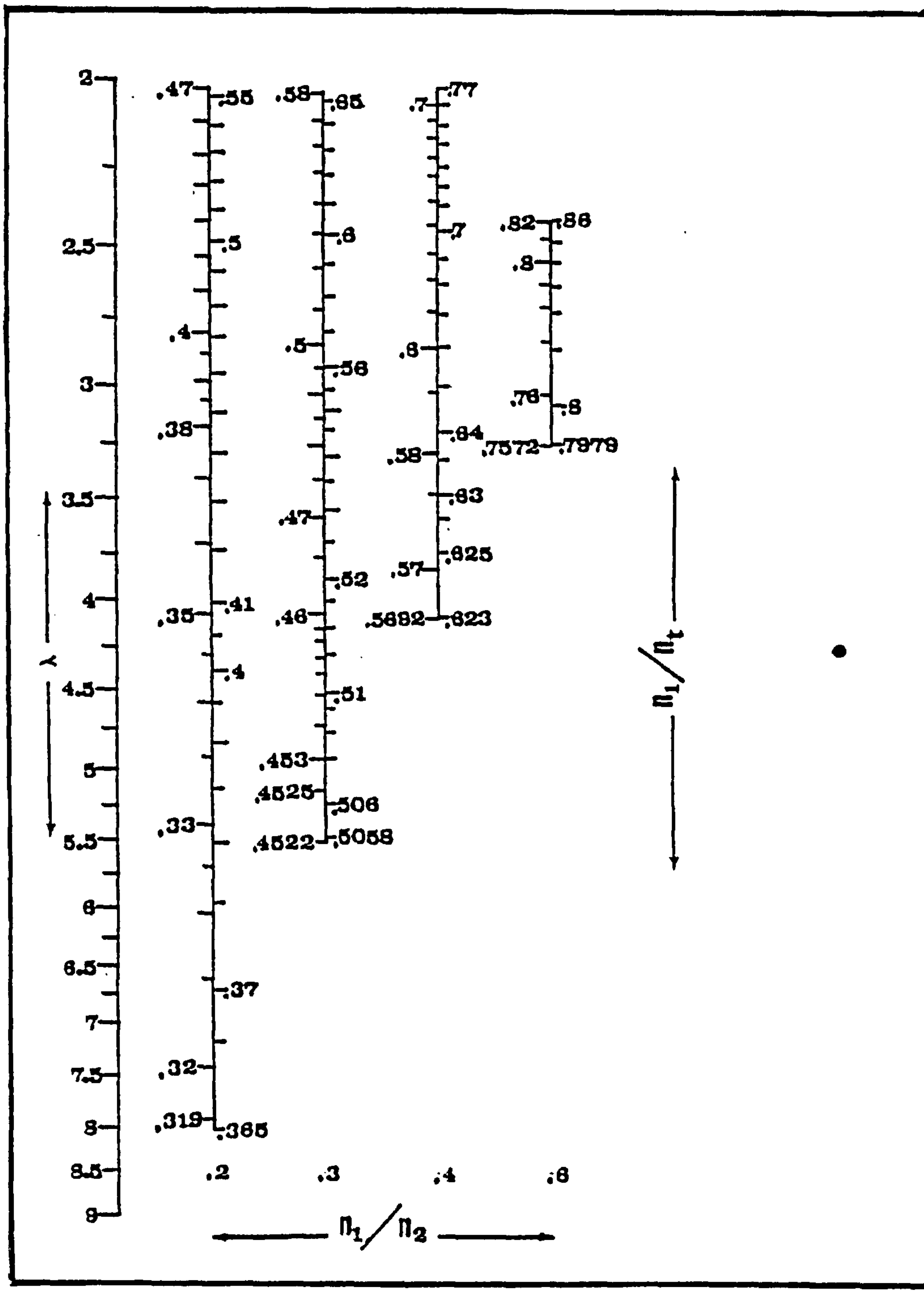

Fig. 5.3.1 Monograph For n_1/n_t Ratio.

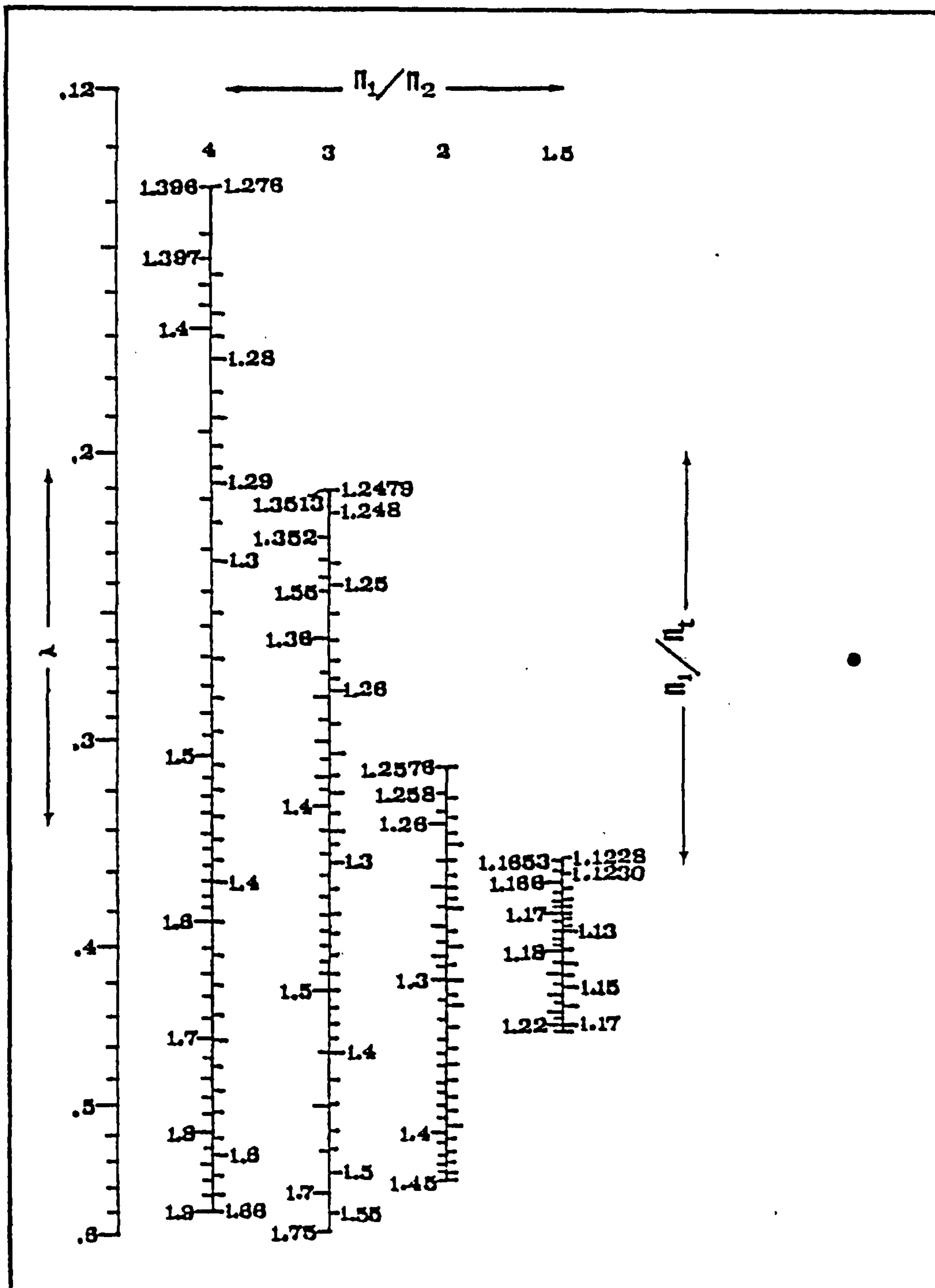

Fig. 5.3.2 Monograph For n_1/n_t Ratio.

of certain given n_1/n_2, α and λ value is demonstrated in Appendix A1.

5.4 Calibration of Roughness Elements

The experimental procedures and settings for these calibration tests had already been mentioned in Chapter IV, Section 4.3.1. The recorded data were then used to evaluate the corresponding hydraulic parameters as well as the roughness coefficients expressed in terms of Manning's n and Chezy's C. The procedures used to carry out the evaluation is listed in Fig. 5.4.1 . All the results are presented in Appendix C1, Table (C.1.1) to (C.1.6). The calculated Manning coefficients for different roughness elements were then plotted against their Reynolds' numbers, and the graphs are shown in Fig. 5.4.2 and Fig. 5.4.3 . It can be seen that all these roughness curves range from the laminar flow region, then passing by a transitional zone, into the turbulent region. The slopes of the curves dn/dN_R are very steep in the laminar region which indicates the persistence of laminar shear under low flow velocity, while the values of dn/dN_R approaching zero when they reach the turbulent region. Usually, most of the practical designs and laboratory studies are based on this region, since the roughness coefficient becomes a constant with respect to the flow velocity.

The curves also show that the fine wire mesh has

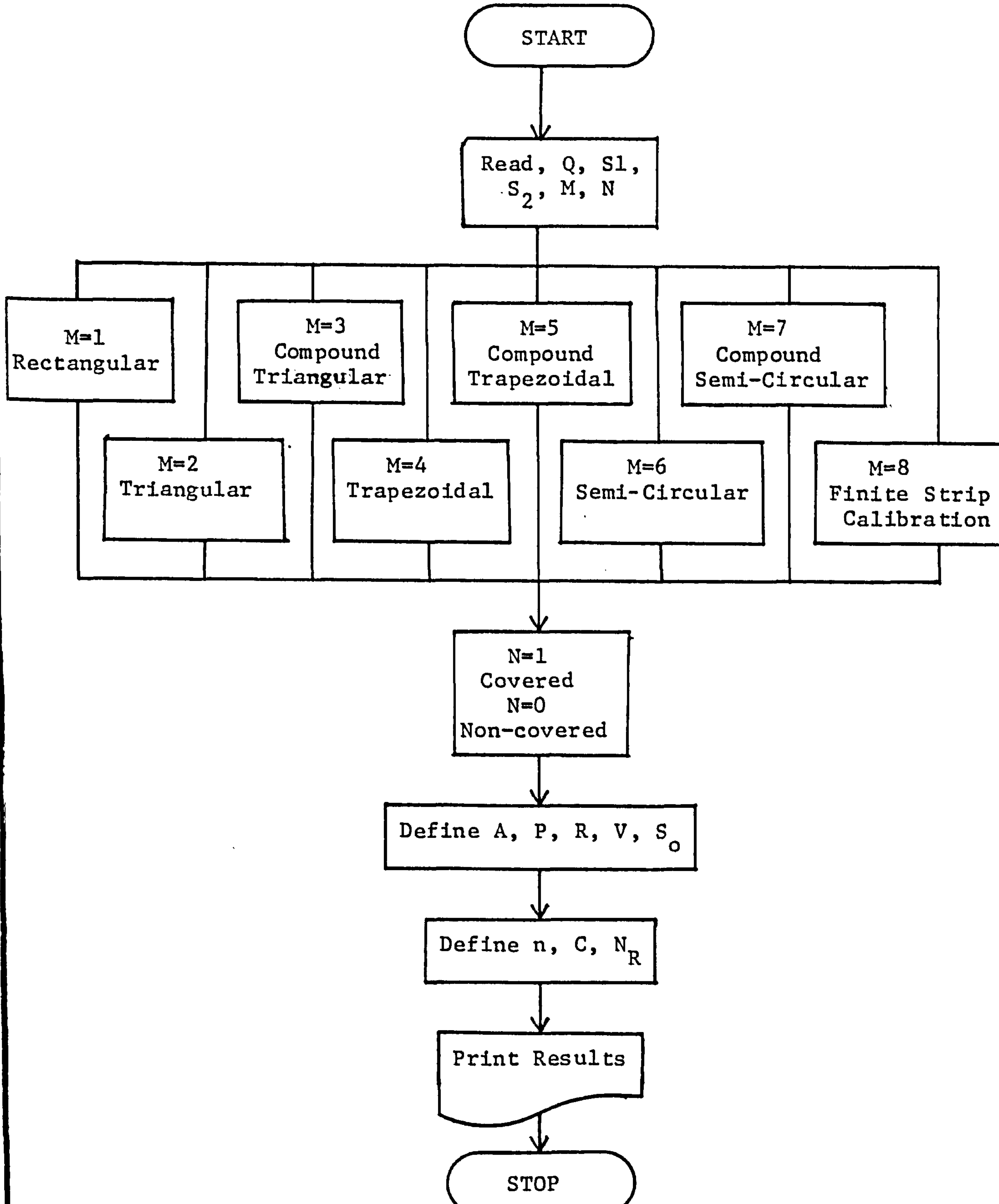

Fig. 5.4.1 Flow Chart for Estimating Experimental Manning's n and Chezy's C.

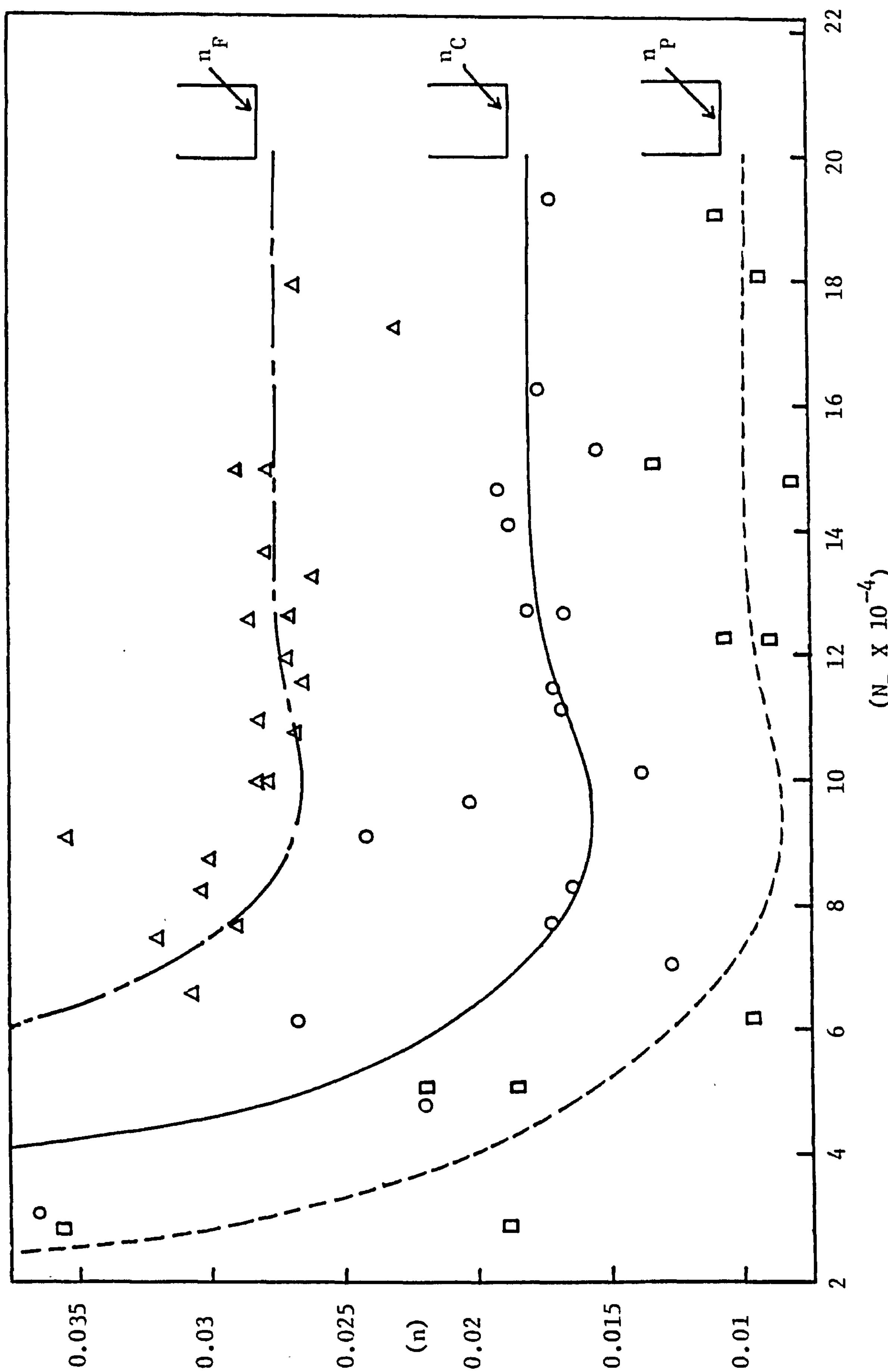

Fig. 5.4.2 Calibration Using the Total Flow Rate

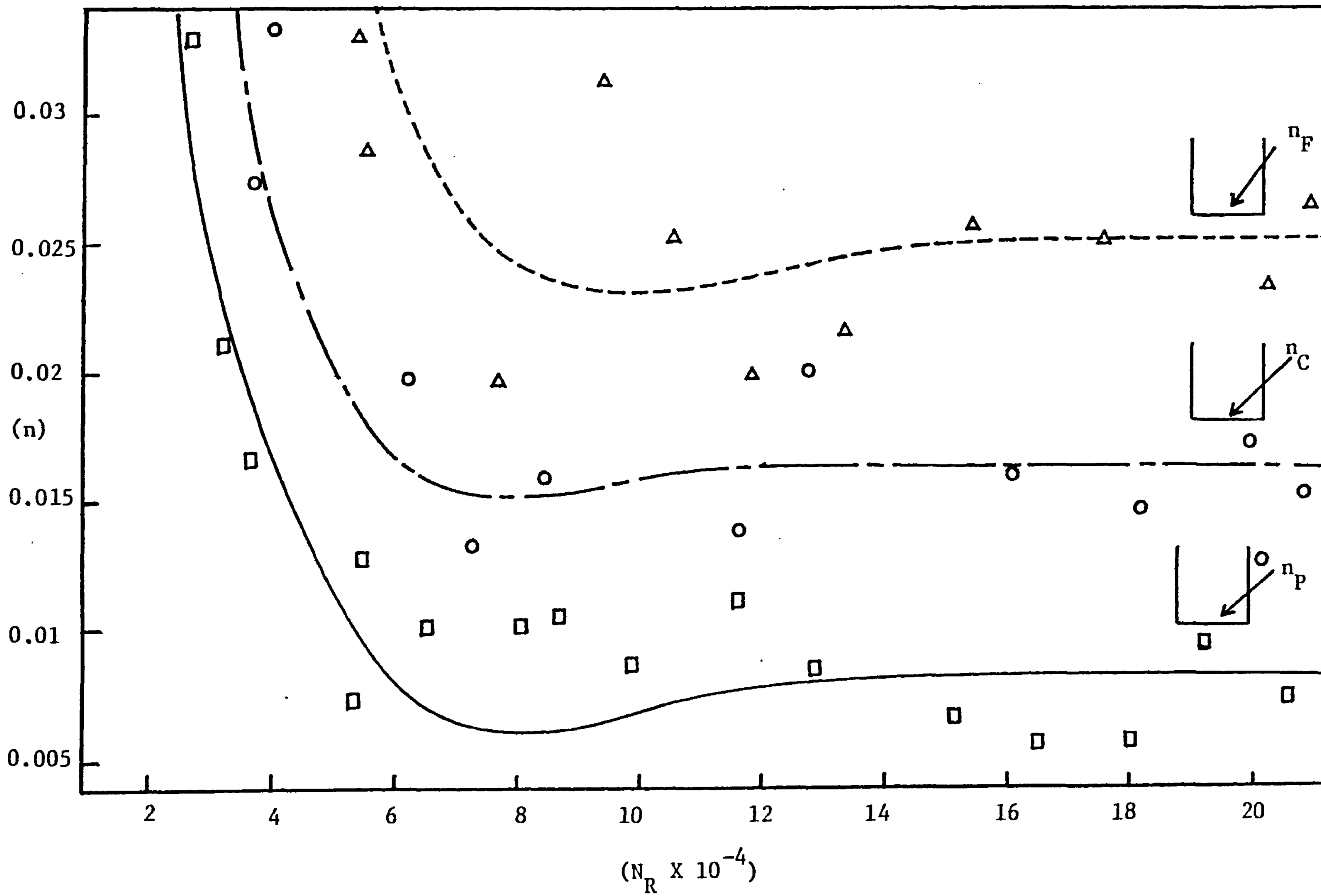

Fig. 5.4.3 Calibration Using Vertical Strip Approach

a higher Manning's value, than the coarse one. It can be explained that, since both of them have almost the same roughness height (manufactured by steel sheet of the same thickness), but the fine one carries a denser pattern within an unit area of wire mesh, so more energy will be lost when flow passed over it. Thus, it shows a higher roughness coefficient, than the coarse one. The figures (5.4.2, 5.4.3) also show that, the centre velocity profile approach will give a lower roughness coefficient due to reduced side wall effect in calibration (Ref. Fig. 5.4.4) and this method is more advantageous in standardizing material roughnesses for design purposes.

5.5 Effects of Geometric Shape and Boundary Roughness

There were twenty two tests carried out according to the procedures mentioned in Chapter IV, Section 4.3.2, in order to verify the effects of geometric shape and multiple boundary roughness.

The testing started with experiments on different geometric shapes with equal lining material and under free surface conditions. The data were analyzed according to the procedures listed in Fig. 5.4.1 in order to obtain the roughness coefficients. The results were then plotted against the corresponding Reynolds' numbers as in Fig. 5.5.1 . It shows that for different shape of channels

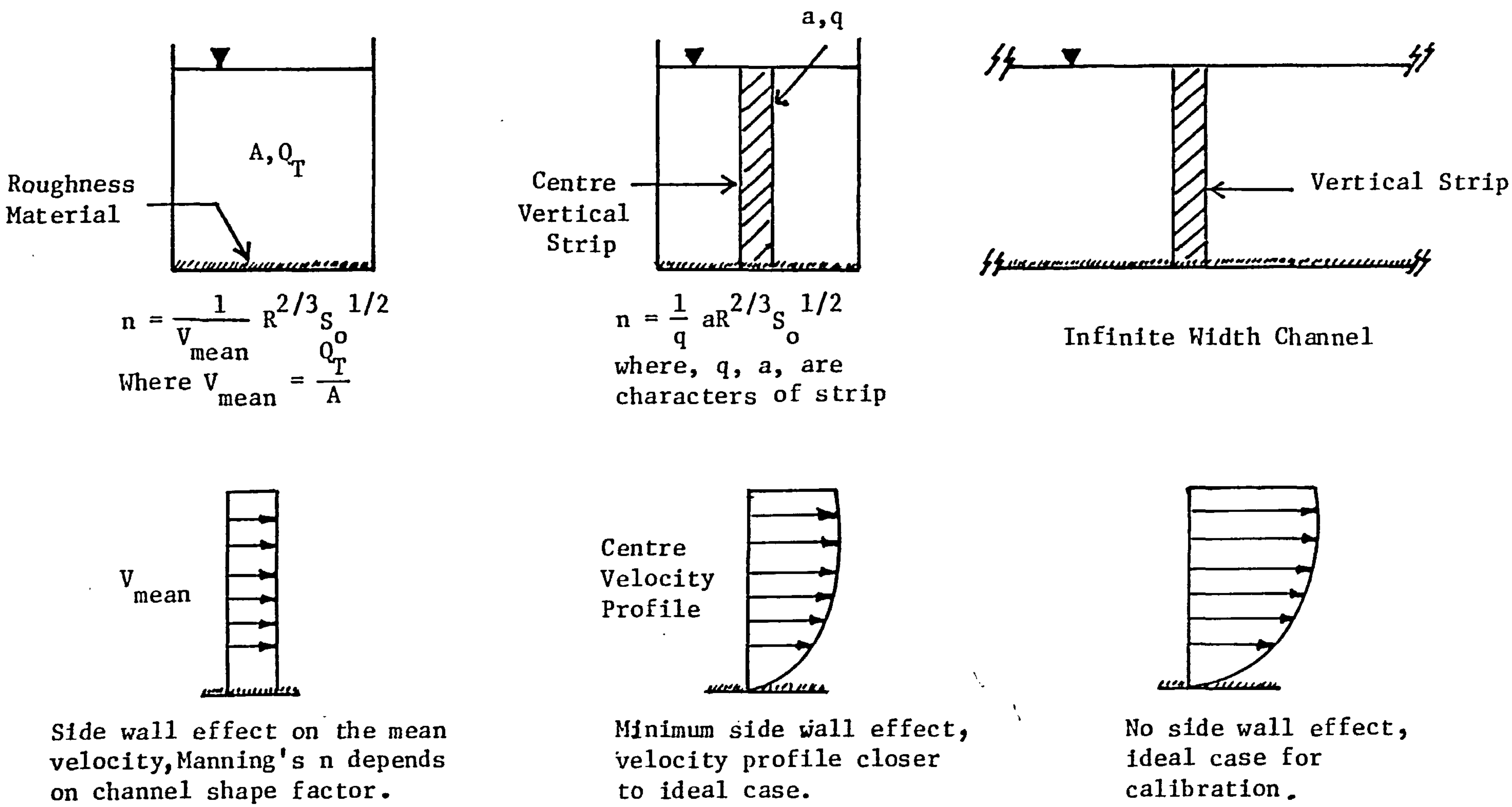

Fig. 5.4.4 Calibration of Manning's Roughness Factor Using Vertical Strip Approach.

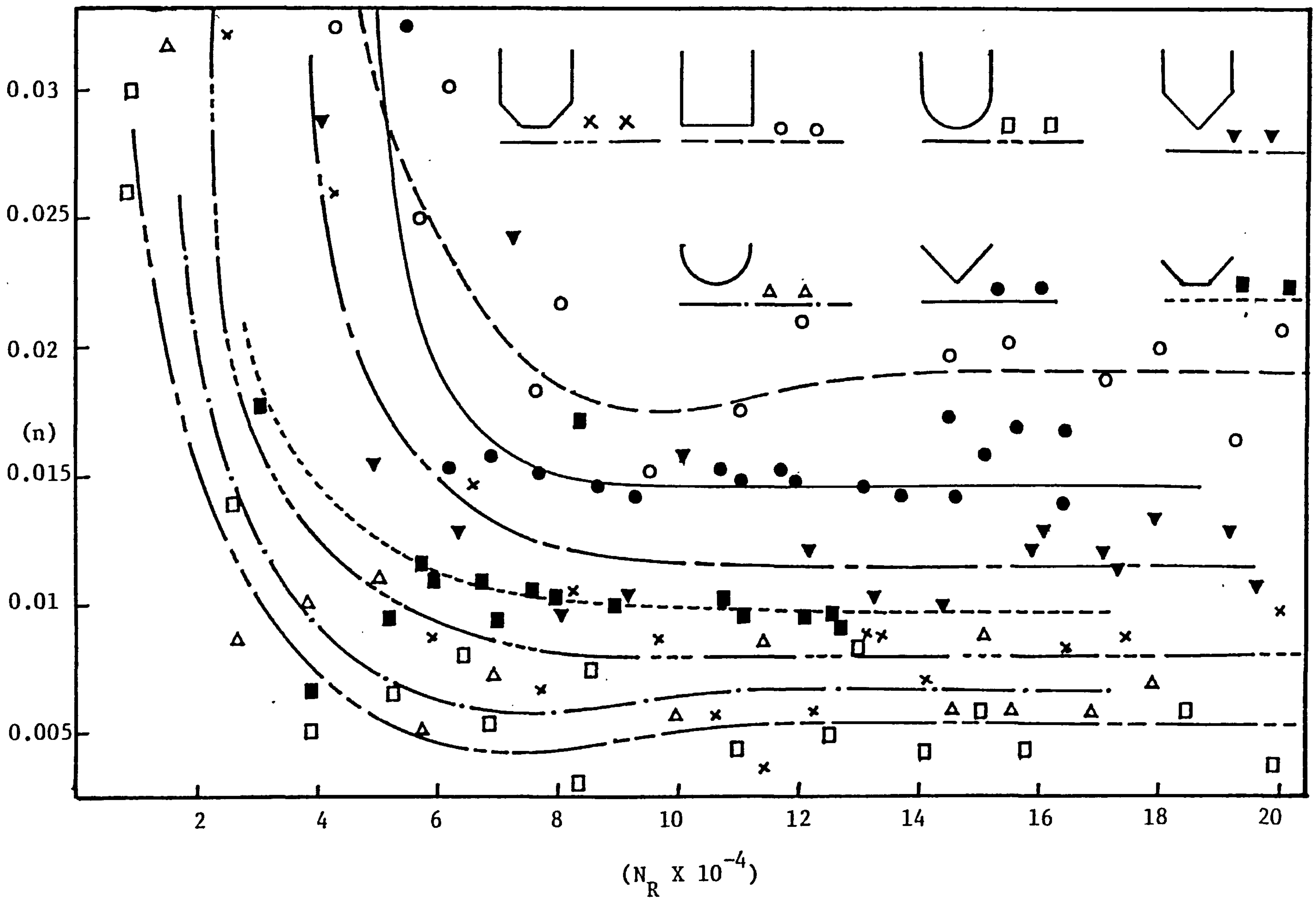

Fig. 5.5.1 n_1 of Different Shapes with Similar Lining Material n_C.

with similar lining material, different roughness coefficients will be expected. The most efficient geometric shape found is the semi-circular section. The reason can be related to the secondary motions mentioned in Chapter II, Section 2.4. The symmetric condition of uniform flow in semi-circular section greatly reduces the existence of secondary motions within the flow. Thus less energy loss will be encountered.

The second part of the testing involved experiments on channels with different geometric shapes, lining materials and buoyant covers. The results were graphed and shown in Fig. 5.5.2a,b to Fig. 5.5.5a,b .

For different combinations of channel shapes and lining materials, different roughness curves can be obtained. Thus, it concludes that mathematical models which involve precise definitions of geometric shapes and boundary roughnesses is needed to solve the complexity of channel hydraulics.

5.6 Comparison Between Experimental and Theoretical Composite Roughness

In verifying the utilization of the Division Surface Equation (3.7.4) and Composite Roughness Equation (3.8.3), fourteen experiments had been carried out on channels with different shapes and buoyant covers.

The experiments were separated into two groups, the

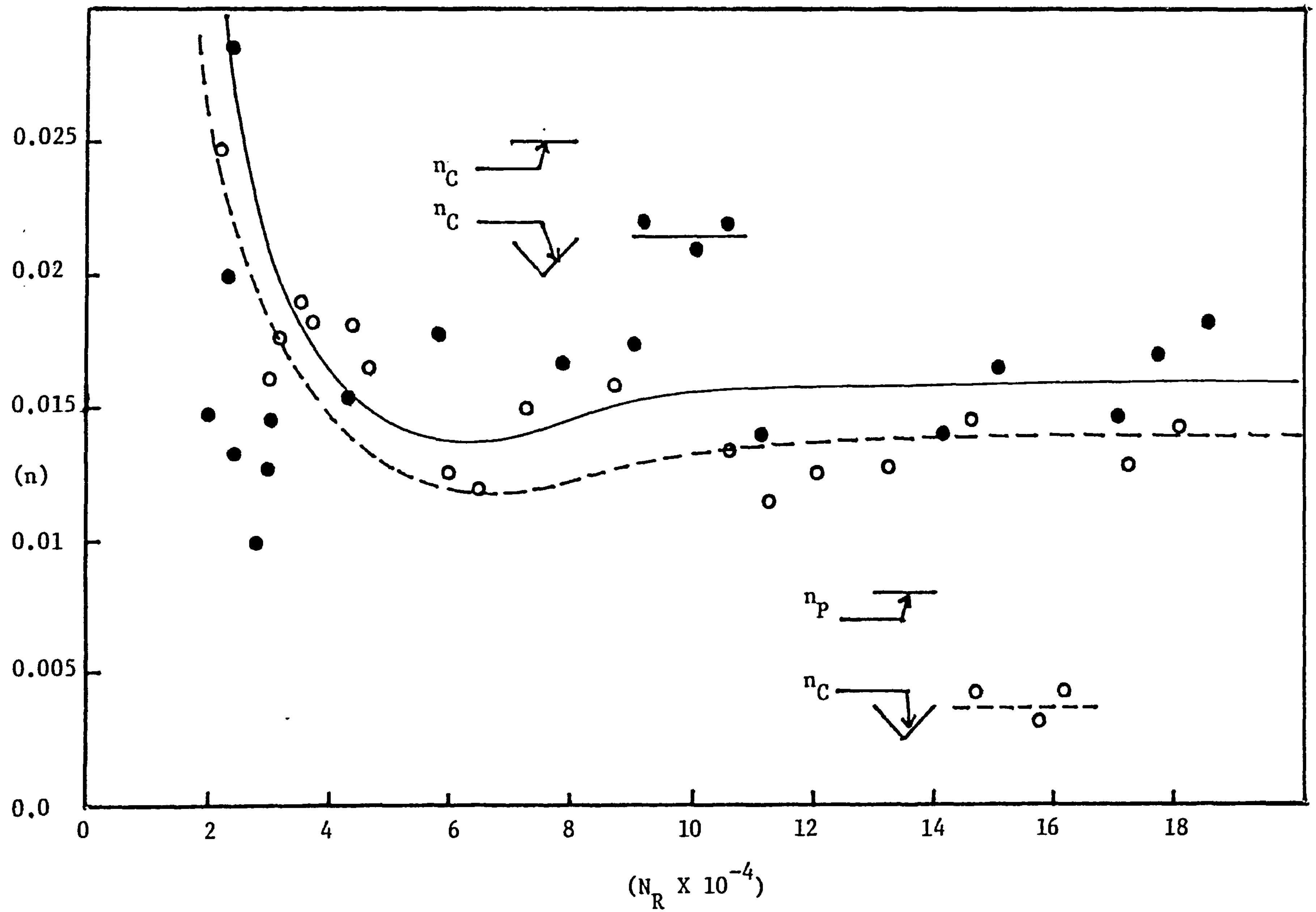

Fig. 5.5.2a Composite Roughness n_t of Channels With Different Cover Roughness.

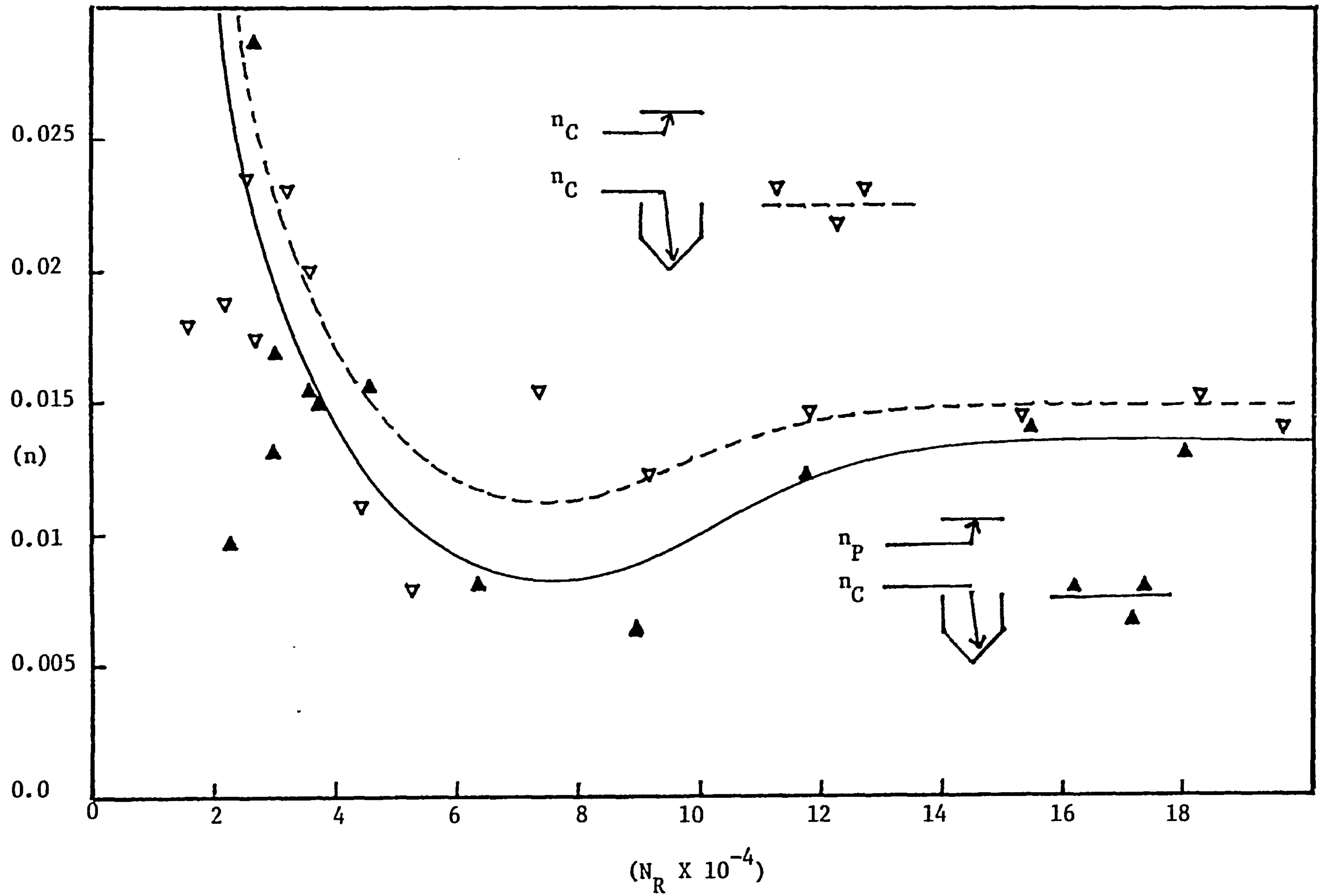

Fig. 5.5.2b Composite Roughness n_t of Channels With Different Cover Roughness

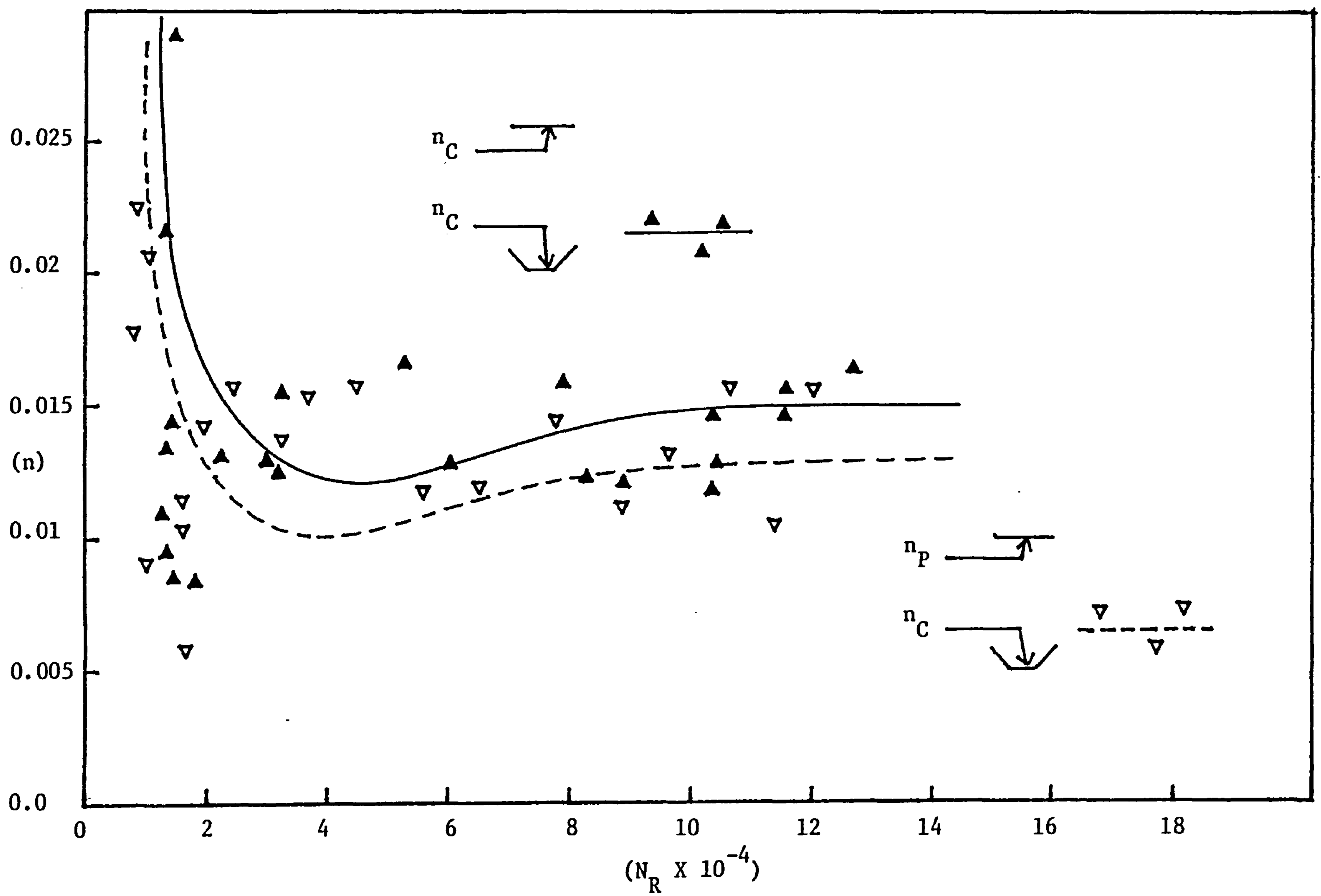

Fig. 5.5.3a Composite Roughness n_t of Channels with Different Cover Roughness.

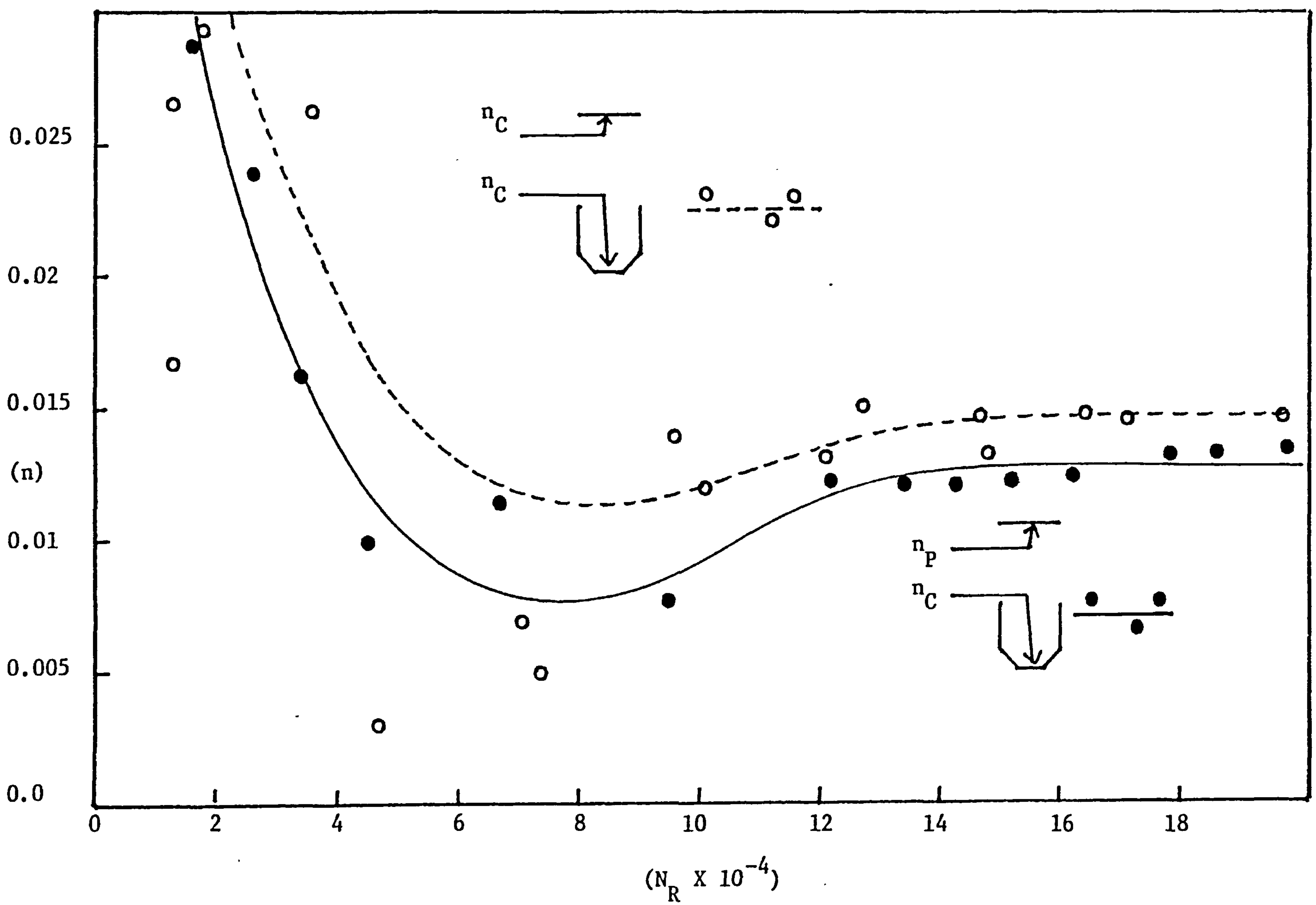

Fig. 5.5.3b Composite Roughness n_t of Channels With Different Cover Roughness.

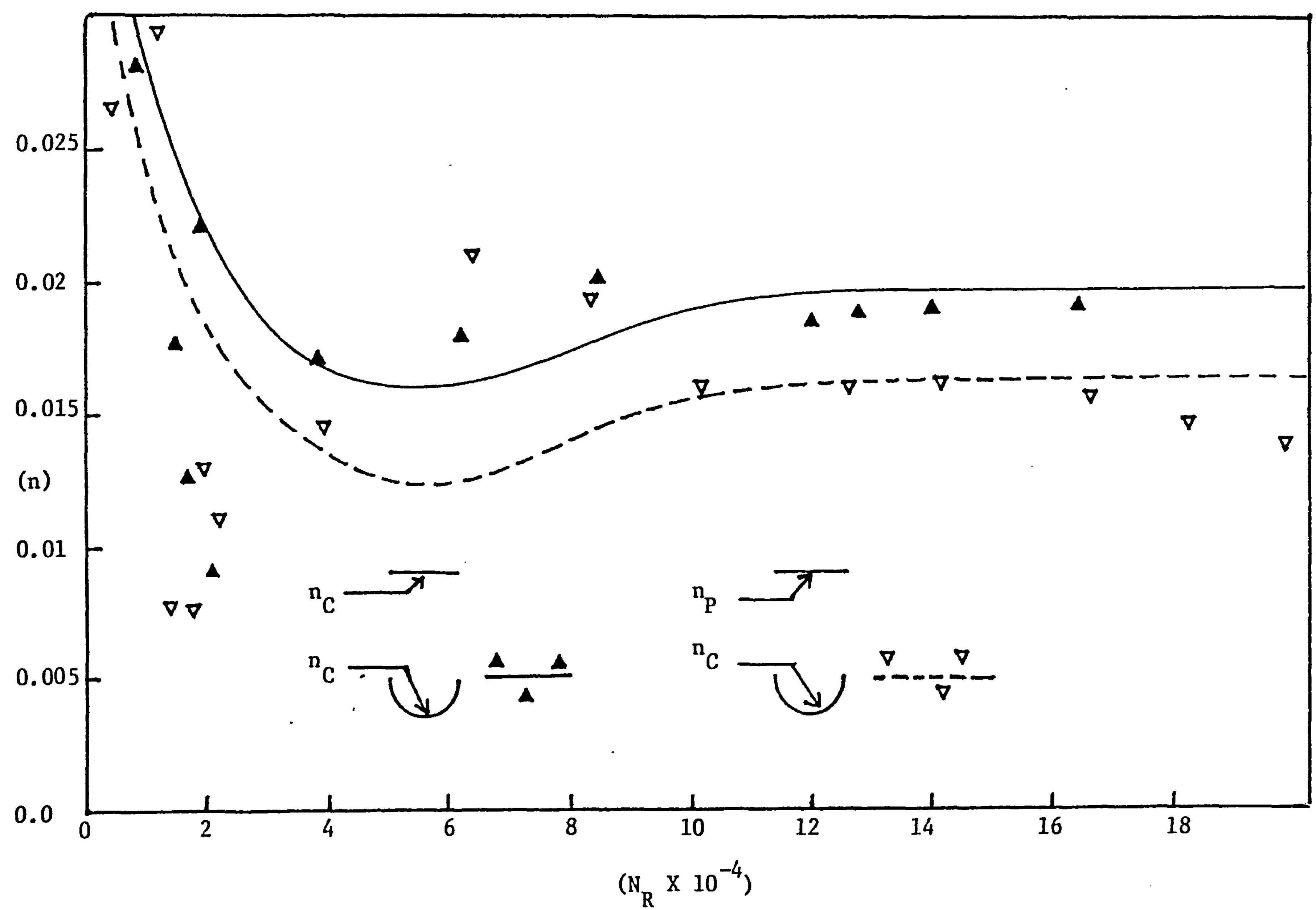

Fig. 5.5.4a Composite Roughness n_t of Channels With Different Cover Roughness.

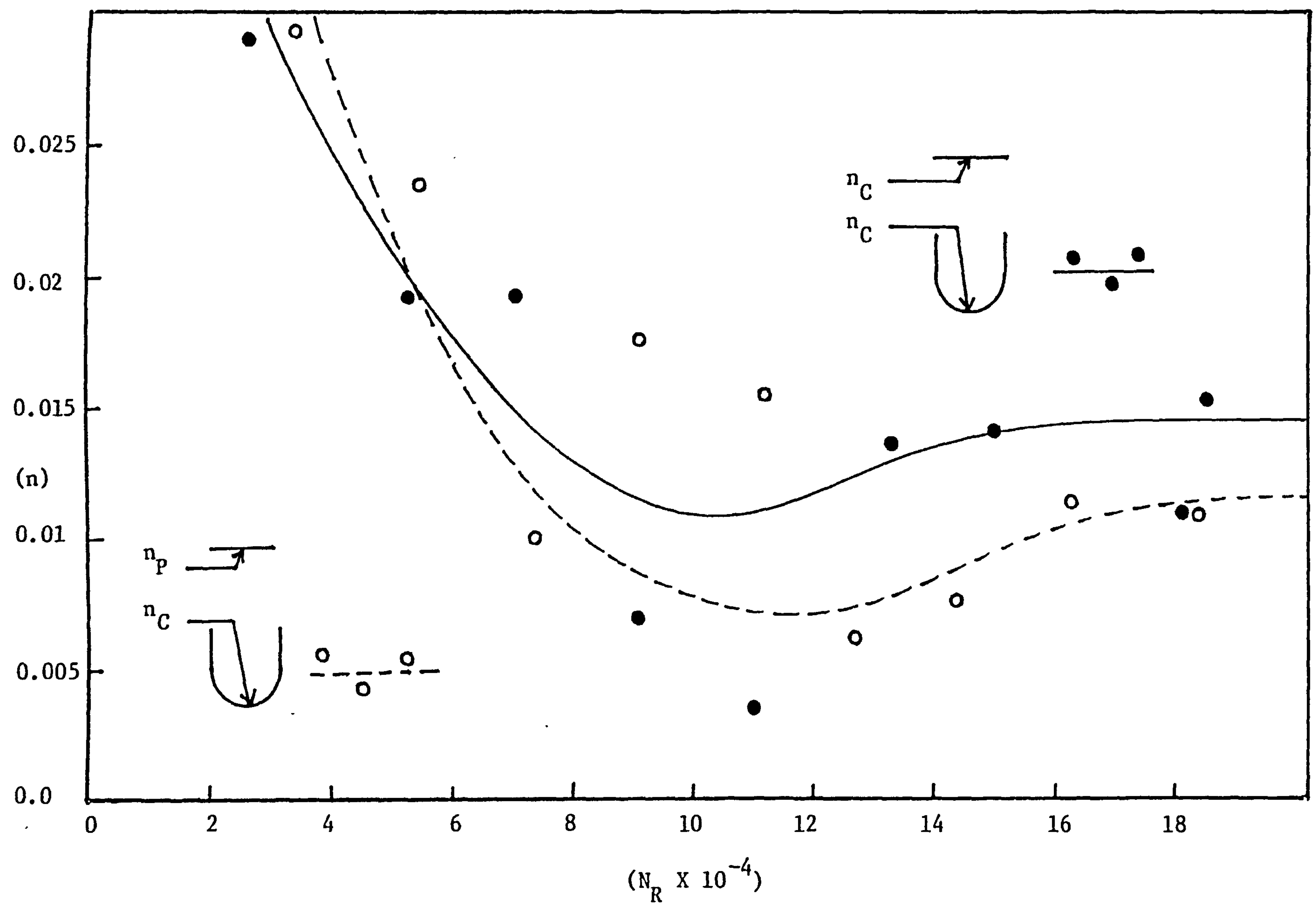

Fig. 5.5.4b Composite Roughness n_t of Channels with Different Cover Roughness.

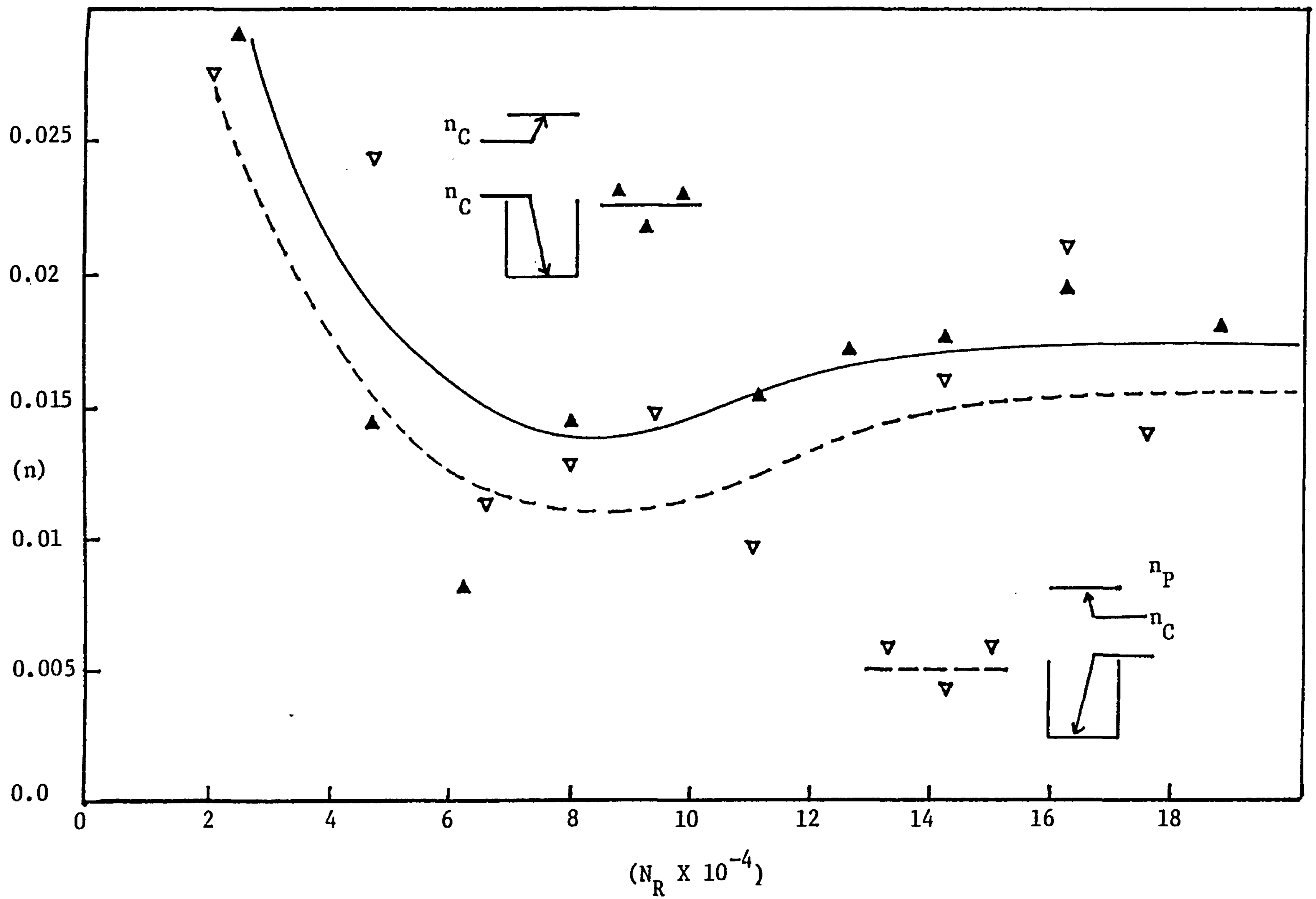

Fig. 5.5.5a Composite Roughness n_t of Channels With Different Cover Roughness.

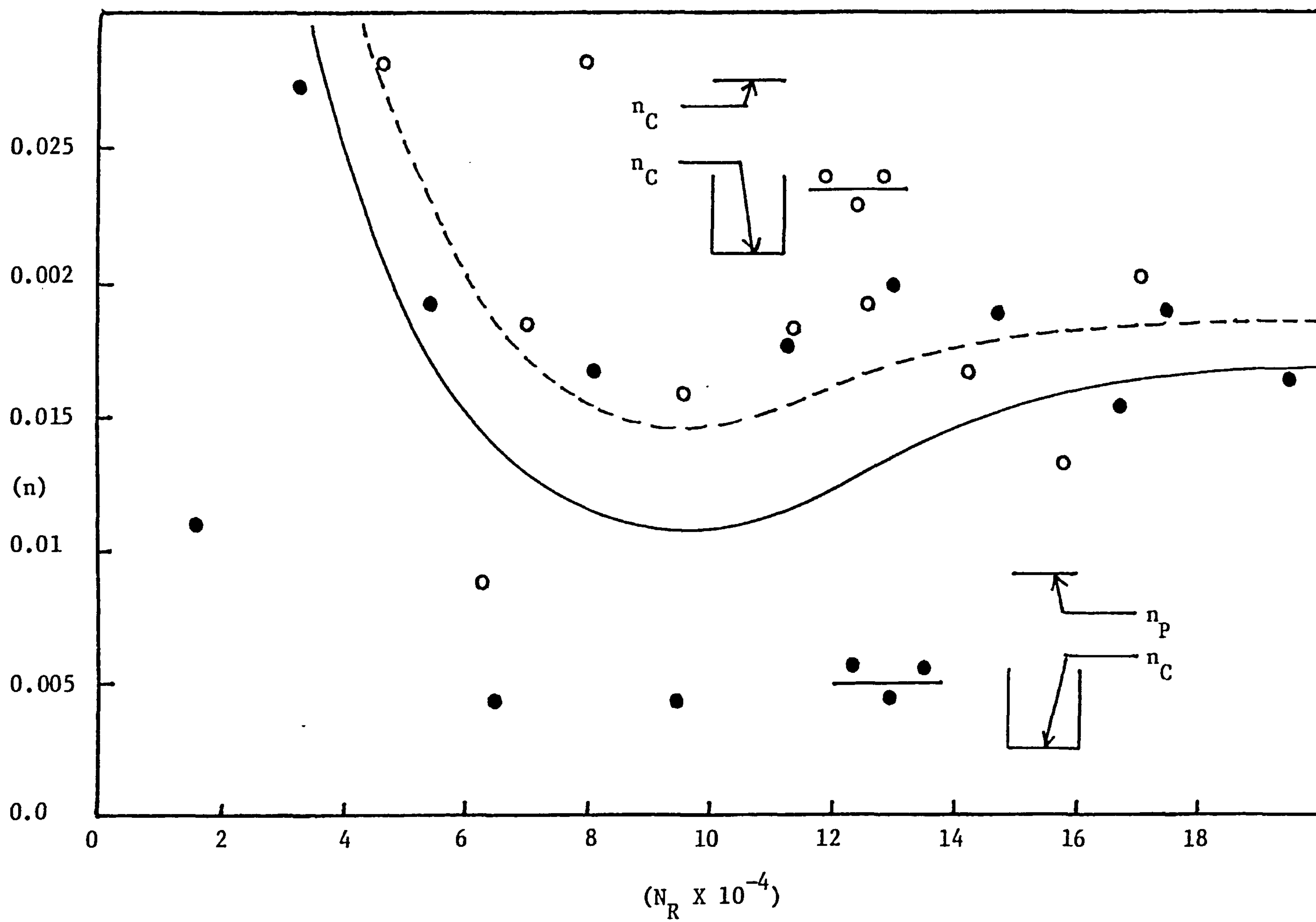

Fig. 5.5.5b Composite Roughness n_t of Channels With Different Cover Roughness.

first one involved channels with plywood blocks for the cover, and the second group with 2 1/2" x 1 1/4" coarse wire mesh. The experimental procedures were described as in Chapter IV, Section 4.3.2. The recorded data were then analyzed according to the procedures as shown in Fig. 5.6.1 . The results were shown in Fig. 5.6.2 to 5.6.15 and in Table(C.2.1) to (C.2.14).

Both cases show that, although there were variations in experimental composite roughness coefficients for different boundary conditions, the theoretical curves generated by Eq. (3.8.3) were more or less the same. This behaviour implies that Eq. (3.8.3) is not so sensitive in response to shape effects as is to be expected. The same argument can also be found as in Chapter II, Section 2.3 and in this chapter, Section 5.2.

In Section 2.3, the introduction of a shape factor ϕ in Eq. (2.3.26) to form the correlation between the experimental and theoretical predicted n_t implied that Eq. (3.8.3) cannot be used to evaluate the composite n_t directly with regards to channel configurations. And in Section 5.2, the insensitivity of λ to the changes of α values also indicated that, the α parameter failed to represent the shape effects within the relation.

It is suspected that the wide channel assumption $R \simeq Y$ used in deriving the relations caused this vital

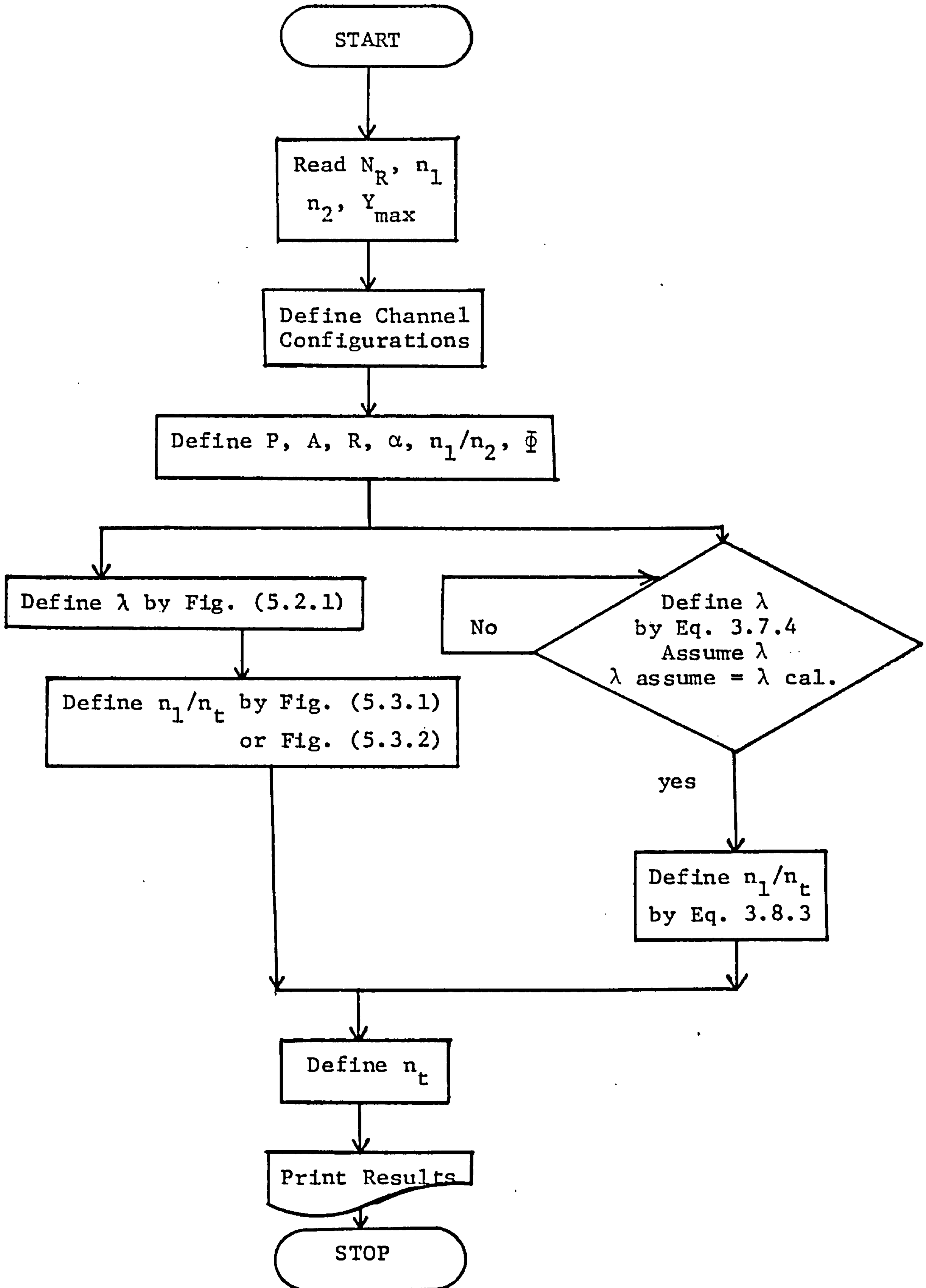

Fig. 5.6.1 Flow Chart for Estimating Theoretical Manning's n of Covered Channels.

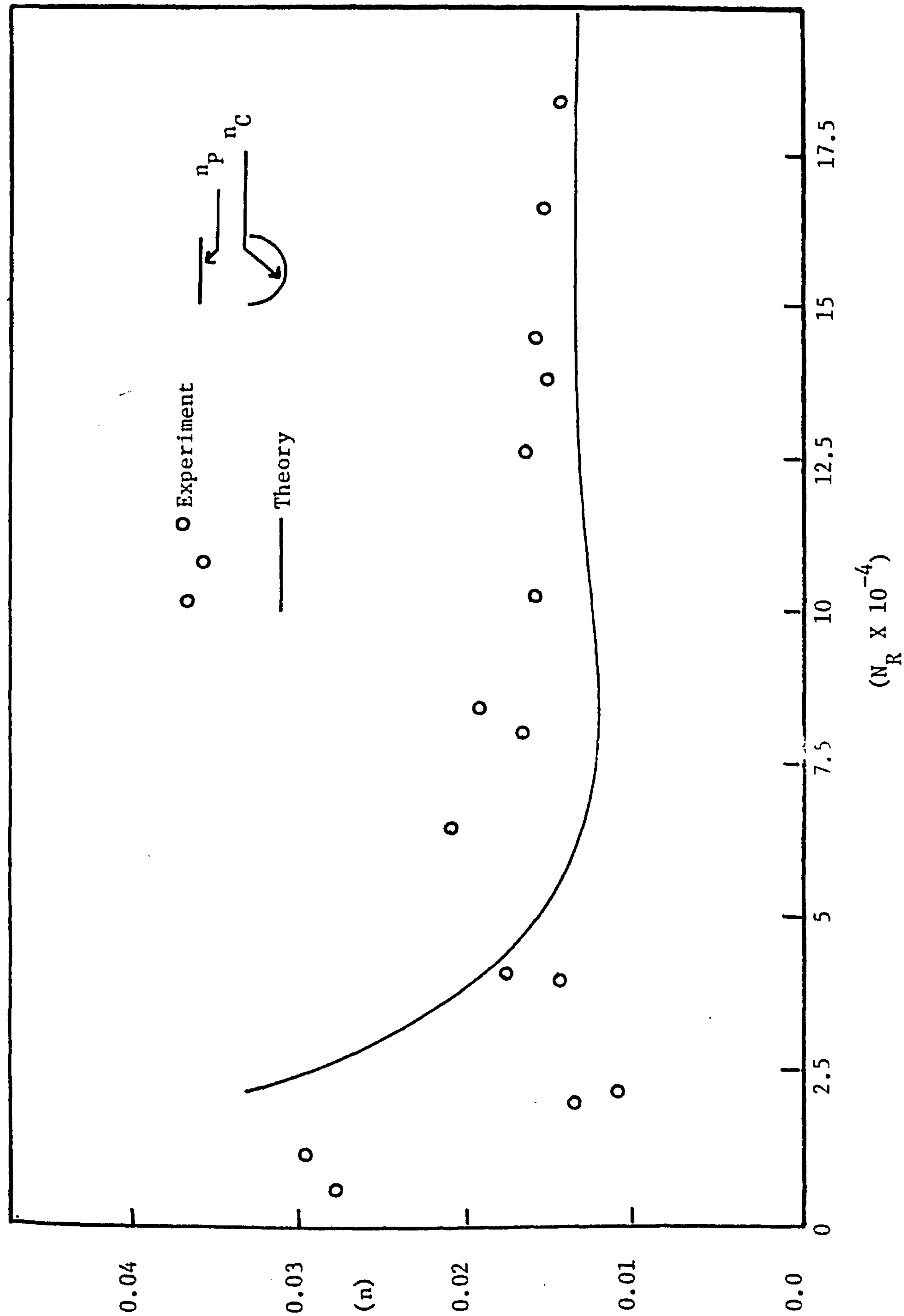

Fig. 5.6.2 Experimental and Theoretical Composite Roughness

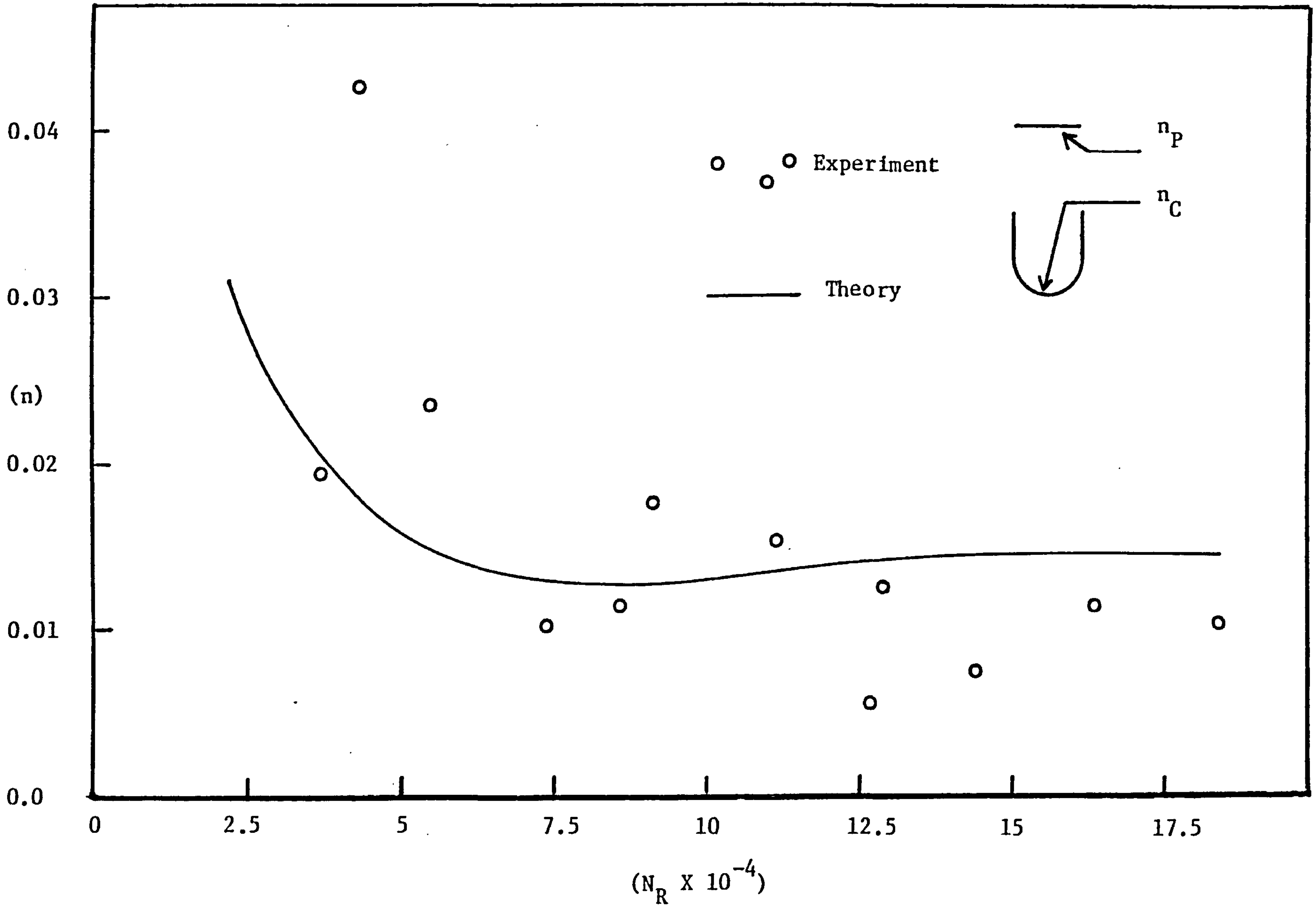

Fig. 5.6.3 Experimental and Theoretical Composite Roughness.

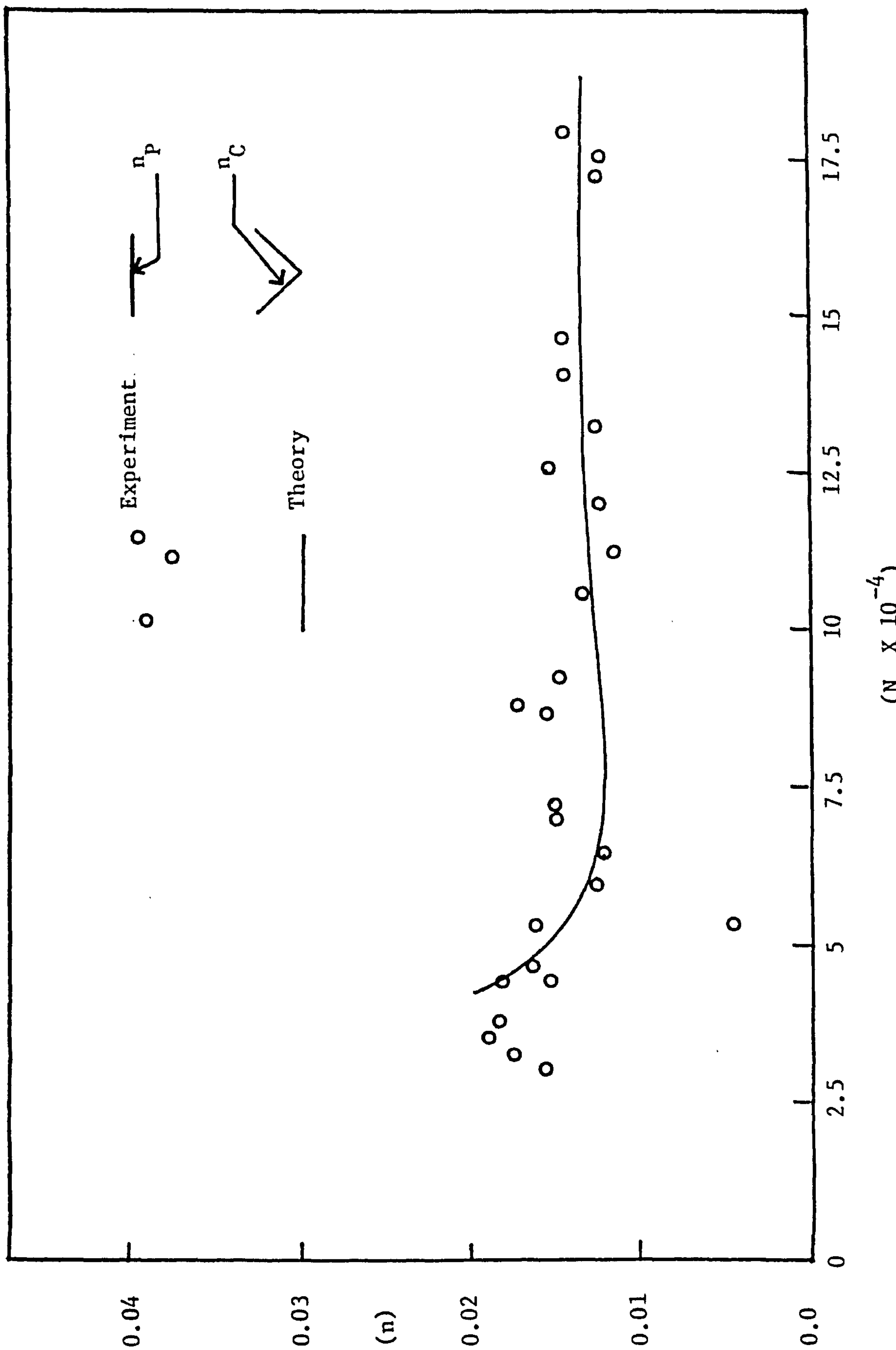

Fig. 5.6.4 Experimental and Theoretical Composite Roughness.

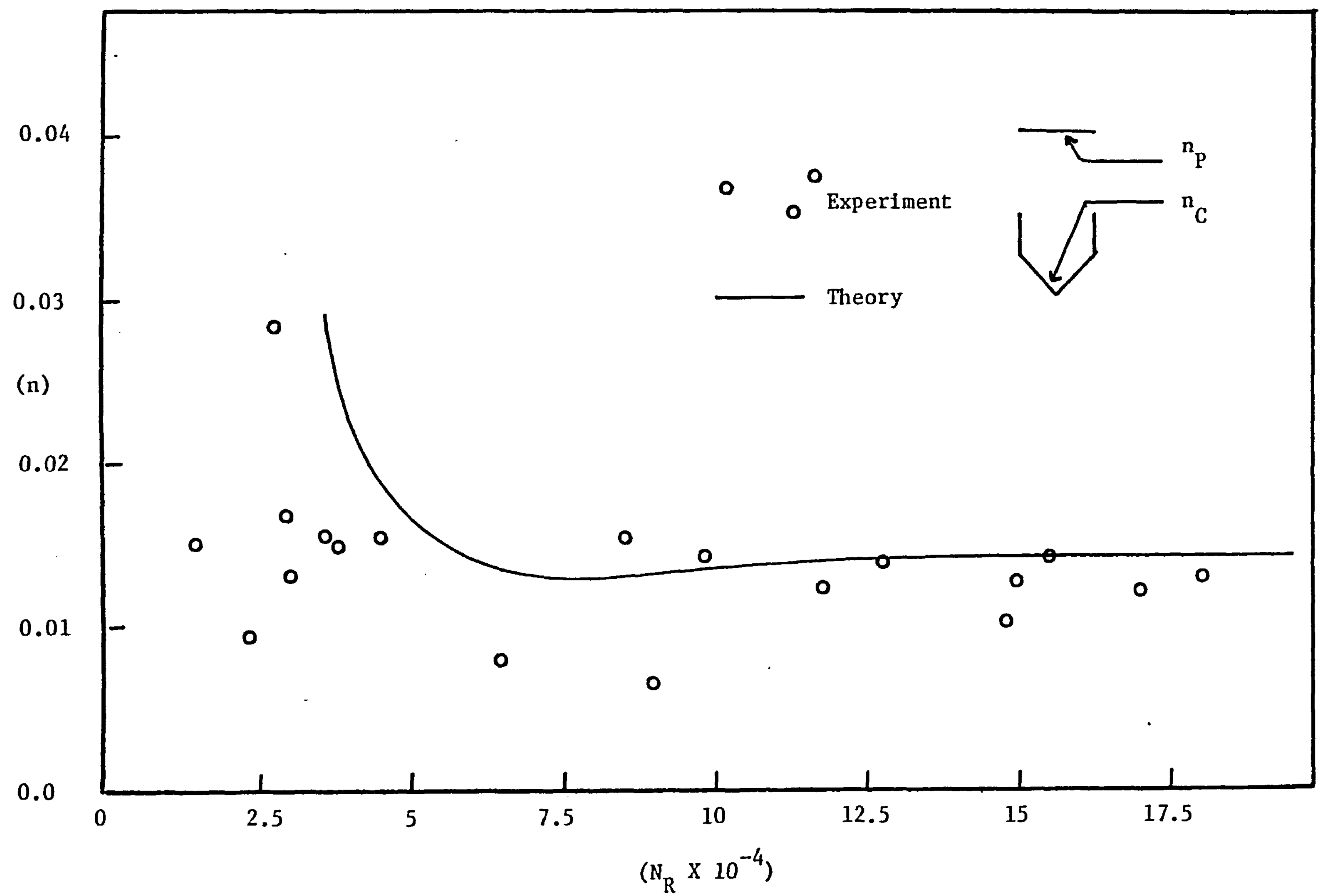

Fig. 5.6.5 Experimental and Theoretical Composite Roughness.

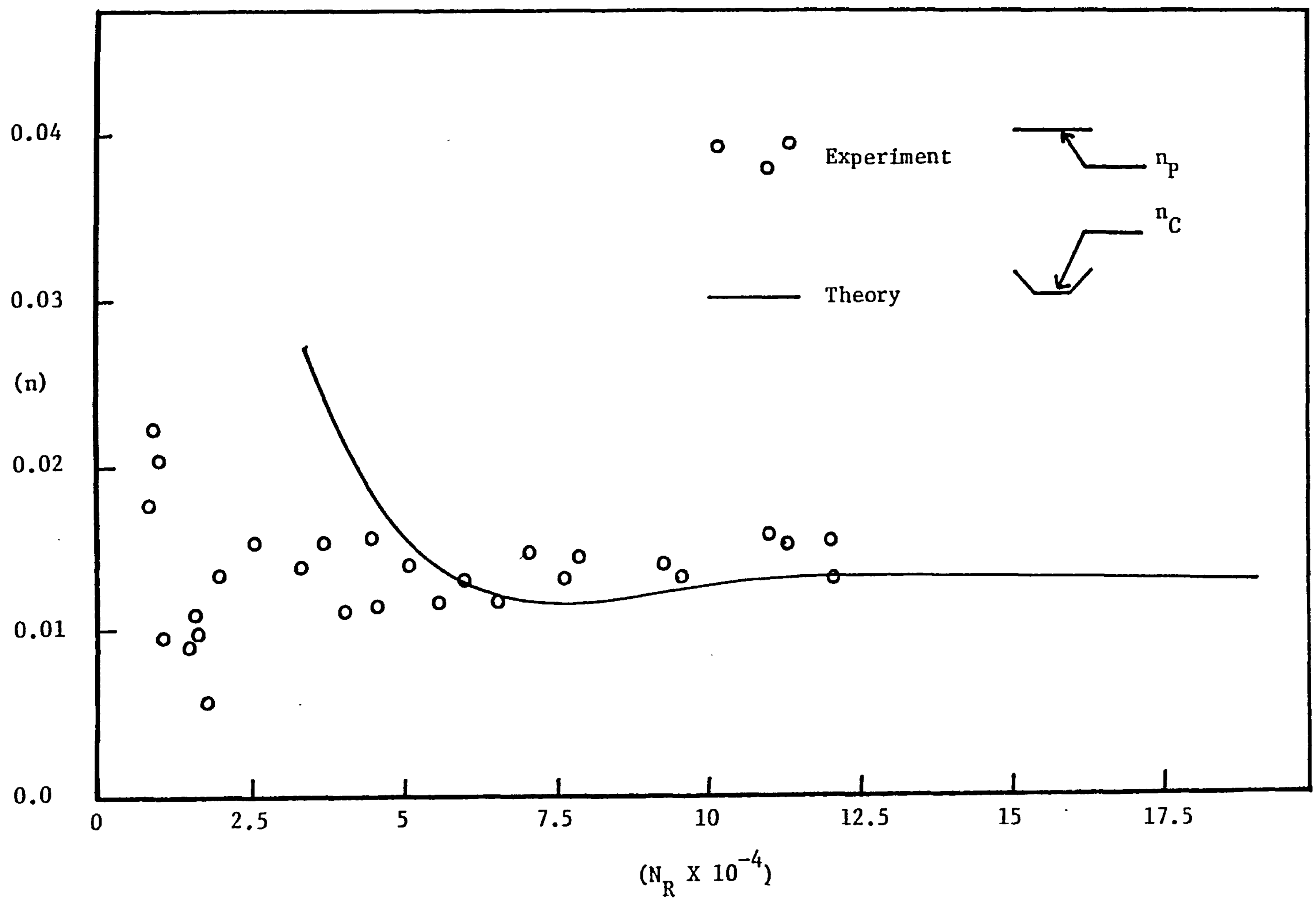

Fig. 5.6.6 Experimental and Theoretical Composite Roughness

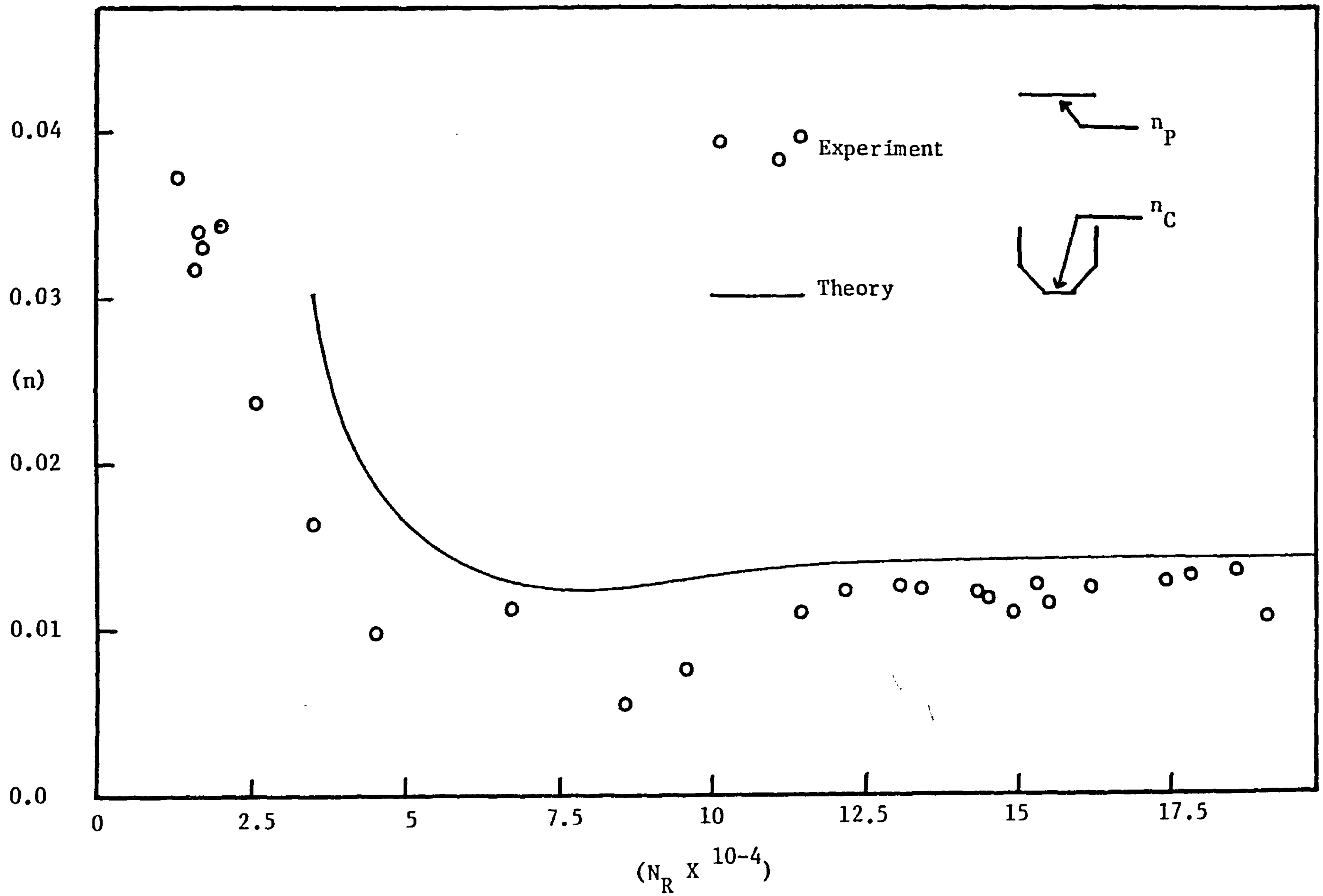

Fig. 5.6.7 Experimental and Theoretical Composite Roughness.

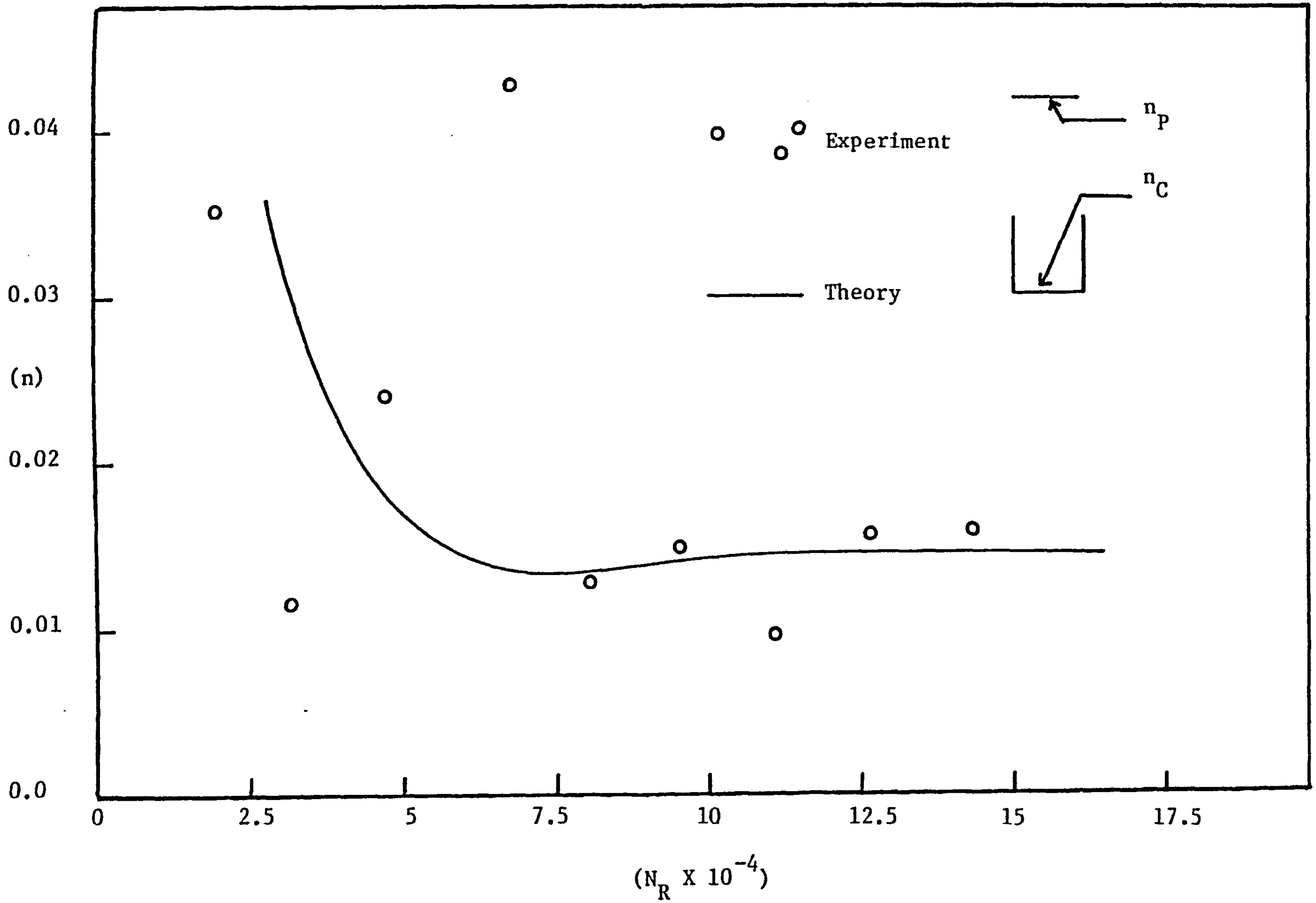

Fig. 5.6.8 Experimental and Theoretical Composite Roughness.

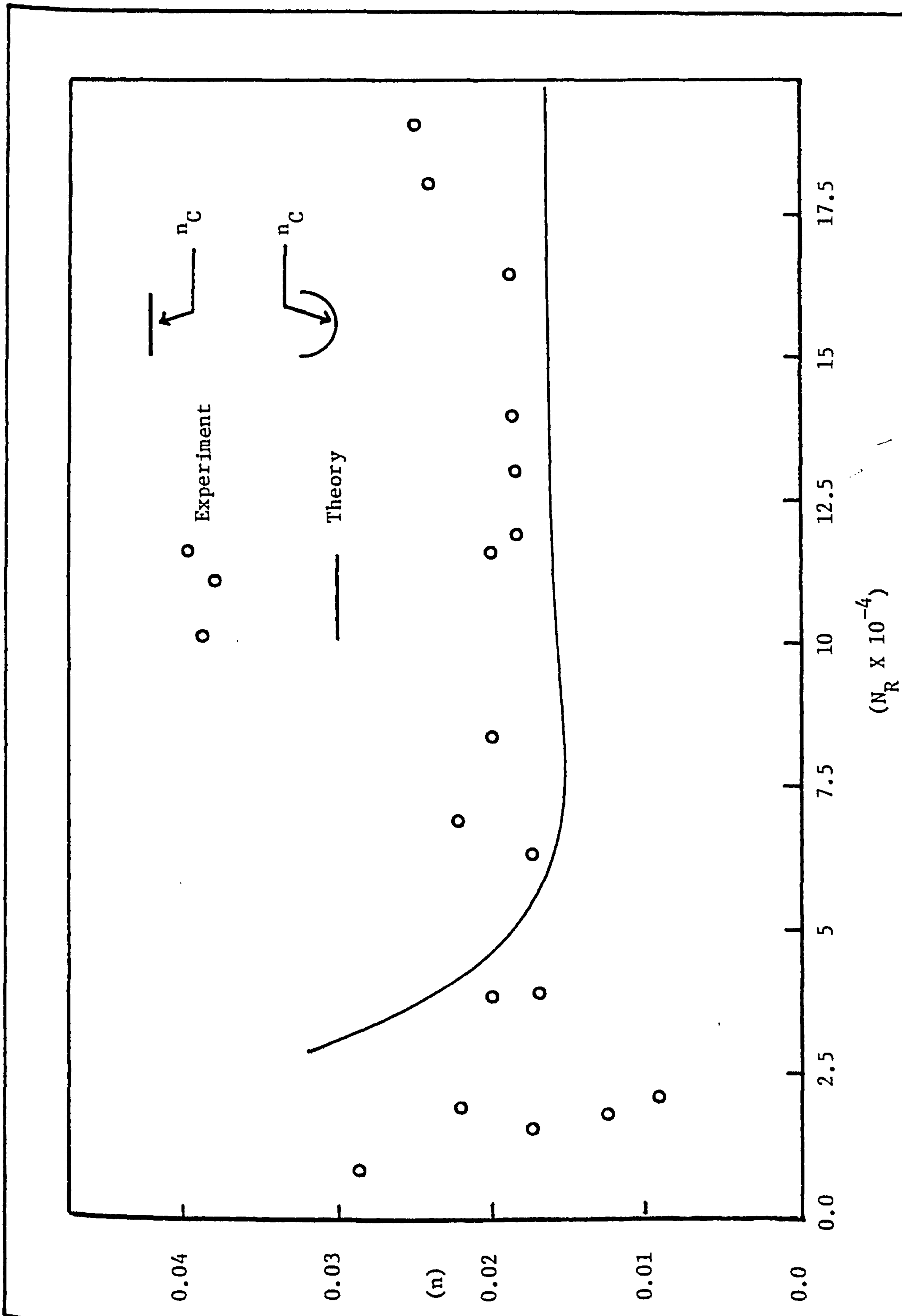

Fig. 5.6.9 Experimental and Theoretical Composite Roughness.

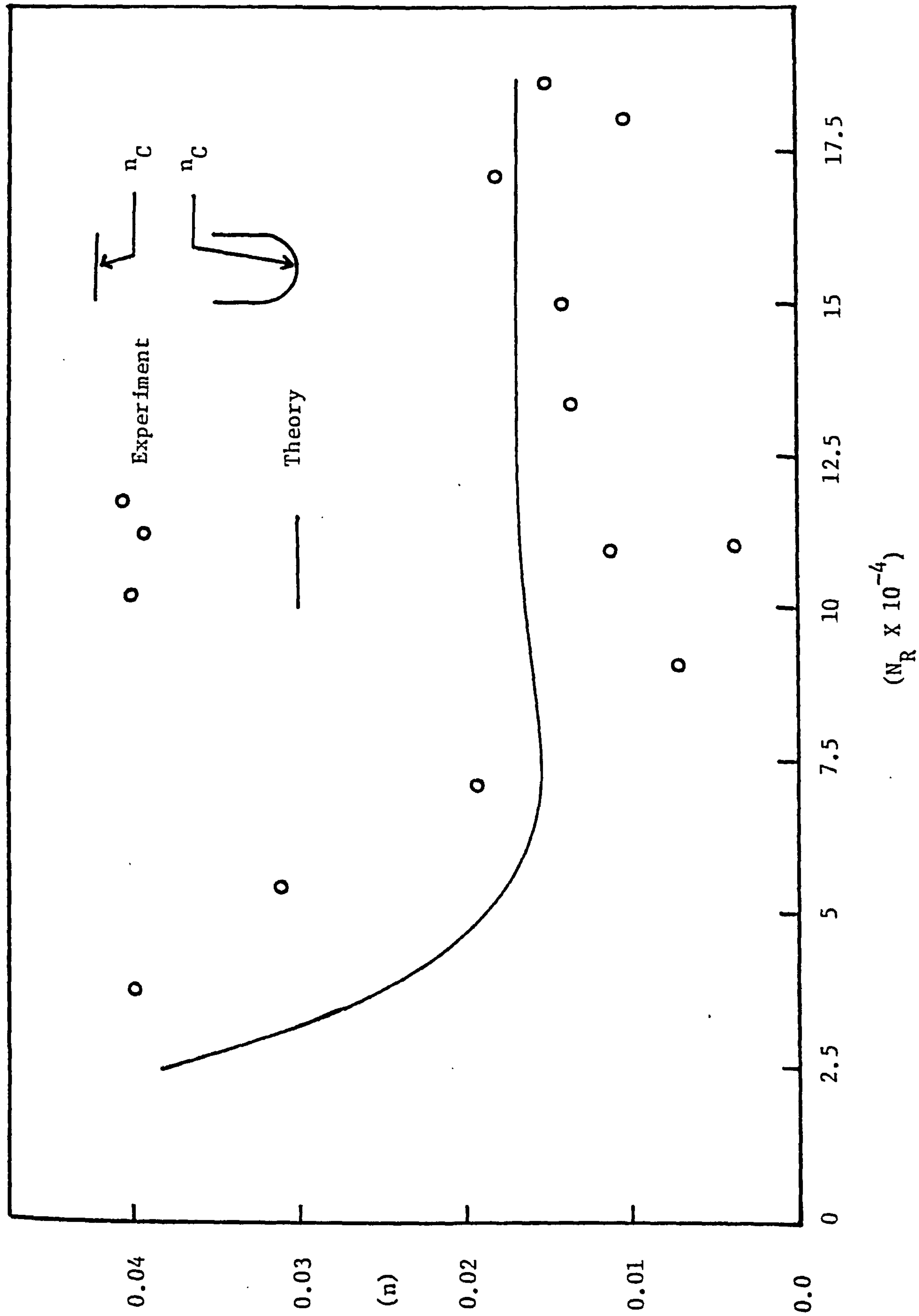

Fig. 5.6.10 Experimental and Theoretical Composite Roughness.

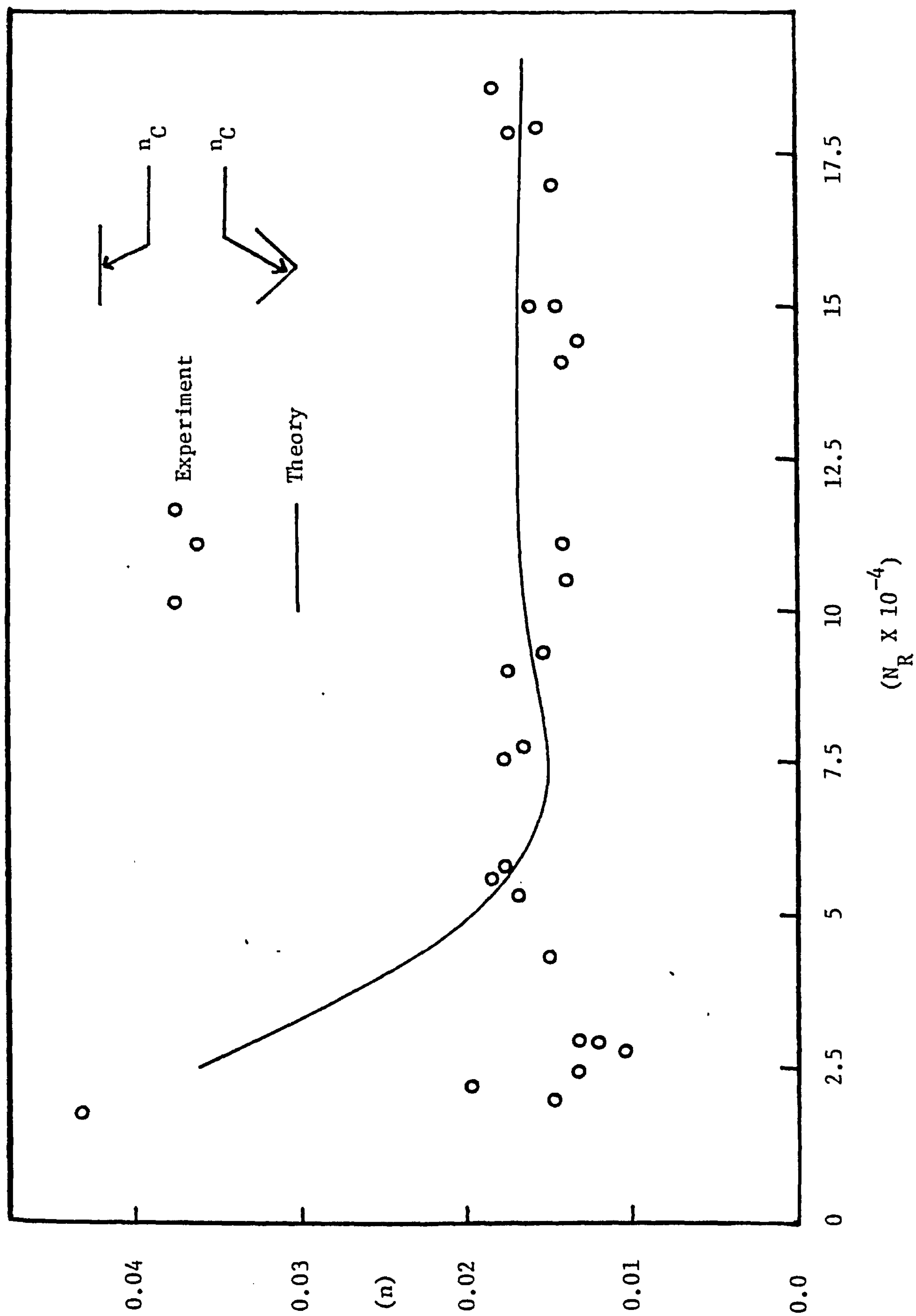

Fig. 5.6.11 Experimental and Theoretical Composite Roughness.

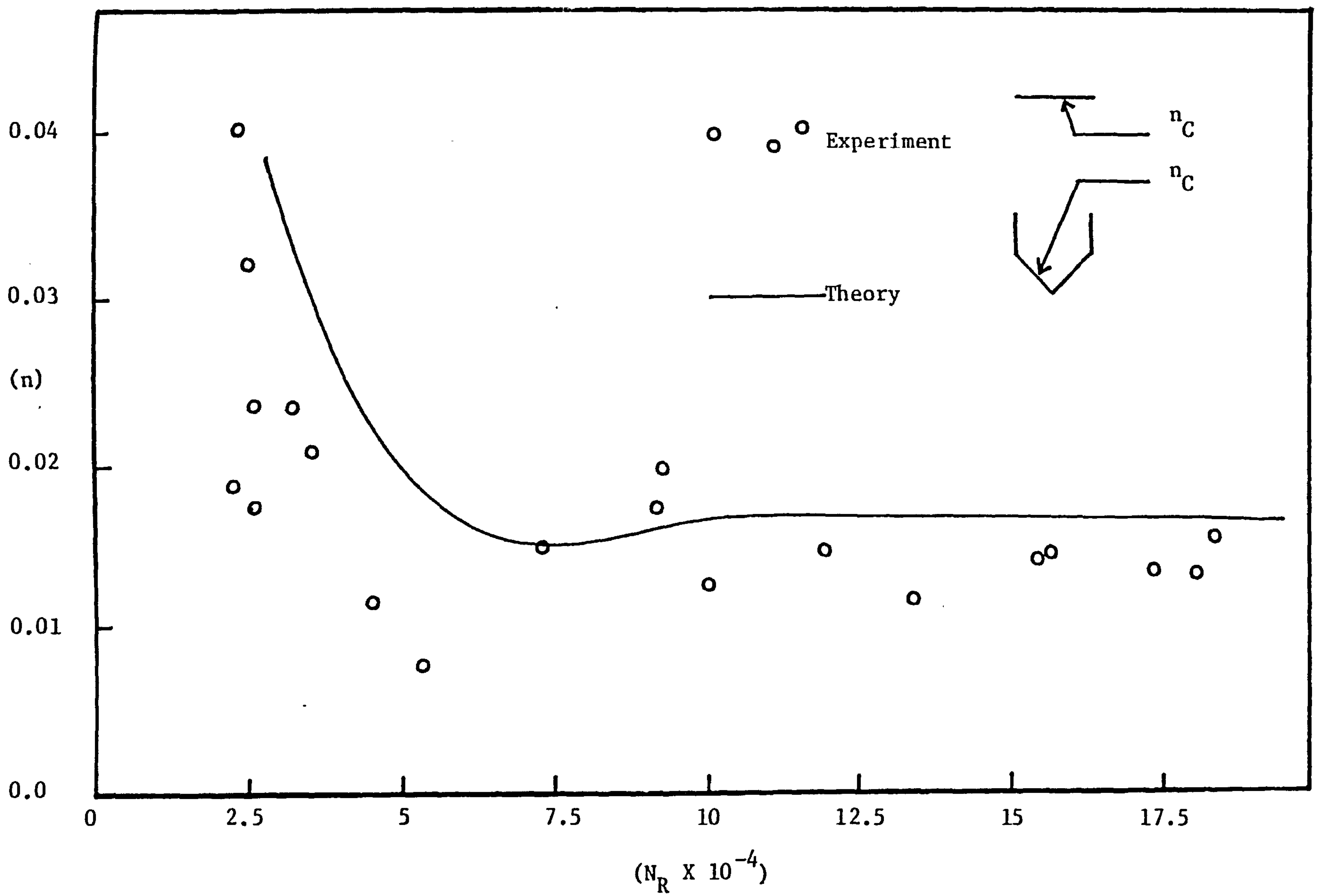

Fig. 5.6.12 Experimental and Theoretical Composite Roughness.

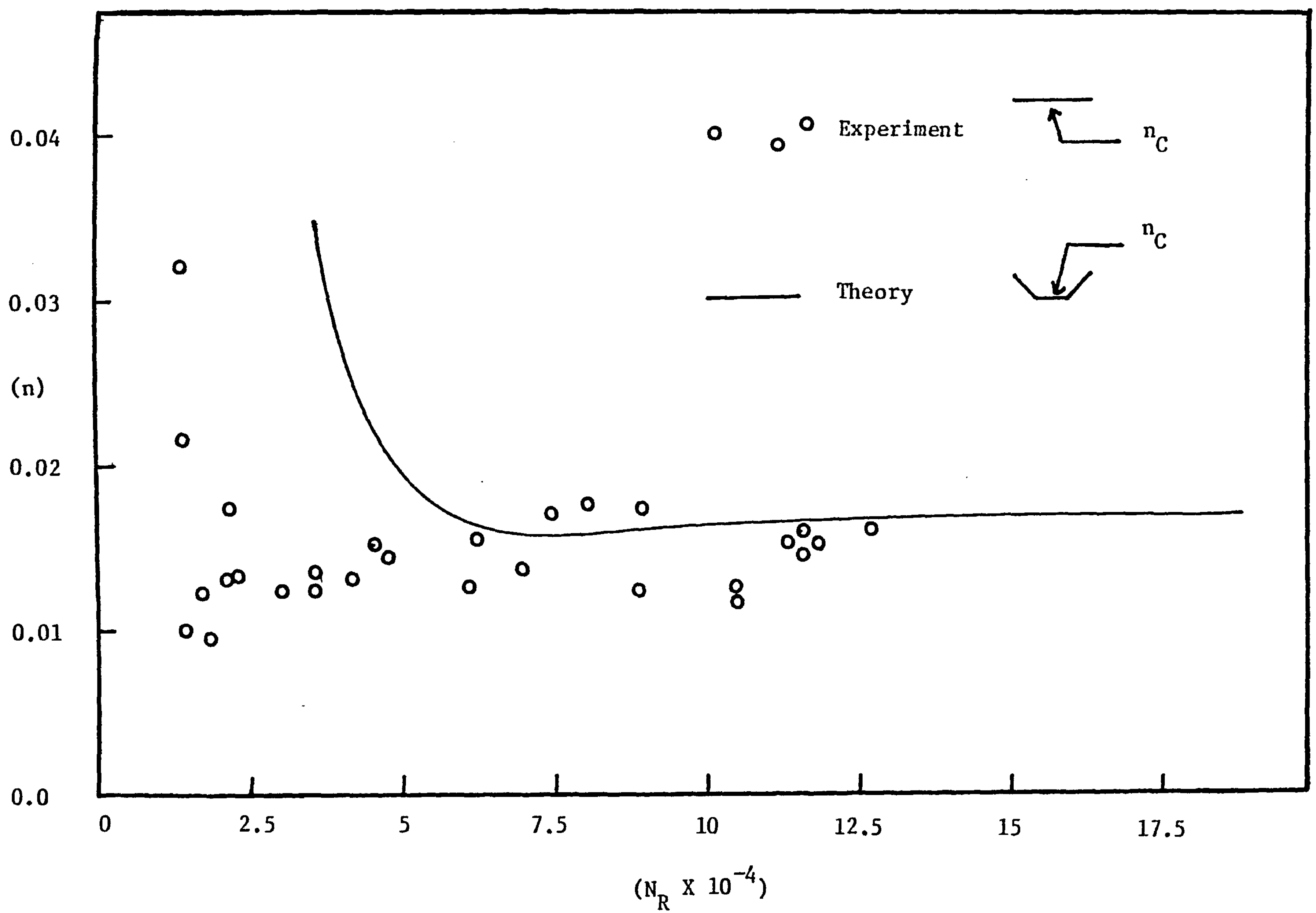

Fig. 5.6.13 Experimental and Theoretical Composite Roughness

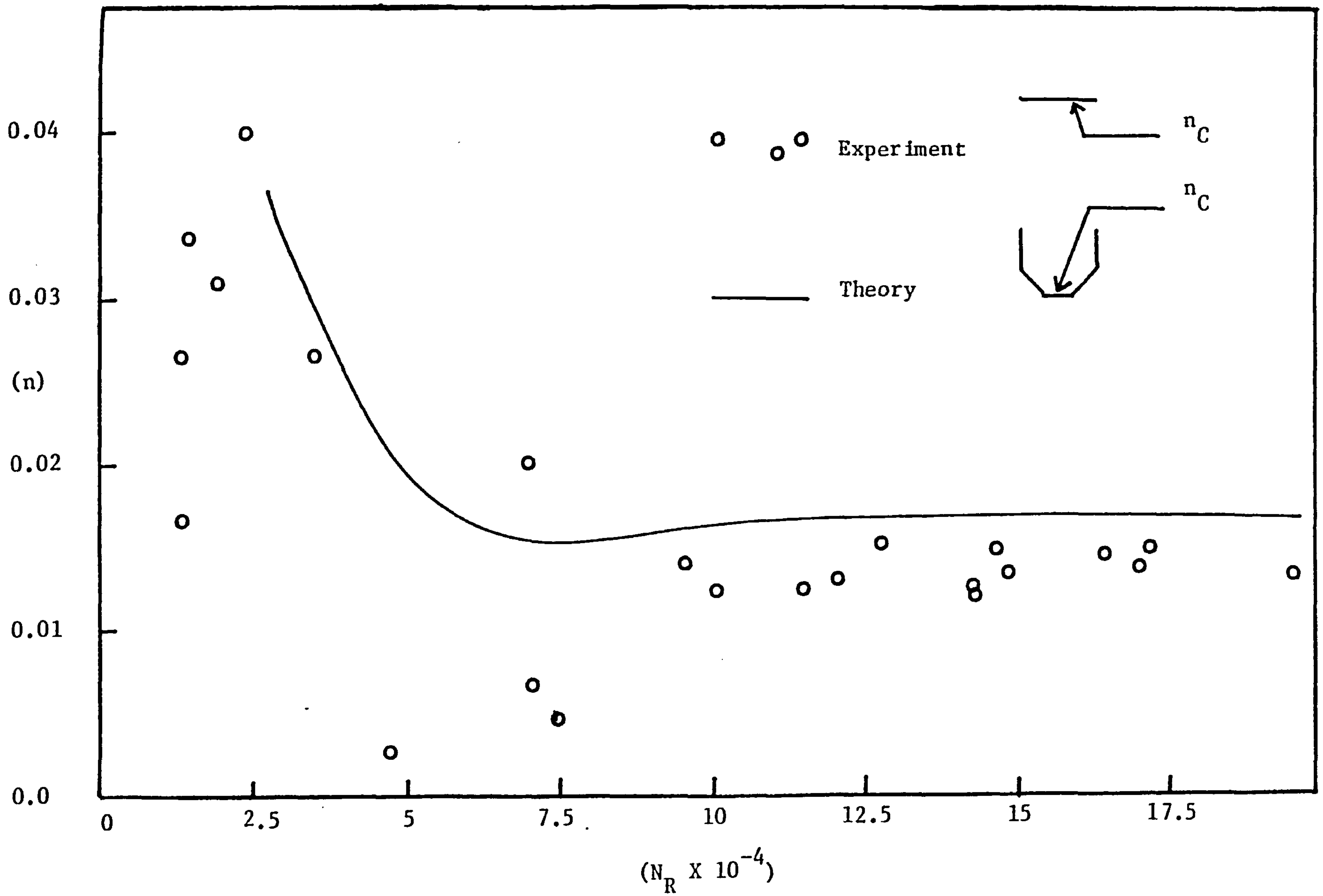

Fig. 5.6.14 Experimental and Theoretical Composite Roughness.

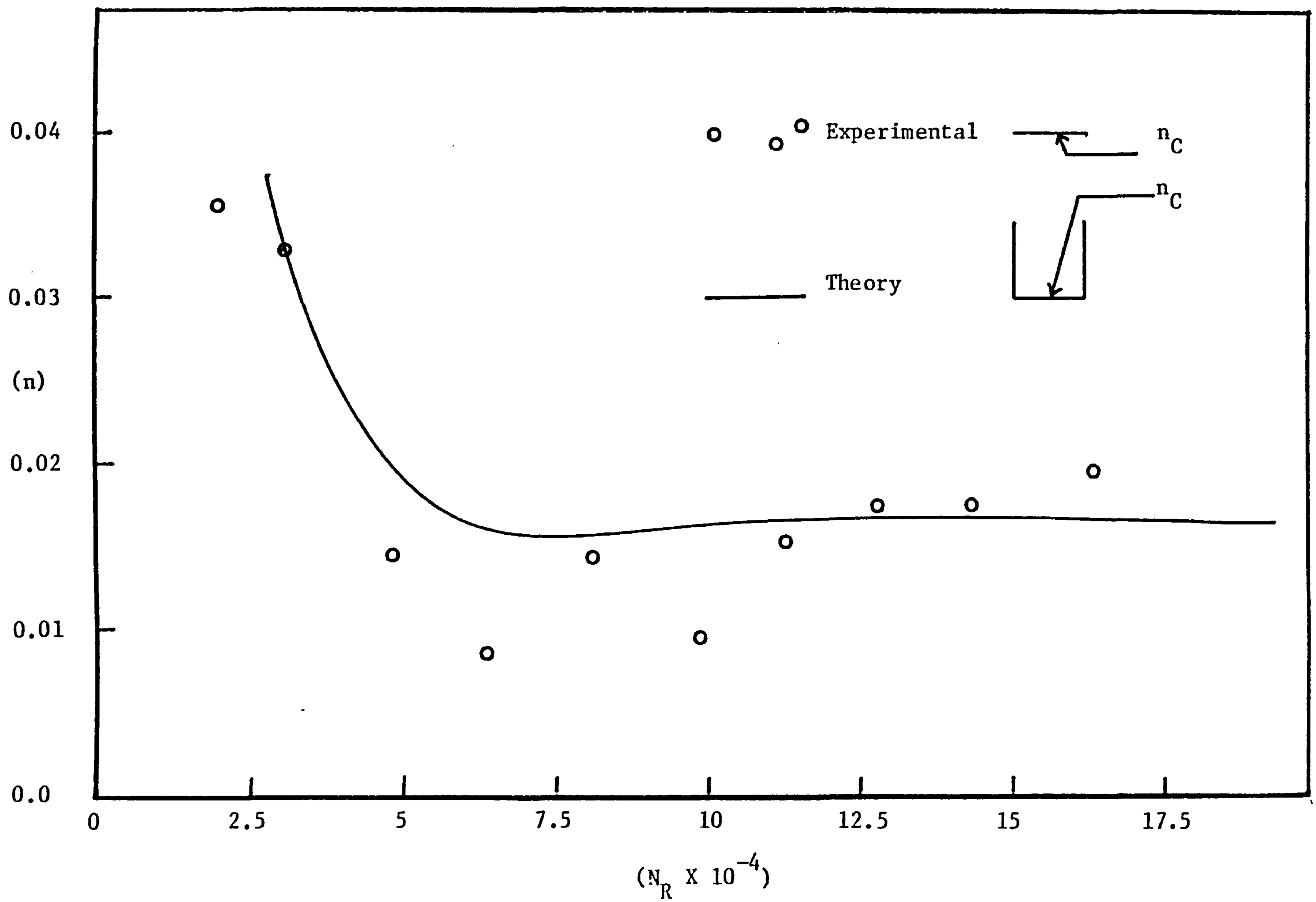

Fig. 5.6. 15 Experimental and Theoretical Composite Roughness.

disadvantage of utilizing Eq. (3.7.4) and Eq. (3.8.3).

In the following section, the introduction of the finite strip method into the analytical model in order to eliminate the above disadvantage is examined.

5.7 Comparison of Velocity Profiles Using Finite Strip Approach

To study the effect of channel shapes and boundary roughnesses on the flow pattern, sixty seven experiments were tested. All seven channel configurations together with three different kinds of roughness elements combined to form different settings for analysis. The experimental procedures were described as in Chapter IV, Section 4.3.3. The recorded velocity traverses were analyzed according to the procedures as shown in Fig. 5.7.1 . The theoretical and experimental velocity traverses are listed in Appendix C.4, Table (E-13)to Table (E-93). There are several important aspects which had been deduced from the data analysis, and they are going to be discussed in the following sections.

5.7.1 Percentage Difference Between Experimental and Predicted Local Velocities

The percentage difference between measured and predicted point velocities ranged from less than 1% minimum, and up to 11% maximum.

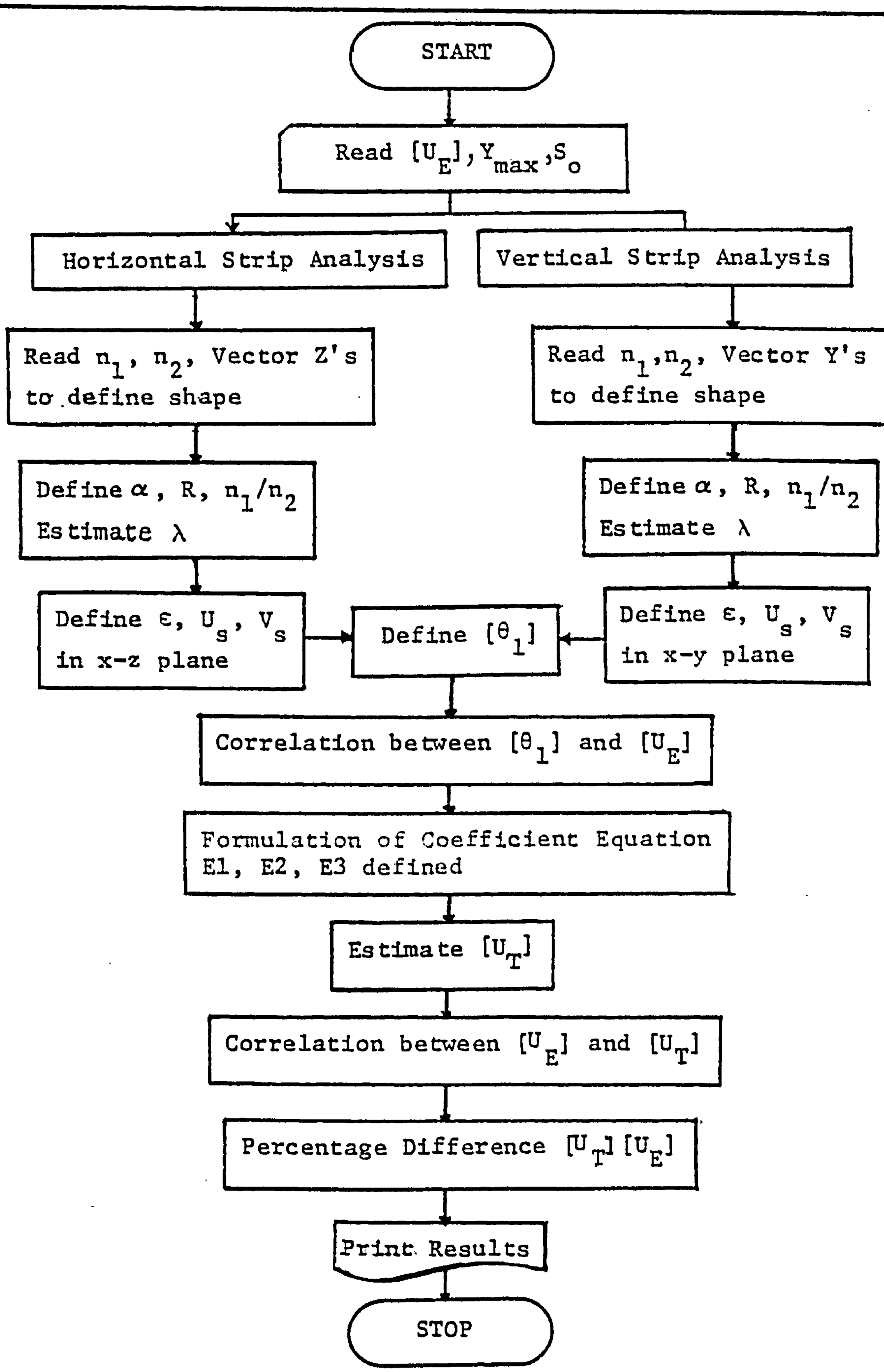

Fig. 5.7.1 Flow Chart for Estimating Velocity Profiles by Finite Strip Approach.

The estimated percentage error in measuring local velocities which is discussed in this chapter, section 5.8 has been found to be ±5%. It seems that both ranges are compatible to each other.

Since, the mean velocity was obtained by integrating the local velocity traverse with respect to the finite areas, it's level of error should fall into the same range as in the above case. Thus, the estimated percentage error in mean velocity of ≈ ±6% described in Section 5.8 is acceptable.

5.7.2 Behavior of Coefficient Equations

The two coefficient equations discussed in Chapter III, Section 3.9, Eq. (3.9.1) and Eq. (3.9.2) had been tested against the experimental data.

The coefficients E1 and E3 had been recorded graphically as in Fig. 5.7.2.1 to Fig. 5.7.2.2 and E2 in Table C.5.1. For all seven configurations with different boundary conditions, the values of E1 shown in Fig. 5.7.2.1 has more or less a constant value of ≈ 0.975, when they were separated from the (V_{max}/V) ratios, the values of E3 can be obtained. Fig. 5.7.2.2 shows that E3 has slightly more scatter than E1 with a mean value of ≈ 1.135. The values of E2 are shown in Table C.5.1. The variations between the data ranged from 0.164 up to 2.600.

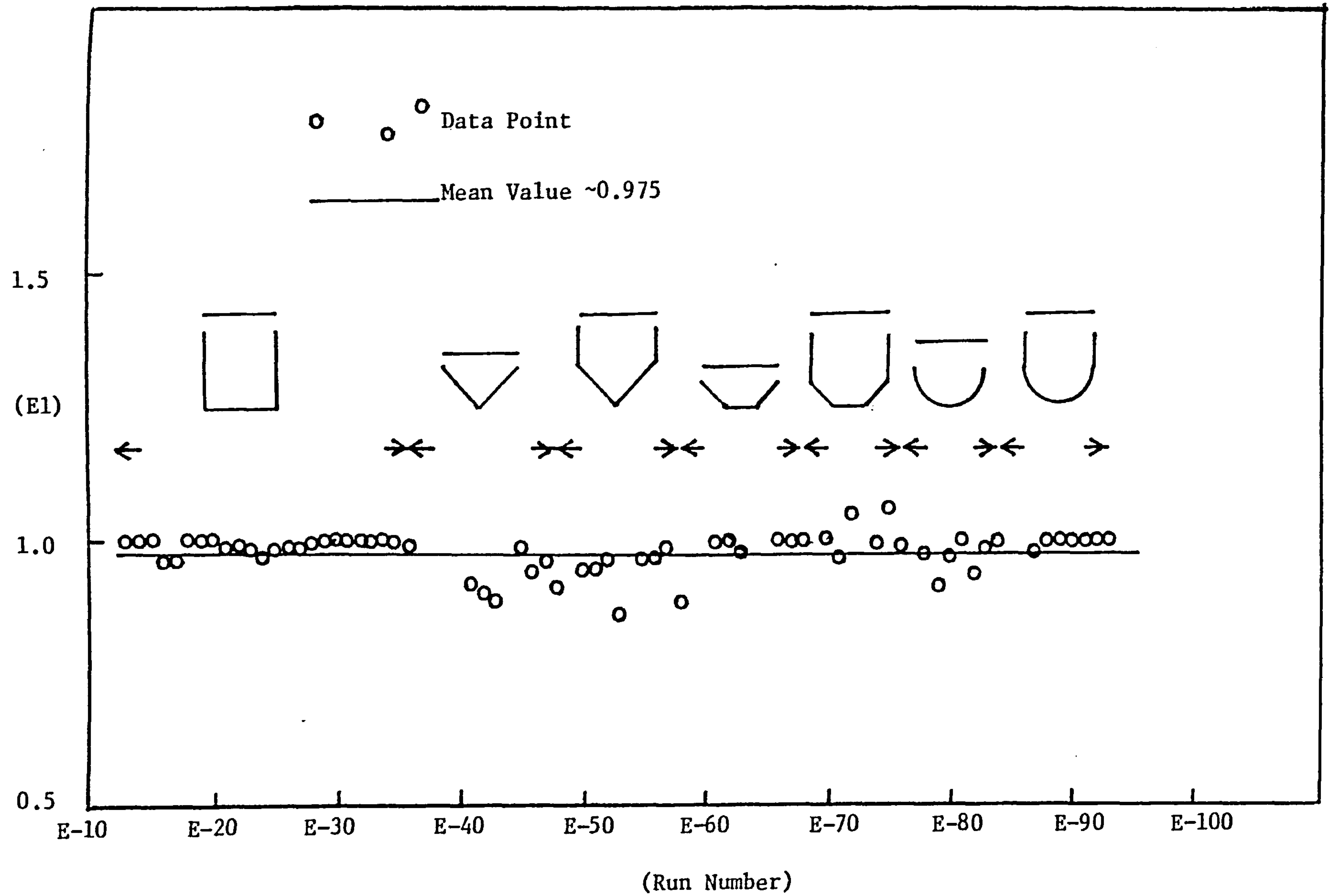

Fig. 5.7.2.1 Velocity Coefficient E1.

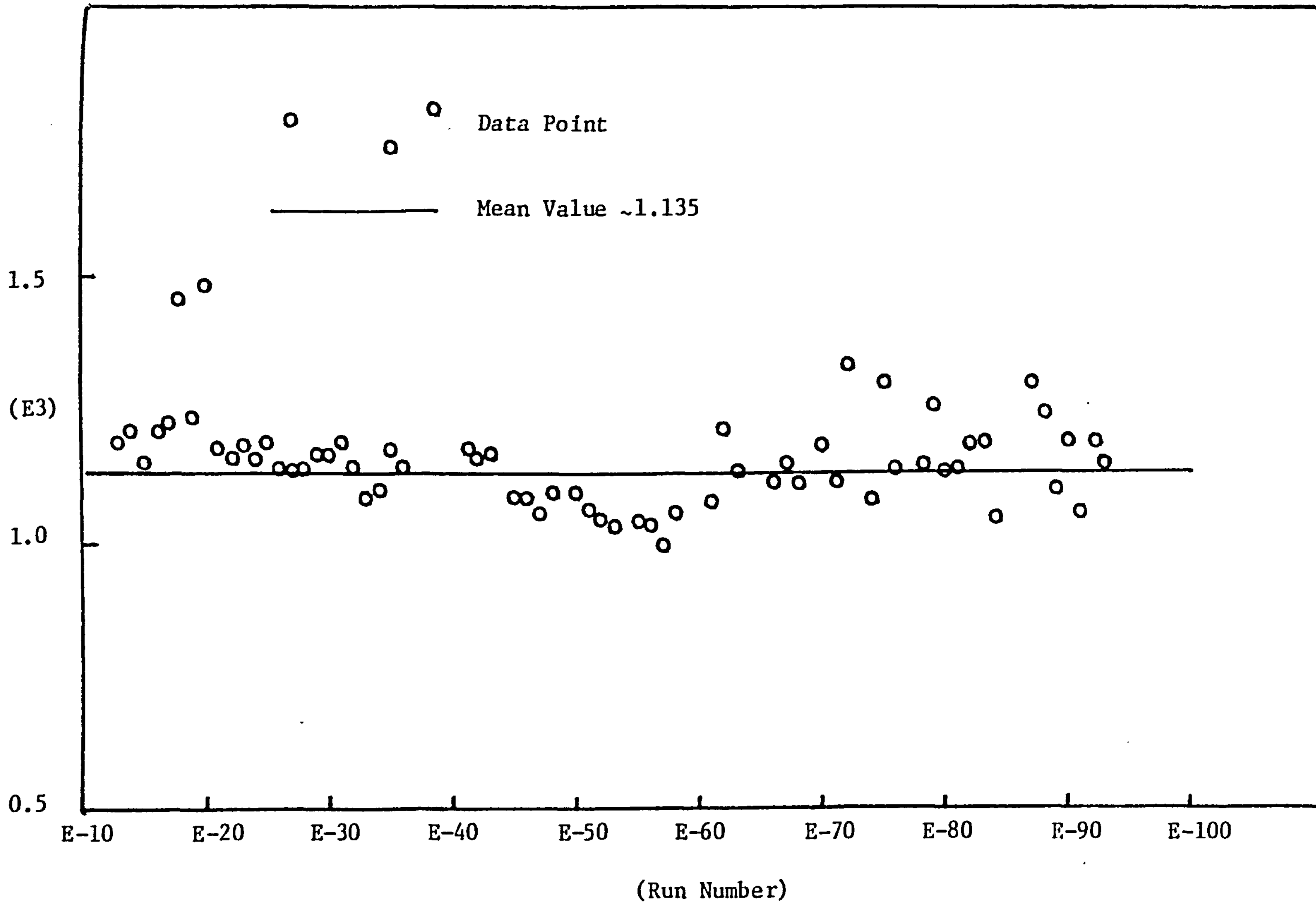

Fig. 5.7.2.2 Velocity Coefficient E3.

Since E1 is obtained by the correlation between dimensionless velocity traverses, a constant value is most likely to be expected. The scattering in values of E2 implies that for different boundary conditions and discharges, different velocity gradient steepness will exist.

The values of E2 was then plotted against E1 as in Fig. 5.7.2.3 and V/V_{maxT} ratio as in Fig. 5.7.2.4. Both cases show good relations between these coefficients. In Fig. 5.7.2.3, a second degree function between E1 and E2 and in Fig. 5.7.2.4 a linear function between V/V_{maxT} and E2 are expected.

The constancies of E1 and E3 together with the relations shown in Fig. 5.7.2.3 and Fig. 5.7.2.4 enable them to be selected as the initial conditions for solving design problems when an iterative method is used, whereas, the value of E2 has to be evaluated successively.

5.7.3 Statistical Analysis Between Theoretical and Experimental Results

A statistical program has been carried out to estimate the correlation between the theoretical and measured velocity traverses. The most commonly used "Least Square Regression" model has been adopted, and the results through all sixty seven velocity traverses are presented in Appendix C.3, Table (C.3.1).

The "Least Square Regression" model is designed to

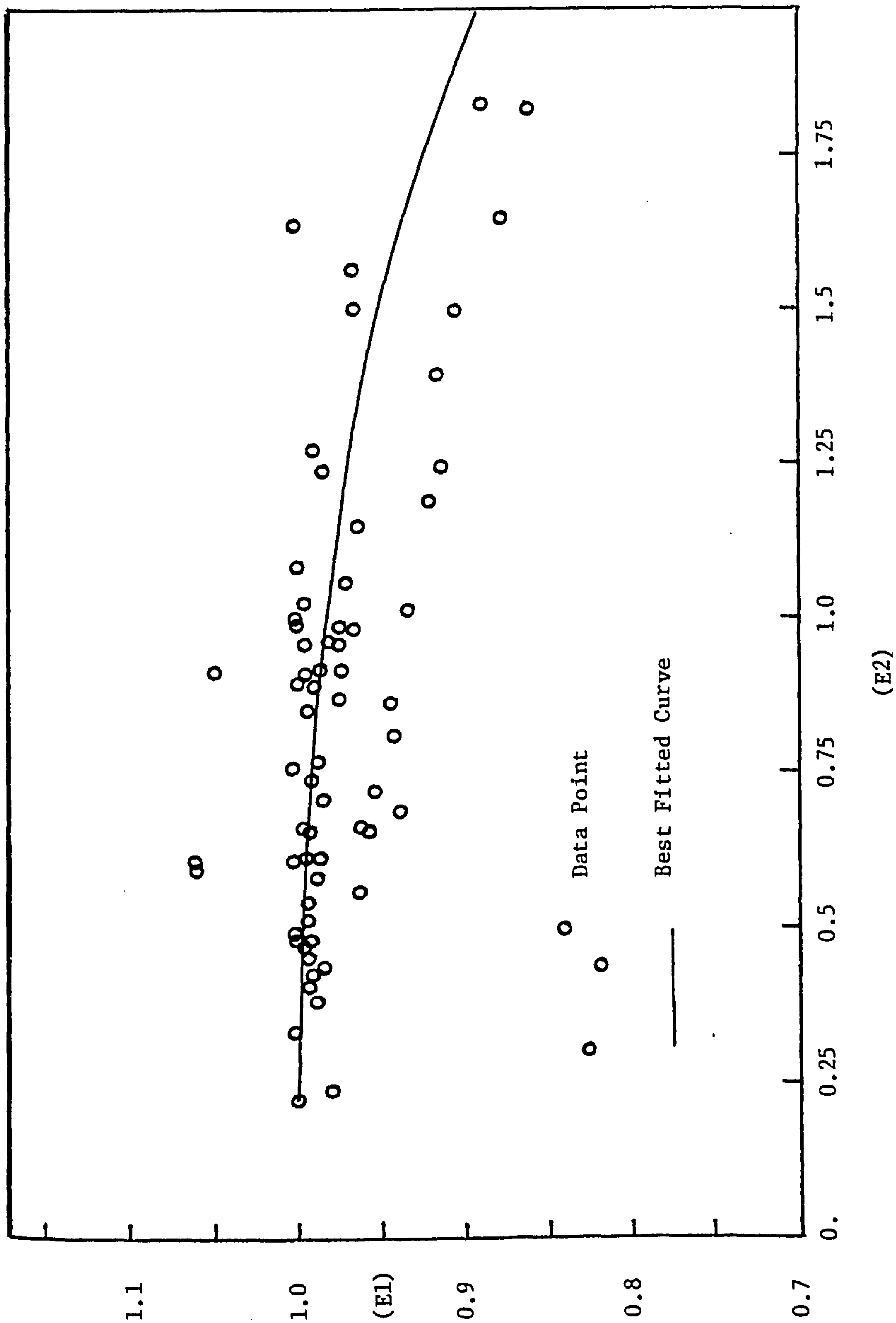

Fig. 5.7.2.3 Plot of E2 V.S. E1

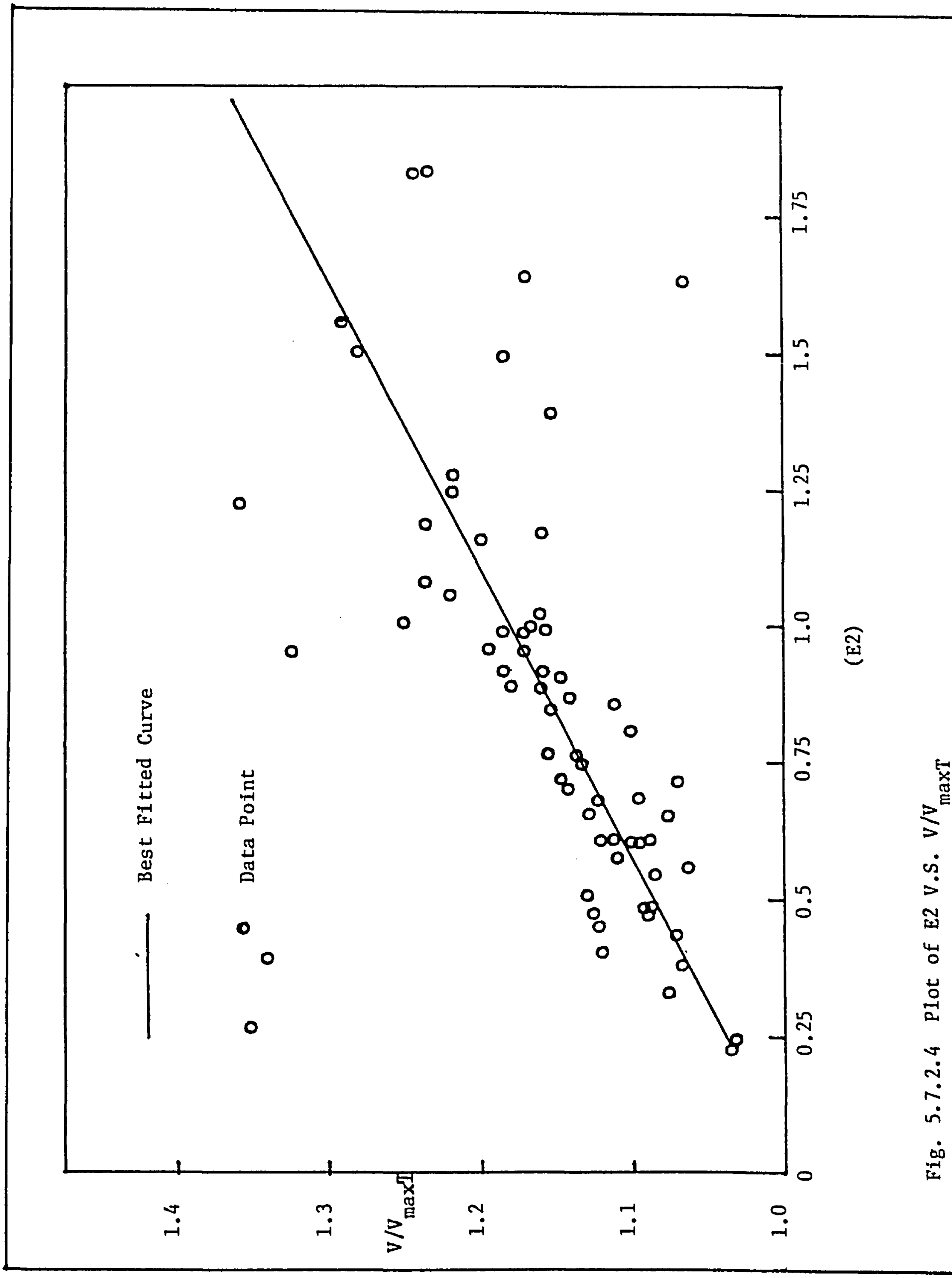

Fig. 5.7.2.4 Plot of E2 V.S. V/V_{maxT}

minimize the sum of the squares of the deviations of the actual data points from the straight line of best fit. The correlation coefficient "r", which measures how well the line fitted to the data, ranged from 0.811 up to 0.999, with value of 1.0 in the ideal case. The slope "m" of the regression line ranged from 0.946 up to 1.052, with 1.0 as the ideal value. The standard deviations of the predicted local velocities were found to be 0.0075 m/s minimum and 0.1238 m/s maximum, and of the measured one with 0.0084 m/s as the minimum and 0.1342 m/s maximum.

In most cases, the higher the standard deviations are the lower the correlation coefficients become.

5.8 Experimental Errors

5.8.1 Sources of Errors

The sources of experimental errors during the laboratory testings can be classified as follows:

1. Flow depth and distance measurements:
   - (a) Variations of channel bed ±0.100" (0.254 cm).
   - (b) Reference datum recording (still water level) ±0.005" (0.0127 cm).
   - (c) Point gauge reading ±0.005" (0.0127 cm).
   - (d) Water surface fluctuation in still water wells upstream ±0.1" (0.254 cm); downstream ±0.05" (0.127 cm).

(e) Distance measurement between station (1) and station (2) ±0.05" (0.127 cm).

2. Local velocity measurements:

(a) For the pitot tube, a common instrument precision error of ±1% was assumed.

(b) Manometer reading ±0.10" (0.254 cm) including fluctuation.

(c) For the miniature current meter, a common instrument precision of ±1% was assumed.

(d) Averaging of dial reading ±1 Hz.

(e) Velocity conversion chart accuracy ±3%.

(f) Vertical displacement in traverse ±0.005" (0.0127 cm).

(g) Horizontal displacement in traverse ±0.10" (0.254 cm).

3. Total flow measurement:

(a) Electro-magnetic flow recorder ±5 USGPM (3.15×10^{-4} $m^3/s.$)

5.8.2 General Equation for Errors Estimation

The general equation of the theory of errors can be written as

$$(\delta Q)^2 = (\partial F/\partial X_1)^2(\delta X_1)^2 + (\partial Q/\partial X_2)^2(\delta X_2)^2 + \ldots \quad (5.8.2.1)$$

in which $Q = F(X_1, X_2, X_3 \ldots)$ is a defined function.

Q is the dependent variable

$X_1, X_2, \ldots$ are the independent variables

δQ is the estimated error in Q

δX_1, δX_2, ... are the specific errors in $X_1, X_2 \ldots$ that were made during their measurements.

Eq. (5.8.2.1) can be applied to each tests in order to estimate its expected experimental error.

5.8.3 <u>Estimation of Experimental Errors</u>

1. For the local velocity, the error was estimated at ±5% maximum

2. For the average velocity, since

$$V = Q/A \tag{5.8.3.1}$$

and applying Eq. (5.8.2.1),

$$\delta V = [\ (\delta Q)^2 + (\delta A)^2\ ]^{1/2} \tag{5.8.3.2}$$

where

δQ = 5% max., δA = 3.4% maximum

Therefore, $\delta V \approx \pm 6.1\%$ maximum

3. For Manning's Coefficient, since

$$n = \frac{1}{V} R^{2/3} S_o^{1/2} \tag{5.8.3.3}$$

applying Eq. (5.8.2.1.)

$$\delta n = [\ (\delta V)^2 + \frac{4}{9} (\delta R)^2 + \frac{1}{4} (\delta S_o)^2\ ]^{1/2} \tag{5.8.3.4}$$

in which $\delta V \approx \pm 6.1\%$ maximum

$$\delta R = [\ (\delta A)^2 + (\delta P)^2\ ]^{1/2} \tag{5.8.3.5}$$

$$= [\ (3.4)^2 + (2.6)^2\ ]^{1/2} = 4.3\%\ \text{maximum}$$

$$\delta S_o = 4.9\%\ \text{maximum}$$

$$\text{Therefore}\ \delta n = [\ (6.1)^2 + \frac{4}{9}(4.3)^2 + \frac{1}{4}(4.9)^2\ ]^{1/2}$$

$$= 7.2\%\ \text{maximum}$$

The above calculations for various experimental errors are only based on the sensitivity of measuring equipments. Therefore, the figures provide conservative estimates.

5.9 Remarks on Discussion of Results

Generally, the theoretical model which had been presented in Chapter III was tested and good agreement was obtained between theoretical and experimental results. However, field measurements are essential in order to prove its general applicability. Since, there was no suitable field data available during this research to serve the purpose, an extensive field study should be carried out to fulfill the need.

CHAPTER VI

CONCLUSIONS AND RESEARCH SUGGESTIONS

6.1 Conclusions

The general goal of the study was an improved understanding of the characteristics of multiple roughness channels and their related flow patterns. The analytical and numerical models developed here satisfactorily predicted the behavior of flow velocities under laboratory conditions. On the basis of the analytical and experimental results the following conclusions may be summarized:

1. The Composite Roughness Equation (3.8.3) mentioned in Chapter III, Section 3.8 has been found to be inadequate in applying to finite channels of different configurations.

2. The experimental investigation proves that the different channel configurations and boundary conditions offer varying resistances to the flow. The use of shape factors by previous investigators to describe the influence are insufficient for wide general applications.

3. The numerical model mentioned in Chapter III, Section 3.9 has proved to be satisfactory under laboratory conditions. Velocity profiles estimate by this model averaged about ±5% error.

4. The velocity profile equation 3.5.15 derived in Chapter III, Section 3.5 can be exmployed by the above numerical model to yield satisfactory results.

5. Precise estimation of composite roughness coefficient for multiple roughness channels can be possible by applying the above model.

6. The Finite Strip Approach for the calibration of roughness elements has been quite successful in defining their friction coefficients.

6.2 Research Suggestions

The results of the present study could probably be extended to further investigations. Some of these suggestions are summarized as follows:

1. The subdivision of a turbulent flow into hydrodynamically independent zones is not in general possible, because the turbulence generated at the bed is definitely diffused throughout the channel. Therefore, more precise experimental investigations are needed and the measurements should be extended to include determinations of turbulence and secondary circulations in three dimensional flows.

2. The laterally varying roughness found in nature is interrelated with the transport of sediment. Investigations are needed to study their complexity.

3. Further investigations on the definition of

friction factor are necessary. Common lining materials should be tested to verify the Finite Strip calibration procedures.

4. Extensive field programs are suggested to verify the model's applicability together with the effects of scale.

APPENDICES

APPENDIX A

Numerical Example

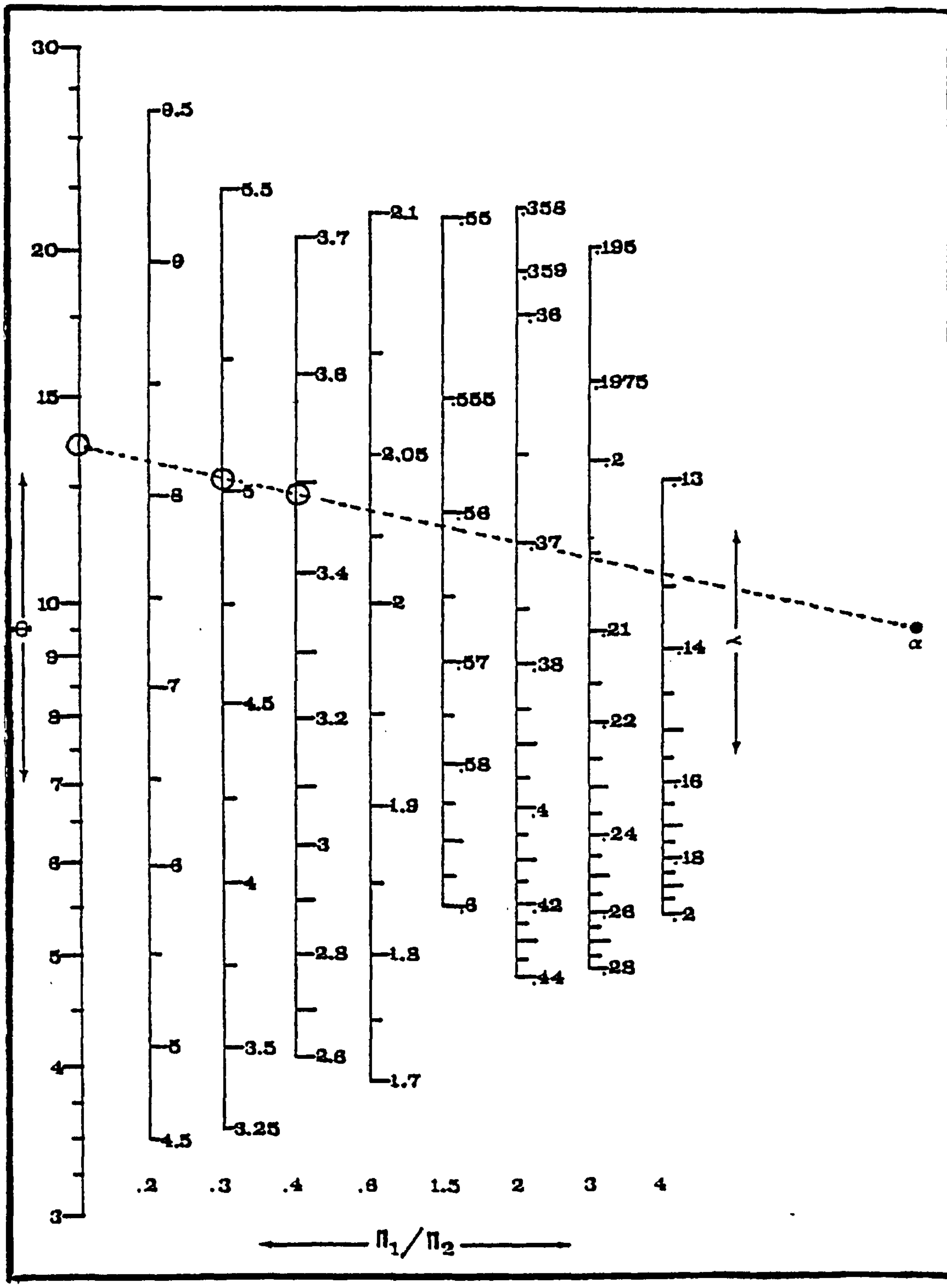

Fig. 5.2.1 Monograph for λ

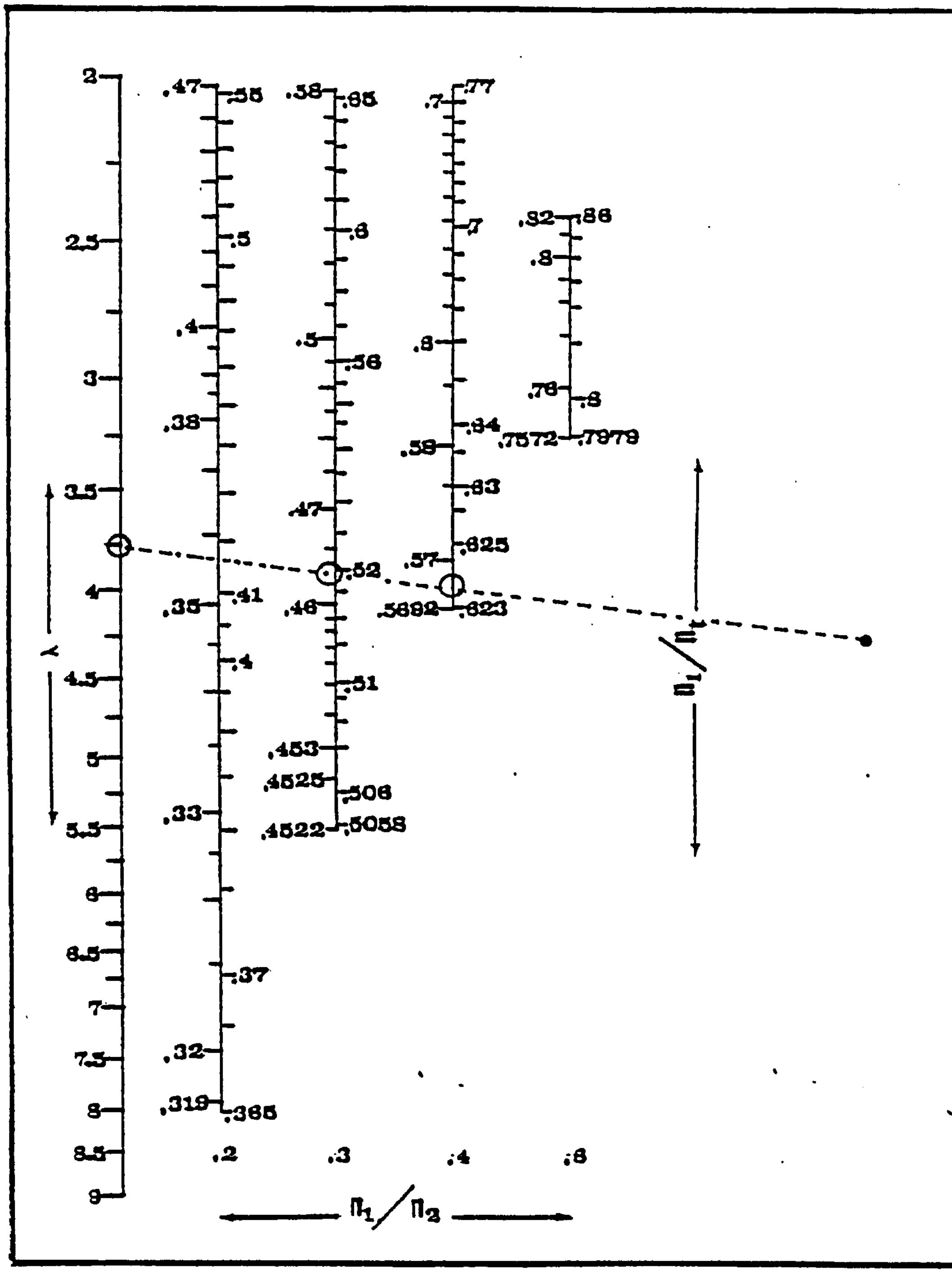

Fig. 5.3.1 Monograph For n_1/n_t Ratio.

A1. Numerical Example in Demonstrating the Use of Monographs in Finding λ and n_1/n_t Ratio

In this section a numerical example is illustrated to explain the use of the developed charts in finding the values of λ and n_1/n_t.

Given: A trapezoidal channel with the following characters are known,

: cover underside Manning's roughness is equal to 0.02616,

: the channel sides and bed roughness is equal to 0.01,

: dimension of the channel;

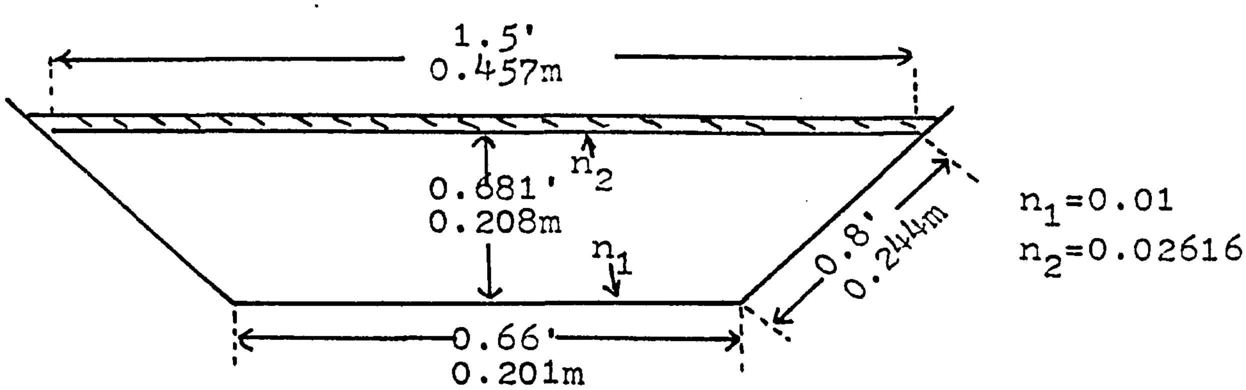

Fig. A.1.1 Channel Cross-Section

Solution:

Wetted perimeter of channel bed and sides
P_1 = 0.8' + 0.66' + 0.8' = 2.26' (0.6889 m)

Wetted perimeter of channel cover
P_2 = 1.5' (0.4572 m)

Total wetted perimeter
$P = P_1 + P_2$ = 2.26' + 1.5' = 3.76' (1.1460 m)

Wetted perimeter ratio
$\alpha = P_1/P = 2.25/3.76 = 0.601064$

The roughness ratio
$n_1/n_2 = 0.01/0.02616 = 0.382263$

The total flow area of the channel
$A = 0.735353$ ft.^{2} (0.06832 m^2)

The hydraulic radius of the channel
$R = A/P = 0.735353/3.76' = 0.195572'$ (0.05961 m)

The value of Φ function

$$\Phi = \frac{R^{1/6}}{n_1 g^{1/2}} = \frac{(0.195572)^{1/6}}{0.01(32.2)^{1/2}} = 13.426305$$

In order to obtain the value of λ we use Fig. 5.2.1 .

By $\Phi = 13.43$, $n_1/n_2 = 0.382263$, we read from the chart.

$(n_1/n_2 = 0.3)$ axis will give $\lambda = 5.03$

$(n_1/n_2 = 0.4)$ axis will give $\lambda = 3.49$

Therefore for $n_1/n_2 = 0.382263$ implies

$$\lambda = 3.49 + \frac{(0.4 - 0.382263)}{(0.4 - 0.3)} (5.03 - 3.49)$$

$$= 3.763150$$

And to obtain the value of n_1/n_t, we use Fig. 5.3.1 .

By $\lambda = 3.76$, $\alpha = 0.601064$, $n_1/n_2 = 0.382263$

From $(n_1/n_2 = 0.3)$ axis, when

$\alpha = 0.55 \rightarrow n_1/n_t = 0.463$

$\alpha = 0.65 \rightarrow n_1/n_t = 0.519$

Therefore for $\alpha = 0.601064$

$$n_1/n_t = 0.519 - \frac{(0.65 - 0.601064)}{(0.65 - 0.85)} (0.519 - 0.463)$$

$$= 0.491596$$

From $(n_1/n_2 = 0.4)$ axis, when

$$\alpha = 0.55 \rightarrow n_1/n_2 = 0.5696$$

$$\alpha = 0.65 \rightarrow n_1/n_t = 0.6235$$

Therefore for $\alpha = 0.601064$

$$n_1/n_t = 0.6235 - \frac{(0.65 - 0.601064)}{(0.65 - 0.55)} (0.6235 - 0.5696)$$

$$= 0.597124.$$

In order to get the final n_1/n_t value for $n_1/n_2 = 0.382263$ we have to take one more interpolation along the n_1/n_2 value.

Therefore for $n_1/n_2 = 0.382263$

$$n_1/n_t = 0.597124 - \frac{(0.4 - 0.382263)}{(0.4 - 0.3)} (0.597124 - 0.491596)$$

$$= 0.578406 \rightarrow n_t = 0.01/0.578406 = 0.01729$$

The percentage in error, using the exact λ and n_1/n_t values as the base.

By the Eq. (3.7.4) and (3.8.3), the exact value of λ and n_1/n_t are

$$\lambda = 3.695937, \; n_1/n_t = 0.576947.$$

$\therefore$ % different in λ value

$$\frac{3.763150 - 3.695937}{3.675937} \times 100\% \simeq 1.82\%$$

And % different in n_1/n_t value

$$\frac{0.578406 - 0.576947}{0.576947} \times 100\% \simeq 0.25\%$$

Notes: The magnitude of the error in percentage depends on two major factors: (1) The accuracy in reading the charts, and (2) the round-off figures during the calculations.

APPENDIX B

List of Computer Programs

B.1 Program for Estimating Local Velocity Profile

In this appendix, the computer program which had been employed in analyzing the local velocity traverses is listed as following :

```
$JOB     WATFIV   XXXXXXXXXX     ANDREW  ANDREW
          REAL N1,N2,N12,LIM,LEV(7,1),X(100),Y(100),INTP,MUH(7,7),MUV(7,7)
          DIMENSION UH(7,7),HD(7,1),HDL1(7,1),HDL2(7,1),HW(1,7),HRW(7,7)
         *,HRMW(7,7),HVS1(7,1),HVS2(7,1),HVM(7,1),HVMAX(7,1),HVM1(7,1),
         *HVM2(7,1),HY1(7,1),HY2(7,1),NUM(7),CSUM(7)
          DIMENSION UV(7,7),VD(1,7),VRD(7,7),VY1(1,7),VY2(1,7),
         *VVS1(1,7),VVS2(1,7),VVM1(1,7),VVM2(1,7),VVM(1,7),VVMAX(1,7)
          DIMENSION A(7,7),B(7,7),C(7,7),UE(7,7),UF(7,7),PCEF(7,7),PCEE(7,7)
          READ ,IE
          READ,V,VMA
          V=V*0.3048
          VMA=VMA*0.3048
          PRINT 160
          PRINT 310,LL,IE
          PRINT 51
          PRINT 50
          PRINT 51
          CALL HORU (UH,MUH,V,VMA)
          PRINT 160
          PRINT 51
          PRINT 60
          PRINT 51
          CALL VERU (UV,MUV,V,VMA,S,YMAX)
          PRINT 160
          MM=7
          CALL MATMUL (MM,MM,MUH,MM,MM,MUV,C,MM)
          READ,((UE(I,J),J=1,7),I=1,7)
          DO 13 I=1,7
          DO 13 J=1,7
   13     UE(I,J)=UE(I,J)*0.3048
          KK=1
          DO 1 I=1,7
          DO 1 J=1,7
          IF ((UE(I,J) .LE. 0.0).OR.(C(I,J) .LE. 0.0)) GO TO 1
          Y(KK)=ALOG10(UE(I,J)/V)
          X(KK)=ALOG10(C(I,J))
  5       KK=KK+1
  1       CONTINUE
          PRINT 70
          NN=KK-1
```

```
      CALL COEFF (X,Y,NN,SLOP,INTP)
      E1=10.**INTP
      E2=SLOP
      E3=E1*VMA/V
      PRINT 110
      PRINT 120,E1
      PRINT 130,E2
      PRINT 180,E3
      DO 2 I=1,7
      DO 2 J=1,7
      IF (C(I,J) .LE. 0.0) GO TO 4
      UF(I,J)=V*E1*(C(I,J)**E2)
      GO TO 2
 4    UF(I,J)=0.0
 2    CONTINUE
      DO 6 I=1,7
      DO 6 J=1,7
      IF((UF(I,J).LE.0.0).OR.(UE(I,J).LE.0.0)) GO TO 9
      PCEF(I,J)=ABS(UF(I,J) UE(I,J))/UF(I,J)*100
      PCEE(I,J)=ABS(UF(I,J)-UE(I,J))/UE(I,J)*100
      GO TO 6
 9    PCEF(I,J)=PCEE(I,J)=0.0
 6    CONTINUE
      PRINT 171
      PRINT 310,LL,IE
      PRINT 150
      PRINT 40
      PRINT 31
      PRINT 150
      PRINT 32
      DO 11 I=1,7
 11   PRINT 25,I,(UE(I,J),J=1,7)
      PRINT 150
      PRINT 170
 4    FORMAT (/,21X,'EXPERIMENTAL LOCAL VELOCITIES (M/S)')
      PRINT 150
      PRINT 10
      PRINT 31
      PRINT 150
      PRINT 32
```

```
      DO 12 I=1,7
12    PRINT 25,I,(UF(I,J),J=1,7)
      PRINT 150
      PRINT 140,YMAX,V,S
      PRINT 80
      PRINT 30
      DO 7 I=1,7
7     PRINT 20,I,(PCEF(I,J),J=1,7)
      PRINT 90
      PRINT 30
      DO 8 I=1,7
8     PRINT 20,I,(PCEE(I,J),J=1,7)
      KK=1
      DO 21 I=1,7
      DO 21 J=1,7
      IF((UF(I,J).LE.0.0).OR.(UE(I,J).LE.0.0)) GO TO 21
      X(KK)=UF(I,J)
      Y(KK)=UE(I,J)
      KK=KK+1
21    CONTINUE
      PRINT 171
      PRINT 100
      NN=KK-1
      CALL COEFF(X,Y,NN,SLOP,INTP)
      CALL MINMAX (X,Y,NN,XMAX,XMIN,YMAX,YMIN)
      CALL MEAN(UF,VMEAN1,7)
      CALL MEAN(UE,VMEAN2,7)
      RF=XMAX/VMEAN1
      RE=YMAX/VMEAN2
      PRINT 210,XMAX
      PRINT 220,XMIN
      PRINT 250,VMEAN1
      PRINT 270,RF
      PRINT 230,YMAX
      PRINT 240,YMIN
      PRINT 260,VMEAN2
      PRINT 280,RE
100   FORMAT(///////,2X,'CORRELATION BETWEEN ESTIMATED AND EXPERIMENTAL
     *LOCAL VELOCITIES',/)
80    FORMAT(////, 2X,'PERCENTAGE DIFFERENT IN LOCAL VELOCITIES USING ES
```

```
     *TIMATED VALUES AS BASE',/)
 90   FORMAT(////, 2X,'PERCENTAGE DIFFERENT IN LOCAL VELOCITIES USING EX
     *PERIMENTAL VALUES AS BASE',/)
 10   FORMAT (/,10X,'ESTIMATED LOCAL VELOCITIES BY THE COEFFICIENT EQUAT
     *ION  (M/S)')
 30   FORMAT(2X,'I',6X,'A', 8X,'B', 8X,'C', 7X,'CL', 8X,'D',
     * 8X,'E', 8X,'F',/)
 20   FORMAT(1X,I2,2X,7(F8.5,1X))
 50   FORMAT(/, 5X,'HORIZONTAL STRIPS ANALYSIS',/)
 60   FORMAT(/, 6X,'VERTICAL STRIPS ANALYSIS',/)
 70   FORMAT(///, 2X,'FORMULATION OF COEFFICIENT EQUATION',/)
 110  FORMAT(//, 2X,'THE COEFFICIENT EQUATION IS   U=V*E1*((UH/HVM)*(UV/
     *VVM))**E2, WHERE',/)
 120  FORMAT( 6X,'*** E1 = ',E14.7,' ***',/)
 130  FORMAT( 6X,'*** E2 = ',E14.7,' ***',/)
 180  FORMAT( 6X,'*** E3 = ',E14.7,' ***',/)
 150  FORMAT(5X,71(' '))
 51   FORMAT(4X,28(' '))
 140  FORMAT(/,6X,'YMAX=',F7.4,' M',4X,'VMEAN=',F7.4,' M/S',4X,'ENERGY
     * SLOPE=',E12.5,////)
 25   FORMAT(7X,I2,4X,7(F8.5,1X))
 31   FORMAT(/,7X,'STN',7X,'A',8X,'B',8X,'C',8X,'CL',7X,'D',8X,'E',8X
     *,'F',/)
 32   FORMAT(6X,'LEVEL')
 160  FORMAT('1')
 170  FORMAT(//)
 171  FORMAT(///)
 210  FORMAT(/, 6X,'*** MAXINUM ESTIMATED LOCAL VELOCITY = ',E14.7,' ***
     *',/)
 220  FORMAT( 6X,'*** MINIMUM ESTIMATED LOCAL VELOCITY = ',E14.7,' ***',
     */)
 230  FORMAT( 6X,'*** MAXINUM EXPERIMENTAL LOCAL VELOCITY = ',E14.7,' **
     **',/)
 240  FORMAT( 6X,'*** MINIMUM EXPERIMENTAL LOCAL VELOCITY = ',E14.7,' **
     **',/)
 250  FORMAT( 6X,'*** MEAN ESTIMATED VELOCITY = ',E14.7,' ***',/)
 260  FORMAT( 6X,'*** MEAN EXPERIMENTAL VELOCITY = ',E14.7,' ***',/)
 270  FORMAT( 6X,'*** ESTIMATED VMAX/VMEAN RATIO = ',E14.7,' ***',/)
 280  FORMAT(6X,'*** EXPERIMENTAL VMAX/VMEAN RATIO = ',E14.7,' ***',///)
 310  FORMAT('+',I2,2X,'RUN NUMBER E ',I2)
```

```
      STOP
      END
C     **************************************************************
C     SUBROUTINE FOR HORIZONTAL STRIPS ANALYSIS

      SUBROUTINE HORU (UH,MUH,V,VMA)
      REAL N1,N2,N12,LIM,MUH(7,7)
      DIMENSION UH(7,7),HD(7,1),HDL1(7,1),HDL2(7,1),HW(1,7),HRW(7,7)
     *,HRMW(7,7),HVS1(7,1),HVS2(7,1),HVM(7,1),HVMAX(7,1),HVM1(7,1),
     *HVM2(7,1),HY1(7,1),HY2(7,1)
      READ,(HD(I,1), I=1,7)
      READ,N1,N2,G,S,ALP,VK
      DO 1 I=1,7
    1 HD(I,1)=HD(I,1)*0.3048
      G=G*0.3048
      PRINT 202
      PRINT 203,V,VMA,S,VK
      PRINT 201
      HW(1,1)=0.083333*0.3048
      HW(1,2)=0.25*0.3048
      HW(1,3)=0.5*0.3048
      HW(1,4)=0.75*0.3048
      HW(1,5)=1.0*0.3048
      HW(1,6)=1.25*0.3048
      HW(1,7)=1.416667*0.3048
      DO 9 J=1,7
      DO 9 I=1,7
      HRW(I,J)=HW(1,J)
    9 CONTINUE
C     ----------------------------------------------
      DO 8 I=1,7
      R=0.5*HD(I,1)
      APHI=(R**0.166666667)/(N1*SQRT(G))*0.6728280275
      CALL LIMDA (N1,N2,ALP,APHI,LIM,I)
      HDL2(I,1)=0.5*((1.5*0.3048) HD(I,1))
      HDL1(I,1)=HDL2(I,1)+HD(I,1)
      HY1(I,1)=HD(I,1)/(1+LIM)
      HY2(I,1)=LIM*HY1(I,I)
      HVS1(I,1)=SQRT(G*HY1(I,1)*S)
      HVS2(I,1)=SQRT(G*HY2(I,1)*S)
```

```
      HVM1(I,1)=1.00*(HY1(I,1)**0.6666667)*SQRT(S)/N1
      HVM2(I,1)=1.00*(HY2(I,1)**0.6666667)*SQRT(S)/N2
      HVM(I,1)=0.5*(HVM1(I,1)+HVM2(I,1))-(1/(3.*VK))*(
     *HVS1(I,1)-HVS2(I,1))*((HY1(I,1)-HY2(I,1))/HD(I,1))
      HVMAX(I,1)=0.5*(HVM1(I,1)+HVM2(I,1))+(1/(3.*VK))*(
     *HVS1(I,1)+HVS2(I,1))
      DO 12 J=1,7
      IF((HRW(I,J).LE.HDL2(I,1)).OR.(HRW(I,J).GE.HDL1(I,1))) GO TO 7
      HRMW(I,J)=HRW(I,J)-HDL2(I,1)
      IF (HRMW(I,J).GE.HY2(I,1)) GO TO 13
      EPS=HRMW(I,J)/(HY2(I,1))
      FNEPS=2*SQRT(1-EPS)-ALOG((1+SQRT(1-EPS))/(1-SQRT(1-EPS)))
      UH(I,J)=HVMAX(I,1)+HVS2(I,1)*FNEPS/VK
      MUH(I,J)=UH(I,J)/HVM(I,1)
      GO TO 12
   13 HRRMW=HD(I,1)-HRMW(I,J)
      EPS=HRRMW/HY1(I,1)
      FNEPS=2*SQRT(1-EPS)-ALOG((1+SQRT(1-EPS))/(1-SQRT(1-EPS)))
      UH(I,J)=HVMAX(I,1)+HVS1(I,1)*FNEPS/VK
      MUH(I,J)=UH(I,J)/HVM(I,I)
      GO TO 12
    7 UH(I,J)=0.0
      HRMW(I,J)=0.0
      MUH(I,J)=0.0
   12 CONTINUE
    8 CONTINUE
C     ------------------------------------------
      PRINT 102
      DO 14 I=1,7
      PRINT 101,I,HDL2(I,1),HY2(I,1),HY1(I,1),HDL1(I,1),HD(I,1)
   14 CONTINUE
  101 FORMAT(1X,I2,2X,5(F8.5,1X))
  102 FORMAT(///,2X,'I',4X,'HDL2', 6X,'HY2', 6X,'HY1', 5X,
     *'HDL1', 6X,'HD',/)
      PRINT 103
      DO 15 I=1,7
      PRINT 104,I,HVS2(I,1),HVM2(I,1),HVM1(I,1),HVS1(I,1),
     *HVM(I,1),HVMAX(I,1)
   15 CONTINUE
  104 FORMAT(1X,I2,2X,6(F8.5,1X))
```

```
103  FORMAT(/////,2X,'I',4X,'HVS2', 5X,'HVM2', 5X,'HVM1', 5X,'HVS1',
    * 6X,'HVM', 5X,'HVMAX',/)
     PRINT 105
     PRINT 107
     DO 16 I=1,7
     PRINT 106,I,(HRMW(I,J),J=1,7)
16   CONTINUE
105  FORMAT(////,14X,'RELATIVE POSITION VECTORS FROM BOUNDARY #2',/)
106  FORMAT(1X,I2,2X,7(F8.5,1X))
107  FORMAT(2X,'I',6X,'A', 8X,'B', 8X,'C', 7X,'CL', 8X,'D',
    * 8X,'E', 8X,'F',/)
     PRINT 108
     PRINT 107
     DO 17 I=1,7
     PRINT 106 , I,(UH(I,J),J=1,7)
17   CONTINUE
108  FORMAT(////,15X,'LOCAL VELOCITIES FOR HORIZONTAL STRIPS',/)
202  FORMAT(///,11X,'V',11X,'VMA',11X,'S',11X, 'VK',/)
203  FORMAT(5X,4(E12.5,1X))
201  FORMAT (///,2X,'I',6X,'N1', 7X,'N2', 6X,'N12', 6X,
    C'ALP', 6X,'DLIM', 5X,'TOL', 7X,'UL', 5X,'APHI',
    C 6X,'LIM',/)
     RETURN
     END
C    ************************************************************
C    SUBROUTINE FOR VERTICAL STRIPS ANALYSIS

     SUBROUTINE VERU (UV,MUV,V,VMA,S,YMAX)
     REAL N1,N2,N12,LIM,LEV(7,1),MUV(7,7)
     DIMENSION UV(7,7),VD(1,7),VRD(7,7),VY1(1,7),VY2(1,7),
    *VVS1(1,7),VVS2(1,7),VVM1(1,7),VVM2(1,7),VVM(1,7),VVMAX(1,7)
     READ ,(VD(1,J),J=1,7)
     READ ,N1,N2,G,S,ALP,VK,YMAX
     DO 1 J=1, 7
1    VD(1,J)=VD(1,J)*0.3048
     G=G*0.3048
     YMAX=YMAX*0.3048
     PRINT 202
     PRINT 203,V,VMA,S,VK
     PRINT 201
```

```
      LEV(1,1)=0.1*YMAX
      LEV(2,1)=0.2*YMAX
      LEV(3,1)=C.4*YMAX
      LEV(4,1)=0.6*YMAX
      LEV(5,1)=0.8*YMAX
      LEV(6,1)=0.9*YMAX
      LEV(7,1)=0.95*YMAX
      DO 9 J=1,7
      DO 9 I=1,7
      VRD(I,J)=LEV(I,1)
    9 CONTINUE
C     ---------------------------------------
      DO 8 J=1,7
      R=0.5*VD(1,J)
      APHI=(R**C.1666666667)/(N1*SQRT(G))*0.6728280275
      CALL LIMCA (N1,N2,ALP,APHI,LIM,J)
      VY1(1,J)=VD(1,J)/(1+LIM)
      VY2(1,J)=LIM*VY1(1,J)
      VVS1(1,J)=SQRT(G*VY1(1,J)*S)
      VVS2(1,J)=SQRT(G*VY2(1,J)*S)
      VVM1(1,J)=1.00*(VY1(1,J)**0.6666667)*SQRT(S)/N1
      VVM2(1,J)=1.00*(VY2(1,J)**0.6666667)*SQRT(S)/N2
      VVM(1,J)=0.5*(VVM1(1,J)+VVM2(1,J))-(1/(3.*VK))*(
     *VVS1(1,J) VVS2(1,J))*((VY1(1,J)-VY2(1,J))/VD(1,J))
      VVMAX(1,J)=0.5*(VVM1(1,J)+VVM2(1,J))+(1/(3.*VK))*(
     *VVS1(1,J)+VVS2(1,J))
      DO 12 I=1,7
      IF (VRD(I,J) .GE. VD(1,J)) GC TO 7
      IF (VRD(I,J) .GE. VY2(1,J)) GO TO 13
      EPS=VRD(I,J)/VY2(1,J)
      FNEPS=2.*SQRT(1-EPS)-ALOG((1+SQRT(1-EPS))/(1-SQRT(1-EPS)))
      UV(I,J)=VVMAX(1,J)+VVS2(1,J)*FNEPS/VK
      MUV(I,J)=UV(I,J)/VVM(1,J)
      GO TO 12
   13 VRRD=VD(1,J)-VRD(I,J)
      EPS=VRRD/VY1(1,J)
      FNEPS=2.*SQRT(1-EPS)-ALOG((1+SQRT(1-EPS))/(1-SQRT(1-EPS)))
      UV(I,J)=VVMAX(1,J)+VVS1(1,J)*FNEPS/VK
      MUV(I,J)=LV(I,J)/VVM(1,J)
      GO TO 12
```

```
7     UV(I,J)=0.0
      VRD(I,J)=0.0
      MUV(I,J)=0.0
12    CONTINUE
8     CONTINUE
C     ----------------------------------------------
      PRINT 102
      DO 14 J=1,7
      PRINT 101,J,VY2(1,J),VY1(1,J),VD(1,J)
14    CONTINUE
101   FORMAT(1X,I2,2X,3(F8.5,1X))
102   FORMAT(///,2X,'J',5X,'VY2', 6X,'VY1', 6X,'VD',/)
      PRINT 103
      DO 15 J=1,7
      PRINT 104,J,VVS2(1,J),VVM2(1,J),VVM1(1,J),VVS1(1,J),
     *VVM(1,J),VVMAX(1,J)
15    CONTINUE
104   FORMAT(1X,I2,2X,6(F8.5,1X))
103   FORMAT(/////,2X,'J',4X,'VVS2', 5X,'VVM2', 5X,'VVM1', 5X,'VVS1',
     * 5X,'VVM', 6X,'VVMAX',/)
      PRINT 105
      PRINT 107
      PRINT 109
      DO 16 I=1,7
      PRINT 106 ,I,(VRD(I,J),J=1,7)
16    CONTINUE
105   FORMAT(////,13X,'RELATIVE POSITION VECTORS FROM BOUNDARY #2',/)
106   FORMAT(1X,I2,2X,7(F8.5,1X))
107   FORMAT(9X,'A', 8X,'B', 8X,'C', 8X,'CL', 7X,'D',
     * 8X,'E', 8X,'F')
      PRINT 108
      PRINT 107
      PRINT 109
      DO 17 I=1,7
      PRINT 106,I,(UV(I,J),J=1,7)
17    CONTINUE
108   FORMAT(////,17X,'LOCAL VELOCITIES FOR VERTICAL STRIPS',/)
109   FORMAT(2X,'I',2X,'J',3X,'1',8X,'2',8X,'3',8X,'4',8X,'5',8X,'6',8X,
     *'7')
202   FORMAT(///,11X,'V',10X,'VMA',12X,'S',11X,'VK',/)
```

```
      203  FURMAT(5X,4(E12.5,1X))
      201  FCRMAT (///,2X,'J',6X,'N1', 7X,'N2', 6X,'N12', 6X,
          C'ALP', 6X,'DLIM', 5X,'TCL', 7X,'UL', 5X,'APHI',
          C 6X,'LIM',/)
           RETURN
           END
     C     **************************************************************
     C     SUBROUTINE FOR SEARCHING LAMDA VALUE

           SUBROUTINE LIMDA (N1,N2,ALP,APHI,LIM,K)
           REAL N1,N2,N12,LIM
           TOL=0.01
           DLIM=0.00025
           N12=N1/N2
           IF ((N12.GE.0.2).AND.(N12.LT.0.3)) UL=9.7
           IF ((N12.GE.0.3).AND.(N12.LT.0.4)) UL=5.75
           IF ((N12.GE.0.4).AND.(N12.LT.0.6)) UL=3.8
           IF ((N12.GE.0.6).AND.(N12.LT.1.0)) UL=2.1
           IF ((N12.GE.1.0).AND.(N12.LT.1.5)) UL=0.95
           IF ((N12.GE.1.5).AND.(N12.LT.2.0)) UL=0.8
           IF ((N12.GE.2.0).AND.(N12.LT.3.0)) UL=0.44
           IF ((N12.GE.3.0).AND.(N12.LT.4.0)) UL=0.28
           IF (N12.GE.4.0) UL=0.2
           IF (N12.EQ.1.0) GO TO 13
           LIM=UL
           DO 11 I=1, 1000000
           CPHI=1.111*(SQRT(LIM)-1)*((ALP+((1-ALP)*LIM))
          C**0.16666667)/(1-(N12*(LIM**0.666667)))
           DPHI=ABS(APHI-CPHI)
           IF (DPHI .LE. TCL ) GC TC 12
           LIM =LIM-(DPHI/10.0)*DLIM
           IF (LIM .LE. 0.0) GO TC 14
       11  CONTINUE
       13  LIM=1.0
           UL=1.0
       12  PRINT 101,K,N1,N2,N12,ALF,DLIM,TCL,UL,APHI,LIM
           GO TO 104
       14  PRINT 103,N12,LIM
      101  FORMAT (1X,I2,2X,9(F8.5,1X))
      103  FORMAT (10X,2(E12.5,1X))
```

```
  104 RETURN
      END
C     ***********************************************************
C     SUBROUTINE FOR POINT MULTIPLICATION

      SUBROUTINE MATMUL(M,N,A,K,L,B,C,NMAX)
      DIMENSION A(NMAX,NMAX),B(NMAX,NMAX),C(NMAX,NMAX)
   12 FORMAT(' ','***MATRIES A AND B ARE NOT COMPATIBLE***')
   20 FORMAT(1X,I2,2X,7(F8.5,1X))
   30 FORMAT(2X,'I',6X,'A', 8X,'B', 8X,'C', 7X,'CL', 8X,'D',
     * 8X,'E', 8X,'F',/)
   40 FORMAT (/,20X,'PRODUCT OF (UH/HVM)*(UV/VVM)',/)
      IF (N.NE.K) GO TO 11
      DO 1 I=1, M
      DO 1 J=1,L
      IF ((A(I,J) .LE. 0.0) .OR. (B(I,J) .LE. 0.0))GO TO 2
      C(I,J)=A(I,J)*B(I,J)
      GO TO 1
    2 C(I,J)=0.0
    1 CONTINUE
      PRINT 40
      PRINT 30
      DO 14 I=1,M
   14 PRINT 20,I,(C(I,J),J=1,L)
      RETURN
   11 PRINT 12
      RETURN
      END
C     ***************************************************************
C     SUBROUTINE FOR CORRELATION

      SUBROUTINE COEFF (X,Y,N,SLOP,INTP)
      REAL X(100),Y(100),INTP
      SXY=SX=SY=SXSQ=SYSQ=0.0
      DO 1 I=1,N
      SXY=X(I)*Y(I)+SXY
      SX=X(I)+SX
      SY=Y(I)+SY
      SXSQ=X(I)**2+SXSQ
      SYSQ=Y(I)**2+SYSQ
```

```
1     CONTINUE
      SLOP=(SXY-(SX*SY)/N)/(SXSQ-(SX**2/N))
      INTP=(SY-SLOP*SX)/N
      STDX=SQRT((SXSQ-(SX**2/N))/(N-1))
      STDY=SQRT((SYSQ-(SY**2/N))/(N-1))
      COEF=SLOP*STDX/STDY
      PRINT 10,SLOP
      PRINT 20,INTP
      PRINT 30,STDX
      PRINT 40,STDY
      PRINT 50,COEF
10    FORMAT( 6X,'*** SLOPE = ',E14.7,' ***',/)
20    FORMAT( 6X,'*** INTERCEPT = ',E14.7,' ***',/)
30    FORMAT( 6X,'*** STANDARD DEVIATION OF X = ',E14.7,' ***',/)
40    FORMAT( 6X,'*** STANDARD DEVIATION OF Y = ',E14.7,' ***',/)
50    FORMAT( 6X,'*** COEFFICIENT OF CORRELATION = ',E14.7,' ***',/)
      RETURN
      END
C     ****************************************************************
C     SUBROUTINE FOR MINIMUM AND MAXIMUM VALUES

      SUBROUTINE MINMAX(X,Y,N,XMAX,XMIN,YMAX,YMIN)
      DIMENSION X(N),Y(N)
      XMIN=X(1)
      XMAX=X(1)
      YMIN=Y(1)
      YMAX=Y(1)
      DO 3 I=2,N
      XMAX=AMAX1(XMAX,X(I))
      XMIN=AMIN1(XMIN,X(I))
      YMAX=AMAX1(YMAX,Y(I))
      YMIN=AMIN1(YMIN,Y(I))
3     CONTINUE
      RETURN
      END
C     ****************************************************************
C     SUBROUTINE FOR MEAN VALUE

      SUBROUTINE MEAN(A,VMEAN,N)
      DIMENSION A(N,N),NUM(7),CSUM(7)
```

```
      DU 2 J=1,7
      SUM=0.0
      K=1
      DU 1 I=1,7
      IF(A(I,J).LE.0.0) GO TC 1
      SUM=SUM+A(I,J)
      K=K+1
    1 CONTINUE
      NUM(J)=K-1
      CSUM(J)=SUM
    2 CONTINUE
      TNUM=NUM(1)+NUM(7)+3*(NUM(2)+NUM(3)+NUM(4)+NUM(5)+NUM(6))
      TSUM=CSUM(1)+CSUM(7)+3*(CSUM(2)+CSUM(3)+CSUM(4)+CSUM(5)+CSUM(6))
      VMEAN=TSUM/TNUM
      RETURN
      END
$ENTRY
```

UU RUN NUMBER E-62

HORIZONTAL STRIPS ANALYSIS

V	VMA	S	VK
0.43779E 00	0.53814E 00	0.15624E-02	0.44000E 00

I	N1	N2	N12	ALP	DLIM	TUL	UL	APHI	LIM
1	0.01580	0.01580	1.00000	0.50000	0.00025	0.01000	1.00000	10.59923	1.00000
2	0.01580	0.01580	1.00000	0.50000	0.00025	0.01000	1.00000	10.46533	1.00000
3	0.01580	0.01580	1.00000	0.50000	0.00025	0.01000	1.00000	10.10079	1.00000
4	0.01580	0.01580	1.00000	0.50000	0.00025	0.01000	1.00000	9.82084	1.00000
5	0.01580	0.01580	1.00000	0.50000	0.00025	0.01000	1.00000	9.39785	1.00000
6	0.01580	0.01580	1.00000	0.50000	0.00025	0.01000	1.00000	9.14463	1.00000
7	0.01580	0.01580	1.00000	0.50000	0.00025	0.01000	1.00000	9.01484	1.00000

I	HDL2	HY2	HY1	HDL1	HD
1	0.00381	0.22479	0.22479	0.45339	0.44958
2	0.02032	0.20828	0.20828	0.43688	0.41656
3	0.05207	0.17653	0.17653	0.40513	0.35306
4	0.08636	0.14224	0.14224	0.37084	0.28448
5	0.11938	0.10922	0.10922	0.33782	0.21844
6	0.13589	0.09271	0.09271	0.32131	0.18542
7	0.14351	0.08509	0.08509	0.31369	0.17018

I	HVS2	HVM2	HVM1	HVS1	HVM	HVMAX
1	0.05871	0.92490	0.92490	0.05871	0.92490	1.01386
2	0.05651	0.87904	0.87904	0.05651	0.87904	0.96467
3	0.05203	0.78727	0.78727	0.05203	0.78727	0.86610
4	0.04670	0.68170	0.68170	0.04670	0.68170	0.75246
5	0.04092	0.57163	0.57163	0.04092	0.57163	0.63363
6	0.03771	0.51246	0.51246	0.03771	0.51246	0.56959
7	0.03612	0.48398	0.48398	0.03612	0.48398	0.53871

RELATIVE POSITION VECTORS FROM BOUNDARY #2

I	A	B	C	CL	D	E	F
1	0.02159	0.07239	0.14859	0.22479	0.30099	0.37719	0.42799
2	0.00508	0.05588	0.13208	0.20828	0.28448	0.36068	0.41148
3	0.00000	0.02413	0.10033	0.17653	0.25273	0.32893	0.00000
4	0.00000	0.00000	0.06604	0.14224	0.21844	0.00000	0.00000
5	0.00000	0.00000	0.03302	0.10922	0.18542	0.00000	0.00000
6	0.00000	0.00000	0.01651	0.09271	0.16891	0.00000	0.00000
7	0.00000	0.00000	0.00889	0.08509	0.16129	0.00000	0.00000

LOCAL VELOCITIES FOR HORIZONTAL STRIPS

I	A	B	C	CL	D	E	F
1	0.77663	0.92209	0.99155	1.01386	0.99155	0.92209	0.77663
2	0.56494	0.85664	0.94003	0.96467	0.94003	0.85664	0.56494
3	0.00000	0.69513	0.83523	0.86610	0.83523	0.69513	0.00000
4	0.00000	0.00000	0.70980	0.75246	0.70980	0.00000	0.00000
5	0.00000	0.00000	0.56480	0.63363	0.56480	0.00000	0.00000
6	0.00000	0.00000	0.46651	0.56959	0.46650	0.00000	0.00000
7	0.00000	0.00000	0.39931	0.53871	0.39931	0.00000	0.00000

VERTICAL STRIPS ANALYSIS

V	VMA	S	VK
0.43779E 00	0.53814E 00	0.15624E-02	0.44000E 00

J	N1	N2	N12	ALP	DLIM	TUL	UL	APHI	LIM
1	0.01580	0.01580	1.00000	0.50000	0.00025	0.01000	1.00000	7.04022	1.00000
2	0.01580	0.01580	1.00000	0.50000	0.00025	0.01000	1.00000	[illegible].09784	1.00000
3	0.01580	0.01580	1.00000	0.50000	0.00025	0.01000	1.00000	8.97402	1.00000
4	0.01580	0.01580	1.00000	0.50000	0.00025	0.01000	1.00000	8.97402	1.00000
5	0.01580	0.01580	1.00000	0.50000	0.00025	0.01000	1.00000	8.97402	1.00000
6	0.01580	0.01580	1.00000	0.50000	0.00025	0.01000	1.00000	8.09784	1.00000
7	0.01580	0.01580	1.00000	0.50000	0.00025	0.01000	1.00000	7.04022	1.00000

J	VY2	VY1	VD
1	0.01930	0.01930	0.03861
2	0.04470	0.04470	0.08941
3	0.08280	0.08280	0.16561
4	0.08280	0.08280	0.16561
5	0.08280	0.08280	0.16561
6	0.04470	0.04470	0.08941
7	0.01930	0.01930	0.03861

J	VVS2	VVM2	VVM1	VVS1	VVM	VVMAX
1	0.01721	0.18003	0.18003	0.01721	0.18003	0.20610
2	0.02618	0.31512	0.31512	0.02618	0.31512	0.35479
3	0.03563	0.47527	0.47527	0.03563	0.47527	0.52927
4	0.03563	0.47527	0.47527	0.03563	0.47527	0.52927
5	0.03563	0.47527	0.47527	0.03563	0.47527	0.52927
6	0.02618	0.31512	0.31512	0.02618	0.31512	0.35479
7	0.01721	0.18003	0.18003	0.01721	0.18003	0.20610

RELATIVE POSITION VECTORS FROM BOUNDARY #2

I \ J	A 1	B 2	C 3	CL 4	D 5	E 6	F 7
1	0.01656	0.01656	0.01656	0.01656	0.01656	0.01656	0.01656
2	0.03312	0.03312	0.03312	0.03312	0.03312	0.03312	0.03312
3	0.00000	0.06624	0.06624	0.06624	0.06624	0.06624	0.00000
4	0.00000	0.00000	0.09936	0.09936	0.09936	0.00000	0.00000
5	0.00000	0.00000	0.13249	0.13249	0.13249	0.00000	0.00000
6	0.00000	0.00000	0.14905	0.14905	0.14905	0.00000	0.00000
7	0.00000	0.00000	0.15733	0.15733	0.15733	0.00000	0.00000

LOCAL VELOCITIES FOR VERTICAL STRIPS

I \ J	A 1	B 2	C 3	CL 4	D 5	E 6	F 7
1	0.20457	0.32061	0.44031	0.44031	0.44031	0.32061	0.20457
2	0.17513	0.34856	0.48762	0.48762	0.48762	0.34856	0.17513
3	0.00000	0.33554	0.52376	0.52376	0.52376	0.33554	0.00000
4	0.00000	0.00000	0.52376	0.52376	0.52376	0.00000	0.00000
5	0.00000	0.00000	0.48762	0.48762	0.48762	0.00000	0.00000
6	0.00000	0.00000	0.44031	0.44031	0.44031	0.00000	0.00000
7	0.00000	0.00000	0.38839	0.38839	0.38839	0.00000	0.00000

PRODUCT OF (UH/HVM)*(UV/VVM)

I	A	B	C	CL	D	E	F
1	0.95414	1.01433	0.99319	1.01553	0.99319	1.01433	0.95414
2	0.62518	1.07792	1.09715	1.12591	1.09715	1.07792	0.62518
3	0.00000	0.94017	1.16915	1.21236	1.16915	0.94017	0.00000
4	0.00000	0.00000	1.14745	1.21640	1.14745	0.00000	0.00000
5	0.00000	0.00000	1.01371	1.13726	1.01371	0.00000	0.00000
6	0.00000	0.00000	0.84335	1.02971	0.84335	0.00000	0.00000
7	0.00000	0.00000	0.67422	0.90960	0.67422	0.00000	0.00000

FORMULATION OF COEFFICIENT EQUATION

*** SLOPE = 0.8906356E 00 ***

*** INTERCEPT = -0.3827922E-02 ***

*** STANDARD DEVIATION OF X = 0.8073747E-01 ***

*** STANDARD DEVIATION OF Y = 0.7233930E 01 ***

*** COEFFICIENT OF CORRELATION = 0.9940878E 00 ***

THE COEFFICIENT EQUATION IS U=V*E1*((UH/HVM)*(UV/VVM))**E2, WHERE

*** E1 = 0.9912246E 00 ***

*** E2 = 0.8906356E 00 ***

*** E3 = 0.1218428E 01 ***

UU RUN NUMBER E-62

EXPERIMENTAL LOCAL VELOCITIES (M/S)

STN / LEVEL	A	B	C	CL	D	E	F
1	0.41386	0.43608	0.42833	0.43653	0.42833	0.43608	0.41386
2	0.28665	0.45932	0.47495	0.50722	0.47495	0.45932	0.28665
3	0.00000	0.40865	0.49216	0.53814	0.49216	0.40865	0.00000
4	0.00000	0.00000	0.48439	0.50894	0.48439	0.00000	0.00000
5	0.00000	0.00000	0.43587	0.48075	0.43587	0.00000	0.00000
6	0.00000	0.00000	0.37217	0.47225	0.37217	0.00000	0.00000
7	0.00000	0.00000	0.30631	0.39722	0.30631	0.00000	0.00000

ESTIMATED LOCAL VELOCITIES BY THE COEFFICIENT EQUATION (M/S)

STN / LEVEL	A	B	C	CL	D	E	F
1	0.41618	0.43948	0.43132	0.43995	0.43132	0.43948	0.41618
2	0.28560	0.46394	0.47131	0.48229	0.47131	0.46394	0.28560
3	0.00000	0.41075	0.49876	0.51514	0.49876	0.41075	0.00000
4	0.00000	0.00000	0.49050	0.51667	0.49050	0.00000	0.00000
5	0.00000	0.00000	0.43925	0.48662	0.43925	0.00000	0.00000
6	0.00000	0.00000	0.37286	0.44541	0.37286	0.00000	0.00000
7	0.00000	0.00000	0.30547	0.39883	0.30547	0.00000	0.00000

YMAX= 0.1656 M VMEAN= 0.4378 M/S ENERGY SLOPE= 0.15624E-02

PERCENTAGE DIFFERENT IN LOCAL VELOCITIES USING ESTIMATED VALUES AS BASE

I	A	B	C	CL	D	E	F
1	0.55683	0.77458	0.69331	0.77598	0.69331	0.77458	0.55686
2	0.36754	0.99591	0.77362	5.16836	0.77362	0.99591	0.36725
3	0.00000	0.51205	1.32281	4.46512	1.32281	0.51208	0.00000
4	0.00000	0.00000	1.24670	1.49588	1.24670	0.00000	0.00000
5	0.00000	0.00000	0.76790	1.20736	0.76790	0.00000	0.00000
6	0.00000	0.00000	0.18309	6.02409	0.18306	0.00000	0.00000
7	0.00000	0.00000	0.27472	0.40465	0.27472	0.00000	0.00000

PERCENTAGE DIFFERENT IN LOCAL VELOCITIES USING EXPERIMENTAL VALUES AS BASE

I	A	B	C	CL	D	E	F
1	0.55995	0.78062	0.69815	0.78205	0.69815	0.78062	0.55998
2	0.36620	1.00593	0.76768	4.91436	0.76768	1.00593	0.36591
3	0.00000	0.51469	1.34054	4.27427	1.34054	0.51472	0.00000
4	0.00000	0.00000	1.26244	1.51859	1.26244	0.00000	0.00000
5	0.00000	0.00000	0.77384	1.22212	0.77384	0.00000	0.00000
6	0.00000	0.00000	0.18342	5.68181	0.18339	0.00000	0.00000
7	0.00000	0.00000	0.27396	0.40629	0.27396	0.00000	0.00000

```
CORRELATION BETWEEN ESTIMATED AND EXPERIMENTAL LOCAL VELOCITIES

    *** SLOPE =  0.1004650E 01 ***

    *** INTERCEPT = -0.1996502E 02 ***

    *** STANDARD DEVIATION OF X =  0.6460851E-01 ***

    *** STANDARD DEVIATION OF Y =  0.6550711E-01 ***

    *** COEFFICIENT OF CORRELATION =  0.9910657E 00 ***

    *** MAXINUM ESTIMATED LOCAL VELOCITY =  0.5166700E 00 ***

    *** MINIMUM ESTIMATED LOCAL VELOCITY =  0.2855985E 00 ***

    *** MEAN ESTIMATED VELOCITY =  0.4376473E 00 ***

    *** ESTIMATED VMAX/VMEAN RATIO =  0.1180562E 01 ***

    *** MAXINUM EXPERIMENTAL LOCAL VELOCITY =  0.5381412E 00 ***

    *** MINIMUM EXPERIMENTAL LOCAL VELOCITY =  0.2866482E 00 ***

    *** MEAN EXPERIMENTAL VELOCITY =  0.4378057E 00 ***

    *** EXPERIMENTAL VMAX/VMEAN RATIC =  0.1229177E 01 ***


STATEMENTS EXECUTED=    3707

CORE USAGE       OBJECT CODE=   25992 BYTES,ARRAY AREA=    5476 BYTES,TOTAL AREA AVAI
```

APPENDIX C

Experimental Results

C.1 Roughness Elements Calibration Data

In this appendix, the data which had been used in calibrating the roughness elements are listed in the following tables. The symbol which had been used are as follows:

- Q Experimental Total Flow Rate
- V Experimental Mean Velocity
- Del Different in elevations between station (1) and (2) per 12 ft. (3.658 m) of channel length.

TABLE C.1.1

Calibtration by Standard Approach

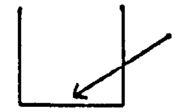

n_P

Q (USGPM)	V (ft/S)	DEL (ft.)	$N_R X10^{-4}$	n	C
180	0.240	0.001167	2.8745	0.0357	6.431
320	0.400	0.000833	5.1103	0.0185	12.474
460	0.548	0.001500	7.3460	0.0182	12.705
590	0.679	0.002166	9.4221	0.0178	13.040
930	0.984	0.000833	14.8520	0.0079	29.524
770	0.848	0.000833	12.2966	0.0089	26.145
180	0.242	0.000333	2.8745	0.0189	12.152
310	0.391	0.001167	4.9506	0.0223	10.334
390	0.478	0.000334	6.2281	0.0098	23,467
500	0.592	0.000001	7.9848	0.0004	542.160
630	0.721	0.000167	10.0608	0.0047	49.260
775	0.855	0.001167	12.3764	0.0106	21.875
950	1.003	0.002501	15.1711	0.0134	17.357
1135	1.157	0.000667	18.1254	0.0059	39.550

*1 USGPM = 6.3×10^{-5} m^3/s

**1 ft. = 0.3084 m

TABLE C.1.2

Calibration by Standard Approach

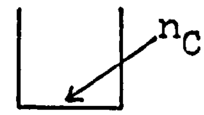

Q (USGPM)	V (ft/S)	DEL (ft.)	$N_R X10^{-4}$	n	C
125	0.174	0.001333	1.996	0.0520	4.4036
200	0.265	0.001500	3.194	0.0368	6.2492
300	0.380	0.001082	4.791	0.0219	1.0481
390	0.478	0.002499	6.228	0.0268	8.6207
490	0.580	0.001499	7.825	0.0172	13.4470
605	0.697	0.002999	9.661	0.0204	11.3730
710	0.797	0.002666	11.338	0.0169	13.7590
800	0.876	0.003166	12.776	0.0168	13.8410
920	0.982	0.005167	14.692	0.0192	12.1060
1020	1.065	0.005167	16.289	0.0178	13.1120
120	0.164	0.000499	1.916	0.0339	6.7490
200	0.264	0.000329	3.193	0.0173	13.2640
260	0.334	0.000499	4.152	0.0169	13.5800
335	0.417	0.000167	5.349	0.0789	29.2220
440	0.528	0.000667	7.026	0.0125	18.3930
520	0.611	0.001517	8.304	0.0165	14.0630
575	0.666	0.003917	9.182	0.0243	9.5193
660	0.747	0.001583	10.540	0.0139	16.7480
720	0.803	0.002749	11.498	0.0170	13.6450
800	0.876	0.003833	12.776	0.0185	12.5670
880	0.948	0.004582	14.053	0.0187	12.4270
960	0.101	0.003583	15.331	0.0155	15.0050

*USGPM = 6.3×10^{-5} m^2/s

**1 ft. = 0.3084 m

TABLE C.1.3

Calibration by Standard Approach

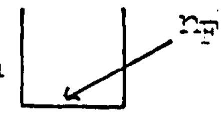

Q (USGPM)	V (ft/s)	DEL (ft.)	$N_R X10^{-4}$	n	C
1085	1.096	0.009333	17.327	0.0234	9.9863
940	0.981	0.011750	15.011	0.0292	7.8960
860	0.916	0.009583	13.734	0.0281	8.2855
790	0.857	0.008833	12.616	0.0288	8.0835
730	0.806	0.008833	11.658	0.0268	8.6602
680	0.761	0.006166	10.859	0.0269	8.6267
630	0.716	0.005999	10.061	0.0281	8.2506
555	0.645	0.005666	8.863	0.0302	7.6745
485	0.578	0.004333	7.745	0.0294	7.8809
415	0.507	0.003749	6.627	0.0310	7.4601
350	0.438	0.004582	5.589	0.0394	5.8614
425	0.517	0.005999	6.787	0.0384	6.0119
475	0.567	0.005080	7.585	0.0324	7.1485
515	0.606	0.005167	8.224	0.0306	7.5607
570	0.660	0.008166	9.102	0.0355	6.5293
630	0.717	0.006249	10.061	0.0287	8.0924
690	0.770	0.006916	11.019	0.0282	8.2365
750	0.823	0.007333	11.977	0.0273	8.5334
800	0.866	0.007999	12.776	0.0271	8.5816
835	0.897	0.007999	13.335	0.0262	8.8859
940	0.983	0.010833	15.011	0.0279	8.3390

*USGPM = 6.3×10^{-5} m^2/s

**1 ft. = 0.3084 m

TABLE C.1.4

Calibration by Vertical Strip Approach

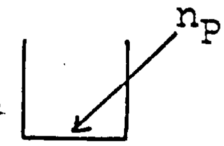

Q (USGPM)	V (ft/s)	DEL (ft.)	$N_R X10^{-4}$	n	C
22.0	0.511	0.000999	6.3384	0.0289	9.271
7.2	0.248	0.001999	2.2697	0.0656	3.839
9.0	0.302	0.002750	2.5871	0.0640	3.949
11.2	0.363	0.000417	3.2339	0.0212	11.996
13.0	0.416	0.000333	3.7513	0.0166	15.317
19.3	0.609	0.000417	5.5622	0.0129	19.710
22.5	0.692	0.000334	6.4677	0.0104	24.667
26.5	0.799	0.001000	7.6319	0.0159	16.239
30.1	0.889	0.000583	8.6667	0.0108	24.007
27.9	0.756	0.000333	8.0199	0.0103	25.314
34.2	0.904	0.000334	9.8309	0.0088	29.742
40.5	1.167	0.001000	11.6419	0.0113	22.928
45.0	1.267	0.000668	12.9354	0.0087	30.019
46.5	1.302	0.000083	13.3752	0.0029	87.181
53.1	1.440	0.000501	15.2638	0.0068	38.453
57.6	1.688	0.000667	16.5573	0.0059	44.113
63.0	1.801	0.000749	18.1096	0.0058	44.098
73.3	1.671	0.000499	21.0847	0.0061	43.889
81.0	1.804	0.000501	23.2838	0.0063	43.249
82.3	1.829	0.000499	23.6719	0.0057	47.763
90.8	1.933	0.000667	26.1296	0.0064	42.912

*USGPM = 6.3×10^{-5} m^3/s

** 1 ft = 0.3084 m

TABLE C.1.5

Calibration by Vertical Strip Approach

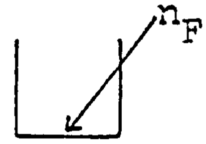

Q (USGPM)	V (ft/s)	DEL (ft.)	$N_R X10^{-4}$	n	C
9.4	0.2137	0.000667	2.7164	0.0579	4.663
14.0	0.3063	0.001167	4.0244	0.0548	4.958
20.0	0.4190	0.000083	5.7347	0.0109	24.904
26.9	0.5533	0.000250	7.7469	0.0146	18.844
32.5	0.6524	0.001916	9.3566	0.0347	7.938
41.3	0.8010	0.000916	11.8719	0.0199	13.896
46.9	0.8951	0.001333	13.4816	0.0217	12.794
53.9	0.1076	0.002920	15.4938	0.0258	10.681
61.2	0.1192	0.003333	17.6066	0.0253	10.954
74.5	0.1636	0.008667	21.4295	0.0267	10.092
82.6	0.1765	0.006833	23.7436	0.0224	12.168
89.6	0.1871	0.008999	25.7557	0.0245	11.152
97.6	0.1988	0.008582	28.0697	0.0228	12.041
102.6	0.2055	0.009667	29.4782	0.0236	11.666
109.9	0.2157	0.009333	31.5910	0.0223	12.384
116.9	0.2254	0.105830	33.6031	0.0229	12.098
123.9	0.2637	0.016833	35.6147	0.0224	12.201
135.1	0.2799	0.021249	38.8337	0.0238	11.488
144.2	0.2929	0.018667	41.4498	0.0214	12.810

*USGPM = $6.3 \times 10^{-5}\ m^3/s$

**1 ft = 0.3084 m

TABLE C.1.6

Calibration by Vertical Strip Approach

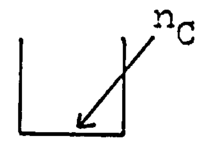

Q (USGPM)	V (ft/s)	DEL (ft.)	$N_R X10^{-4}$	n	C
13.3	0.506	0.001667	3.8231	0.027	9.105
17.6	0.635	0.011167	5.0519	0.058	4.314
21.8	0.775	0.001833	6.2809	0.019	12.619
25.5	0.769	0.000668	7.3186	0.013	19.181
29.4	0.868	0.001167	8.4652	0.016	16.125
34.9	0.997	0.003333	10.0221	0.024	10.754
46.5	1.072	0.003167	13.3809	0.025	10.658
56.0	1.244	0.001667	16.1117	0.016	16.671
63.4	1.543	0.002666	18.2145	0.015	18.072
70.3	1.676	0.002333	20.2079	0.013	20.893
78.6	1.821	0.004499	22.5838	0.016	16.221
89.0	1.999	0.005168	25.5877	0.018	14.854
96.6	2.131	0.004333	27.7723	0.014	19.146
105.0	2.269	0.005332	30.3119	0.015	18.273
114.0	2.412	0.004667	33.0428	0.013	20.669
124.0	2.555	0.006166	35.7735	0.014	18.991
145.0	3.948	0.032500	41.6938	0.014	19.005
155.0	3.224	0.013998	44.6481	0.016	16.981
165.0	3.372	0.013332	47.6521	0.015	18.236
180.0	3.578	0.014166	51.8847	0.015	18.865
193.0	3.965	0.019999	55.5704	0.014	19.012

*USGPM = 6.3 x 10^{-5} m^3/s

**1 ft = 0.3084 m.

C.2 Theoretical Results on Covered Channels

In this Appendix, the theoretical results on covered channels with different shapes and boundary roughness are presented. The symbols which had been used in the tables are as follows:

n_C - Manning's Coefficient for Coarse Wire Mesh (2 1/2" x 1 1/4")

n_F - Manning's Coefficient for Fine Wire Mesh (1 1/2" x 3/4")

n_P - Manning's Coefficient for Plywood

n_{tT} - Theoretical Composite Manning's Coefficient

n_{tE} - Experimental Composite Manning's Coefficient

TABLE C.2.1

Composite Roughness for Covered Channel

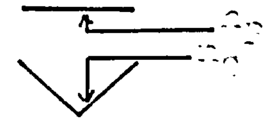

$N_R X10^{-4}$	n_1	n_2	A (ft^2)	R (ft)	λ	α	n_{tT}	n_{tE}
4.41	0.0225	0.0135	0.7096	0.1745	0.583	0.5858	0.0189	0.0181
4.67	0.0210	0.0123	0.7149	0.1751	0.577	0.5858	0.0175	0.0164
5.97	0.0166	0.0077	0.5817	0.1579	0.381	0.5858	0.0133	0.0126
7.25	0.0152	0.0063	0.6285	0.1642	0.296	0.5858	0.0119	0.0150
8.70	0.0157	0.0062	0.6816	0.1710	0.296	0.5858	0.0122	0.0158
10.63	0.0165	0.0072	0.5524	0.1539	0.380	0.5858	0.0129	0.0133
12.06	0.0167	0.0077	0.6144	0.1623	0.381	0.5858	0.0133	0.0126
14.65	0.0167	0.0082	0.6795	0.1707	0.382	0.5858	0.0135	0.0146
17.23	0.0167	0.0083	0.6582	0.1680	0.382	0.5858	0.0135	0.0127
18.03	0.0167	0.0083	0.6956	0.1727	0.382	0.5858	0.0135	0.0142

* 1 ft = 0.3084 m

TABLE C.2.2

Composite Roughness for Covered Channel

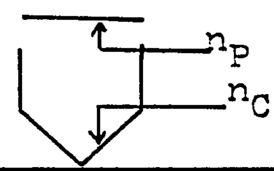

$N_R X10^{-4}$	n_1	n_2	A (ft^2)	R (ft)	λ	α	n_{tT}	n_{tE}
3.62	0.0320	0.0200	1.3535	0.2894	0.590	0.6792	0.0284	0.0156
3.72	0.0307	0.0193	1.3640	0.2908	0.588	0.6802	0.0272	0.0153
4.58	0.0215	0.0127	1.4069	0.2964	0.500	0.6871	0.0189	0.0158
6.48	0.0160	0.007	1.3302	0.2864	0.336	0.6771	0.0134	0.0081
9.02	0.0160	0.0062	1.4255	0.2987	0.294	0.6857	0.0133	0.0065
11.82	0.0166	0.0075	1.3732	0.2920	0.337	0.6810	0.0140	0.0122
15.50	0.0167	0.0083	1.2836	0.2801	0.379	0.6727	0.0142	0.0139
18.08	0.0167	0.0083	1.3521	0.2893	0.379	0.6791	0.0143	0.0129
20.54	0.0167	0.0083	1.4122	0.2970	0.379	0.6845	0.0143	0.0131
23.69	0.0167	0.0083	1.3173	0.2847	0.379	0.6759	0.0143	0.0144

*1 ft = 0.3084 m

TABLE C.2.3

Composite Roughness for Covered Channel

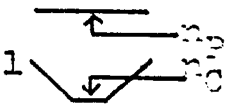

$N_R X10^{-4}$	n_1	n_2	A (ft^2)	R (ft)	λ	α	n_{tT}	n_{tE}
3.71	0.0290	0.0192	0.6038	0.1617	0.587	0.5628	0.0249	0.0153
4.58	0.0220	0.0130	0.6574	0.1690	0.507	0.5637	0.0183	0.0114
5.65	0.0175	0.0087	0.5274	0.1506	0.381	0.5613	0.0139	0.0118
6.53	0.0160	0.0070	0.5695	0.1568	0.333	0.5622	0.0125	0.0119
7.08	0.0155	0.0065	0.7159	0.1767	0.315	0.5646	0.0119	0.0148
7.84	0.0153	0.0060	0.6335	0.1658	0.287	0.5633	0.0117	0.0145
9.68	0.0162	0.0067	0.5977	0.1608	0.311	0.5627	0.0125	0.0133
10.97	0.0165	0.0075	0.6986	0.1744	0.347	0.5644	0.0129	0.0157
11.24	0.0165	0.0075	0.7266	0.1799	0.347	0.5648	0.0129	0.0153
12.07	0.0166	0.0077	0.6701	0.1707	0.347	0.5639	0.0131	0.0156

*1 ft = 0.3084 m

TABLE C.2.4

Composite Roughness for Covered Channel

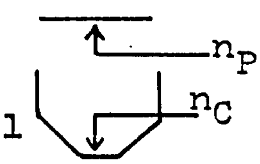

$N_R X10^{-4}$	n_1	n_2	A (ft^2)	R (ft)	λ	α	n_{tT}	n_{tE}
3.46	0.0350	0.0220	1.2350	0.2810	0.561	0.6586	0.0308	0.0161
4.58	0.0220	0.0130	1.2903	0.2888	0.504	0.6643	0.0192	0.0096
6.74	0.0157	0.0067	1.2113	0.2776	0.320	0.6562	0.0129	0.0114
9.59	0.0162	0.0067	1.3173	0.2925	0.308	0.6669	0.0134	0.0076
12.23	0.0167	0.0077	1.2158	0.2783	0.351	0.6566	0.1390	0.0123
14.32	0.0167	0.0082	1.2793	0.2873	0.273	0.6632	0.0137	0.0121
16.21	0.0167	0.0083	1.3357	0.2949	0.377	0.6688	0.0142	0.0125
17.81	0.0167	0.0083	1.1069	0.2621	0.378	0.6448	0.0140	0.0132
18.63	0.0167	0.0083	1.1262	0.2651	0.378	0.6469	0.0140	0.0132
20.88	0.0167	0.0083	1.1832	0.2736	0.378	0.6531	0.0141	0.0126

*1 ft = 0.3084 m

TABLE C.2.5

Composite Roughness For Covered Channel

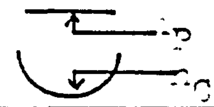

$N_R X10^{-4}$	n_1	n_2	A (ft^2)	R (ft)	λ	α	n_{tT}	n_{tE}
2.22	0.0350	0.0270	0.9110	0.2341	0.760	0.6147	0.0319	0.0111
4.06	0.0270	0.0167	0.8879	0.2299	0.542	0.6116	0.0233	0.0146
6.42	0.0160	0.0071	0.8749	0.2276	0.337	0.6098	0.0128	0.0209
8.41	0.0155	0.0060	0.8500	0.2230	0.281	0.6066	0.0122	0.0195
10.28	0.0163	0.0070	0.8043	0.2147	0.325	0.6006	0.0129	0.0160
12.66	0.0166	0.0078	0.8660	0.2259	0.359	0.6087	0.0135	0.0165
14.49	0.0166	0.0082	0.8659	0.2258	0.376	0.6087	0.0136	0.0160
16.68	0.0166	0.0083	0.8395	0.2209	0.380	0.6052	0.0136	0.0156
18.34	0.0166	0.0083	0.8242	0.2179	0.380	0.6032	0.0136	0.0145
20.55	0.0166	0.0083	0.8295	0.2187	0.380	0.6039	0.0136	0.0142

*1 ft = 0.3084 m

TABLE C.2.6

Composite Roughness For Covered Channel

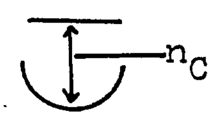

$N_R X10^{-4}$	n_1	n_2	A (ft^2)	R (ft)	λ	α	n_{tT}	n_{tE}
3.91	0.028	0.028	0.7473	0.2040	1.000	0.5935	0.0280	0.0170
6.33	0.016	0.016	0.7488	0.2043	1.000	0.5937	0.0160	0.0178
8.40	0.016	0.016	0.7644	0.2072	1.000	0.5956	0.0155	0.0205
11.93	0.017	0.017	0.7735	0.2088	1.000	0.5967	0.0166	0.0185
12.89	0.017	0.017	0.7944	0.2126	1.000	0.8994	0.0166	0.0189
14.09	0.017	0.017	0.8035	0.2142	1.000	0.6006	0.0166	0.0189
16.47	0.017	0.017	0.8239	0.2177	1.000	0.6032	0.0166	0.0189
17.96	0.017	0.017	0.8854	0.2279	1.000	0.6115	0.0166	0.0243
19.03	0.017	0.017	0.9010	0.2299	1.000	0.6138	0.0166	0.0253
20.06	0.017	0.017	0.9107	0.2314	1.000	0.6152	0.0166	0.0247

*1ft = 0.3084 m

TABLE C.2.7

Composite Roughness for Covered Channel

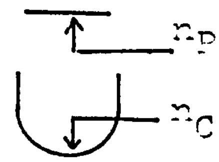

$N_R X10^{-4}$	n_1	n_2	A (ft^2)	R (ft)	λ	α	n_{tT}	n_{tE}
2.00	0.0350	0.0270	1.8250	0.3570	0.746	0.7065	0.0327	0.0850
4.34	0.0185	0.0145	1.8161	0.3561	0.763	0.7059	0.0174	0.0426
5.52	0.0175	0.0090	1.7725	0.3516	0.398	0.7025	0.0152	0.0236
7.44	0.0153	0.0062	1.8279	0.3573	0.299	0.7068	0.0129	0.0100
9.13	0.0160	0.0064	1.7085	0.3447	0.295	0.6973	0.0134	0.0175
11.21	0.0150	0.0075	1.7694	0.3513	0.378	0.7022	0.0130	0.0153
12.70	0.0166	0.0079	1.7508	0.3493	0.361	0.7007	0.0143	0.0055
14.45	0.0166	0.0082	1.8024	0.3547	0.374	0.7048	0.0144	0.0076
16.29	0.0166	0.0083	1.7688	0.3512	0.378	0.7022	0.0144	0.0133
18.39	0.0166	0.0083	1.7362	0.3477	0.378	0.6996	0.0144	0.0108

*1 ft = 0.3084 m

TABLE C.2.8

Composite Roughness for Covered Channel

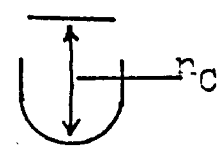

$N_R X10^{-4}$	n_1	n_2	A (ft^2)	R (ft)	λ	α	n_{tT}	n_{tE}
1.89	0.0350	0.3500	1.8378	0.3583	1.000	0.7075	0.0350	0.1018
3.83	0.0290	0.0290	1.6902	0.3427	1.000	0.6958	0.0290	0.0404
5.44	0.0180	0.0180	1.7713	0.3515	1.000	0.7024	0.0180	0.0311
7.13	0.0153	0.0153	1.8476	0.3595	1.000	0.7083	0.0153	0.0191
9.13	0.0160	0.0160	1.6727	0.3408	1.000	0.6944	0.0160	0.0069
11.09	0.0166	0.0166	1.7362	0.3477	1.000	0.6996	0.0166	0.0035
13.30	0.0166	0.0166	1.8116	0.3556	1.000	0.7055	0.0166	0.0134
14.95	0.0166	0.0166	1.7051	0.3444	1.000	0.6971	0.0166	0.0141
18.09	0.0166	0.0166	1.7418	0.3483	1.000	0.7000	0.0166	0.0107
18.55	0.0166	0.0166	1.8116	0.3556	1.000	0.7055	0.0166	0.0152

*1 ft = 0.3084 m

TABLE C.2.9

Composite Roughness for Covered Channel

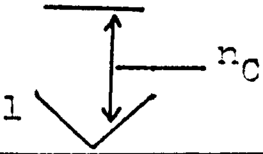

$N_R X10^{-4}$	n_1	n_2	A (ft^2)	R (ft)	λ	α	n_{tT}	n_{tE}
4.31	0.0235	0.0235	0.6046	0.1610	1.000	0.5858	0.0235	0.0153
5.87	0.0170	0.0170	0.6656	0.1689	1.000	0.5858	0.0170	0.0177
7.88	0.0153	0.0153	0.6247	0.1636	1.000	0.5858	0.0153	0.0165
9.00	0.0160	0.0160	0.6795	0.1706	1.000	0.5858	0.0160	0.0174
11.17	0.0165	0.0165	0.6116	0.1619	1.000	0.5858	0.0165	0.0139
14.18	0.0166	0.0166	0.6152	0.1622	1.000	0.5858	0.0166	0.0139
14.93	0.0166	0.0166	0.6788	0.1702	1.000	0.5858	0.0166	0.0166
17.07	0.0166	0.0166	0.6572	0.1673	1.000	0.5858	0.0166	0.0146
17.79	0.0166	0.0166	0.6989	0.1722	1.000	0.5858	0.0166	0.0169
18.55	0.0166	0.0166	0.7613	0.1797	1.000	0.5858	0.0166	0.0182

*1 ft. = 0.3084 m

TABLE C2.10

Composite Roughness for Covered Channel

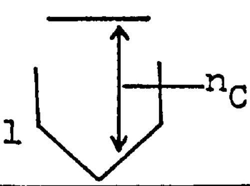

$N_R X10^{-4}$	n_1	n_2	A (ft^2)	R (ft)	λ	α	n_{tT}	n_{tE}
3.69	0.0310	0.0310	1.4062	0.2963	1.000	0.6839	0.0310	0.0208
4.50	0.0217	0.0217	1.2635	0.2773	1.000	0.6707	0.0220	0.0113
5.37	0.0182	0.0182	1.2487	0.2830	1.000	0.6747	0.0180	0.0078
7.29	0.0153	0.0153	1.3177	0.2753	1.000	0.6693	0.0160	0.0151
9.23	0.0160	0.0160	1.4053	0.2847	1.000	0.6759	0.0166	0.0174
11.85	0.0166	0.0166	1.2826	0.2962	1.000	0.6839	0.0166	0.0147
15.37	0.0166	0.0166	1.3592	0.2799	1.000	0.6726	0.0166	0.0143
18.29	0.0166	0.0166	1.3936	0.2902	1.000	0.6797	0.0166	0.0153
19.61	0.0166	0.0166	1.3936	0.2946	1.000	0.6828	0.0166	0.0141
22.99	0.0166	0.0166	1.2774	0.2792	1.000	0.6721	0.0166	0.0154

*1 ft = 0.3084 m

TABLE C.2.11

Composite Roughness for Covered Channel

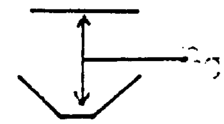

$N_R X10^{-4}$	n_1	n_2	A (ft^2)	R (ft)	λ	α	n_{tT}	n_{tE}
3.58	0.0350	0.0350	0.5545	0.1546	1.000	0.5619	0.0350	0.0134
4.18	0.0250	0.0250	0.5916	0.1599	1.000	0.5626	0.0250	0.0131
4.67	0.0207	0.0207	0.6223	0.1642	1.000	0.5631	0.0207	0.0149
6.06	0.0166	0.0166	0.5403	0.1525	1.000	0.5616	0.0166	0.0128
8.05	0.0155	0.0155	0.4571	0.1385	1.000	0.5594	0.0155	0.0178
8.95	0.0159	0.0159	0.5440	0.1529	1.000	0.5616	0.0159	0.0121
10.53	0.0163	0.0163	0.5662	0.1560	1.000	0.5621	0.0163	0.0123
11.65	0.0167	0.0167	0.6516	0.1676	1.000	0.5636	0.0167	0.0158
12.74	0.0167	0.0167	0.7323	0.1781	1.000	0.5648	0.0167	0.0164
11.59	0.0167	0.0167	0.6243	0.1739	1.000	0.5631	0.0167	0.0148

*1 ft = 0.3084 m

TABLE C.2.12

Composite Roughness for Covered Channel

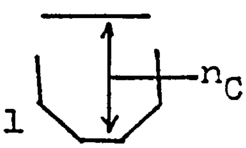

$N_R X10^{-4}$	n_1	n_2	A (ft^2)	R (ft)	λ	α	n_{tT}	n_{tE}
3.64	0.0320	0.0320	1.2526	0.2836	1.000	0.6605	0.032	0.0263
4.75	0.0205	0.0205	1.3100	0.2915	1.000	0.6662	0.0205	0.0025
7.15	0.0153	0.0153	1.2924	0.2891	1.000	0.6645	0.0153	0.0068
9.66	0.0162	0.0162	1.2623	0.2849	1.000	0.6614	0.0162	0.0138
12.78	0.0166	0.0166	1.1736	0.2721	1.000	0.6522	0.0166	0.0150
14.69	0.0166	0.0166	1.2340	0.2809	1.000	0.6585	0.0166	0.0146
17.12	0.0166	0.0166	1.3079	0.2912	1.000	0.6660	0.0166	0.0146
19.77	0.0166	0.0166	1.2012	0.2761	1.000	0.6550	0.0166	0.0147
16.46	0.0166	0.0166	1.3024	0.2904	1.000	0.6655	0.0166	0.0149
14.85	0.0166	0.0166	1.2502	0.2832	1.000	0.6602	0.0166	0.0132

*1 ft = 0.3084 m

TABLE C.2.13

Composite Roughness for Covered Channel

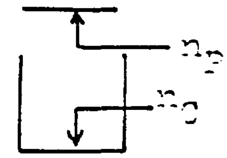

$N_R X10^{-4}$	n_1	n_2	A (ft^2)	R (ft)	λ	α	n_{tT}	n_{tE}
6.79	0.0156	0.0066	1.8937	0.3428	0.315	0.7285	0.0135	0.0115
4.87	0.0200	0.0112	1.8155	0.3349	0.465	0.7233	0.0178	0.0245
3.19	0.0350	0.0235	1.7353	0.3266	0.603	0.7177	0.0319	0.0428
8.14	0.0155	0.0060	2.0021	0.3531	0.279	0.7354	0.0133	0.0129
9.58	0.0162	0.0065	2.0465	0.3572	0.295	0.7382	0.0140	0.0147
11.18	0.0165	0.0075	2.0952	0.3616	0.344	0.7411	0.0145	0.0096
12.72	0.0166	0.0079	2.2937	0.3770	0.361	0.7519	0.0149	0.0153
14.37	0.0166	0.0082	1.8703	0.3404	0.374	0.7269	0.0146	0.0161
16.29	0.0166	0.0083	1.9287	0.3462	0.378	0.7308	0.0146	0.2161

*1 ft = 0.3084 m

TABLE C.2.14

Composite Roughness for Covered Channel

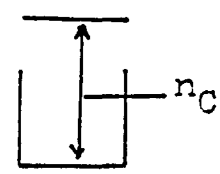

$N_R X10^{-4}$	n_1	n_2	A (ft^2)	R (ft)	λ	α	n_{tT}	n_{tE}
3.11	0.0350	0.0350	2.0869	0.3609	1.000	0.7406	0.0350	0.0330
4.87	0.0200	0.0200	2.0484	0.3574	1.000	0.7383	0.0200	0.0146
6.31	0.0162	0.0162	2.1067	0.3627	1.000	0.7418	0.0162	0.0083
8.14	0.0155	0.0155	2.0454	0.3572	1.000	0.7381	0.0155	0.0146
9.89	0.0162	0.0162	2.1741	0.3685	1.000	0.7457	0.0162	0.0932
11.24	0.0165	0.0165	1.7641	0.3296	1.000	0.7197	0.0165	0.0154
12.78	0.0166	0.0166	1.8176	0.3351	1.000	0.7234	0.0166	0.0172
14.37	0.0166	0.0166	1.8708	0.3405	1.000	0.7269	0.0166	0.0176
16.29	0.0166	0.0166	1.9353	0.3468	1.000	0.7312	0.0166	0.0196

*1 ft = 0.3084 m

C.3 Results of Statistical Analysis on Velocity Profiles

In this appendix, the results obtained from statistical analysis on velocity profiles are presented. The symbols which had been used in the tables are as follows:

E-13	Experiment run number
σ_{UT}	Standard deviation for theoretical velocity profile
σ_{UE}	Standard deviation for experimental velocity profile
m	Slope of regression line
r	Correlation coefficient
V_{maxT}	Theoretical maximum point velocity
V_{maxE}	Experimental maximum point velocity
V_{meanT}	Theoretical mean velocity
V_{meanE}	Experimental mean velocity

TABLE C.3.1

Results of Statistical Analysis on Velocity Profile

Run No.	σ_{UT} Theory	σ_{UE} Exper.	m Slope	r Cor.	V_{maxT}	V_{meanT}	V_{maxE}	V_{meanE}
E-13	0.034	0.0350	0.999	0.956	0.2907	0.2510	0.2982	0.2511
E-14	0.0490	0.0515	1.007	0.957	0.4092	0.3509	0.4251	0.3509
E-15	0.0522	0.0539	0.983	0.952	0.4768	0.4146	0.4785	0.4152
E-16	0.0409	0.0402	0.965	0.982	0.2711	0.2100	0.2648	0.2102
E-17	0.0394	0.0401	1.005	0.989	0.2670	0.2085	0.2639	0.2086
E-18	0.0639	0.0692	1.000	0.980	0.3503	0.2525	0.3491	0.2526
E-19	0.0391	0.0403	1.001	0.971	0.2860	0.2347	0.2915	0.2345
E-20	0.0275	0.0287	1.014	0.968	0.2902	0.2565	0.2975	0.2572
E-21	0.0682	0.0707	0.999	0.964	0.4893	0.4012	0.4785	0.4015
E-22	0.0298	0.0316	1.003	0.944	0.2940	0.2570	0.2980	0.2570
E-23	0.0530	0.0550	1.004	0.968	0.4213	0.3522	0.4251	0.3512
E-24	0.0683	0.0732	1.033	0.963	0.4967	0.4069	0.4910	0.4083
E-25	0.0338	0.0356	1.013	0.962	0.3009	0.2606	0.3116	0.2612
E-26	0.0552	0.0568	0.995	0.967	0.4238	0.3582	0.4184	0.3591
E-27	0.0521	0.0576	0.997	0.901	0.4829	0.4225	0.4919	0.4247
E-28	0.0287	0.0327	1.007	0.887	0.3173	0.2808	0.3249	0.2830
E-29	0.0373	0.0422	1.010	0.893	0.4242	0.3769	0.4451	0.3777
E-30	0.0381	0.0447	1.029	0.878	0.4402	0.3923	0.4652	0.3946
E-31	0.0367	0.0399	1.001	0.920	0.3802	0.3343	0.3975	0.3330
E-32	0.0222	0.0258	1.005	0.867	0.3333	0.3062	0.3459	0.3036
E-33	0.0267	0.0282	0.946	0.896	0.3375	0.3009	0.3265	0.2995
E-34	0.0273	0.0293	0.949	0.882	0.3370	0.3034	0.3329	0.3070
E-35	0.0335	0.0364	0.979	0.899	0.3439	0.3046	0.3620	0.3054
E-36	0.0267	0.0293	1.011	0.922	0.3332	0.3000	0.3459	0.3000
E-41	0.0621	0.0627	1.002	0.991	0.3539	0.2861	0.3650	0.2863
E-42	0.0593	0.0773	1.026	0.788	0.5205	0.4402	0.5720	0.4456
E-43	0.1238	0.1342	1.052	0.971	0.8775	0.7043	0.9267	0.7043
E-45	0.0446	0.0499	0.977	0.873	0.6458	0.6024	0.6599	0.6029
E-46	0.0246	0.0296	1.029	0.854	0.3266	0.2973	0.3449	0.2977
E-47	0.0486	0.0591	0.995	0.818	0.7662	0.7156	0.7976	0.7192
E-48	0.1100	0.1157	1.005	0.957	0.8911	0.7732	0.9267	0.7748
E-50	0.0279	0.0294	1.000	0.951	0.3485	0.3163	0.3683	0.3164
E-51	0.0296	0.0299	1.007	0.993	0.2915	0.2626	0.2924	0.2624
E-52	0.0514	0.0514	0.999	0.999	0.5232	0.4800	0.5232	0.4800
E-53	0.0995	0.0991	0.977	0.982	0.8203	0.6656	0.7976	0.6675
E-55	0.0324	0.0341	1.013	0.963	0.3582	0.3367	0.3624	0.3374
E-56	0.0251	0.0251	1.000	0.999	0.2568	0.2389	0.2568	0.2389
E-57	0.0091	0.0136	0.983	0.655	0.4123	0.3989	0.4123	0.4027
E-58	0.0960	0.0996	1.007	0.970	0.7788	0.6660	0.7976	0.6657
E-60	0.0501	0.0519	1.020	0.983	0.4310	0.3583	0.4611	0.3593
E-61	0.0152	0.0171	0.998	0.886	0.2655	0.2496	0.2679	0.2502
E-62	0.0646	0.0655	1.005	0.991	0.5167	0.4376	0.5381	0.4378

TABLE C.3.1 - continued

Run No.	σ_{UT} Theory	σ_{UE} Exper.	m Slope	r Cor.	V_{maxT}	V_{meanT}	V_{maxE}	V_{meanE}
E-63	0.0716	0.0779	1.021	0.938	0.7798	0.6803	0.7976	0.6842
E-65	0.0356	0.0383	1.027	0.954	0.4183	0.3781	0.4478	0.3799
E-66	0.0215	0.0221	1.014	0.982	0.2315	0.2065	0.2332	0.2067
E-67	0.0399	0.0477	1.010	0.846	0.6553	0.6137	0.7170	0.6171
E-68	0.0689	0.7063	1.001	0.976	0.8242	0.7550	0.8429	0.7568
E-70	0.0317	0.0324	0.979	0.958	0.3179	0.2722	0.3123	0.2729
E-71	0.0567	0.0596	1.012	0.962	0.5563	0.4749	0.5520	0.4759
E-72	0.0809	0.0910	1.048	0.931	0.8210	0.7078	0.8299	0.7089
E-74	0.0239	0.0246	1.007	0.976	0.3491	0.3214	0.3516	0.3217
E-75	0.0427	0.0460	1.027	0.952	0.5506	0.5017	0.5735	0.5037
E-76	0.0545	0.0599	1.021	0.927	0.6899	0.6278	0.7331	0.6295
E-78	0.0873	0.0909	1.018	0.978	0.6021	0.5084	0.6044	0.5092
E-79	0.0276	0.0279	1.010	0.998	0.1475	0.1082	0.1499	0.1086
E-80	0.0499	0.0551	1.051	0.951	0.4249	0.3666	0.4345	0.3679
E-81	0.0804	0.0805	0.985	0.983	0.7611	0.6604	0.7559	0.6590
E-82	0.0334	0.0353	1.048	0.989	0.1869	0.1485	0.1887	0.1497
E-83	0.0463	0.0531	1.029	0.896	0.5805	0.5429	0.6068	0.5473
E-84	0.0276	0.0341	1.003	0.811	0.7143	0.6890	0.7262	0.6860
E-87	0.0190	0.0199	1.022	0.979	0.9930	0.0748	0.1010	0.0754
E-88	0.0283	0.0295	1.011	0.972	0.2159	0.1841	0.2297	0.1843
E-89	0.0265	0.0272	0.981	0.956	0.3264	0.2985	0.3285	0.2981
E-90	0.0075	0.0084	1.013	0.913	0.1061	0.9849	0.1164	0.9849
E-91	0.0178	0.0189	0.956	0.901	0.1913	0.1705	0.1827	0.1713
E-92	0.0551	0.0550	0.982	0.984	0.3286	0.2657	0.3152	0.2653
E-93	0.0246	0.0247	0.994	0.992	0.1846	0.1581	0.1827	0.1582

C.4 Experimental and Theoretical Velocity Profiles

In this appendix, the theoretical results on velocity profiles are listed as below. The symbols which had been used in the tables are as follows:

STN A	represents the stations shown in Fig. 4.3.3.1
Level 1	represents the dimensionless depths shown in Fig. 4.3.3.1
M	in meter
M/s	in meter per second
E-13	Experiment run number
n_C	Manning's Coefficient for Coarse Wire Mesh (2 1/2" x 1 1/4")
n_F	Manning's Coefficient for Fine Wire Mesh (1 1/2" x 3/4")
n_P	Manning's Coefficient for plywood.

1 RUN NUMBER E-13

EXPERIMENTAL LOCAL VELOCITIES (M/S)

STN	A	B	C	CL	D	E	F
LEVEL							
1	0.26319	0.27816	0.28484	0.28484	0.27148	0.24477	0.21162
2	0.25145	0.29152	0.29820	0.29152	0.28484	0.27816	0.21606
3	0.27148	0.29820	0.29152	0.27148	0.27148	0.25282	0.21803
4	0.26434	0.27148	0.26488	0.26480	0.27148	0.24513	0.21140
5	0.26480	0.25145	0.25850	0.24477	0.25813	0.24477	0.19802
6	0.22458	0.22473	0.21806	0.23309	0.24477	0.22473	0.18467
7	0.20223	0.20964	0.20664	0.20470	0.18467	0.17799	0.16463

ESTIMATED LOCAL VELOCITIES BY THE COEFFICIENT EQUATION (M/S)

STN	A	B	C	CL	D	E	F
LEVEL							
1	0.26922	0.28326	0.28333	0.27840	0.26898	0.24951	0.21489
2	0.27624	0.29065	0.29071	0.28566	0.27599	0.25601	0.22050
3	0.27548	0.28774	0.28781	0.28280	0.27323	0.25346	0.21829
4	0.26509	0.27892	0.27898	0.27413	0.26485	0.24569	0.21160
5	0.24630	0.25915	0.25921	0.25470	0.24608	0.22827	0.19660
6	0.22491	0.23665	0.23670	0.23258	0.22471	0.20845	0.17953
7	0.20234	0.21290	0.21294	0.20924	0.20216	0.18753	0.16151

YMAX= 0.3492 M VMEAN= 0.2511 M/S ENERGY SLOPE= 0.13090E-02

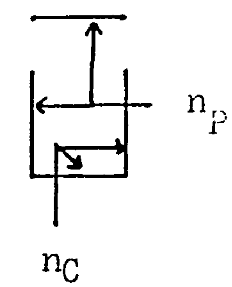

2 RUN NUMBER E-14

EXPERIMENTAL LOCAL VELOCITIES (M/S)

STN LEVEL	A	B	C	CL	D	E	F
1	0.35539	0.41173	0.41841	0.40505	0.38501	0.31823	0.31155
2	0.38501	0.41841	0.42508	0.40505	0.36498	0.36498	0.31823
3	0.39169	0.41173	0.40505	0.40505	0.37834	0.37834	0.30169
4	0.35830	0.37166	0.39837	0.37834	0.33827	0.33827	0.30169
5	0.33159	0.34203	0.35162	0.36501	0.32491	0.31155	0.26480
6	0.30487	0.30487	0.33566	0.33073	0.34494	0.28484	0.25145
7	0.26189	0.28484	0.31155	0.29255	0.28484	0.25813	0.21806

ESTIMATED LOCAL VELOCITIES BY THE COEFFICIENT EQUATION (M/S)

STN LEVEL	A	B	C	CL	D	E	F
1	0.36122	0.39003	0.39440	0.38760	0.37378	0.34465	0.29243
2	0.37789	0.40466	0.40919	0.40214	0.38780	0.35758	0.30340
3	0.37726	0.40398	0.40851	0.40147	0.38716	0.35699	0.30289
4	0.36551	0.39140	0.39579	0.38896	0.37510	0.34587	0.29346
5	0.33823	0.36219	0.36625	0.35993	0.34710	0.32005	0.27156
6	0.30635	0.32356	0.33226	0.32654	0.31490	0.29036	0.24636
7	0.27362	0.29300	0.29629	0.29118	0.28080	0.25692	0.21963

YMAX= 0.3879 M VMEAN= 0.3509 M/S ENERGY SLOPE= 0.27776E-03

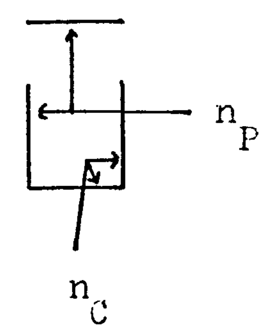

3 RUN NUMBER E-15

EXPERIMENTAL LOCAL VELOCITIES (M/S)

STN / LEVEL	A	B	C	CL	D	E	F
1	0.40505	0.43176	0.45180	0.41841	0.40505	0.39169	0.32826
2	0.41641	0.45848	0.47163	0.46515	0.45848	0.44512	0.35530
3	0.44512	0.46515	0.47851	0.47851	0.47851	0.45180	0.36594
4	0.44512	0.44512	0.46515	0.44512	0.45848	0.41251	0.35601
5	0.40505	0.41841	0.43844	0.43176	0.43176	0.39837	0.33627
6	0.37834	0.38501	0.40505	0.42508	0.41173	0.35353	0.32491
7	0.32491	0.33827	0.35162	0.36498	0.32491	0.29820	0.25813

ESTIMATED LOCAL VELOCITIES BY THE COEFFICIENT EQUATION (M/S)

STN / LEVEL	A	B	C	CL	D	E	F
1	0.42394	0.45304	0.45929	0.45231	0.43773	0.40659	0.34999
2	0.43953	0.46953	0.47601	0.46877	0.45366	0.42139	0.36274
3	0.44007	0.47027	0.47676	0.46951	0.45436	0.42206	0.36331
4	0.42792	0.45729	0.46359	0.45655	0.44183	0.41040	0.35328
5	0.39917	0.42657	0.43245	0.42588	0.41215	0.38284	0.32955
6	0.36573	0.39083	0.39622	0.39020	0.37762	0.35076	0.30194
7	0.32936	0.35280	0.35747	0.35203	0.34069	0.31645	0.27240

YMAX= 0.4200 M VMEAN= 0.4152 M/S ENERGY SLOPE= 0.56042E-03

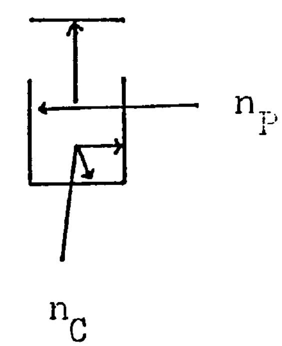

4 RUN NUMBER L-16

EXPERIMENTAL LOCAL VELOCITIES (M/S)

STN LEVEL	A	B	C	CL	D	E	F
1	0.14335	0.18334	0.21797	0.23141	0.21806	0.18334	0.14335
2	0.16558	0.21177	0.23669	0.25145	0.23669	0.21177	0.16558
3	0.18332	0.23445	0.26480	0.25145	0.26480	0.23445	0.18332
4	0.18332	0.24477	0.24477	0.24811	0.24477	0.24477	0.18332
5	0.16558	0.21138	0.23669	0.23342	0.23669	0.21138	0.16553
6	0.14126	0.18334	0.20492	0.21214	0.20492	0.18334	0.14126
7	0.11120	0.15385	0.17196	0.17802	0.17196	0.15385	0.11120

ESTIMATED LOCAL VELOCITIES BY THE COEFFICIENT EQUATION (M/S)

STN LEVEL	A	B	C	CL	D	E	F
1	0.14233	0.18248	0.20419	0.21146	0.20419	0.18248	0.14233
2	0.16464	0.21109	0.23619	0.24460	0.23619	0.21109	0.16464
3	0.18245	0.23393	0.26175	0.27107	0.26175	0.23393	0.18245
4	0.18245	0.23393	0.26175	0.27107	0.26175	0.23393	0.18245
5	0.16464	0.21109	0.23619	0.24460	0.23619	0.21109	0.16464
6	0.14233	0.18248	0.20419	0.21146	0.20419	0.18248	0.14233
7	0.11922	0.15286	0.17103	0.17712	0.17103	0.15286	0.11922

YMAX= 0.3643 4 VMEAN= 0.2101 M/S ENERGY SLOPE= 0.27736E-04

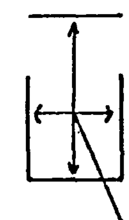

n_C

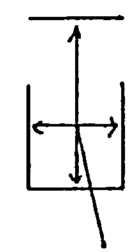

5 RUN NUMBER E-17

EXPERIMENTAL LOCAL VELOCITIES (M/S)

STN / LEVEL	A	B	C	CL	D	E	F
1	0.14146	0.17660	0.19769	0.20688	0.19769	0.17660	0.14146
2	0.16257	0.21259	0.23279	0.26390	0.23279	0.21259	0.16257
3	0.17839	0.23053	0.25630	0.26390	0.25630	0.23053	0.17839
4	0.18234	0.23053	0.26390	0.24680	0.26390	0.23053	0.18234
5	0.16662	0.20938	0.23279	0.26390	0.23279	0.20938	0.16662
6	0.14451	0.18270	0.20312	0.20993	0.20312	0.18270	0.14451
7	0.12243	0.15478	0.17209	0.17786	0.17209	0.15478	0.12243

ESTIMATED LOCAL VELOCITIES BY THE COEFFICIENT EQUATION (M/S)

STN / LEVEL	A	B	C	CL	D	E	F
1	0.14306	0.18213	0.20312	0.21013	0.20312	0.18213	0.14306
2	0.16462	0.20957	0.23372	0.24179	0.23372	0.20957	0.16462
3	0.18176	0.23139	0.25806	0.26697	0.25806	0.23139	0.18176
4	0.18176	0.23139	0.25806	0.26697	0.25806	0.23139	0.18176
5	0.16462	0.20957	0.23372	0.24179	0.23372	0.20957	0.16462
6	0.14306	0.18213	0.20312	0.21013	0.20312	0.18213	0.14306
7	0.12060	0.15354	0.17123	0.17715	0.17123	0.15354	0.12060

YMAX= 0.3305 M   VMEAN= 0.2066 M/S   ENERGY SLOPE= 0.43742E-03

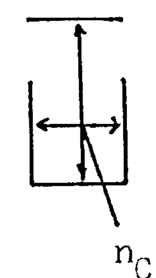

6 RUN NUMBER E-18

EXPERIMENTAL LOCAL VELOCITIES (M/S)

STN / LEVEL	A	B	C	CL	D	E	F
1	0.15734	0.21259	0.26390	0.26390	0.26390	0.21259	0.15734
2	0.16813	0.25465	0.31521	0.31521	0.31521	0.25465	0.16813
3	0.22280	0.29213	0.31863	0.34911	0.31863	0.29213	0.22280
4	0.20760	0.29213	0.31521	0.34909	0.31521	0.29213	0.20760
5	0.15057	0.22970	0.31521	0.31521	0.31521	0.22970	0.15057
6	0.16129	0.20665	0.22970	0.25370	0.22970	0.20665	0.16129
7	0.12708	0.16263	0.17839	0.19980	0.17839	0.16263	0.12708

ESTIMATED LOCAL VELOCITIES BY THE COEFFICIENT EQUATION (M/S)

STN / LEVEL	A	B	C	CL	D	E	F
1	0.15009	0.20891	0.24257	0.25412	0.24257	0.20891	0.15009
2	0.16113	0.25212	0.29274	0.30668	0.29274	0.25212	0.16113
3	0.20687	0.28795	0.33435	0.35027	0.33435	0.28795	0.20687
4	0.20687	0.28795	0.33435	0.35027	0.33435	0.28795	0.20687
5	0.16113	0.25212	0.29274	0.30668	0.29274	0.25212	0.16113
6	0.15009	0.20891	0.24257	0.25412	0.24257	0.20891	0.15009
7	0.11947	0.16629	0.19309	0.20228	0.19309	0.16629	0.11947

YMAX= 0.4[illegible] VMEAN= 0.2393 M/S ENERGY SLOPE= 0.83327E-03

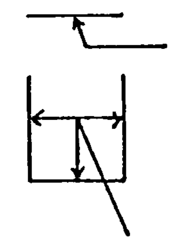

7 RUN NUMBER E-19

EXPERIMENTAL LOCAL VELOCITIES (M/S)

STN LEVEL	A	B	C	CL	D	E	F
1	0.21138	0.23141	0.25813	0.25813	0.25813	0.23141	0.21138
2	0.22473	0.25813	0.29152	0.29152	0.29152	0.25813	0.22473
3	0.20866	0.25202	0.28484	0.28484	0.28484	0.25202	0.20866
4	0.20058	0.24224	0.28484	0.25145	0.28484	0.24224	0.20058
5	0.18266	0.23141	0.22473	0.24394	0.22473	0.23141	0.18266
6	0.16271	0.21138	0.21113	0.21697	0.21113	0.21138	0.16271
7	0.14224	0.17179	0.18419	0.18929	0.18419	0.17179	0.14224

ESTIMATED LOCAL VELOCITIES BY THE COEFFICIENT EQUATION (M/S)

STN LEVEL	A	B	C	CL	D	E	F
1	0.20525	0.24738	0.26937	0.27663	0.26937	0.24738	0.20525
2	0.21225	0.25582	0.27856	0.28607	0.27856	0.25582	0.21225
3	0.20975	0.25231	0.27527	0.28269	0.27527	0.25231	0.20975
4	0.20170	0.24310	0.26471	0.27184	0.26471	0.24310	0.20170
5	0.18336	0.22160	0.24130	0.24780	0.24130	0.22160	0.18336
6	0.16399	0.19765	0.21522	0.22102	0.21522	0.19765	0.16399
7	0.14356	0.17303	0.18840	0.19348	0.18840	0.17303	0.14356

YMAX= 0.3742 M VMEAN= 0.2344 M/S ENERGY SLOPE= 0.29167E-03

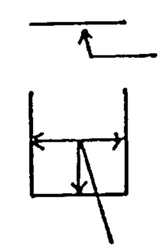

8 RUN NUMBER E-20

EXPERIMENTAL LOCAL VELOCITIES (M/S)

STN / LEVEL	A	B	C	CL	D	E	F
1	0.21806	0.25145	0.28406	0.28905	0.28710	0.25145	0.21806
2	0.24722	0.27641	0.28686	0.29743	0.29234	0.27946	0.24722
3	0.22970	0.26390	0.28910	0.29728	0.29215	0.26390	0.22970
4	0.23654	0.26390	0.26390	0.29020	0.26390	0.26390	0.23654
5	0.21259	0.24680	0.26390	0.26390	0.26390	0.24680	0.21259
6	0.20831	0.23588	0.24680	0.24680	0.24680	0.23588	0.20831
7	0.19384	0.21912	0.22844	0.23259	0.23161	0.21608	0.19[illegible]

ESTIMATED LOCAL VELOCITIES BY THE COEFFICIENT EQUATION (M/S)

STN / LEVEL	A	B	C	CL	D	E	F
1	0.23317	0.26288	0.27752	0.28224	0.27752	0.26288	0.23317
2	0.23974	0.27029	0.28535	0.29020	0.28535	0.27029	0.23974
3	0.23959	0.27012	0.28517	0.29002	0.28517	0.27012	0.23959
4	0.23407	0.26390	0.27859	0.28333	0.27859	0.26390	0.23407
5	0.22102	0.24919	0.26306	0.26754	0.26306	0.24919	0.22102
6	0.20567	0.23187	0.24479	0.24895	0.24479	0.23187	0.20567
7	0.18397	0.21305	0.22491	0.22874	0.22491	0.21305	0.18397

YMAX= 0.4058 M VMEAN= 0.2572 M/S ENERGY SLOPE= 0.39577E-03

9 RUN NUMBER E-21

EXPERIMENTAL LOCAL VELOCITIES (M/S)							
STN	A	B	C	CL	D	E	F
LEVEL							
1	0.31017	0.38439	0.42309	0.43583	0.42309	0.38439	0.31017
2	0.33159	0.44512	0.47851	0.47851	0.47851	0.44512	0.33159
3	0.37166	0.46849	0.47851	0.47851	0.47851	0.46849	0.37166
4	0.34491	0.42010	0.47851	0.47851	0.47851	0.42010	0.34491
5	0.34494	0.40505	0.41840	0.43020	0.41840	0.40505	0.34494
6	0.29152	0.31823	0.39169	0.39169	0.39169	0.31823	0.29152
7	0.23609	0.28484	0.31823	0.31823	0.31823	0.28484	0.23809

ESTIMATED LOCAL VELOCITIES BY THE COEFFICIENT EQUATION (M/S)							
STN	A	B	C	CL	D	E	F
LEVEL							
1	0.33885	0.41351	0.45243	0.46528	0.45243	0.41351	0.33885
2	0.35562	0.43398	0.47483	0.48832	0.47483	0.43398	0.35562
3	0.35637	0.43489	0.47583	0.48935	0.47583	0.43489	0.35637
4	0.34313	0.41874	0.45816	0.47117	0.45816	0.41874	0.34313
5	0.31236	0.38119	0.41707	0.42892	0.41707	0.38119	0.31236
6	0.27754	0.33870	0.37058	0.38111	0.37058	0.33870	0.27754
7	0.24154	0.29476	0.32251	0.33167	0.32251	0.29476	0.24154

YMAX= 0.434[illegible] VMEAN= 0.4015 M/S ENERGY SLOPE= 0.47223E-03

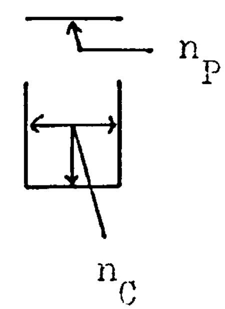

10 RUN NUMBER E-22

EXPERIMENTAL LOCAL VELOCITIES (M/S)

STN LEVEL	A	B	C	CL	D	E	F
1	0.22675	0.25144	0.25813	0.25813	0.23141	0.22593	0.17799
2	0.23141	0.28484	0.29820	0.29152	0.26480	0.24027	0.20470
3	0.25813	0.29820	0.29152	0.29152	0.29152	0.25144	0.20717
4	0.27148	0.29152	0.28484	0.27816	0.29152	0.27148	0.21022
5	0.25144	0.25144	0.26480	0.27148	0.27148	0.26480	0.20717
6	0.21806	0.25023	0.25144	0.25144	0.25144	0.25144	0.20470
7	0.21047	0.23141	0.23809	0.23809	0.23809	0.21617	0.17131

ESTIMATED LOCAL VELOCITIES BY THE COEFFICIENT EQUATION (M/S)

STN LEVEL	A	B	C	CL	D	E	F
1	0.25000	0.25497	0.26387	0.26018	0.25086	0.22975	0.18595
2	0.24552	0.27147	0.28095	0.27702	0.26710	0.24461	0.20113
3	0.25663	0.28380	0.29371	0.28960	0.27923	0.25574	0.21052
4	0.25663	0.28380	0.29371	0.28960	0.27923	0.25574	0.21052
5	0.24552	0.27147	0.28095	0.27702	0.26710	0.24461	0.20113
6	0.25000	0.25497	0.26387	0.26018	0.25086	0.22975	0.18595
7	0.21376	0.23634	0.24460	0.24117	0.23254	0.21297	0.1751[illegible]

YMAX= 0.3451 M VMEAN= 0.2573 M/S ENERGY SLOPE= 0.13356E-0[illegible]

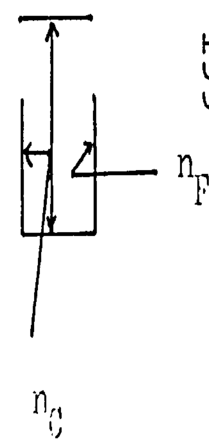

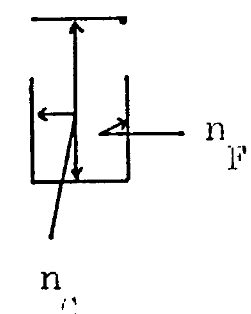

11 RUN NUMBER E-23

EXPERIMENTAL LOCAL VELOCITIES (M/S)

STN	A	B	C	CL	D	E	F
LEVEL							
1	0.29827	0.33159	0.35830	0.33827	0.31437	0.27974	0.24477
2	0.31155	0.37166	0.41173	0.39169	0.35162	0.30722	0.27143
3	0.34494	0.41173	0.42508	0.40505	0.38501	0.36498	0.28341
4	0.35433	0.41172	0.41841	0.39837	0.39169	0.38501	0.28341
5	0.33827	0.37834	0.41173	0.40505	0.39169	0.33771	0.26692
6	0.29820	0.33159	0.37834	0.35994	0.34487	0.31021	0.24519
7	0.25689	0.26026	0.31155	0.32491	0.31155	0.25813	0.20479

ESTIMATED LOCAL VELOCITIES BY THE COEFFICIENT EQUATION (M/S)

STN	A	B	C	CL	D	E	F
LEVEL							
1	0.29371	0.34108	0.38122	0.35723	0.34140	0.30506	0.23733
2	0.32146	0.37329	0.39534	0.39103	0.37365	0.33389	0.26002
3	0.34260	0.39785	0.42134	0.41674	0.39823	0.35585	0.27712
4	0.34260	0.39785	0.42134	0.41674	0.39823	0.35585	0.27712
5	0.32146	0.37329	0.39534	0.39103	0.37365	0.33389	0.26002
6	0.29371	0.34108	0.38122	0.35723	0.34140	0.30506	0.23733
7	0.26316	0.30560	0.3236	0.32012	0.30589	0.27334	0.21286

YMAX= 0.37[illegible] M VMEAN= 0.35[illegible] M/S ENERGY SLOPE= 0.[illegible]271E-03

12 RUN NUMBER E-24

EXPERIMENTAL LOCAL VELOCITIES (M/S)

STN	A	B	C	CL	D	E	F
LEVEL							
1	0.31362	0.37815	0.44269	0.44269	0.36202	0.34589	0.24909
2	0.34589	0.42655	0.47495	0.47495	0.44269	0.37815	0.31362
3	0.36202	0.47495	0.49109	0.49109	0.45882	0.44269	0.30552
4	0.39427	0.47495	0.49109	0.49109	0.47495	0.44269	0.30854
5	0.34589	0.44269	0.47495	0.47495	0.45882	0.38237	0.31362
6	0.31362	0.37815	0.44269	0.44269	0.37815	0.34711	0.28135
7	0.29717	0.32223	0.34408	0.33841	0.31984	0.28135	0.24909

ESTIMATED LOCAL VELOCITIES BY THE COEFFICIENT EQUATION (M/S)

STN	A	B	C	CL	D	E	F
LEVEL							
1	0.33531	0.39502	0.41993	0.41348	0.39233	0.34484	0.25354
2	0.37000	0.43589	0.46338	0.45626	0.43292	0.38052	0.28523
3	0.39664	0.46727	0.49673	0.48910	0.46408	0.40791	0.30582
4	0.39664	0.46727	0.49673	0.48910	0.46408	0.40791	0.30582
5	0.37000	0.43589	0.46338	0.45626	0.43292	0.38052	0.28528
6	0.33531	0.39502	0.41993	0.41348	0.39233	0.34484	0.25354
7	0.29750	0.35048	0.37258	0.36685	0.34809	0.30596	0.22439

YMAX= 0.4011 M VMEAN= 0.4083 M/S ENERGY SLOPE= 0.14722E-02

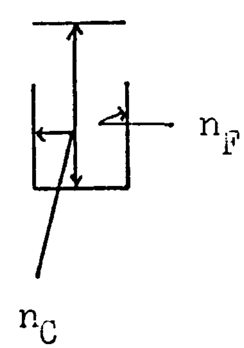

13 RUN NUMBER E-25

EXPERIMENTAL LOCAL VELOCITIES (M/S)

STN	A	B	C	CL	D	E	F
LEVEL							
1	0.25040	0.26480	0.27816	0.27816	0.25813	0.24477	0.20470
2	0.25526	0.27816	0.31155	0.31155	0.29820	0.25912	0.21306
3	0.25813	0.29152	0.31155	0.30487	0.29820	0.25702	0.21036
4	0.24477	0.29152	0.29820	0.28484	0.28484	0.25093	0.20338
5	0.24477	0.25144	0.27816	0.27816	0.27148	0.25144	0.19412
6	0.20470	0.24477	0.25144	0.25813	0.26480	0.23141	0.19134
7	0.20033	0.22332	0.23210	0.22889	0.22034	0.20097	0.17131

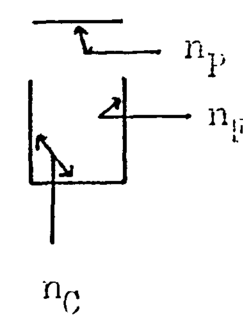

ESTIMATED LOCAL VELOCITIES BY THE COEFFICIENT EQUATION (M/S)

STN	A	B	C	CL	D	E	F
LEVEL							
1	0.25510	0.28416	0.29525	0.29120	0.28039	0.25591	0.2091[illegible]
2	0.26003	0.28966	0.30096	0.29683	0.28582	0.2606[illegible]	0.2131[illegible]
3	0.25791	0.28726	0.29850	0.29440	0.28348	0.25872	0.2114[illegible]
4	0.25176	0.28043	0.29138	0.28738	0.27672	0.25255	0.20[illegible]
5	0.23785	0.26495	0.27529	0.27151	0.26144	0.23861	0.19493
6	0.22175	0.24701	0.25665	0.25312	0.24373	0.22245	0.1517[illegible]
7	0.20437	0.22765	0.23653	0.23328	0.22463	0.20502	0.1675[illegible]

YMAX= 0.3492 M VMEAN= 0.2612 M/S ENERGY SLOPE= 0.2636[illegible]E-03

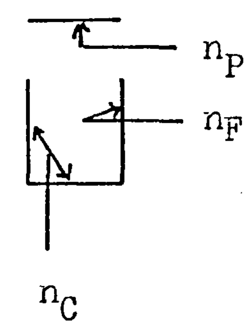

14 RUN NUMBER E-28

EXPERIMENTAL LOCAL VELOCITIES (M/S)

STN LEVEL	A	B	C	CL	D	E	F
1	0.30819	0.35980	0.39169	0.39169	0.36498	0.33734	0.27622
2	0.33159	0.38501	0.41841	0.41841	0.39837	0.35162	0.27316
3	0.33162	0.40505	0.41841	0.41841	0.40505	0.39169	0.28539
4	0.33159	0.40505	0.41841	0.40505	0.40505	0.35115	0.27750
5	0.32491	0.36498	0.40505	0.41173	0.39169	0.32776	0.25904
6	0.28434	0.36498	0.35271	0.34881	0.33418	0.30061	0.23759
7	0.26014	0.29922	0.29820	0.32491	0.27148	0.27156	0.20470

ESTIMATED LOCAL VELOCITIES BY THE COEFFICIENT EQUATION (M/S)

STN LEVEL	A	B	C	CL	D	E	F
1	0.33657	0.33797	0.40952	0.40486	0.38744	0.34757	0.27294
2	0.34833	0.40150	0.42380	0.41898	0.40095	0.35969	0.28245
3	0.34803	0.40119	0.42348	0.41866	0.40064	0.35941	0.28223
4	0.33817	0.38982	0.41147	0.40679	0.38928	0.34922	0.27423
5	0.31503	0.36321	0.38338	0.37902	0.36271	0.32538	0.25551
6	0.28852	0.33235	0.35081	0.34682	0.33190	0.29774	0.23381
7	0.25973	0.29940	0.31603	0.31244	0.29899	0.26822	0.21063

YMAX= 0.4072 M VMEAN= 0.3591 M/S ENERGY SLOPE= 0.7032E-03

15 RUN NUMBER E-27

EXPERIMENTAL LOCAL VELOCITIES (M/S)

STN	A	B	C	CL	D	L	F
LEVEL							
1	0.36498	0.41841	0.43176	0.43176	0.42508	0.39837	0.31823
2	0.38501	0.44512	0.46515	0.47851	0.45180	0.41173	0.33159
3	0.40505	0.45848	0.49187	0.48519	0.47183	0.45180	0.36493
4	0.39169	0.47183	0.47851	0.48519	0.47183	0.45848	0.38501
5	0.37834	0.45180	0.47183	0.47851	0.45848	0.43176	0.36493
6	0.35827	0.42508	0.45848	0.43176	0.40505	0.36495	0.33826
7	0.28484	0.34494	0.36498	0.36498	0.35162	0.31823	0.27148

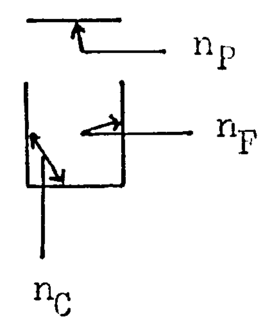

ESTIMATED LOCAL VELOCITIES BY THE COEFFICIENT EQUATION (M/S)

STN	A	B	C	CL	D	E	F
LEVEL							
1	0.40329	0.45015	0.46899	0.46415	0.44809	0.41094	0.33575
2	0.41476	0.46294	0.48233	0.47734	0.46083	0.42265	0.34533
3	0.41527	0.46352	0.48292	0.47793	0.46140	0.42315	0.34631
4	0.40625	0.45346	0.47244	0.46756	0.45133	0.41396	0.34124
5	0.38470	0.42940	0.44738	0.44276	0.42744	0.39200	0.32313
6	0.35919	0.40095	0.41771	0.41340	0.39909	0.36601	0.30171
7	0.33133	0.36983	0.38531	0.38133	0.36814	0.33762	0.27831

YMAX= 0.4135 M V MEAN= 0.4247 M/S ENERGY SLOPE= 0.83327E-03

16 RUN NUMBER E-28

EXPERIMENTAL LOCAL VELOCITIES (M/S)

STN / LEVEL	A	B	C	CL	D	E	F
1	0.21138	0.25144	0.27148	0.27148	0.28392	0.27979	0.26150
2	0.21806	0.28484	0.31155	0.31155	0.30487	0.28774	0.26874
3	0.25144	0.31155	0.32491	0.32491	0.32491	0.29152	0.27148
4	0.25813	0.30487	0.31823	0.31155	0.31823	0.29152	0.27816
5	0.25144	0.27148	0.31155	0.30487	0.31155	0.28484	0.25144
6	0.23141	0.25144	0.26480	0.29820	0.29820	0.26480	0.23141
7	0.20470	0.22473	0.24477	0.25813	0.27816	0.23809	0.22473

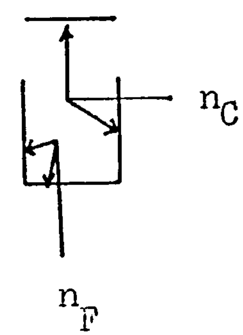

ESTIMATED LOCAL VELOCITIES BY THE COEFFICIENT EQUATION (M/S)

STN / LEVEL	A	B	C	CL	D	E	F
1	0.24030	0.27316	0.28954	0.29653	0.29865	0.29052	0.26990
2	0.25061	0.28488	0.30197	0.30926	0.31147	0.30299	0.28148
3	0.25533	0.29024	0.30764	0.31507	0.31733	0.30869	0.28677
4	0.25045	0.28470	0.30177	0.30905	0.31127	0.30279	0.28130
5	0.23697	0.26938	0.28553	0.29242	0.29452	0.28650	0.26616
6	0.21995	0.25002	0.26502	0.27141	0.27336	0.26592	0.24704
7	0.20023	0.22761	0.24126	0.24708	0.24885	0.24205	0.22489

YMAX= 0.3523 M   VMEAN= 0.2830 M/S   ENERGY SLOPE= 0.40976E-03

17 RUN NUMBER E-29

EXPERIMENTAL LOCAL VELOCITIES (M/S)

STN LEVEL	A	B	C	CL	D	E	F
1	0.30255	0.33788	0.36348	0.36256	0.36498	0.37000	0.32955
2	0.31155	0.35046	0.40505	0.43170	0.41841	0.39169	0.34552
3	0.34434	0.36498	0.43176	0.44512	0.43170	0.41841	0.39337
4	0.35162	0.39169	0.41841	0.41841	0.43170	0.41841	0.40505
5	0.32491	0.39169	0.40505	0.38933	0.39153	0.39169	0.37834
6	0.29820	0.36458	0.35677	0.36436	0.38501	0.35162	0.33827
7	0.27148	0.31139	0.32801	0.35162	0.36493	0.29820	0.31155

ESTIMATED LOCAL VELOCITIES BY THE COEFFICIENT EQUATION (M/S)

STN LEVEL	A	B	C	CL	D	E	F
1	0.32330	0.36658	0.38785	0.39682	0.39924	0.38826	0.36076
2	0.33097	0.38207	0.40424	0.41359	0.41612	0.40469	0.37604
3	0.34355	0.33953	0.41213	0.42166	0.42424	0.41259	0.38337
4	0.33738	0.33254	0.40473	0.41409	0.41662	0.40518	0.37649
5	0.32001	0.36284	0.38390	0.39278	0.39518	0.38432	0.35711
6	0.29734	0.33771	0.35730	0.36557	0.36780	0.35770	0.33237
7	0.27169	0.30828	0.32617	0.33371	0.33575	0.32655	0.30341

YMAX= 0.37694 VMEAN= 0.3787 M/S ENERGY SLOPE= 0.69435E-03

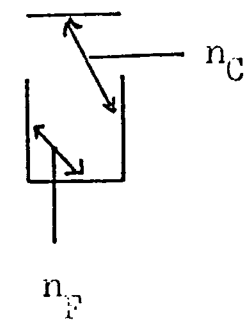

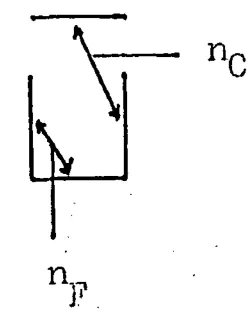

1 RUN NUMBER E-30

EXPERIMENTAL LOCAL VELOCITIES (M/S)

STN LEVEL	A	B	C	CL	D	E	F
1	0.31275	0.35474	0.37523	0.37834	0.37834	0.37634	0.35043
2	0.35599	0.36498	0.39837	0.44512	0.42508	0.40505	0.36466
3	0.36498	0.39169	0.43176	0.46515	0.45848	0.45848	0.36498
4	0.35162	0.43176	0.44512	0.45349	0.45348	0.45843	0.39837
5	0.35159	0.41841	0.40092	0.40946	0.41202	0.43176	0.36498
6	0.32491	0.35668	0.37565	0.38364	0.38605	0.37834	0.33327
7	0.29820	0.32839	0.34583	0.35320	0.37834	0.32491	0.31155

ESTIMATED LOCAL VELOCITIES BY THE COEFFICIENT EQUATION (M/S)

STN LEVEL	A	B	C	CL	D	E	F
1	0.35771	0.38222	0.40401	0.41323	0.41599	0.40520	0.37765
2	0.35120	0.39748	0.42014	0.42973	0.43260	0.42133	0.39273
3	0.35736	0.40445	0.42751	0.43727	0.44019	0.42878	0.39962
4	0.35104	0.39730	0.41995	0.42953	0.43240	0.42119	0.39255
5	0.33345	0.37739	0.39891	0.40301	0.41073	0.40008	0.37288
6	0.31099	0.35197	0.37203	0.38052	0.38306	0.37313	0.34776
7	0.28460	0.32210	0.34047	0.34824	0.35056	0.34147	0.31825

YMAX= 0.4041 M VMEAN= 0.3946 M/S ENERGY SLOPE= 0.10139E-02

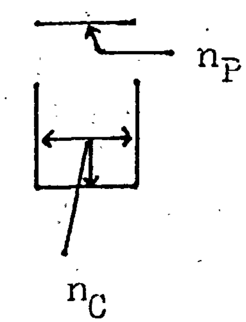

2 RUN NUMBER E-31

EXPERIMENTAL LOCAL VELOCITIES (M/S)

STN	A	B	C	CL	D	E	F
LEVEL							
1	0.30464	0.31362	0.34589	0.34589	0.34589	0.31362	0.30464
2	0.31362	0.34589	0.37815	0.37815	0.37815	0.34589	0.31362
3	0.34539	0.36525	0.37815	0.39751	0.37815	0.36525	0.34539
4	0.31362	0.34589	0.37815	0.39106	0.37815	0.34589	0.31362
5	0.30071	0.31362	0.33298	0.35579	0.33298	0.31362	0.30071
6	0.26199	0.28135	0.31362	0.34589	0.31362	0.28135	0.26199
7	0.24909	0.26199	0.28135	0.32653	0.28135	0.26199	0.24909

ESTIMATED LOCAL VELOCITIES BY THE COEFFICIENT EQUATION (M/S)

STN	A	B	C	CL	D	E	F
LEVEL							
1	0.30766	0.34644	0.36559	0.37177	0.36559	0.34644	0.30766
2	0.31462	0.35428	0.37386	0.38018	0.37386	0.35428	0.31462
3	0.31250	0.35189	0.37134	0.37761	0.37134	0.35189	0.31250
4	0.30433	0.34326	0.36223	0.36835	0.36223	0.34326	0.30463
5	0.28731	0.32353	0.34141	0.34718	0.34141	0.32353	0.28731
6	0.26690	0.30055	0.31715	0.32252	0.31715	0.30055	0.26690
7	0.24430	0.27566	0.29090	0.29581	0.29090	0.27566	0.24430

YMAX= 0.3472 M VMEAN= 0.3330 M/S ENERGY SLOPE= 0.25694E-03

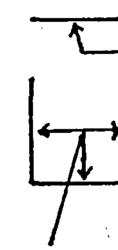

3 RUN NUMBER L-32

EXPLRIMENTAL LOCAL VELOCITIES (M/S)

STN LEVEL	A	B	C	CL	D	E	F
1	0.29426	0.31362	0.32007	0.32007	0.32007	0.31362	0.29426
2	0.32653	0.33298	0.33943	0.34589	0.33943	0.33298	0.32653
3	0.32007	0.32653	0.33298	0.33298	0.33298	0.32653	0.32007
4	0.30071	0.30717	0.31362	0.32007	0.31362	0.30717	0.30071
5	0.28135	0.28731	0.29426	0.30071	0.29426	0.28781	0.28135
6	0.26845	0.27490	0.28135	0.28135	0.28135	0.27490	0.26845
7	0.25554	0.26199	0.26845	0.26845	0.26845	0.26199	0.25554

ESTIMATED LOCAL VELOCITIES BY THE COEFFICIENT EQUATION (M/S)

STN LEVEL	A	B	C	CL	D	E	F
1	0.29054	0.31379	0.32493	0.32843	0.32493	0.31379	0.29054
2	0.29479	0.31338	0.32968	0.33123	0.32968	0.31838	0.29479
3	0.29850	0.31698	0.32823	0.33152	0.32823	0.31698	0.29550
4	0.28880	0.31191	0.32298	0.32651	0.32298	0.31191	0.28880
5	0.27791	0.30015	0.31080	0.31420	0.31080	0.30015	0.27791
6	0.26492	0.28612	0.29628	0.29952	0.29628	0.28612	0.26492
7	0.25046	0.27050	0.28010	0.28317	0.28010	0.27050	0.25046

YMAX= 0.3442 M VMEAN= 0.3036 M/S ENERGY SLOPE= 0.22912E-03

4 RUN NUMBER E-33

EXPERIMENTAL LOCAL VELOCITIES (M/S)

STN / LEVEL	A	B	C	CL	D	E	F
1	0.24909	0.29426	0.30394	0.30394	0.30394	0.29426	0.24909
2	0.28135	0.30717	0.31685	0.32555	0.31685	0.30717	0.28135
3	0.31362	0.32330	0.32653	0.32653	0.32653	0.32330	0.31362
4	0.30717	0.31362	0.31362	0.32007	0.31362	0.31362	0.30717
5	0.28135	0.29749	0.31039	0.31362	0.31039	0.29749	0.28135
6	0.26199	0.28135	0.30071	0.30717	0.30071	0.28135	0.26199
7	0.21682	0.23618	0.28135	0.29426	0.28135	0.23618	0.21682

ESTIMATED LOCAL VELOCITIES BY THE COEFFICIENT EQUATION (M/S)

STN / LEVEL	A	B	C	CL	D	E	F
1	0.25540	0.28426	0.29838	0.30292	0.29838	0.28426	0.25540
2	0.27210	0.30285	0.31789	0.32273	0.31789	0.30285	0.27210
3	0.28455	0.31670	0.33243	0.33749	0.33243	0.31670	0.28455
4	0.28455	0.31670	0.33243	0.33749	0.33243	0.31670	0.28455
5	0.27210	0.30285	0.31789	0.32273	0.31789	0.30285	0.27210
6	0.25540	0.28426	0.29838	0.30292	0.29838	0.28426	0.25540
7	0.23646	0.26318	0.27625	0.28045	0.27625	0.26318	0.23646

YMAX= 0.3449 M   VMEAN= 0.2995 M/S   ENERGY SLOPE= 0.51587E-03

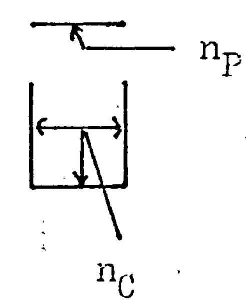

5 RUN NUMBER E-34

EXPERIMENTAL LOCAL VELOCITIES (M/S)

STN LEVEL	A	B	C	CL	D	E	F
1	0.27796	0.29749	0.31039	0.31362	0.31039	0.29749	0.27796
2	0.30394	0.32653	0.32975	0.33298	0.32975	0.32653	0.30394
3	0.32007	0.32330	0.33298	0.33298	0.33298	0.32330	0.32007
4	0.30071	0.31039	0.31039	0.31362	0.31039	0.31039	0.30071
5	0.29426	0.29749	0.30717	0.31039	0.30717	0.29749	0.29426
6	0.24909	0.28135	0.29426	0.30071	0.29426	0.28135	0.24909
7	0.21682	0.23295	0.28135	0.28135	0.28135	0.23295	0.21682

ESTIMATED LOCAL VELOCITIES BY THE COEFFICIENT EQUATION (M/S)

STN LEVEL	A	B	C	CL	D	E	F
1	0.28349	0.31223	0.32619	0.33067	0.32619	0.31223	0.28349
2	0.28892	0.31822	0.33244	0.33700	0.33244	0.31822	0.28892
3	0.28754	0.31670	0.33086	0.33539	0.33086	0.31670	0.28754
4	0.28183	0.31041	0.32429	0.32874	0.32429	0.31041	0.28183
5	0.28863	0.29587	0.30909	0.31333	0.30909	0.29587	0.28863
6	0.28302	0.27868	0.29114	0.29513	0.29114	0.27868	0.28302
7	0.28585	0.25977	0.27138	0.27510	0.27138	0.25977	0.28585

YMAX= 0.3455 M VMEAN= 0.3016 M/S ENERGY SLOPE= 0.37773E-03

6 • RUN NUMBER E-35

EXPERIMENTAL LOCAL VELOCITIES (M/S)

STN LEVEL	A	B	C	CL	D	E	F
1	0.28829	0.28927	0.3067[illegible]	0.29749	0.29426	0.29703	0.25552
2	0.28135	0.32653	0.345[illegible]	0.33298	0.32975	0.32007	0.26135
3	0.31362	0.34589	0.362[illegible]	0.34589	0.33943	0.33298	0.25903
4	0.30071	0.32007	0.3397[illegible]	0.32653	0.32653	0.32007	0.28135
5	0.24909	0.31362	0.332[illegible]	0.32307	0.32007	0.30071	0.24196
6	0.24909	0.28135	0.32067	0.31362	0.30717	0.26522	0.23618
7	0.22973	0.24909	0.2613[illegible]	0.27490	0.27167	0.24909	0.19746

ESTIMATED LOCAL VELOCITIES BY THE COEFFICIENT EQUATION (M/S)

STN LEVEL	A	B	C	CL	D	E	F
1	0.29342	0.32419	0.33713	0.33524	0.32562	0.30287	0.25817
2	0.29929	0.33068	0.34357	0.34194	0.33213	0.30893	0.26333
3	0.29769	0.32890	0.34203	0.34011	0.33035	0.30727	0.26192
4	0.29141	0.32197	0.33481	0.33294	0.32338	0.30079	0.25640
5	0.27694	0.30598	0.31819	0.31641	0.30733	0.28586	0.24367
6	0.25994	0.28719	0.29865	0.29698	0.28845	0.26830	0.22870
7	0.24132	0.26663	0.27726	0.27571	0.26780	0.24909	0.21233

YMAX= 0.3632 M VMEAN= 0.3054 M/S ENERGY SLOPE= 0.29353E-03

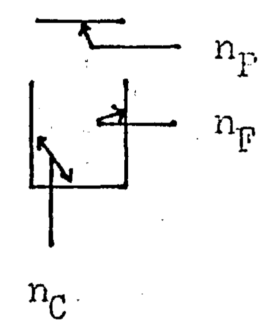

7 RUN NUMBER E-36

EXPERIMENTAL LOCAL VELOCITIES (M/S)

STN LEVEL	A	B	C	CL	D	E	F
1	0.24909	0.26845	0.27490	0.28135	0.29095	0.27242	0.23574
2	0.28135	0.32653	0.32653	0.33943	0.32007	0.29749	0.25197
3	0.29368	0.33298	0.34589	0.34589	0.33943	0.31362	0.26179
4	0.30717	0.31362	0.32653	0.32007	0.31362	0.31039	0.28135
5	0.28781	0.30717	0.31362	0.31362	0.30717	0.29749	0.26845
6	0.26199	0.29426	0.29749	0.30717	0.30071	0.28135	0.24909
7	0.24909	0.26845	0.28135	0.29749	0.28781	0.24909	0.23295

ESTIMATED LOCAL VELOCITIES BY THE COEFFICIENT EQUATION (M/S)

STN LEVEL	A	B	C	CL	D	E	F
1	0.26974	0.29431	0.30455	0.30306	0.29544	0.27732	0.24118
2	0.28434	0.31024	0.32104	0.31946	0.31143	0.29233	0.25423
3	0.29513	0.32202	0.33322	0.33159	0.32326	0.30342	0.26388
4	0.29513	0.32202	0.33322	0.33159	0.32326	0.30342	0.26388
5	0.28434	0.31024	0.32104	0.31946	0.31143	0.29233	0.25423
6	0.26974	0.29431	0.30455	0.30306	0.29544	0.27732	0.24118
7	0.25302	0.27607	0.28567	0.28427	0.27713	0.26013	0.22623

YMAX= 0.0683 M VMEAN= 0.3000 M/S ENERGY SLOPE= 0.56934E-03

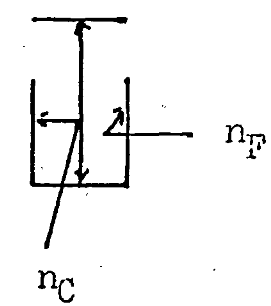

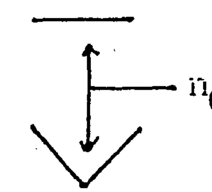

8 RUN NUMBER E-41

EXPERIMENTAL LOCAL VELOCITIES (M/S)

STN / LEVEL	A	B	C	CL	D	E	F
1	0.13124	0.28212	0.28226	0.25813	0.28226	0.28212	0.13124
2	0.00000	0.27074	0.31823	0.33827	0.31823	0.27074	0.00000
3	0.00000	0.00000	0.32491	0.36498	0.32491	0.00000	0.00000
4	0.00000	0.00000	0.21406	0.34209	0.21406	0.00000	0.00000
5	0.00000	0.00000	0.00000	0.32491	0.00000	0.00000	0.00000
6	0.00000	0.00000	0.00000	0.29152	0.00000	0.00000	0.00000
7	0.00000	0.00000	0.00000	0.23809	0.00000	0.00000	0.00000

ESTIMATED LOCAL VELOCITIES BY THE COEFFICIENT EQUATION (M/S)

STN / LEVEL	A	B	C	CL	D	E	F
1	0.13219	0.28541	0.28525	0.27158	0.28525	0.28541	0.13219
2	0.00000	0.27240	0.32224	0.31502	0.32224	0.27240	0.00000
3	0.00000	0.00000	0.32349	0.35044	0.32349	0.00000	0.00000
4	0.00000	0.00000	0.20621	0.35387	0.20621	0.00000	0.00000
5	0.00000	0.00000	0.00000	0.32572	0.00000	0.00000	0.00000
6	0.00000	0.00000	0.00000	0.28739	0.00000	0.00000	0.00000
7	0.00000	0.00000	0.00000	0.24445	0.00000	0.00000	0.00000

YMAX= 0.2314 VMEAN= 0.2663 M/S ENERGY SLOPE= 0.55552E-03

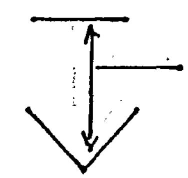

9 RUN NUMBER E-42

EXPERIMENTAL LOCAL VELOCITIES (M/S)

STN / LEVEL	A	B	C	CL	D	E	F
1	0.28698	0.39772	0.39458	0.37166	0.39458	0.39772	0.28698
2	0.00000	0.39169	0.48519	0.47637	0.48519	0.39169	0.00000
3	0.00000	0.00000	0.50522	0.57201	0.50522	0.00000	0.00000
4	0.00000	0.00000	0.45848	0.55865	0.45848	0.00000	0.00000
5	0.00000	0.00000	0.00000	0.51190	0.00000	0.00000	0.00000
6	0.00000	0.00000	0.00000	0.44512	0.00000	0.00000	0.00000
7	0.00000	0.00000	0.00000	0.37166	0.00000	0.00000	0.00000

ESTIMATED LOCAL VELOCITIES BY THE COEFFICIENT EQUATION (M/S)

STN / LEVEL	A	B	C	CL	D	E	F
1	0.32388	0.43428	0.43186	0.41557	0.43186	0.43428	0.32388
2	0.00000	0.43078	0.47993	0.47653	0.47993	0.43078	0.00000
3	0.00000	0.00000	0.48429	0.51612	0.48429	0.00000	0.00000
4	0.00000	0.00000	0.34472	0.52055	0.34472	0.00000	0.00000
5	0.00000	0.00000	0.00000	0.48498	0.00000	0.00000	0.00000
6	0.00000	0.00000	0.00000	0.43659	0.00000	0.00000	0.00000
7	0.00000	0.00000	0.00000	0.38512	0.00000	0.00000	0.00000

YMAX= 0.2580 M VMEAN= 0.4456 M/S ENERGY SLOPE= 0.13889E-02

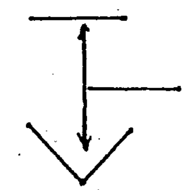

n_C

10 RUN NUMBER E-43

EXPERIMENTAL LOCAL VELOCITIES (M/S)

STN / LEVEL	A	B	C	CL	D	E	F
1	0.48371	0.67240	0.63629	0.63629	0.63629	0.67240	0.48371
2	0.00000	0.63629	0.79762	0.82989	0.79762	0.63629	0.00000
3	0.00000	0.00000	0.82989	0.92669	0.82989	0.00000	0.00000
4	0.00000	0.00000	0.52511	0.89442	0.52511	0.00000	0.00000
5	0.00000	0.00000	0.00000	0.79762	0.00000	0.00000	0.00000
6	0.00000	0.00000	0.00000	0.67683	0.00000	0.00000	0.00000
7	0.00000	0.00000	0.00000	0.57175	0.00000	0.00000	0.00000

ESTIMATED LOCAL VELOCITIES BY THE COEFFICIENT EQUATION (M/S)

STN / LEVEL	A	B	C	CL	D	E	F
1	0.46568	0.68965	0.68479	0.85036	0.68479	0.68965	0.46568
2	0.00000	0.68219	0.78792	0.76750	0.78792	0.68219	0.00000
3	0.00000	0.00000	0.79746	0.86761	0.79746	0.00000	0.00000
4	0.00000	0.00000	0.50775	0.87750	0.50774	0.00000	0.00000
5	0.00000	0.00000	0.00000	0.79382	0.00000	0.00000	0.00000
6	0.00000	0.00000	0.00000	0.69419	0.00000	0.00000	0.00000
7	0.00000	0.00000	0.00000	0.58619	0.00000	0.00000	0.00000

YMAX= 0.2383 M VMEAN= 0.7043 M/S ENERGY SLOPE= 0.36458E-02

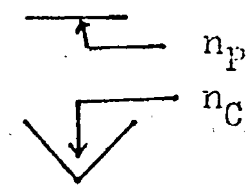

11 RUN NUMBER E-45

EXPERIMENTAL LOCAL VELOCITIES (M/S)

STN	A	B	C	CL	D	E	F
LEVEL							
1	0.00000	0.6333[illegible]	0.62384	0.62481	0.62384	0.63038	0.00000
2	0.00000	0.60687	0.62995	0.63053	0.62995	0.60687	0.00000
3	0.00000	0.00000	0.60731	0.63358	0.60731	0.00000	0.00000
4	0.00000	0.00000	0.49028	0.63120	0.49028	0.00000	0.00000
5	0.00000	0.00000	0.00000	0.59989	0.00000	0.00000	0.00000
6	0.00000	0.00000	0.00000	0.55801	0.00000	0.00000	0.00000
7	0.00000	0.00000	0.00000	0.52543	0.00000	0.00000	0.00000

ESTIMATED LOCAL VELOCITIES BY THE COEFFICIENT EQUATION (M/S)

STN	A	B	C	CL	D	E	F
LEVEL							
1	0.00000	0.60762	0.6[illegible]	0.63117	0.63201	0.60762	0.00000
2	0.00000	0.56286	0.[illegible]	0.64584	0.63794	0.56286	0.00000
3	0.00000	0.00000	0.613[illegible]	0.64580	0.61503	0.00000	0.00000
4	0.00000	0.00000	0.500[illegible]	0.63525	0.50068	0.00000	0.00000
5	0.00000	0.00000	0.00[illegible]	0.61851	0.00000	0.00000	0.00000
6	0.00000	0.00000	0.00[illegible]	0.59379	0.00000	0.00000	0.00000
7	0.00000	0.00000	0.00[illegible]	0.56491	0.00000	0.00000	0.00000

YMAX= 0.2159 [illegible] VMEAN= 0.6[illegible] M/S ENERGY SLOPE= 0.6680[illegible]E-02

12 RUN NUMBER E-46

STN	A	B	C	CL	D	E	F
EXPERIMENTAL LOCAL VELOCITIES (M/S)							
LEVEL							
1	0.26235	0.29927	0.28484	0.27816	0.28484	0.29927	0.26235
2	0.00000	0.29152	0.31155	0.33327	0.31155	0.29152	0.00000
3	0.00000	0.00000	0.33159	0.34494	0.33159	0.00000	0.00000
4	0.00000	0.00000	0.25490	0.34494	0.25490	0.00000	0.00000
5	0.00000	0.00000	0.00000	0.28484	0.00000	0.00000	0.00000
6	0.00000	0.00000	0.00000	0.28250	0.00000	0.00000	0.00000
7	0.00000	0.00000	0.00000	0.25856	0.00000	0.00000	0.00000

STN	A	B	C	CL	D	E	F
ESTIMATED LOCAL VELOCITIES BY THE COEFFICIENT EQUATION (M/S)							
LEVEL							
1	0.26268	0.30194	0.30848	0.30581	0.30848	0.30194	0.26268
2	0.00000	0.29033	0.31910	0.32040	0.31910	0.29033	0.00000
3	0.00000	0.00000	0.30765	0.32664	0.30765	0.00000	0.00000
4	0.00000	0.00000	0.25159	0.32054	0.25159	0.00000	0.00000
5	0.00000	0.00000	0.00000	0.30304	0.00000	0.00000	0.00000
6	0.00000	0.00000	0.00000	0.28082	0.00000	0.00000	0.00000
7	0.00000	0.00000	0.00000	0.25543	0.00000	0.00000	0.00000

YMAX= 0.2518 M VMEAN= 0.2977 M/S ENERGY SLOPE= 0.42559E-03

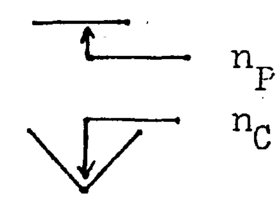

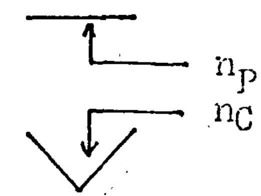

13 RUN NUMBER E-47

EXPERIMENTAL LOCAL VELOCITIES (M/S)

STN LEVEL	A	B	C	CL	D	E	F
1	0.60045	0.70435	0.70082	0.71695	0.70082	0.70435	0.60045
2	0.00000	0.71373	0.74922	0.79762	0.74922	0.71373	0.00000
3	0.00000	0.00000	0.76535	0.79763	0.76535	0.00000	0.00000
4	0.00000	0.00000	0.66855	0.78003	0.66855	0.00000	0.00000
5	0.00000	0.00000	0.00000	0.73309	0.00000	0.00000	0.00000
6	0.00000	0.00000	0.00000	0.71373	0.00000	0.00000	0.00000
7	0.00000	0.00000	0.00000	0.60021	0.00000	0.00000	0.00000

ESTIMATED LOCAL VELOCITIES BY THE COEFFICIENT EQUATION (M/S)

STN LEVEL	A	B	C	CL	D	E	F
1	0.64063	0.72693	0.75113	0.75139	0.75113	0.72693	0.64063
2	0.00000	0.69773	0.75486	0.76623	0.75486	0.69773	0.00000
3	0.00000	0.00000	0.72794	0.76557	0.72794	0.00000	0.00000
4	0.00000	0.00000	0.62746	0.75065	0.62746	0.00000	0.00000
5	0.00000	0.00000	0.00000	0.71939	0.00000	0.00000	0.00000
6	0.00000	0.00000	0.00000	0.68214	0.00000	0.00000	0.00000
7	0.00000	0.00000	0.00000	0.64088	0.00000	0.00000	0.00000

YMAX= 0.2310 M   VMEAN= 0.7192 M/S   ENERGY SLOPE= 0.13750E-02

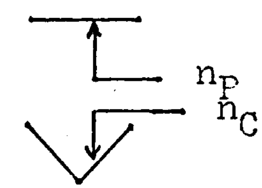

14 RUN NUMBER E-48

EXPERIMENTAL LOCAL VELOCITIES (M/S)

STN LEVEL	A	B	C	CL	D	E	F
1	0.58537	0.79002	0.79762	0.82989	0.79762	0.79002	0.58537
2	0.00000	0.71695	0.84602	0.92669	0.84602	0.71695	0.00000
3	0.00000	0.00000	0.86215	0.92669	0.86215	0.00000	0.00000
4	0.00000	0.00000	0.59559	0.89442	0.59559	0.00000	0.00000
5	0.00000	0.00000	0.00000	0.76535	0.00000	0.00000	0.00000
6	0.00000	0.00000	0.00000	0.68469	0.00000	0.00000	0.00000
7	0.00000	0.00000	0.00000	0.60372	0.00000	0.00000	0.00000

ESTIMATED LOCAL VELOCITIES BY THE COEFFICIENT EQUATION (M/S)

STN LEVEL	A	B	C	CL	D	E	F
1	0.59884	0.79723	0.85562	0.85626	0.85562	0.79723	0.59884
2	0.00000	0.72314	0.86242	0.89113	0.86242	0.72314	0.00000
3	0.00000	0.00000	0.79808	0.88422	0.79808	0.00000	0.00000
4	0.00000	0.00000	0.57814	0.85339	0.57814	0.00000	0.00000
5	0.00000	0.00000	0.00000	0.78123	0.00000	0.00000	0.00000
6	0.00000	0.00000	0.00000	0.69898	0.00000	0.00000	0.00000
7	0.00000	0.00000	0.00000	0.61269	0.00000	0.00000	0.00000

YMAX= 0.2469 M VMEAN= 0.7748 M/S ENERGY SLOPE= 0.29722E-02

15 RUN NUMBER E-50

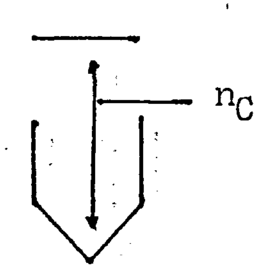

EXPERIMENTAL LOCAL VELOCITIES (M/S)

STN LEVEL	A	B	C	CL	D	E	F
1	0.28078	0.30199	0.30729	0.31524	0.30729	0.30199	0.28078
2	0.28028	0.32850	0.34175	0.32081	0.34175	0.32850	0.28028
3	0.24342	0.31018	0.34175	0.36826	0.34175	0.31018	0.24342
4	0.00000	0.00000	0.31495	0.33973	0.31495	0.00000	0.00000
5	0.00000	0.00000	0.00000	0.31524	0.00000	0.00000	0.00000
6	0.00000	0.00000	0.00000	0.30543	0.00000	0.00000	0.00000
7	0.00000	0.00000	0.00000	0.28252	0.00000	0.00000	0.00000

ESTIMATED LOCAL VELOCITIES BY THE COEFFICIENT EQUATION (M/S)

STN LEVEL	A	B	C	CL	D	E	F
1	0.27038	0.29912	0.30676	0.30449	0.30676	0.29912	0.27038
2	0.28532	0.31937	0.32979	0.32350	0.32979	0.31937	0.28532
3	0.24717	0.31728	0.34383	0.34664	0.34383	0.31728	0.24717
4	0.00000	0.00000	0.32232	0.34848	0.32232	0.00000	0.00000
5	0.00000	0.00000	0.00000	0.33548	0.00000	0.00000	0.00000
6	0.00000	0.00000	0.00000	0.31234	0.00000	0.00000	0.00000
7	0.00000	0.00000	0.00000	0.28817	0.00000	0.00000	0.00000

YMAX= 0.3734 M   VMEAN= 0.3164 M/S   ENERGY SLOPE= 0.97219E-03

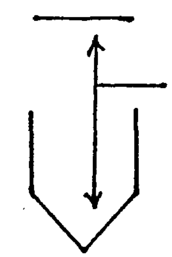

n_C

16 RUN NUMBER E-51

EXPERIMENTAL LOCAL VELOCITIES (M/S)

STN LEVEL	A	B	C	CL	D	E	F
1	0.22705	0.25088	0.25681	0.25453	0.25681	0.25088	0.22705
2	0.23969	0.26809	0.27655	0.27511	0.27655	0.26809	0.23969
3	0.17500	0.26137	0.28798	0.29089	0.28798	0.26137	0.17500
4	0.00000	0.00000	0.26813	0.29244	0.26813	0.00000	0.00000
5	0.00000	0.00000	0.00000	0.27952	0.00000	0.00000	0.00000
6	0.00000	0.00000	0.00000	0.25145	0.00000	0.00000	0.00000
7	0.00000	0.00000	0.00000	0.22473	0.00000	0.00000	0.00000

ESTIMATED LOCAL VELOCITIES BY THE COEFFICIENT EQUATION (M/S)

STN LEVEL	A	B	C	CL	D	E	F
1	0.22598	0.24986	0.25580	0.25351	0.25580	0.24986	0.22598
2	0.23864	0.26710	0.27558	0.27414	0.27558	0.26710	0.23864
3	0.17388	0.26037	0.28704	0.28996	0.28704	0.26037	0.17388
4	0.00000	0.00000	0.26714	0.29151	0.26714	0.00000	0.00000
5	0.00000	0.00000	0.00000	0.27855	0.00000	0.00000	0.00000
6	0.00000	0.00000	0.00000	0.26054	0.00000	0.00000	0.00000
7	0.00000	0.00000	0.00000	0.23583	0.00000	0.00000	0.00000

YMAX= 0.3381 M VMEAN= 0.2684 M/S ENERGY SLOPE= 0.41068E-03

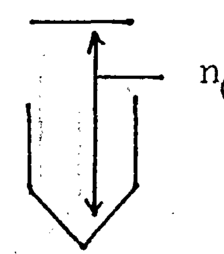

17 RUN NUMBER E-52

EXPERIMENTAL LOCAL VELOCITIES (M/S)

STN	A	B	C	CL	D	E	F
LEVEL							
1	0.42819	0.46347	0.47176	0.46811	0.47176	0.46347	0.42819
2	0.44661	0.48852	0.50051	0.49820	0.50051	0.48852	0.44661
3	0.31339	0.47549	0.51657	0.52323	0.51657	0.47549	0.31339
4	0.00000	0.00000	0.48689	0.52100	0.48689	0.00000	0.00000
5	0.00000	0.00000	0.00000	0.50476	0.00000	0.00000	0.00000
6	0.00000	0.00000	0.00000	0.47859	0.00000	0.00000	0.00000
7	0.00000	0.00000	0.00000	0.44804	0.00000	0.00000	0.00000

ESTIMATED LOCAL VELOCITIES BY THE COEFFICIENT EQUATION (M/S)

STN	A	B	C	CL	D	E	F
LEVEL							
1	0.42823	0.46348	0.47177	0.46814	0.47177	0.46348	0.42823
2	0.44663	0.48854	0.50052	0.49822	0.50052	0.48854	0.44663
3	0.31390	0.47551	0.51655	0.52101	0.51655	0.47551	0.31390
4	0.00000	0.00000	0.48689	0.52322	0.48689	0.00000	0.00000
5	0.00000	0.00000	0.00000	0.50478	0.00000	0.00000	0.00000
6	0.00000	0.00000	0.00000	0.47860	0.00000	0.00000	0.00000
7	0.00000	0.00000	0.00000	0.44773	0.00000	0.00000	0.00000

YMAX= 0.3520 M VMEAN= 0.4800 M/S ENERGY SLOPE= 0.88882E-03

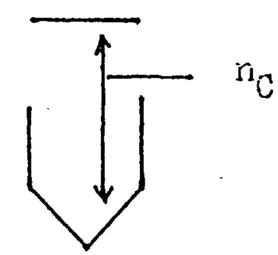

1 RUN NUMBER E-53

EXPERIMENTAL LOCAL VELOCITIES (M/S)

STN / LEVEL	A	B	C	CL	D	E	F
1	0.46181	0.60402	0.60402	0.60402	0.60402	0.60402	0.46181
2	0.51735	0.70082	0.74922	0.73309	0.74922	0.70082	0.51735
3	0.00000	0.63629	0.76535	0.79762	0.76535	0.63629	0.00000
4	0.00000	0.00000	0.64694	0.79762	0.64694	0.00000	0.00000
5	0.00000	0.00000	0.00000	0.73309	0.00000	0.00000	0.00000
6	0.00000	0.00000	0.00000	0.62015	0.00000	0.00000	0.00000
7	0.00000	0.00000	0.00000	0.55562	0.00000	0.00000	0.00000

ESTIMATED LOCAL VELOCITIES BY THE COEFFICIENT EQUATION (M/S)

STN / LEVEL	A	B	C	CL	D	E	F
1	0.47626	0.58948	0.61627	0.60170	0.61627	0.58948	0.47626
2	0.53142	0.68091	0.72587	0.71517	0.72587	0.68091	0.53142
3	0.00000	0.60600	0.78851	0.81044	0.78851	0.60600	0.00000
4	0.00000	0.00000	0.65941	0.82023	0.65941	0.00000	0.00000
5	0.00000	0.00000	0.00000	0.74234	0.00000	0.00000	0.00000
6	0.00000	0.00000	0.00000	0.63951	0.00000	0.00000	0.00000
7	0.00000	0.00000	0.00000	0.53139	0.00000	0.00000	0.00000

YMAX= 0.3411 M VMEAN= 0.6675 M/S ENERGY SLOPE= 0.18194E-02

2 RUN NUMBER E-55

EXPERIMENTAL LOCAL VELOCITIES (M/S)							
STN	A	B	C	CL	D	E	F
LEVEL							
1	0.29880	0.31320	0.35362	0.35468	0.35362	0.31320	0.29880
2	0.31414	0.34562	0.35988	0.36234	0.35988	0.34562	0.31414
3	0.23362	0.32769	0.35481	0.36240	0.35481	0.32769	0.23362
4	0.00000	0.00000	0.33378	0.35728	0.33378	0.00000	0.00000
5	0.00000	0.00000	0.00000	0.34422	0.00000	0.00000	0.00000
6	0.00000	0.00000	0.00000	0.32804	0.00000	0.00000	0.00000
7	0.00000	0.00000	0.00000	0.30982	0.00000	0.00000	0.00000

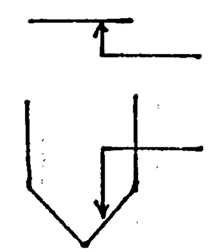

ESTIMATED LOCAL VELOCITIES BY THE COEFFICIENT EQUATION (M/S)							
STN	A	B	C	CL	D	E	F
LEVEL							
1	0.31356	0.33977	0.34953	0.35056	0.34953	0.33977	0.31356
2	0.31073	0.34167	0.35565	0.35808	0.35565	0.34167	0.31073
3	0.23147	0.32404	0.35068	0.35615	0.35068	0.32404	0.23147
4	0.00000	0.00000	0.33003	0.35312	0.33003	0.00000	0.00000
5	0.00000	0.00000	0.00000	0.34029	0.00000	0.00000	0.00000
6	0.00000	0.00000	0.00000	0.32438	0.00000	0.00000	0.00000
7	0.00000	0.00000	0.00000	0.30646	0.00000	0.00000	0.00000

YMAX= 0.3531 M VMEAN= 0.3375 M/S ENERGY SLOPE= 0.12083E-02

3 RUN NUMBER E-56

EXPERIMENTAL LOCAL VELOCITIES (M/S)

STN LEVEL	A	B	C	CL	D	E	F
1	0.22094	0.24267	0.25155	0.25294	0.25155	0.24287	0.22094
2	0.21770	0.24203	0.25355	0.25684	0.25355	0.24203	0.21770
3	0.15908	0.22773	0.24884	0.25499	0.24884	0.22773	0.15908
4	0.00000	0.00000	0.23235	0.25067	0.23235	0.00000	0.00000
5	0.00000	0.00000	0.00000	0.24032	0.00000	0.00000	0.00000
6	0.00000	0.00000	0.00000	0.22796	0.00000	0.00000	0.00000
7	0.00000	0.00000	0.00000	0.21425	0.00000	0.00000	0.00000

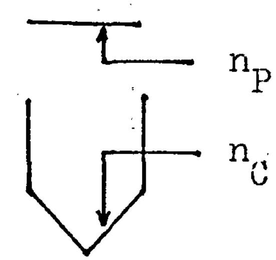

ESTIMATED LOCAL VELOCITIES BY THE COEFFICIENT EQUATION (M/S)

STN LEVEL	A	B	C	CL	D	F	F
1	0.22094	0.24287	0.25154	0.25294	0.25154	0.24287	0.22094
2	0.21771	0.24203	0.25355	0.25683	0.25355	0.24203	0.21771
3	0.15908	0.22774	0.24884	0.25499	0.24884	0.22774	0.15908
4	0.00000	0.00000	0.23235	0.25067	0.23235	0.00000	0.00000
5	0.00000	0.00000	0.00000	0.24032	0.00000	0.00000	0.00000
6	0.00000	0.00000	0.00000	0.22796	0.00000	0.00000	0.00000
7	0.00000	0.00000	0.00000	0.21424	0.00000	0.00000	0.00000

YMAX= 0.3547 M VMEAN= 0.2389 M/S ENERGY SLOPE= 0.22920E-03

4 RUN NUMBER E-57

EXPERIMENTAL LOCAL VELOCITIES (M/S)

STN LEVEL	A	B	C	CL	D	E	F
1	0.36202	0.40319	0.40788	0.40825	0.40788	0.40319	0.36202
2	0.41042	0.40417	0.41099	0.41210	0.41099	0.40417	0.41042
3	0.00000	0.39355	0.40847	0.41235	0.40847	0.39355	0.00000
4	0.00000	0.00000	0.39788	0.40992	0.39788	0.00000	0.00000
5	0.00000	0.00000	0.00000	0.40558	0.00000	0.00000	0.00000
6	0.00000	0.00000	0.00000	0.39429	0.00000	0.00000	0.00000
7	0.00000	0.00000	0.00000	0.38624	0.00000	0.00000	0.00000

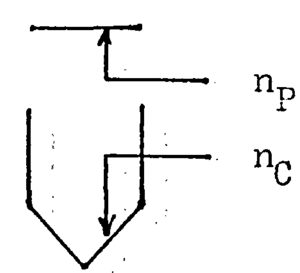

ESTIMATED LOCAL VELOCITIES BY THE COEFFICIENT EQUATION (M/S)

STN LEVEL	A	B	C	CL	D	E	F
1	0.38865	0.40264	0.40758	0.40801	0.40758	0.40264	0.38865
2	0.38686	0.40369	0.41091	0.41204	0.41091	0.40369	0.38686
3	0.28176	0.39245	0.40824	0.41232	0.40824	0.39245	0.28176
4	0.00000	0.00000	0.39703	0.40972	0.39703	0.00000	0.00000
5	0.00000	0.00000	0.00000	0.40304	0.00000	0.00000	0.00000
6	0.00000	0.00000	0.00000	0.39456	0.00000	0.00000	0.00000
7	0.00000	0.00000	0.00000	0.38476	0.00000	0.00000	0.00000

YMAX= 0.3442 M VMEAN= 0.4027 M/S ENERGY SLOPE= 0.35413E-03

5 RUN NUMBER E-58

EXPERIMENTAL LOCAL VELOCITIES (M/S)

STN / LEVEL	A	B	C	CL	D	E	F
1	0.57175	0.63629	0.70082	0.70082	0.70082	0.63629	0.57175
2	0.47860	0.68469	0.74922	0.79762	0.74922	0.68469	0.47860
3	0.00000	0.55055	0.76535	0.79762	0.76535	0.55055	0.00000
4	0.00000	0.00000	0.59216	0.76535	0.59216	0.00000	0.00000
5	0.00000	0.00000	0.00000	0.66855	0.00000	0.00000	0.00000
6	0.00000	0.00000	0.00000	0.57175	0.00000	0.00000	0.00000
7	0.00000	0.00000	0.00000	0.50722	0.00000	0.00000	0.00000

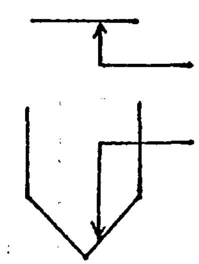

ESTIMATED LOCAL VELOCITIES BY THE COEFFICIENT EQUATION (M/S)

STN / LEVEL	A	B	C	CL	D	E	F
1	0.52732	0.66634	0.72166	0.72617	0.72166	0.66634	0.52732
2	0.50850	0.67664	0.76145	0.77525	0.76145	0.67664	0.50851
3	0.00000	0.55373	0.72814	0.77883	0.72814	0.55373	0.00000
4	0.00000	0.00000	0.59938	0.74725	0.59938	0.00000	0.00000
5	0.00000	0.00000	0.00000	0.66959	0.00000	0.00000	0.00000
6	0.00000	0.00000	0.00000	0.58089	0.00000	0.00000	0.00000
7	0.00000	0.00000	0.00000	0.49134	0.00000	0.00000	0.00000

YMAX= 0.3373 M VMEAN= 0.6657 M/S ENERGY SLOPE= 0.95828E-03

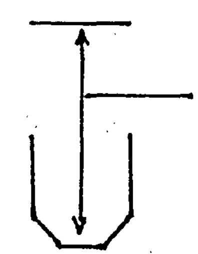

6 RUN NUMBER E-60

EXPERIMENTAL LOCAL VELOCITIES (M/S)

STN LEVEL	A	B	C	CL	D	E	F
1	0.27818	0.33791	0.34665	0.35485	0.34765	0.33791	0.27818
2	0.31524	0.37139	0.38385	0.39291	0.38385	0.37139	0.31524
3	0.31267	0.38726	0.41234	0.46105	0.41234	0.38726	0.31267
4	0.00000	0.31940	0.40890	0.46105	0.40890	0.31940	0.00000
5	0.00000	0.00000	0.36706	0.39652	0.36706	0.00000	0.00000
6	0.00000	0.00000	0.31131	0.35959	0.31131	0.00000	0.00000
7	0.00000	0.00000	0.24943	0.31836	0.24943	0.00000	0.00000

ESTIMATED LOCAL VELOCITIES BY THE COEFFICIENT EQUATION (M/S)

STN LEVEL	A	B	C	CL	D	E	F
1	0.29476	0.33645	0.34602	0.35500	0.34602	0.33645	0.29476
2	0.32304	0.37319	0.38692	0.39696	0.38692	0.37319	0.32304
3	0.30898	0.39070	0.41857	0.42943	0.41857	0.39070	0.30898
4	0.00000	0.31628	0.41472	0.43096	0.41472	0.31628	0.00000
5	0.00000	0.00000	0.36839	0.40099	0.36839	0.00000	0.00000
6	0.00000	0.00000	0.30749	0.36018	0.30749	0.00000	0.00000
7	0.00000	0.00000	0.24114	0.31512	0.24114	0.00000	0.00000

YMAX= 0.2743 M VMEAN= 0.3593 M/S ENERGY SLOPE= 0.14194E-02

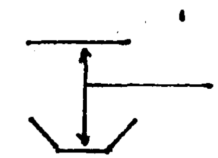

7 RUN NUMBER E-61

EXPERIMENTAL LOCAL VELOCITIES (M/S)

STN LEVEL	A	B	C	CL	D	E	F
1	0.24340	0.24900	0.24949	0.25129	0.24949	0.24900	0.24340
2	0.20501	0.25400	0.25813	0.26234	0.25313	0.25400	0.20501
3	0.00000	0.24361	0.26445	0.26769	0.26445	0.24361	0.00000
4	0.00000	0.00000	0.26284	0.26797	0.26284	0.00000	0.00000
5	0.00000	0.00000	0.25171	0.26191	0.25171	0.00000	0.00000
6	0.00000	0.00000	0.23499	0.25813	0.23499	0.00000	0.00000
7	0.00000	0.00000	0.21384	0.21806	0.25145	0.00000	0.00000

ESTIMATED LOCAL VELOCITIES BY THE COEFFICIENT EQUATION (M/S)

STN LEVEL	A	B	C	CL	D	E	F
1	0.24641	0.25142	0.24913	0.25074	0.24913	0.25142	0.24641
2	0.21174	0.25586	0.25743	0.25941	0.25743	0.25586	0.21174
3	0.00000	0.24451	0.26243	0.26530	0.26243	0.24451	0.00000
4	0.00000	0.00000	0.26101	0.26555	0.26101	0.00000	0.00000
5	0.00000	0.00000	0.25111	0.26018	0.25111	0.00000	0.00000
6	0.00000	0.00000	0.23615	0.25173	0.23615	0.00000	0.00000
7	0.00000	0.00000	0.21705	0.24029	0.21705	0.00000	0.00000

YMAX= 0.1671 M VMEAN= 0.2488 M/S ENERGY SLOPE= 0.36112E-03

8 RUN NUMBER E-62

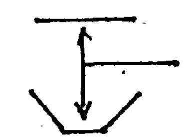

EXPERIMENTAL LOCAL VELOCITIES (M/S)

STN	A	B	C	CL	D	E	F
LEVEL							
1	0.41386	0.43608	0.42833	0.43653	0.42833	0.43608	0.41386
2	0.28665	0.45932	0.47495	0.50722	0.47495	0.45932	0.28665
3	0.00000	0.40865	0.49216	0.53814	0.49216	0.40865	0.00000
4	0.00000	0.00000	0.48439	0.50894	0.48439	0.00000	0.00000
5	0.00000	0.00000	0.43587	0.48075	0.43587	0.00000	0.00000
6	0.00000	0.00000	0.37217	0.47225	0.37217	0.00000	0.00000
7	0.00000	0.00000	0.30631	0.39722	0.30631	0.00000	0.00000

ESTIMATED LOCAL VELOCITIES BY THE COEFFICIENT EQUATION (M/S)

STN	A	B	C	CL	D	E	F
LEVEL							
1	0.41618	0.43948	0.43132	0.43995	0.43132	0.43948	0.41618
2	0.28560	0.46394	0.47131	0.48229	0.47131	0.46394	0.28560
3	0.00000	0.41075	0.49876	0.51514	0.49876	0.41075	0.00000
4	0.00000	0.00000	0.49050	0.51667	0.49050	0.00000	0.00000
5	0.00000	0.00000	0.43925	0.48662	0.43925	0.00000	0.00000
6	0.00000	0.00000	0.37286	0.44541	0.37286	0.00000	0.00000
7	0.00000	0.00000	0.30547	0.39383	0.30547	0.00000	0.00000

YMAX= 0.1656 M VMEAN= 0.4378 M/S ENERGY SLOPE= 0.15624E-02

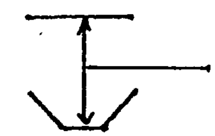

n_C

9 RUN NUMBER E-63

EXPERIMENTAL LOCAL VELOCITIES (M/S)

STN	A	B	C	CL	D	E	F
LEVEL							
1	0.61503	0.64536	0.67056	0.68158	0.67056	0.64536	0.61503
2	0.58160	0.66855	0.76535	0.79762	0.76535	0.66855	0.58160
3	0.00000	0.70082	0.75799	0.77676	0.75799	0.70082	0.00000
4	0.00000	0.00000	0.74882	0.77875	0.74882	0.00000	0.00000
5	0.00000	0.00000	0.68479	0.74092	0.68479	0.00000	0.00000
6	0.00000	0.00000	0.60138	0.68869	0.60138	0.00000	0.00000
7	0.00000	0.00000	0.50283	0.62938	0.50283	0.00000	0.00000

ESTIMATED LOCAL VELOCITIES BY THE COEFFICIENT EQUATION (M/S)

STN	A	B	C	CL	D	E	F
LEVEL							
1	0.63865	0.67066	0.66503	0.67663	0.66503	0.67066	0.63865
2	0.62693	0.71534	0.72914	0.73332	0.72914	0.71534	0.62693
3	0.00000	0.67025	0.75772	0.77771	0.75772	0.67025	0.00000
4	0.00000	0.00000	0.74795	0.77983	0.74795	0.00000	0.00000
5	0.00000	0.00000	0.68008	0.73057	0.68008	0.00000	0.00000
6	0.00000	0.00000	0.59230	0.68413	0.59230	0.00000	0.00000
7	0.00000	0.00000	0.48954	0.62167	0.48954	0.00000	0.00000

YMAX= 0.1839 M   VMEAN= 0.6841 M/S   ENERGY SLOPE= 0.42917E-02

10 RUN NUMBER E-65

EXPERIMENTAL LOCAL VELOCITIES (M/S)							
STN	A	B	C	CL	D	E	F
LEVEL							
1	0.35776	0.39478	0.40803	0.41214	0.40803	0.39478	0.35776
2	0.34175	0.42129	0.41021	0.41594	0.41021	0.42129	0.34175
3	0.31524	0.38458	0.40829	0.44780	0.40829	0.38458	0.31524
4	0.00000	0.32540	0.39698	0.40622	0.39698	0.32540	0.00000
5	0.00000	0.00000	0.36852	0.38718	0.36852	0.00000	0.00000
6	0.00000	0.00000	0.33166	0.36386	0.33166	0.00000	0.00000
7	0.00000	0.00000	0.31524	0.33763	0.31524	0.00000	0.00000

ESTIMATED LOCAL VELOCITIES BY THE COEFFICIENT ECUATION (M/S)							
STN	A	B	C	CL	D	F	F
LEVEL							
1	0.36097	0.39281	0.40445	0.40997	0.40445	0.39281	0.36094
2	0.35920	0.39670	0.41272	0.41835	0.41272	0.39670	0.35921
3	0.33174	0.38747	0.41081	0.41642	0.41081	0.38747	0.33174
4	0.00000	0.32898	0.39967	0.40877	0.39967	0.32898	0.00000
5	0.00000	0.00000	0.37162	0.39000	0.37162	0.00000	0.00000
6	0.00000	0.00000	0.33521	0.36699	0.33521	0.00000	0.00000
7	0.00000	0.00000	0.29325	0.34107	0.29325	0.00000	0.00000

YMAX= 0.2540 1 VMEAN= 0.3536 M/S ENERGY SLOPE= 0.95828E-03

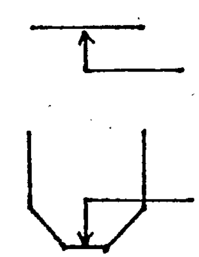

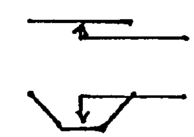

n_P
n_C

11 RUN NUMBER E-66

EXPERIMENTAL LOCAL VELOCITIES (M/S)

STN	A	B	C	CL	D	E	F
LEVEL							
1	0.19599	0.21112	0.21806	0.21506	0.21806	0.21112	0.19599
2	0.18597	0.21674	0.22527	0.22852	0.22527	0.21674	0.18597
3	0.00000	0.18467	0.22841	0.23524	0.22841	0.18467	0.00000
4	0.00000	0.00000	0.22238	0.22959	0.22238	0.00000	0.00000
5	0.00000	0.00000	0.20430	0.21860	0.20430	0.00000	0.00000
6	0.00000	0.00000	0.18075	0.20369	0.18075	0.00000	0.00000
7	0.00000	0.00000	0.15053	0.18535	0.15053	0.00000	0.00000

ESTIMATED LOCAL VELOCITIES BY THE COEFFICIENT EQUATION (M/S)

STN	A	B	C	CL	D	E	F
LEVEL							
1	0.19715	0.21236	0.21460	0.21761	0.21460	0.21236	0.19715
2	0.18708	0.21801	0.22353	0.22680	0.22353	0.21801	0.18708
3	0.00000	0.19916	0.22669	0.23154	0.22669	0.19916	0.00000
4	0.00000	0.00000	0.22062	0.22788	0.22062	0.00000	0.00000
5	0.00000	0.00000	0.20244	0.21082	0.20244	0.00000	0.00000
6	0.00000	0.00000	0.17879	0.20182	0.17379	0.00000	0.00000
7	0.00000	0.00000	0.14856	0.13349	0.14850	0.00000	0.00000

YMAX= 0.1[illegible] VMEAN= 0.2067 M/S ENERGY SLOPE= 0.27984E-03

12 RUN NUMBER E-67

EXPERIMENTAL LOCAL VELOCITIES (M/S)

STN / LEVEL	A	B	C	CL	D	E	F
1	0.56964	0.60105	0.60865	0.60364	0.60865	0.60105	0.56964
2	0.54373	0.62942	0.68469	0.71695	0.68469	0.62942	0.54373
3	0.00000	0.62015	0.64645	0.65492	0.64645	0.62015	0.00000
4	0.00000	0.00000	0.63361	0.64703	0.63361	0.00000	0.00000
5	0.00000	0.00000	0.63629	0.63629	0.63629	0.00000	0.00000
6	0.00000	0.00000	0.57354	0.60232	0.57354	0.00000	0.00000
7	0.00000	0.00000	0.51006	0.58789	0.51006	0.00000	0.00000

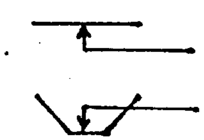

ESTIMATED LOCAL VELOCITIES BY THE COEFFICIENT EQUATION (M/S)

STN / LEVEL	A	B	C	CL	D	E	F
1	0.60008	0.63172	0.63935	0.64488	0.63935	0.63172	0.60003
2	0.57397	0.63267	0.64922	0.65515	0.64922	0.63267	0.57397
3	0.00000	0.59626	0.64676	0.65528	0.64676	0.59626	0.00000
4	0.00000	0.00000	0.63380	0.64732	0.63380	0.00000	0.00000
5	0.00000	0.00000	0.60166	0.62723	0.60166	0.00000	0.00000
6	0.00000	0.00000	0.55857	0.60229	0.55857	0.00000	0.00000
7	0.00000	0.00000	0.50945	0.57373	0.50945	0.00000	0.00000

YMAX= 0.1321 M VMEAN= 0.6171 M/S ENERGY SLOPE= 0.14167E-02

13 RUN NUMBER E-68

EXPERIMENTAL LOCAL VELOCITIES (M/S)							
STN	A	B	C	CL	D	E	F
LEVEL							
1	0.72084	0.77566	0.78689	0.79589	0.78689	0.77566	0.72084
2	0.60991	0.76946	0.80210	0.81267	0.80210	0.76945	0.60991
3	0.00000	0.69744	0.82780	0.84295	0.82780	0.69744	0.00000
4	0.00000	0.00000	0.80600	0.82971	0.80600	0.00000	0.00000
5	0.00000	0.00000	0.75138	0.79659	0.75138	0.00000	0.00000
6	0.00000	0.00000	0.68234	0.75528	0.68234	0.00000	0.00000
7	0.00000	0.00000	0.60774	0.70304	0.60774	0.00000	0.00000

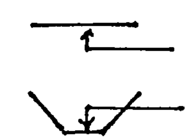

n_P

n_C

ESTIMATED LOCAL VELOCITIES BY THE COEFFICIENT EQUATION (M/S)							
STN	A	B	C	CL	D	E	F
LEVEL							
1	0.73601	0.78867	0.79945	0.80806	0.79945	0.78867	0.73601
2	0.62922	0.78273	0.81402	0.82419	0.81402	0.78273	0.62922
3	0.00000	0.71351	0.80945	0.82396	0.80945	0.71351	0.00000
4	0.00000	0.00000	0.78854	0.81129	0.78854	0.00000	0.00000
5	0.00000	0.00000	0.73609	0.77948	0.73609	0.00000	0.00000
6	0.00000	0.00000	0.66967	0.73583	0.66967	0.00000	0.00000
7	0.00000	0.00000	0.59775	0.69435	0.59775	0.00000	0.00000

YMAX= 0.1704 M VMEAN= 0.7567 M/S ENERGY SLOPE= 0.45834E-02

14 RUN NUMBER E-70

EXPERIMENTAL LOCAL VELOCITIES (M/S)

STN LEVEL	A	B	C	CL	D	E	F
1	0.21138	0.27148	0.28484	0.28484	0.28484	0.27148	0.21138
2	0.24616	0.27744	0.28575	0.29186	0.28575	0.27744	0.24616
3	0.25145	0.29152	0.30486	0.31136	0.30486	0.29152	0.25145
4	0.00000	0.24402	0.31229	0.31227	0.31229	0.24402	0.00000
5	0.00000	0.00000	0.27476	0.29426	0.27476	0.00000	0.00000
6	0.00000	0.00000	0.23870	0.26943	0.23870	0.00000	0.00000
7	0.00000	0.00000	0.19645	0.25813	0.19645	0.00000	0.00000

ESTIMATED LOCAL VELOCITIES BY THE COEFFICIENT EQUATION (M/S)

STN LEVEL	A	B	C	CL	D	E	F
1	0.23050	0.25782	0.26429	0.27008	0.26429	0.25782	0.23050
2	0.24915	0.28135	0.29029	0.29665	0.29029	0.28135	0.24915
3	0.24124	0.29273	0.31018	0.31698	0.31018	0.29273	0.24124
4	0.00000	0.24693	0.30788	0.31791	0.30788	0.24693	0.00000
5	0.00000	0.00000	0.27892	0.29915	0.27892	0.00000	0.00000
6	0.00000	0.00000	0.24142	0.27331	0.24142	0.00000	0.00000
7	0.00000	0.00000	0.19773	0.24450	0.19773	0.00000	0.00000

YMAX= 0.2785 M VMEAN= 0.2645 M/S ENERGY SLOPE= 0.55552E-03

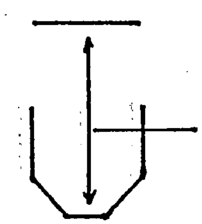

n_C

15 RUN NUMBER E-71

STN	A	B	C	CL	D	E	F
EXPERIMENTAL LOCAL VELOCITIES (M/S)							
LEVEL							
1	0.37837	0.41000	0.45291	0.44404	0.45291	0.41000	0.37837
2	0.43000	0.52000	0.50757	0.51784	0.50757	0.52000	0.43000
3	0.43000	0.54000	0.53968	0.55062	0.53968	0.54000	0.43000
4	0.00000	0.44082	0.53630	0.55202	0.53630	0.44082	0.00000
5	0.00000	0.00000	0.48910	0.52191	0.48910	0.00000	0.00000
6	0.00000	0.00000	0.42396	0.47996	0.42396	0.00000	0.00000
7	0.00000	0.00000	0.35466	0.43216	0.35466	0.00000	0.00000

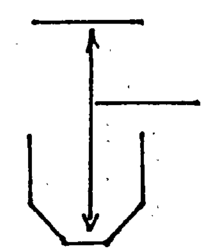

n_C

STN	A	B	C	CL	D	E	F
ESTIMATED LOCAL VELOCITIES BY THE COEFFICIENT EQUATION (M/S)							
LEVEL							
1	0.39990	0.44914	0.46080	0.47108	0.46080	0.44914	0.39990
2	0.43301	0.49108	0.50725	0.51856	0.50725	0.49108	0.43301
3	0.42030	0.51154	0.54267	0.55477	0.54267	0.51154	0.42030
4	0.00000	0.43440	0.53892	0.55631	0.53892	0.43440	0.00000
5	0.00000	0.00000	0.48699	0.52301	0.48699	0.00000	0.00000
6	0.00000	0.00000	0.41618	0.47699	0.41618	0.00000	0.00000
7	0.00000	0.00000	0.34200	0.42504	0.34200	0.00000	0.00000

YMAX= 0.2311 M VMEAN= 0.4759 M/S ENERGY SLOPE= 0.74300E-03

16 RUN NUMBER E-72

EXPERIMENTAL LOCAL VELOCITIES (M/S)							
STN	A	B	C	CL	D	E	F
LEVEL							
1	0.57175	0.60402	0.62015	0.63629	0.62015	0.60402	0.57175
2	0.66855	0.73309	0.76535	0.76535	0.76535	0.73309	0.66855
3	0.64226	0.78149	0.82989	0.82989	0.82989	0.78149	0.64226
4	0.00000	0.66036	0.82989	0.82989	0.82989	0.66036	0.00000
5	0.00000	0.00000	0.70758	0.81375	0.70758	0.00000	0.00000
6	0.00000	0.00000	0.63699	0.74922	0.63699	0.00000	0.00000
7	0.00000	0.00000	0.54527	0.66855	0.54527	0.00000	0.00000

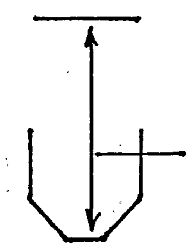

ESTIMATED LOCAL VELOCITIES BY THE COEFFICIENT EQUATION (M/S)							
STN	A	B	C	CL	D	E	F
LEVEL							
1	0.60004	0.67081	0.68858	0.70301	0.68858	0.67081	0.60004
2	0.64709	0.72940	0.75321	0.76399	0.75321	0.72940	0.64709
3	0.63573	0.75924	0.80225	0.81906	0.80225	0.75924	0.63573
4	0.00000	0.66068	0.79752	0.82103	0.79752	0.66068	0.00000
5	0.00000	0.00000	0.72688	0.77497	0.72688	0.00000	0.00000
6	0.00000	0.00000	0.62858	0.71117	0.62858	0.00000	0.00000
7	0.00000	0.00000	0.50699	0.63902	0.50699	0.00000	0.00000

YMAX= 0.2016 1   VMEAN= 0.6547 M/S   ENERGY SLOPE= 0.16666E-02

17 RUN NUMBER E-74

EXPERIMENTAL LOCAL VELOCITIES (M/S)

STN LEVEL	A	B	C	CL	D	E	F
1	0.31155	0.33111	0.34178	0.34632	0.34178	0.33111	0.31155
2	0.30279	0.33295	0.34695	0.35155	0.34695	0.33295	0.30279
3	0.28740	0.32609	0.34427	0.34887	0.34427	0.32609	0.28740
4	0.00000	0.29245	0.33585	0.34231	0.33585	0.29245	0.00000
5	0.00000	0.00000	0.31386	0.32721	0.31386	0.00000	0.00000
6	0.00000	0.00000	0.28562	0.30892	0.28562	0.00000	0.00000
7	0.00000	0.00000	0.25341	0.30487	0.28484	0.00000	0.00000

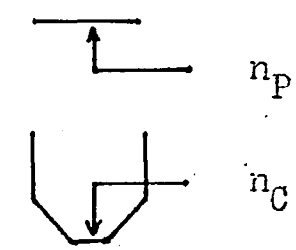

ESTIMATED LOCAL VELOCITIES BY THE COEFFICIENT EQUATION . (M/S)

STN LEVEL	A	B	C	CL	D	E	F
1	0.30760	0.33132	0.34063	0.34459	0.34063	0.33132	0.30760
2	0.30637	0.33291	0.34512	0.34913	0.34512	0.33291	0.30637
3	0.29269	0.32690	0.34281	0.34680	0.34281	0.32690	0.29269
4	0.00000	0.29719	0.33546	0.34109	0.33546	0.29719	0.00000
5	0.00000	0.00000	0.31616	0.32790	0.31616	0.00000	0.00000
6	0.00000	0.00000	0.29111	0.31178	0.29111	0.00000	0.00000
7	0.00000	0.00000	0.26214	0.29358	0.26214	0.00000	0.00000

YMAX= 0.2632 M VMEAN= 0.3206 M/S ENERGY SLOPE= 0.11810E-03

1 RUN NUMBER F-75.

EXPERIMENTAL LOCAL VELOCITIES (M/S)

STN	A	B	C	CL	D	E	F
LEVEL							
1	0.43937	0.50722	0.53949	0.53949	0.53949	0.50722	0.43937
2	0.45882	0.52514	0.54242	0.57354	0.54242	0.52514	0.45882
3	0.45882	0.51295	0.54272	0.57354	0.54272	0.51295	0.45882
4	0.00000	0.45708	0.52949	0.55741	0.52949	0.45708	0.00000
5	0.00000	0.00000	0.49305	0.51547	0.49305	0.00000	0.00000
6	0.00000	0.00000	0.44434	0.48472	0.44434	0.00000	0.00000
7	0.00000	0.00000	0.39169	0.44447	0.44269	0.00000	0.00000

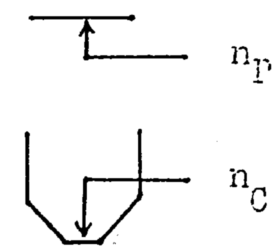

ESTIMATED LOCAL VELOCITIES BY THE COEFFICIENT EQUATION (M/S)

STN	A	B	C	CL	D	E	F
LEVEL							
1	0.47198	0.51393	0.52938	0.53667	0.52938	0.51393	0.47198
2	0.47487	0.52361	0.54272	0.55019	0.54272	0.52361	0.47487
3	0.45098	0.51403	0.54308	0.55056	0.54308	0.51403	0.45098
4	0.00000	0.45951	0.53014	0.54068	0.53014	0.45951	0.00000
5	0.00000	0.00000	0.49463	0.51647	0.49463	0.00000	0.00000
6	0.00000	0.00000	0.44705	0.48649	0.44705	0.00000	0.00000
7	0.00000	0.00000	0.39540	0.45243	0.39540	0.00000	0.00000

YMAX= 0.28241 VMEAN= 0.4673 M/S ENERGY SLOPE= 0.61107E-03

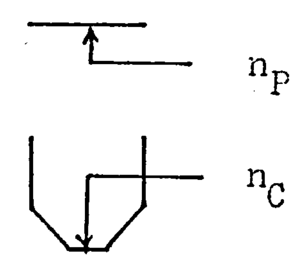

2 RUN NUMBER E-76

EXPERIMENTAL LOCAL VELOCITIES (M/S)

STN LEVEL	A	B	C	CL	D	E	F
1	0.55934	0.60402	0.65242	0.65242	0.65242	0.60402	0.55934
2	0.58789	0.70082	0.71695	0.73309	0.71695	0.70082	0.58789
3	0.57175	0.66855	0.67213	0.67464	0.67213	0.66855	0.57175
4	0.00000	0.57481	0.65262	0.66408	0.65262	0.57481	0.00000
5	0.00000	0.00000	0.61410	0.63805	0.61410	0.00000	0.00000
6	0.00000	0.00000	0.56280	0.60555	0.56280	0.00000	0.00000
7	0.00000	0.00000	0.50247	0.55741	0.50247	0.00000	0.00000

ESTIMATED LOCAL VELOCITIES BY THE COEFFICIENT EQUATION (M/S)

STN LEVEL	A	B	C	CL	D	E	F
1	0.59053	0.64356	0.66309	0.67232	0.66309	0.64356	0.59053
2	0.59416	0.65580	0.67998	0.68944	0.67998	0.65580	0.59416
3	0.56388	0.64367	0.68044	0.68991	0.68044	0.64367	0.56388
4	0.00000	0.57320	0.66392	0.67744	0.66392	0.57320	0.00000
5	0.00000	0.00000	0.61879	0.64680	0.61879	0.00000	0.00000
6	0.00000	0.00000	0.55935	0.60882	0.55935	0.00000	0.00000
7	0.00000	0.00000	0.49056	0.56586	0.49056	0.00000	0.00000

YMAX= 0.2822 M VMEAN= 0.6255 M/S ENERGY SLOPE= 0.10069E-02

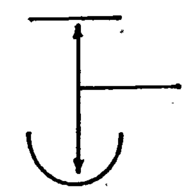

3 RUN NUMBER E-78

EXPERIMENTAL LOCAL VELOCITIES (M/S)

STN LEVEL	A	B	C	CL	D	E	F
1	0.41335	0.45395	0.47132	0.47814	0.47132	0.45395	0.41335
2	0.47495	0.57175	0.57175	0.53949	0.57175	0.57175	0.47495
3	0.24821	0.54101	0.59022	0.60308	0.59022	0.54101	0.24821
4	0.00000	0.45390	0.57976	0.60439	0.57976	0.45390	0.00000
5	0.00000	0.00000	0.50956	0.56634	0.50956	0.00000	0.00000
6	0.00000	0.00000	0.37867	0.51531	0.37867	0.00000	0.00000
7	0.00000	0.00000	0.00000	0.45888	0.00000	0.00000	0.00000

ESTIMATED LOCAL VELOCITIES BY THE COEFFICIENT EQUATION (M/S)

STN LEVEL	A	B	C	CL	D	E	F
1	0.44035	0.48123	0.49871	0.50556	0.49371	0.48123	0.44035
2	0.45740	0.52610	0.55068	0.55932	0.55068	0.52610	0.45740
3	0.24430	0.53820	0.58783	0.60081	0.58783	0.53820	0.24430
4	0.00000	0.45048	0.57729	0.60215	0.57729	0.45048	0.00000
5	0.00000	0.00000	0.50651	0.56373	0.50651	0.00000	0.00000
6	0.00000	0.00000	0.37491	0.51229	0.37491	0.00000	0.00000
7	0.00000	0.00000	0.00000	0.45548	0.00000	0.00000	0.00000

YMAX= 0.2177 M VMEAN= 0.5092 M/S ENERGY SLOPE= 0.48056E-02

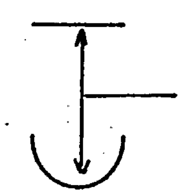

n_C

4 RUN NUMBER E-79

EXPERIMENTAL LOCAL VELOCITIES (M/S)

STN LEVEL	A	B	C	CL	D	E	F
1	0.07351	0.09206	0.09979	0.10545	0.09979	0.09206	0.07351
2	0.07958	0.11175	0.12315	0.12992	0.12315	0.11175	0.07958
3	0.05370	0.11865	0.14045	0.14935	0.14045	0.11865	0.05370
4	0.00000	0.09104	0.13601	0.14993	0.13601	0.09104	0.00000
5	0.00000	0.00000	0.10586	0.13174	0.10586	0.00000	0.00000
6	0.00000	0.00000	0.05955	0.10805	0.05955	0.00000	0.00000
7	0.00000	0.00000	0.00000	0.07958	0.00000	0.00000	0.00000

ESTIMATED LOCAL VELOCITIES BY THE COEFFICIENT EQUATION (M/S)

STN LEVEL	A	B	C	CL	D	E	F
1	0.07380	0.09229	0.10001	0.10263	0.10001	0.09229	0.07380
2	0.08457	0.11202	0.12348	0.12723	0.12348	0.11202	0.08457
3	0.05420	0.12005	0.14094	0.14686	0.14094	0.12005	0.05420
4	0.00000	0.09133	0.13646	0.14746	0.13646	0.09133	0.00000
5	0.00000	0.00000	0.10611	0.12907	0.10611	0.00000	0.00000
6	0.00000	0.00000	0.05697	0.10524	0.05697	0.00000	0.00000
7	0.00000	0.00000	0.00000	0.07967	0.00000	0.00000	0.00000

YMAX= 0.2499 M VMEAN= 0.1066 M/S ENERGY SLOPE= 0.25686E-03

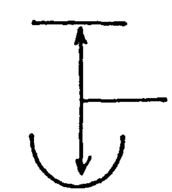
n_C

5 RUN NUMBER E-80

STN	A	B	C	CL	D	E	F
	EXPERIMENTAL LOCAL VELOCITIES (M/S)						
LEVEL							
1	0.30657	0.33012	0.34078	0.34456	0.34078	0.33012	0.30657
2	0.31524	0.38152	0.43454	0.40479	0.43434	0.38152	0.31524
3	0.25397	0.39397	0.42092	0.42788	0.42092	0.39397	0.25327
4	0.00000	0.34716	0.41494	0.42863	0.41494	0.34716	0.00000
5	0.00000	0.00000	0.37537	0.40748	0.37537	0.00000	0.00000
6	0.00000	0.00000	0.26478	0.34842	0.26478	0.00000	0.00000
7	0.00000	0.00000	0.00000	0.31588	0.00000	0.00000	0.00000

STN	A	B	C	CL	D	E	F
	ESTIMATED LOCAL VELOCITIES BY THE COEFFICIENT EQUATION (M/S)						
LEVEL							
1	0.32211	0.34817	0.36006	0.36428	0.36006	0.34817	0.32211
2	0.33518	0.37680	0.39282	0.39410	0.39282	0.37680	0.33518
3	0.23233	0.38555	0.41610	0.42408	0.41610	0.38555	0.23234
4	0.00000	0.33326	0.40931	0.42451	0.40931	0.33326	0.00000
5	0.00000	0.00000	0.36467	0.40082	0.36467	0.00000	0.00000
6	0.00000	0.00000	0.27654	0.36862	0.27654	0.00000	0.00000
7	0.00000	0.00000	0.00000	0.33238	0.00000	0.00000	0.00000

YMAX= 0.2278 M VMEAN= 0.3679 M/S ENERGY SLOPE= 0.12639E-02

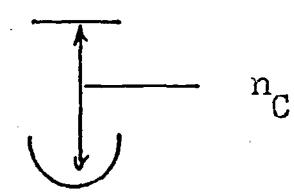

6 RUN NUMBER E-81

EXPERIMENTAL LOCAL VELOCITIES (M/S)							
STN	A	B	C	CL	D	E	F
LEVEL							
1	0.61628	0.63549	0.64745	0.65898	0.64745	0.63549	0.61628
2	0.58035	0.71291	0.71291	0.72617	0.71291	0.71291	0.58035
3	0.00000	0.67713	0.72355	0.75454	0.72355	0.67713	0.00000
4	0.00000	0.53614	0.72698	0.75596	0.72698	0.53614	0.00000
5	0.00000	0.00000	0.64471	0.71782	0.64471	0.00000	0.00000
6	0.00000	0.00000	0.45235	0.71291	0.45235	0.00000	0.00000
7	0.00000	0.00000	0.00000	0.60973	0.00000	0.00000	0.00000

ESTIMATED LOCAL VELOCITIES BY THE COEFFICIENT EQUATION (M/S)							
STN	A	B	C	CL	D	E	F
LEVEL							
1	0.59198	0.64128	0.65847	0.66460	0.65847	0.64128	0.59198
2	0.57306	0.68558	0.71051	0.71838	0.71051	0.68558	0.57306
3	0.00000	0.68260	0.74609	0.75970	0.74609	0.68261	0.00000
4	0.00000	0.54292	0.73223	0.76108	0.73223	0.54292	0.00000
5	0.00000	0.00000	0.65043	0.72309	0.65043	0.00000	0.00000
6	0.00000	0.00000	0.46035	0.67187	0.46035	0.00000	0.00000
7	0.00000	0.00000	0.00000	0.61472	0.00000	0.00000	0.00000

YMAX= 0.1531 M VMEAN= 0.6590 M/S ENERGY SLOPE= 0.39167E-02

7 RUN NUMBER E-82

EXPERIMENTAL LOCAL VELOCITIES (M/S)

STN / LEVEL	A	B	C	CL	D	E	F
1	0.10979	0.14556	0.15667	0.16222	0.15667	0.14556	0.10979
2	0.11176	0.16002	0.18609	0.18683	0.18609	0.16002	0.11176
3	0.05813	0.15180	0.18388	0.18373	0.18388	0.15180	0.05813
4	0.00000	0.11217	0.17054	0.18096	0.17054	0.11217	0.00000
5	0.00000	0.00000	0.14165	0.15356	0.14165	0.00000	0.00000
6	0.00000	0.00000	0.10640	0.13392	0.10640	0.00000	0.00000
7	0.00000	0.00000	0.00000	0.11176	0.00000	0.00000	0.00000

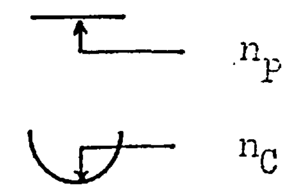

ESTIMATED LOCAL VELOCITIES BY THE COEFFICIENT EQUATION (M/S)

STN / LEVEL	A	B	C	CL	D	E	F
1	0.12025	0.14668	0.15708	0.16227	0.15708	0.14668	0.12025
2	0.12182	0.15929	0.17283	0.17967	0.17283	0.15929	0.12182
3	0.05542	0.15253	0.17960	0.18692	0.17960	0.15253	0.05542
4	0.00000	0.11514	0.17003	0.17972	0.17003	0.11514	0.00000
5	0.00000	0.00000	0.14301	0.15978	0.14301	0.00000	0.00000
6	0.00000	0.00000	0.10200	0.13372	0.10200	0.00000	0.00000
7	0.00000	0.00000	0.00000	0.10958	0.00000	0.00000	0.00000

YMAX= 0.2276 M VMEAN= 0.1497 M/S ENERGY SLOPE= 0.27800E-03

8 RUN NUMBER E-83

n_P

n_C

EXPERIMENTAL LOCAL VELOCITIES (M/S)

STN / LEVEL	A	B	C	CL	D	E	F
1	0.46482	0.52670	0.54048	0.57551	0.54048	0.52670	0.46483
2	0.48756	0.58035	0.58766	0.60687	0.58766	0.58035	0.48756
3	0.40803	0.55370	0.58402	0.59200	0.58402	0.55370	0.40903
4	0.00000	0.54059	0.57123	0.58377	0.57123	0.54059	0.00000
5	0.00000	0.00000	0.55384	0.56296	0.55384	0.00000	0.00000
6	0.00000	0.00000	0.46105	0.53679	0.46105	0.00000	0.00000
7	0.00000	0.00000	0.00000	0.50699	0.00000	0.00000	0.00000

ESTIMATED LOCAL VELOCITIES BY THE COEFFICIENT EQUATION (M/S)

STN / LEVEL	A	B	C	CL	D	E	F
1	0.52556	0.55175	0.56316	0.56693	0.56316	0.55175	0.52556
2	0.51882	0.55964	0.57367	0.57798	0.57367	0.55964	0.51882
3	0.39640	0.54887	0.57394	0.58050	0.57394	0.54887	0.39640
4	0.00000	0.50869	0.56339	0.57373	0.56339	0.50869	0.00000
5	0.00000	0.00000	0.53154	0.55645	0.53154	0.00000	0.00000
6	0.00000	0.00000	0.46756	0.53478	0.46756	0.00000	0.00000
7	0.00000	0.00000	0.00000	0.50974	0.00000	0.00000	0.00000

YMAX= 0.2220 M VMEAN= 0.5473 M/S ENERGY SLOPE= 0.10972E-02

9 RUN NUMBER E-84

EXPERIMENTAL LOCAL VELOCITIES (M/S)

STN / LEVEL	A	B	C	CL	D	E	F
1	0.66180	0.69153	0.70498	0.70936	0.70498	0.69153	0.66180
2	0.72617	0.69927	0.71561	0.72063	0.71561	0.69927	0.72617
3	0.64663	0.68809	0.71459	0.72174	0.71459	0.68809	0.64663
4	0.00000	0.64782	0.70275	0.71388	0.70275	0.64782	0.00000
5	0.00000	0.00000	0.66843	0.69435	0.66843	0.00000	0.00000
6	0.00000	0.00000	0.59915	0.67011	0.59915	0.00000	0.00000
7	0.00000	0.00000	0.00000	0.64205	0.00000	0.00000	0.00000

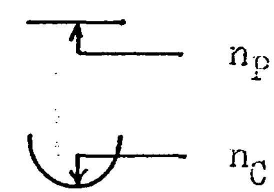

ESTIMATED LOCAL VELOCITIES BY THE COEFFICIENT EQUATION (M/S)

STN / LEVEL	A	B	C	CL	D	E	F
1	0.67570	0.69500	0.70361	0.70641	0.70362	0.69500	0.67570
2	0.67129	0.69996	0.71036	0.71353	0.71037	0.69996	0.67129
3	0.61454	0.69278	0.70972	0.71427	0.70972	0.69278	0.61454
4	0.00000	0.66655	0.70218	0.70929	0.70217	0.66655	0.00000
5	0.00000	0.00000	0.68005	0.69680	0.68000	0.00000	0.00000
6	0.00000	0.00000	0.63428	0.68115	0.63401	0.00000	0.00000
7	0.00000	0.00000	0.00000	0.66281	0.00000	0.00000	0.00000

YMAX= 0.2357 M VMEAN= 0.6859 M/S ENERGY SLOPE= 0.24583E-02

10 RUN NUMBER E-87

EXPERIMENTAL LOCAL VELOCITIES (M/S)

STN LEVEL	A	B	C	CL	D	E	F
1	0.05503	0.07280	0.08109	0.08392	0.08109	0.07280	0.05503
2	0.06018	0.08030	0.08495	0.09031	0.08495	0.08030	0.06018
3	0.05868	0.09299	0.09567	0.10103	0.09567	0.09299	0.05868
4	0.04400	0.08495	0.09567	0.09567	0.09567	0.08495	0.04400
5	0.00000	0.04368	0.08495	0.08589	0.08495	0.04368	0.00000
6	0.00000	0.00000	0.05545	0.07284	0.05545	0.00000	0.00000
7	0.00000	0.00000	0.03060	0.05813	0.03060	0.00000	0.00000

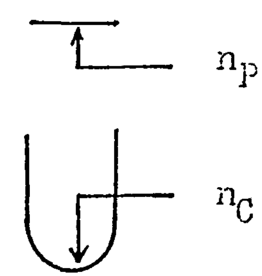

ESTIMATED LOCAL VELOCITIES BY THE COEFFICIENT EQUATION (M/S)

STN LEVEL	A	B	C	CL	D	E	F
1	0.05757	0.07502	0.08314	0.08581	0.08314	0.07502	0.05757
2	0.06262	0.08237	0.09166	0.09470	0.09166	0.08237	0.06262
3	0.06134	0.08437	0.09569	0.09930	0.09569	0.08437	0.06134
4	0.04671	0.07752	0.09125	0.09536	0.09125	0.07752	0.04671
5	0.00000	0.04340	0.07755	0.08486	0.07755	0.04340	0.00000
6	0.00000	0.00000	0.05819	0.07206	0.05819	0.00000	0.00000
7	0.00000	0.00000	0.02855	0.05907	0.02855	0.00000	0.00000

YMAX= 0.4234 M   VMEAN= 0.0754 M/S   ENERGY SLOPE= 0.41723E-04

11 RUN NUMBER L-38

EXPERIMENTAL LOCAL VELOCITIES (M/S)

STN	A	B	C	CL	D	E	F
LEVEL							
1	0.16816	0.19059	0.20146	0.20504	0.20146	0.19059	0.16816
2	0.16889	0.20292	0.21901	0.22437	0.21901	0.20292	0.16889
3	0.17611	0.18987	0.20285	0.22973	0.20285	0.18987	0.17611
4	0.12735	0.17918	0.19638	0.21901	0.19638	0.17918	0.12735
5	0.00000	0.13420	0.18015	0.20828	0.18015	0.13420	0.00000
6	0.00000	0.00000	0.16538	0.17611	0.16538	0.00000	0.00000
7	0.00000	0.00000	0.12068	0.14930	0.12068	0.00000	0.00000

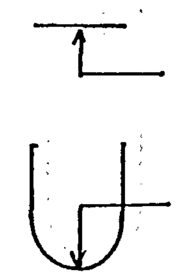

ESTIMATED LOCAL VELOCITIES BY THE COEFFICIENT EQUATION (M/S)

STN	A	B	C	CL	D	E	F
LEVEL							
1	0.17082	0.19537	0.20737	0.21133	0.20737	0.19537	0.17082
2	0.17161	0.19831	0.21160	0.21591	0.21160	0.19831	0.17161
3	0.16545	0.19458	0.20889	0.21344	0.20889	0.19458	0.16545
4	0.13397	0.18285	0.20175	0.20719	0.20175	0.18285	0.13397
5	0.00000	0.13421	0.18391	0.19362	0.18391	0.13421	0.00000
6	0.00000	0.00000	0.15878	0.17818	0.15878	0.00000	0.00000
7	0.00000	0.00000	0.11662	0.16176	0.11662	0.00000	0.00000

YMAX= 0.4094 M VMEAN= 0.1843 M/S ENERGY SLOPE= 0.76373E-04

12 RUN NUMBER E-89

STN	A	B	C	CL	D	E	F
	EXPERIMENTAL LOCAL VELOCITIES (M/S)						
LEVEL							
1	0.28001	0.30941	0.32181	0.32580	0.32181	0.30941	0.28001
2	0.28261	0.30565	0.32419	0.32848	0.32419	0.30565	0.28261
3	0.30199	0.30660	0.32114	0.32568	0.32114	0.30660	0.30199
4	0.26222	0.29452	0.31383	0.31925	0.31383	0.29452	0.26222
5	0.00000	0.26222	0.29518	0.30538	0.29518	0.26222	0.00000
6	0.00000	0.00000	0.28873	0.28921	0.28873	0.00000	0.00000
7	0.00000	0.00000	0.21590	0.27137	0.21590	0.00000	0.00000

STN	A	B	C	CL	D	E	F
	ESTIMATED LOCAL VELOCITIES BY THE COEFFICIENT EQUATION (M/S)						
LEVEL							
1	0.28894	0.31080	0.32096	0.32424	0.32096	0.31080	0.28894
2	0.28856	0.31139	0.32292	0.32642	0.32292	0.31189	0.28856
3	0.28268	0.30849	0.32043	0.32413	0.32043	0.30849	0.28268
4	0.25343	0.29849	0.31443	0.31889	0.31443	0.29849	0.25343
5	0.00000	0.25102	0.29905	0.30749	0.29905	0.25102	0.00000
6	0.00000	0.00000	0.27590	0.29467	0.27590	0.00000	0.00000
7	0.00000	0.00000	0.23139	0.27911	0.23139	0.00000	0.00000

YMAX= 0.4049 M   VMEAN= 0.2950 M/S   ENERGY SLOPE= 0.23603E-03

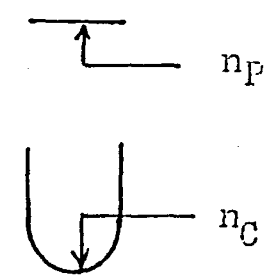

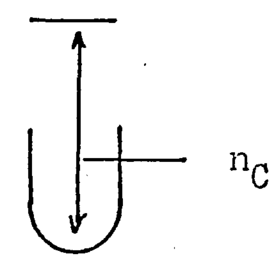

13 RUN NUMBER E-90

EXPERIMENTAL LOCAL VELOCITIES (M/S)

STN LEVEL	A	B	C	CL	D	E	F
1	0.09528	0.09623	0.09652	0.09652	0.09652	0.09623	0.09528
2	0.09652	0.09652	0.10315	0.10315	0.10315	0.09652	0.09652
3	0.09652	0.10073	0.10315	0.11641	0.10315	0.10073	0.09652
4	0.08245	0.09652	0.10315	0.11111	0.10315	0.09652	0.08245
5	0.00000	0.08491	0.10845	0.11111	0.10845	0.08491	0.00000
6	0.00000	0.00000	0.09652	0.10315	0.09652	0.00000	0.00000
7	0.00000	0.00000	0.08007	0.09920	0.08007	0.00000	0.00000

ESTIMATED LOCAL VELOCITIES BY THE COEFFICIENT EQUATION (M/S)

STN LEVEL	A	B	C	CL	D	E	F
1	0.09361	0.09778	0.09959	0.10020	0.09959	0.09773	0.09361
2	0.09642	0.10097	0.10294	0.10360	0.10294	0.10097	0.09642
3	0.09697	0.10299	0.10532	0.10605	0.10532	0.10299	0.09697
4	0.08214	0.10073	0.10499	0.10610	0.10499	0.10073	0.08214
5	0.00000	0.08424	0.10148	0.10373	0.10148	0.08424	0.00000
6	0.00000	0.00000	0.09519	0.10056	0.09519	0.00000	0.00000
7	0.00000	0.00000	0.08009	0.09673	0.08009	0.00000	0.00000

YMAX= 0.3536 1.   VMEAN= 0.0985 M/S   ENERGY SLOPE= 0.97911E-03

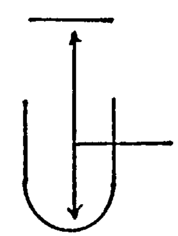

14 RUN NUMBER E-91

EXPERIMENTAL LOCAL VELOCITIES (M/S)

STN	A	B	C	CL	D	E	F
LEVEL							
1	0.15074	0.16618	0.17324	0.17563	0.17324	0.16618	0.15074
2	0.16071	0.18269	0.18269	0.18269	0.18269	0.18269	0.16071
3	0.16405	0.18269	0.18269	0.18269	0.18269	0.18269	0.16405
4	0.12966	0.18269	0.18269	0.18269	0.18269	0.18269	0.12966
5	0.00000	0.16943	0.18269	0.18269	0.18269	0.16943	0.00000
6	0.00000	0.00000	0.15617	0.17688	0.15617	0.00000	0.00000
7	0.00000	0.00000	0.11552	0.16317	0.11552	0.00000	0.00000

ESTIMATED LOCAL VELOCITIES BY THE COEFFICIENT EQUATION (M/S)

STN	A	B	C	CL	D	E	F
LEVEL							
1	0.15342	0.16598	0.17164	0.17355	0.17164	0.16598	0.15342
2	0.16155	0.17536	0.18161	0.18368	0.18161	0.17536	0.16155
3	0.16425	0.18157	0.18886	0.19120	0.18886	0.18157	0.16425
4	0.14096	0.17639	0.18604	0.19129	0.18604	0.17639	0.14096
5	0.00000	0.14110	0.17785	0.18418	0.17785	0.14110	0.00000
6	0.00000	0.00000	0.16053	0.17455	0.16053	0.00000	0.00000
7	0.00000	0.00000	0.12388	0.16354	0.12388	0.00000	0.00000

YMAX= 0.3931 M   VMEAN= 0.1713 M/S   ENERGY SLOPE= 0.15275E-03

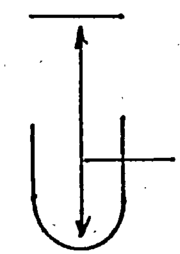

15 RUN NUMBER E-92

EXPERIMENTAL LOCAL VELOCITIES (M/S)

STN / LEVEL	A	B	C	CL	D	E	F
1	0.22452	0.25993	0.27659	0.28238	0.27659	0.25993	0.22452
2	0.24818	0.28963	0.28873	0.28843	0.28873	0.28963	0.24818
3	0.25189	0.28873	0.31524	0.31524	0.31524	0.28873	0.25189
4	0.15617	0.28733	0.31524	0.31524	0.31524	0.28733	0.15617
5	0.00000	0.15617	0.29440	0.31524	0.29440	0.15617	0.00000
6	0.00000	0.00000	0.22245	0.31524	0.22245	0.00000	0.00000
7	0.00000	0.00000	0.13613	0.25391	0.13613	0.00000	0.00000

ESTIMATED LOCAL VELOCITIES BY THE COEFFICIENT EQUATION (M/S)

STN / LEVEL	A	B	C	CL	D	E	F
1	0.22357	0.25551	0.27041	0.27558	0.27041	0.25551	0.22357
2	0.24494	0.28203	0.29936	0.30528	0.29936	0.28203	0.24494
3	0.24827	0.29959	0.32115	0.32815	0.32115	0.29959	0.24827
4	0.15034	0.27999	0.31810	0.32858	0.31810	0.27999	0.15034
5	0.00000	0.15872	0.28627	0.30702	0.28627	0.15872	0.00000
6	0.00000	0.00000	0.23540	0.27860	0.23540	0.00000	0.00000
7	0.00000	0.00000	0.14194	0.24739	0.14194	0.00000	0.00000

YMAX= 0.35381 VMEAN= 0.2661 M/S ENERGY SLOPE= 0.13541E-02

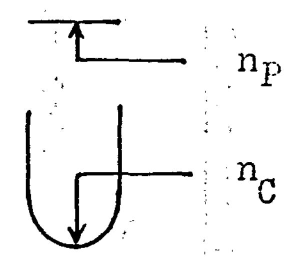

16 RUN NUMBER E-93

EXPERIMENTAL LOCAL VELOCITIES (M/S)

STN	A	B	C	CL	D	E	F
LEVEL							
1	0.14558	0.16667	0.17688	0.18025	0.17688	0.16667	0.14558
2	0.14794	0.16696	0.17857	0.18268	0.17857	0.16757	0.14794
3	0.14265	0.16943	0.18268	0.18268	0.18268	0.16943	0.14265
4	0.11339	0.16132	0.17473	0.17473	0.17473	0.16132	0.11339
5	0.00000	0.12171	0.15917	0.16943	0.15917	0.12171	0.00000
6	0.00000	0.00000	0.13583	0.16143	0.13583	0.00000	0.00000
7	0.00000	0.00000	0.09436	0.13231	0.09436	0.00000	0.00000

ESTIMATED LOCAL VELOCITIES BY THE COEFFICIENT ECLATION (M/S)

STN	A	B	C	CL	D	E	F
LEVEL							
1	0.14617	0.16626	0.17594	0.17914	0.17594	0.16626	0.14617
2	0.14642	0.17067	0.18119	0.18461	0.18119	0.17067	0.14642
3	0.14337	0.16810	0.18007	0.18366	0.18007	0.16810	0.14337
4	0.11535	0.15827	0.17427	0.17885	0.17427	0.15827	0.11535
5	0.00000	0.11390	0.15912	0.16756	0.15912	0.11390	0.00000
6	0.00000	0.00000	0.13686	0.15450	0.13686	0.00000	0.00000
7	0.00000	0.00000	0.09699	0.14042	0.09699	0.00000	0.00000

YMAX= 0.3977 I VMEAN= 0.1552 M/S ENERGY SLOPE= 0.11369E-02

C.5 Values of Velocity Exponent E2

In this appendix, the experimental values of velocity exponent E2 had been recorded.

TABLE C.5.1

Values of E2

Run Number	E2	Run Number	E2	Run Number	E2	Run Number	E2
E13	0.9979	E33	9.6816	E61	0.1638	E87	0.9578
E14	0.1002	E34	0.6149	E62	0.8906	E88	0.9587
E15	0.9148	E35	0.6600	E63	0.8728	E89	0.4834
E16	0.1561	E36	0.5771	E65	0.6082	E90	0.3387
E17	0.1507	E41	0.1186	E66	0.4051	E91	0.6164
E18	0.2064	E42	0.1493	E67	0.4249	E92	0.1086
E19	0.1273	E43	0.1838	E68	0.4750	E93	0.8895
E20	0.7487	E45	0.4369	E70	0.1025		
E21	0.1243	E46	0.6870	E71	0.9792		
E22	0.7103	E47	0.7205	E72	0.9204		
E23	0.9683	E48	0.1399	E74	0.5430		
E24	0.1067	E50	0.8122	E75	0.6070		
E25	0.7701	E51	0.8631	E76	0.6132		
E26	0.9220	E52	0.6599	E78	0.9837		
E27	0.7153	E53	0.1821	E79	0.1226		
E28	0.5148	E55	0.5579	E80	0.9222		
E29	0.4767	E56	0.6585	E81	0.8507		
E30	0.4583	E57	0.2478	E82	0.1015		
E31	0.7608	E58	0.1643	E83	0.3804		
E32	0.4934	E60	0.1156	E84	0.2243		

APPENDIX D

Nomenclature

D.1 List of Nomenclature

In this appendix, the nomenclature and subscripts used in this thesis are presented. Each term is also defined as it first appears.

NOMENCLATURE

A_i	- effective flow area of section
a	- P_2/P_1
a_r'	- experimental coefficient
a_s'	- experimental coefficient
B	- the width of the channel
C_i	- Chezy's coefficient for the section
C_t	- Chezy's coefficient for the channel
E	- coefficient
E1	- velocity coefficient which indicates the magnitude of the flow
E2	- velocity exponent which indicates the velocity gradient steepness
E3	- velocity coefficient where $E3=E1 \cdot (V_{max}/V)$
e	- the rate of dissipation of turbulent energy
exp	- exponent of e
F	- general function
F_{ix}	- body force
Funct	- general function
f_i	- Darcy-Weisbach friction factor of section
f_{MOD}	- modified Darcy-Weisbach friction factor for the channel
G	- turbulent energy production by the mean motion
g	- gravitational acceleration
H	- the mean elevation of the bottom of a transverse cross-section of open-channel
h_ξ	- scale factor

h_η - scale factor

i - number of strips within one section

j - number of sections within the reach

k - kinetic energy of turbulent motion

k_i - absolute roughness height of the boundary

k_s - Nikuradse's sand roughness size

L - length along each section

ln - natural logarithm

log - logarithm to base 10

N_R - Reynolds number

n_1 - channel roughness

n_2 - covered channel roughness

n_C - Manning's coefficient for coarse wire mesh

n_F - Manning's coefficient for fine wire mesh

n_P - Manning's coefficient for plywood

n_t - composite channel roughness

n_{tE} - experimental composite Manning's coefficient

n_{tT} - theoretical composite Manning's coefficient

P_i - wetted perimeter of section

$\overline{P}$ - average pressure

Q - total measured flow rate

q - unit flow rate

R_i - effective hydraulic radius of section

R' - effective hydraulic radius

R_t - hydraulic radius of the channel

r - coefficient of correlation

r - nondimensional coefficient

S_o - energy slope of the channel (bed slope)

S_ϕ - volumetric source rate of ϕ

t - time

U_i - local velocity

$\bar{U}$ - average velocity in x-direction

U' - local velocity variation x-direction

U_s - point velocity within the strip

u - instantaneous velocity fluctuation in x

V - channel mean velocity

V_i - mean velocity of sections

V_* - local shear velocity

$\bar{V}_*$ - mean shear velocity

V_{max} - maximum velocity of cross-section

V_s - mean velocity for the particular strip

$\bar{V}$ - average velocity in y-direction

$V_{\eta *}$ - the value of V_η at a boundary point

V' - local velocity in y-direction

V_1 - x_1 component of flow velocity

v - instantaneous velocity fluctuation in y

W - mean velocity in z-direction

w - instantaneous velocity fluctuation in z

$|x|$ - absolute value of x

Y - maximum flow depth of the channel

Y_i - flow depth of section

y_i - distance from the boundary

z - empirical constant

α - wetted perimeter ratio P_1/P

β_i - empirical coefficient

γ - unit weight of the fluid

δ_i - laminar sublayer thickness

ε - sand roughness

ε_i - relative depth ratio

ξ_* - ratio between local shear velocity and mean shear velocity

ξ_R - rotation of fluid particle

ξ_o - empirical coefficient

η_* - depth ratio from the boundary

κ - Von Karman's constant

λ_i - hydraulic radius ratio R_2/R_1

λ'_i - composite friction coefficient

μ - viscosity

ν - kinematic viscosity

ρ - fluid density

σ - normal stress

τ_i - shear stress

τ_L - turbulent shear

ϕ - shape factor

ϕ - scalar quantity such as concentration in mass transfer

Φ - a functional group

ψ - sectional shape coefficient

θ - channel bed slope

θ_l - local product of point velocities

Σ - summation

REFERENCES

1. Bruk, S. and Volf, Z., "Determination of Roughness Coefficients for very Irregular Rivers with Large Dloodplains," 12th Contress, International Association for Hydraulics Research, 1967, pp. 95-99.

2. Carey, K. L. "Observed Configuration and Computed Roughness of the Underside of River Ice," U.S. Geological Survey Prof. Paper 550B, 1966, pp. B192-B198.

3. Carey, K. L., "The Underside of River Ice, St. Croix River, Wisconsin," U.S. Geological Survey Prof. Paper 575C, 1967, pp. C195-199.

4. Carey, K. L., "Analytical Approaches to Computation of Discharge of an Ice-covered Stream," U.S. Geological Survey Prof. Paper 575C, 1967, pp. C200-C207.

5. Chatfield, C., Statistics for Technology, 2nd ed. London, Chapman and Hall Ltd., 1976, pp. 166-196.

6. Chee, S. P., Haggag, M. R. and Wong, Y. F., "Channel Configuration and Streamflow," International Conference on Water Resources Development, Taiwan, Republic of China, May 1980, pp. 651-660.

7. Chin, C. L., Lin, H. C., and Mizumura, K. "Simulation of Hydraulic Processes in Open Channels," Journal of the Hydraulics Division, ASCE, Vol. 102, No. HY2, Proc. Paper 11905, Feb. 1976, pp. 185-206.

8. Chin, C. L., Hsuing, D. E., and Lin, H. C., "Three-Dimensional Open Channel Flow," Journal of the Hydraulics Division, ASCE, Vol. 104, No. HY8, Proc. Paper 13963, Aug. 1978, pp. 1119-1136.

9. Chin, C. L., Hsuing, D. E., and Lin, R. C. "Secondary Currents under Turbulence in Open Channels of Various Geometrical Shapes," Proceedings of the XVIIIth Congress of the International Association for Hydraulic Research, Sept. 1979, pp. 10-14.

10. Chin, C. L., and Hsiung, D. E., "Secondary Flow, Shear Stress and Sediment Transport," Journal of the Hydraulics Division, ASCE, No. HY7, Proc. Paper 16365, July 1981, pp. 879-898.

11. Chow, V. T., Open Channel Hydraulics, McGraw-Hill Book Co., New York, N.Y., 1959.

12. Chuang H. and Cermak, J. E., "Turbulence Measured by Electrokinetic Transducers," Journal of the Hydraulics Division, ASCE, No. HY6, Proc. Paper 4526, Nov. 1965, pp. 1-8.

13. Dul'nev, V. B. (1962), On the Motion of the Flow Under an Cover. Meteorology and Hydrology, No. 7.

14. Einstein, H. A., and Li, Huon, "Secondary Currents in Straight Channels," Trans. Amer. Geophys. Union, V. 39, 1958, pp. 1085-1088.

15. Emelyanov, K. S., I. M. Konovalov, and P. N. Orlov (1952), Principles of Ice Technology of the River Transport. Rechizdat, L-M.

16. "Factors Influencing Flow in Large Conduits," Progress Report of the Task Force on Flow in Large Conduits of the Committee on Hydraulic Structures, Journal of Hydraulics Division, ASCE, No. HY6, Nov. 1965, pp. 123-149.

17. Haggag, M. R., "Hydraulics of Ice Covered Channels," M.A.Sc. thesis presented to the Faculty of Graduate Studies, University of Windsor, Windsor, Ontario. Canada, 1976.

18. Hancu, S. (1967). Modelarea Hidraulica in Curenti de aer sub presiune, Editura Academiei Rpublicii Socialiste Romania (text in Romanian).

19. Hey, R. D., "Flow Resistance in Gravel-Bed Rivers," Journal of the Hydraulics Division, ASCE, No. HY4, Proc. Paper 14500, April 1979, pp. 365-379.

20. Howarth, L., "Concerning Secondary Flow in Straight Pipes," Proc. Camb. Phil. Soc., V. 34, 1938, pp. 335-344.

21. Hwang, L. S. and Laursen, E. M., "Shear Measurement Technique for Rough Surfaces," Journal of the Hydraulics Division, ASCE, No. HY2, Proc. Paper 3451, March 1963, pp. 19-37.

22. Kazemipour, A. K., and Apett, C. J., "Shape Effects On Resistance to Uniform Flow in Open Channels," Journal of Hydraulics Division, IAHR., Jan. 1979.

23. Ko, S.C., "Measurements of Turbulence in Water at High Velocity," Journal of the Hydraulics Division, ASCE, No. HY12, Dec. 1972, pp. 2253-2257.

24. Krishnamurthy, M., and Christensen, B.A., "Equivalent Roughness for Shallow Channels," Journal of Hydraulics Division, ASCE, No. HY12, Dec. 1972, pp. 2257-2263.

25. Larsen, P. A. (1969). Head Losses Caused by an Ice Cover on Open Channels, J. Boston Society Civil Engineers, Vol. 56, No. 1, pp. 45-67.

26. Lau, Y. L. and Krishnappan, B. G., "Ice Cover Effects on Stream Flows and Mixing," Journal of the Hydraulics Division, ASCE, No. HY10, Proc. Paper 16602, Oct. 1981, pp. 1225-1242.

27. Launder, B. E., and Spalding, D. B., "The Numerical Calculation of Turbulent Flows," Computer Methods in Applied Mechanics and Engineering, Vol. 3, 1974, pp. 269-289.

28. Levi, I. I. (1948). Dynamics of Open Channel Flows, (text in Russian).

29. Marchi, E., "Sid moto uniforme turbolento delle correnti liquide," Rend. Accad. Naz. dei Lincei, Serie VIII, Vol. XXIX, Fasc. 5,6 - Nov. Dec. 1960.

30. Marchi, E.,""Resistance to Flow in Fixed-Bed Channels with the Influence of Cross-Sectional Shape and Free Surface," 12th Congress, International Association for Hydraulics Research, 1967, pp. 32-40.

31. McQuivey, R. S., and Keefer, T. N., "Measurements of Velocity-Concentration Covariance," Journal of the Hydraulics Division, ASCE, No. HY9, Proc. Paper 9184, Sept. 1972, pp. 1625-1646.

32. Morris, M. H., and Wiggert, J. M., "Applied Hydraulics in Engineering," 2nd ed., New York, The Ronald Press Company, 1972.

33. Nezhikhovskiy, R. A. (1964), Coefficients of Roughness of Bottom Surface of Slush-Ice Cover, Soviet Hydrology: Selected Papers, No. 2, pp. 127-150.

34. Nakuradse, J., "Untersuchung uber die geschwindigkeitsventeilung in turbulenten stromungen," VDI Forschungsarbeiten, Heft 281, 1926.

35. Nikuradse, Johann, "Stromungsgesetze in rauhen Rohren," Foreschungs. Arb. Ing.-Wesen, n. 361, Berlin, 1933.

36. Overton, D. E., "Flow Retardance Coefficients for Selected Prismatic Channels," Transactions, American Society of Agricultural Engineers, Vol. 10, No. 3, 1967.

37. Patankar, S. V., and Spalding, D. B., "Heat and Mass Transfer in Boundary Layers," Intertext Publishers, London, England, 1970.

38. Rouse, H., "Critical Analysis of Open-Channel Resistance," Journal of the Hydraulics Division, ASCE, No. HY4, Proc. Paper 4387, July 1965, pp. 1-25.

39. Shiperko, E. E. (1961), Hydraulic Design of Channels with Nonuniform Roughness. Bull. Inst. of Higher Learning. Mining Journal No. 7.

40. Sinotin, V. J., "Velocity Structures of Flow Under Ice Cover," 11th Congress, International Association for Hydraulics Research, Leningrad, 1965, pp. 435-437.

41. Sumbal, J. and Komora, J., "Determination of the Tangential Stress Acting on the Ice Cover in a Rectangular Flume," 12th Congress, International Association for Hydraulics Research, 1967, pp. 255-259.

42. Taylor, R. H., "Exploratory Studies of Open-Channel Flow over Boundaries of Laterally Varying Roughness," U.S. Department of the Interior, Geological Survey, Report No. KH-R-4, July 1961.

43. Tracy, H. J., "Turbulent Flow in a Three-Dimensional Channel," Journal of the Hydraulics Division, ASCE, No. HY6, Proc. Paper 4530, Nov. 1965, pp. 9-35.

44. Trufanov, A. A. (1954), On the Question of Hydraulics of the Flow Under Ice Cover. Meteorology and Hydrology.

45. Uzuner, M. S., "The Composite Roughness of Ice Covered Streams," Journal of Hydraulics Research, IAWH, No. 1, 1975, pp. 79-102.

46. Yen, C. L., and Overton, D. E., "Shape Effects on Resistance in Flood-Plain Channel," Journal of Hydraulics Division, ASCE, No. HY1, Proc. Paper 9506, Jan. 1973, pp. 219-238.

47. Yu, K. H., W. H. Grah, and G. Levine (1968), "The Effect of Ice on the Roughness Coefficients of the St. Croix River, Proc. 11th Conf. Great Lakes Res., Assoc. Great Lakes Res., pp. 668-680.

VITA AUCTORIS

1954 Born on the 30th of December in Hong Kong.

1973 Matriculated from Rosaryhill Secondary School, Hong Kong.

1979 Graduated with a B.A.Sc. in Civil Engineering University of Windsor, Windsor, Ontario, Canada.

1979 Enrolled in the Faculty of Graduate Studies, Department of Civil Engineering in Master program at the University of Windsor, Windsor, Ontario, Canada.

1981 Degree of B.A. in Mathematics was conferred at the University of Windsor, Windsor, Ontario, Canada.